Simulating sand nourishment strategies

from morphology towards multifunctionality

Tosca Kettler

Simulating Sand Nourishment Strategies

from morphology towards multifunctionality

Dissertation

for the purpose of obtaining the degree of doctor
at Delft University of Technology
by the authority of the Rector Magnificus, Prof.dr.ir. H. Bijl,
Chair of the Board for Doctorates
to be defended publicly on
Thursday 5 March 2026 at 10:00

by

Tosca Thalia KETTLER

This dissertation has been approved by the (co)promotors.

Composition of the doctoral committee:

Prof.dr.ir. H. Bijl,	Delft University of Technology, Rector Magnificus
Dr.ir. M.A. de Schipper,	Delft University of Technology, promotor
Dr.ir. A.P. Luijendijk,	Delft University of Technology, copromotor

Independent members:

Prof.dr.ir. J.A. Roelvink,	Delft University of Technology
Prof.dr. J.A. Jiménez,	Universitat Politècnica de Catalunya, Spain
Dr. J.E.A. Storms,	Delft University of Technology
Dr. E.C. Hallin,	Delft University of Technology & Lund University, Sweden
Dr. Q.J. Lodder,	Rijkswaterstaat
Prof.dr. C.A. Katsman,	Delft University of Technology, reserve member

The PhD position was funded by the Netherlands Organization for Scientific Research through the C-SCAPE project (grant number 17595).

In addition, the C-SCAPE project was financially supported by:

Public sector
- Rijkswaterstaat (Dutch ministry of Public Works)
- Province of Noord-Holland
- Municipality of Veere / Region Fund Zeeuwse Kust

Private sector
- Van Oord (dredging, Building with Nature)
- Witteveen+Bos (coastal engineering)

The CSCAPE project received in-kind support (expertise, staff time, equipment, data) from:

Public sector
- HHNK Water Board
- Staatsbosbeheer

Private sector / Public-private initiatives
- Dutch Coastline Challenge
- Svasek Hydraulics

NGOs
- OBN
- Natuurmonumenten
- World Wildlife Fund (WWF)

An electronic version of this thesis is available at: http://repository.tudelft.nl

Contents

7

Summary

This thesis addresses the growing challenge of designing sustainable and adaptive sand nourishment strategies for sandy coasts facing sea level rise, ecological pressures, and intensified human use. While sand nourishment is increasingly adopted as a nature-based alternative to hard coastal defence, its long-term morphological and functional impacts remain insufficiently understood - particularly across decadal timescales and under varying design conditions such as sand volume, placement location and frequency of implementation. The central aim of this thesis is to develop, validate, and apply a modelling framework capable of simulating the multi-decadal evolution of nourished sandy coasts under diverse nourishment strategies and sea level rise rates, thereby supporting the multifunctional and adaptive strategic planning.

The research was structured around four interlinked subcomponents. First, the multi-decadal cross-shore profile evolution of repeatedly nourished sandy coasts was simulated, focusing on equilibration timescales, profile change, and shoreline migration. This included the development of a cross-shore behavioural model, Crocodile, that comprises diffusion-based formulations and incorporates site-specific parameters governing profile shape, depth-dependent diffusion timescales and alongshore transport losses. Its performance was validated against three decades of bathymetric data at nourished Dutch beaches and adjacent nearshore areas. Crocodile was shown to reproduce key morphological indicators (beach width, shoreline position, profile volume) at these nourished sites with sufficient accuracy to distinguish between nourishment strategies.

Second, Crocodile was used to assess how nourishment strategies, that vary in policy, placement volume and frequency, perform under different rates of sea level rise. Results showed that profile response is nonlinear and depth-dependent, with large nourishment volumes leading to profile steepening and reduced nourishment lifetimes by up to 30%. The choice of strategy led to differences of up to 75% in total sand demand over a 50-year horizon. High-frequency (e.g., hold-the-line) strategies may require biannual return periods under high sea level rise rates, while proactive volume-based strategies may lead to overnourished coasts. These findings underscore the need for a nourishment strategy design to be flexible in timing and nourishment dimensions, as present-day design choices may constrain future adaptation options.

The third part of the study explored the depth-dependent alongshore dispersion of mega nourishments. These are high-volume sand nourishments designed to last for one to several decades. Crocodile was coupled with the one-line shoreline model ShorelineS to simulate the depth- and time-dependent dispersion of Gaussian-shaped mega nourishments over 50 years. Results revealed a two-phase evolution: an initial phase of roughly a decade during which sand redistributes both by cross-shore equilibration and alongshore dispersion, followed by longer-term phase dominated

by alongshore dispersion. More seaward deposited sand at lower bed elevations remained largely immobile, suggesting that functional outcomes (e.g., beach width, dune growth) do not scale linearly with sand volume or cross-shore extent.

The fourth subcomponent of this thesis comprised a synthesis on how modelled morphological indicators can be systematically linked to coastal functions such as recreation, ecology, and flood protection. A conceptual framework was developed to translate morphological model outputs to functional indices, and applied in case studies to compare nourishment scenarios. This work moreover exemplifies quantification of trade-offs and synergies in multifunctional nourishment strategy design. It also discusses future directions for integrating this work with ecosystem service modelling and adaptive coastal management.

Collectively, the modelling framework and applications presented in this thesis demonstrate how cross-shore redistribution impacts both morphological evolution and functional outcomes of nourishment strategies. Morphodynamic responses are nonlinear, spatially variable, and depth-dependent, highlighting the need for integrated modelling approaches in strategic planning. As future nourishment strategies must accommodate growing sand demands while minimizing ecological disruption, careful optimization of placement in both time and space becomes essential for both morphologic performance and functional value. This research demonstrates that coupling morphologic modelling with multi-objective planning provides foundation for designing nourishment interventions that are sustainable, resilient, and multifunctional in the face of accelerating coastal change.

Samenvatting

Dit proefschrift behandelt de toenemende uitdaging om duurzame en adaptieve zandsuppletiestrategieën te ontwikkelen voor zandige kusten onder de druk van zeespiegelstijging, druk op ecologische systemen en een toename van menselijke activiteiten. Hoewel zandsuppletie steeds vaker wordt toegepast als een natuur-gebaseerd alternatief voor harde kustverdediging, zijn de langetermijneffecten op de morfologie en functionaliteit – met name over decennialange tijdschalen en onder uiteenlopende ontwerpcondities zoals suppletievolume, plaatsingslocatie en uitvoeringsfrequentie – nog onvoldoende begrepen. Het centrale doel van dit onderzoek is het ontwikkelen, valideren en toepassen van een modelleringskader dat de decadale evolutie van gesuppleerde zandige kusten kan simuleren onder diverse suppletiestrategieën en verschillende snelheden van zeespiegelstijging, en daarmee het multifunctionele en adaptieve strategische planningsproces ondersteunt.

Het onderzoek is opgebouwd uit vier onderling verbonden componenten. Ten eerste is de decadale dwarsprofielontwikkeling van herhaaldelijk gesuppleerde zandige kusten gesimuleerd, met aandacht voor tijdschalen van herverdeling, profielverandering en kustlijnmigratie. Hiervoor is het dwarsprofielgedragsmodel Crocodile ontwikkeld, dat gebruikmaakt van diffusie-gebaseerde formuleringen en locatie-specifieke parameters voor profielvorm, diepte-afhankelijke diffusietijdschalen en langstransportverliezen. De prestaties van Crocodile zijn gevalideerd met drie decennia aan alti- en bathymetrische metingen van gesuppleerde Nederlandse stranden en aangrenzende vooroevergebieden. Het model reproduceert belangrijke morfologische indicatoren (strandbreedte, kustlijnpositie, profielvolume) met voldoende nauwkeurigheid om verschillen tussen suppletiestrategieën zichtbaar te maken.

Ten tweede is Crocodile gebruikt om te analyseren hoe suppletiestrategieën, die variëren in beleid, plaatsingsvolume en plaatsingsfrequentie, presteren onder verschillende snelheden van zeespiegelstijging. De resultaten tonen aan dat de profielrespons niet-lineair en diepte-afhankelijk is, waarbij grote suppletievolumes leiden tot versteiling van het kustprofiel en een tot 30% kortere levensduur van de suppletie. De keuze voor een strategie leidde tot verschillen tot 75% in de totale zandvraag over een periode van 50 jaar. Hoge-frequentiestrategieën (bijvoorbeeld reactief op basis van kustlijnpositie) kunnen bij hoge zeespiegelstijging een terugkeerfrequentie van twee jaar vereisen, terwijl proactieve strategieën op basis van volumebehoud kunnen resulteren in 'over-suppletie' van kusten. Deze bevindingen benadrukken de noodzaak van flexibiliteit in timing en dimensies van zandsuppleties, aangezien ontwerpkeuzes in het heden de toekomstige aanpassingsruimte kunnen beperken.

Het derde onderdeel richt zich op de diepte-afhankelijke langstransportspreiding van megasuppleties – grootschalige zandsuppleties ontworpen om een tot meerdere decennia mee te gaan. Crocodile is gekoppeld aan het één-lijns kustlijnmodel

ShorelineS om de diepte- en tijdsafhankelijke spreiding van normaalverdelingsvormige megasuppleties over een periode van 50 jaar te simuleren. De resultaten laten een evolutie in twee fasen zien: in de eerste tien jaar vindt herverdeling van zand plaats zowel langs- als dwars op de kust, waarna een langdurige fase volgt waarin het langstransport van zand naar aangrenzende kustvakken de dynamiek domineert. Dieper gelegen zand bleek grotendeels immobiel, wat suggereert dat functionele effecten (zoals strandverbreding en duinvorming)niet lineair schalen met suppletievolume of dwarsprofieluitbreiding.

In een synthese is onderzocht hoe gemodelleerde morfologische indicatoren systematisch kunnen worden gekoppeld aan kustfuncties zoals recreatie, ecologie en kustveiligheid. Hiervoor is een conceptueel kader ontwikkeld dat morfologische modeluitvoer vertaalt naar functionele indices, en toegepast in casestudies ter vergelijking van suppletiescenario's. Dit raamwerk maakt het mogelijk om afwegingen en synergiën in multifunctioneel suppletieontwerp te kwantificeren. Ook wordt ingegaan op toekomstige integratie met ecosysteemdienstenmodellering en adaptief kustbeheer.

Gezamenlijk laten het ontwikkelde modelleringskader en de toepassingen in dit proefschrift zien hoe kustdwarse herverdeling van zand zowel de morfologische ontwikkeling als de functionele uitkomsten van suppletiestrategieën beinvloedt. Morfodynamische reacties zijn niet-lineair, ruimtelijk variabel en diepte-afhankelijk, wat de noodzaak onderstreept van geïntegreerde modelleringsbenaderingen in strategische planning. Aangezien toekomstige suppletiestrategieën zowel aan een groeiende zandvraag moeten voldoen als ecologische verstoring moeten minimaliseren, wordt een zorgvuldige optimalisatie van plaatsing in tijd en ruimte essentieel voor zowel morfologische uitkomsten als functionele waarde. Dit onderzoek laat zien dat de integratie van morfologische modellering en multifunctionele kustplanning een sterke basis vormt voor suppletie-interventies die duurzaam, veerkrachtig en multifunctioneel blijven bij versnellende kustveranderingen.

1 Introduction

1.1 Dynamic coasts in a changing climate

The Earth's coastal zones comprise a rich diversity of landforms, ranging from high-energy rocky shores with cliffs to gently sloping sedimentary shores such as tidal flats and sandy coasts (Calkoen et al., 2025; Woodroffe, 2002). Since the beginning of life, these areas have offered geomorphological variability that support biological innovation and diversity (Alongi, 2020). Among them are sandy coasts, which represent approximately one-third of the world's ice-free shoreline (Luijendijk et al., 2018). Their gently sloping profiles and dynamic character comprise intertidal areas, beaches, freshwater lenses and a variety of dune forms, supporting a wide range of habitats (Defeo et al., 2009). The permeability of sand allows for groundwater exchange and nutrient cycling, sustaining both microbial life and higher trophic organisms (Defeo et al., 2009). Moreover, sandy coasts often lie adjacent to nutrient-rich estuaries or upwelling zones, making them particularly productive and supportive of biodiversity (Barbier et al., 2011).

Given their resource richness and accessibility, sandy shores have also played a foundational role in the spatial development and sustenance of human societies throughout history. Archaeological evidence suggests that some of the earliest anatomically modern humans settled near coasts as early as 160.000 years ago, (Marean, 2010). Coastal zones offered reliable access to food like shellfish, fish, and seaweed, as well as freshwater and a relatively stable climate buffered by the ocean (Richards and Schulting, 2006). Today, over 40% of the global population lives within 100 kilometres of a coastline, with also many of the world's major cities, such as Tokyo, New York and Jakarta, located on low-lying coastal land (Small and Nicholls, 2003). Sandy coasts worldwide provide essential functions such as storm protection, recreation, biodiversity, and supporting coastal economies (Barbier et al., 2011; Paprotny et al., 2025) (Figure 1.1).

Figure 1.1 Sandy coasts worldwide provide essential functions such as (A) storm protection, (B) recreation, (C) biodiversity, and (D) supporting coastal economies. Photo sources: (A) KNMI/Jannes Wiersema, (B/D) ANP, (C) Ecomare/Salko de Wolf.

Yet this growing concentration of people and infrastructure along coasts has come with mounting pressure. Accelerating sea level rise, increased storm intensity, land subsidence, the extraction of sand for construction, port development and other economic activities - compounded by coastal squeeze from fixed infrastructure - are placing unprecedented stress on sandy coastlines (Bendixen et al., 2019; Hinkel et al., 2014; Lansu et al., 2024; Paprotny et al., 2025; Temmerman et al., 2013a; Vousdoukas et al., 2020a). These pressures are particularly acute along erosive or highly engineered coasts where natural sand transport is disrupted (Hinkel, 2011). To address these threats, coastal managers increasingly rely on active intervention to maintain shoreline stability and protect coastal functions. Thereby, there is growing awareness that present-day coastal planning decisions can heavily influence - and even constrain - the range of future adaptation options (Haasnoot et al., 2013a). This recognition has led to increasing emphasis on adaptive strategies that avoid path dependency and preserve flexibility to instead keep future pathways open as conditions change (e.g. Haasnoot et al., 2019)

Over the last decades, sand nourishment has emerged as an adaptive nature-based alternative to traditional hard-engineering solutions like seawalls and groynes (Hanson et al., 2002), which are increasingly viewed as inflexible and unsustainable due to their high maintenance costs, limited adaptability to sea level rise, and negative ecological impacts (Cooper and Pilkey, 2012). By artificially adding sand to the beach or shoreface, roughly between the MSL (Mean Sea Level) + 3 m and – 5 m elevation

contours, nourishments aim to reinforce the coast while maintaining the natural dynamics and multifunctionality of the system (Gittman et al., 2016; Temmerman et al., 2013b). Nourishments are thereby increasingly expected not only to prevent shoreline retreat, but also to deliver multifunctionality, supplying ecosystem services that meet multiple policy goals (Borsje et al., 2011; Cooke et al., 2012; Manning et al., 2018; De Schipper et al., 2021). These include supporting coastal habitats, facilitating dune development, and maintaining recreational beach width.

However, despite this optimistic framing of nourishment as a 'win-win' solution, the long-term, system-wide impacts of nourishment are not yet fully understood. Most past nourishments have been evaluated at project-level and over short (sub-decadal) timescales. Yet, evidence shows that repeated nourishments can alter coastal functioning in multiple ways (De Schipper et al., 2021). To enable climate-resilient coastal planning, it is essential to understand how these interventions perform over multi-decadal horizons, including their cumulative consequences. As sea level rise accelerates, nourishment strategies will need to scale up - either through increased sand volumes or more frequent interventions - to maintain their intended functions (Haasnoot et al., 2020; Hinkel et al., 2014; Vousdoukas et al., 2020). This raises critical questions about the sustainability of current strategies, which have also been articulated at the policy and political level (e.g. Rijkswaterstaat, 2020). How much sand will be required under higher sea level scenarios? How fast and whereto does the nourished sand redistribute? How does nourished sand shape ecological, recreational, and safety outcomes? And how can we plan a sustainable long-term nourishment strategy in the face of an uncertain future? This thesis contributes to that need by developing and applying new tools to simulate the decadal morphological evolution of nourished sandy coasts, aiming to support their sustainable and multifunctional design under future boundary conditions.

1.2 Nourishment strategies: from morphology to multifunctionality

Sand nourishment has emerged in many contexts and scales. This ranges from small, frequent sand nourishments with typical cross-shore volumes of $O{\sim}100\ m^3/m$ aimed at maintaining local recreational value or mitigating minor erosion (e.g., Brand et al., 2022; Elko et al., 2021). These can either be implemented as 'beach nourishment' with their top above the waterline or completely submerged as 'shoreface nourishment' (Fig. 1.2). The choice between beach and shoreface placement depends on desired timescales of impact (shoreface nourishments feed the upper beach more gradually), available equipment, and environmental constraints. Implementation typically involves dredging sand from offshore borrow areas using trailing suction hopper dredgers, which pump or rainbow the sediment onto the beach or nearshore, followed by shaping with bulldozers to meet design profiles. There are also interventions that combine nourishment with hard structures such as groynes, breakwaters and sea walls (Capobianco et al., 2002; Ranasinghe and Turner, 2006). At the high end of the spectrum are mega-nourishments, designed with much larger sand volumes to influence long stretches of coastline over multi-decadal timescales (Fig. 1.2). Notable examples include the Dutch Sand Engine implemented as an

explorative pilot project (Fig. 1.3) (Stive et al., 2013), the UK's first Sand Engine constructed at Bacton in 2019 to protect critical energy infrastructure (Lorenzoni et al., 2024), and a large-scale sand nourishment recently implemented in Benin, West Africa, as part of a regional climate adaptation effort (Alves et al., 2020).

Figure 1.2 Schematic cross-shore representation of beach, shoreface, and mega-nourishment types. Blue dashed lines indicate the post-placement equilibration process, where nourished sand redistributes toward a more natural beach profile under wave and current forcing.

An increasing number of nourishments has been implemented and has been described in the scientific literature (De Schipper et al., 2014; Hamm et al., 2002; Luo et al., 2016; Stronkhorst et al., 2018; Valverde et al., 1999). Immediately following placement, beach nourishments often exhibit artificially steep profiles. In response to wave and current forcing, this sand is redistributed seaward and alongshore in a process known as equilibration, which gradually reshapes the profile toward a more natural slope (Fig. 1.2). This adjustment can lead to a rapid reduction in beach width and shoreline retreat shortly after implementation, although the sediment typically remains within the active coastal profile. In contrast, shoreface nourishments, that are placed entirely below the waterline, tend to exhibit less visible short-term morphological changes. Over sufficiently long temporal and spatial scales, the nourishment is diffused in cross-shore and alongshore directions. The rate and extent of profile equilibration depend on the scale of the nourishment relative to its environment and the hydrodynamic climate. This equilibration is generally faster when the maximum elevation of the nourishment is located above the waterline, its cross-shore volume is smaller, and under a highly energetic wave climate (Hamm et al., 2002).

Figure 1.3 The Dutch Sand Engine, a mega nourishment. Aerial foto's from (A) August 2011 and (B) August 2020 by Joop van Houdt (Rijkswaterstaat).

There are notable variations among countries in their coastal management practices concerning nourishment (Brand et al., 2022; Cooke et al., 2012; Defeo et al., 2009; Hanson et al., 2002). Some countries, such as Italy and France, apply nourishment mostly in a reactive strategy in response to local requirements. Typically, the need for nourishment revolves around mitigating erosion at the local scale to prevent coastline retreat, but it may also include creating space for recreation. Long-term planning, an overarching strategy, or regular monitoring of the coastline may not always be present in these cases. Other countries, such as Germany and the Netherlands, established proactive long-term nourishment programs that involve operational objectives on factors such as the volume of sand applied and coastal state indicators such as coastline position, beach width and sand volume in the profile (Brand et al., 2022; Hanson et al., 2002).

Research has shown that nourishment programs can be highly effective at preserving beach width and delaying coastal retreat (Brand et al., 2022; Elko et al., 2021; Stive, 1991). Their long-term morphologic effects depend on local morphology, wave climate, and the specifics of nourishment design - including volume, frequency, and placement location (Beck et al., 2012; Ludka et al., 2016). For instance, cross-shore placement depth strongly influences sediment redistribution timescales (Dean, 1991; Silva et al., 2019) while nourishment frequency affects ecological recovery (Hanley et al., 2014; Herman et al., 2022; Leewis et al., 2012; Ocaña et al., 2022)

These design choices affect the extent of trade-offs that sand nourishment inherently involves. Frequent nourishments can disrupt benthic communities, as the construction process can cause widespread mortality among intertidal fauna, alter sediment characteristics, and disrupt prey availability for shorebirds and other species (Gittman et al., 2016; De Schipper et al., 2021; Schlacher et al., 2012; González & Holtmann-Ahumada, 2017). Recovery times vary; some species recolonize within a year, while long-lived or site-dependent species may take decades or never fully return (Hanley et al., 2014; Leewis et al., 2012). Additionally, redistributing nourishments can degrade offshore water quality and may degrade adjacent habitats such as seagrass beds and reefs, while sand mining for nourishment supply can degrade source environments (Nunes da Silva and Barbosa Viana, 2024). Large volumes of nourishment may cause profile steepening (Walstra et al., 2011), and suppress recreational quality if beaches are too wide or narrow (Broer et al., 2011; Cabezas-Rabadán et al., 2019a). Particularly in low-lying deltas and urbanized coasts, maintaining flood safety while preserving ecological and recreational values presents a growing challenge (Gittman et al., 2016; Haasnoot et al., 2019).

A more nuanced understanding – and preferably quantification - of morphological evolution can therefore help informing multifunctional nourishment strategy design. Morphologic indicators - such as beach width, dune volume, and intertidal area - can be systematically linked to ecosystem service delivery (Manning et al., 2018). For instance, wider beaches tend to improve recreational quality and increase aeolian sand supply to dunes, enhancing both safety and dune biodiversity (Keijsers et al.,

2014; Puijenbroek et al., 2017). Similarly, nourishment return periods, when considered relative to the recovery times of benthic organisms, provide insight into the degree of ecological recovery and cumulative impacts, and thus into ecological resilience (Leewis et al., 2012; Ocaña et al., 2022). A critical process in this respect is cross-shore equilibration: the redistribution of nourished sand across the profile strongly influences how long functional benefits persist (Stive et al., 2013). At present, strategic planning frameworks for these interventions generally operate at a higher level of abstraction and do not yet adequately incorporate time-dependent morphological effects at the operational scale. By quantifying how nourishment design influences morphological outcomes, and how those outcomes influence functional performance, it becomes possible to assess trade-offs and design strategies that balance objectives over time and space.

1.3 Morphologic modelling: a time gap to be bridged

Despite decades of progress in coastal morphodynamic modelling, a fundamental challenge remains: bridging the temporal scale between short-term process-based simulations and long-term coastal evolution (Ranasinghe, 2020). Traditional models have largely operated at either end of this spectrum (Fig. 1.4). On one hand, process-based models such as XBeach (Roelvink et al., 2010), SBeach (Larson, 1998), Delft-3D (Lesser et al., 2004), UNIBEST-TC (Walstra, 2000) and the wave-resolving CROCO model (Marchesiello et al., 2022) resolve hydrodynamics and sediment transport processes at high spatial and temporal resolution. These models have proven high skill in simulating storm events, dune erosion, and nearshore wave-driven transport, and acceleration techniques has stretched their spatial and temporal reach (e.g. up to 30 years by Luijendijk et al., 2019). However, these models require large computational resources, detailed boundary conditions, and often suffer from cumulative uncertainty when applied over longer timeframes, complicating their suitability for exploring nourishment evolution over decadal timescales.

On the other hand, reduced-complexity models and empirical formulations provide efficient approximations of long-term coastal change. The classic Bruun Rule (Bruun, 1962) and its later refinements (e.g. Atkinson & Baldock, 2020; McCarroll et al., 2021b; Rosati et al., 2013) predict shoreline retreat under sea level rise and response to total sediment budget changes by assuming by equilibrium-type profile evolution (Dean, 1991). The ShoreTrans model (McCarroll et al., 2021b) extends this concept by allowing the cross-shore translation of profiles to vary with depth, thereby overcoming one of the main limitations of the Bruun Rule, which assumes uniform translation of the entire profile. Additionally, one-line models such as GENESIS (Hanson and Kraus, 1989) or the ShorelineS model (Roelvink et al., 2020) treat the coastline in planform, focusing on alongshore sediment transport gradients to simulate shoreline change (see Ranasinghe (2020) for an overview). These approaches are computationally fast and have been used for regional, decadal shoreline change studies (e.g. Splinter & Coco, 2021). However, their simplifications come at the cost of physical detail on cross-shore development. While computationally efficient, these models typically focus on shoreline retreat and alongshore transport and lack the ability to represent

cross-shore profile change or vertical sediment redistribution. (Montaño et al., 2021). In an effort to bridge the gap between process-based models and long-term empirical approaches, a number of semi-empirical morphodynamic models have emerged in recent years (e.g. Hallin, 2019; Ranasinghe et al., 2012). While models like the CS-model (Hallin, 2019) and the PCR model (Ranasinghe et al., 2012) offer valuable semi-empirical approaches for long-term coastal evolution, they do not explicitly resolve depth-dependent sediment redistribution following nourishment.

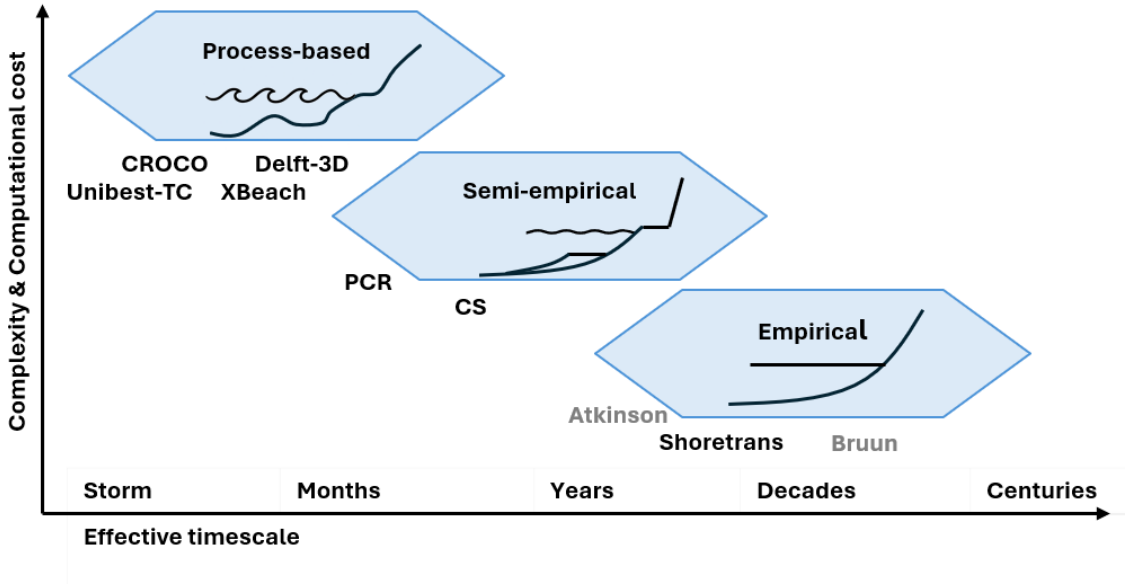

Figure 1.4 Typical modelling timescales of a selection of cross-shore process-based, semi-empirical, and empirical morphodynamic rules (in grey) and models (in black). Schematic beach profile representations illustrate the typical level of detail captured by each model class. These profile shapes are indicative and reflect generalized model resolution rather than exact predictions.

For nourishment strategy planning we need a method that bridges the gap between short-and long-term morphodynamic modelling with specific focus on profile deformation. One promising direction lies in representing coastal profile evolution as a response toward a dynamic equilibrium profile shaped by sediment budget and hydrodynamic climate, around which the actual morphology fluctuates. This concept, initially proposed by Stive et al. (1991), views nourishment as a perturbation that gradually disperses over the profile with a depth-dependent rate. Early implementations of this approach were either embedded within process-based models or relied heavily on site-specific empirical tuning (e.g., Capobianco et al., 1994; Lavrentiev, 2015; Marinho et al., 2017; Chen & Dodd, 2019). However, the growing availability of long-term coastal datasets enables a return to and refinement of this behavioural modelling philosophy, improving generalizability across coastal settings. These developments pave the way for more robust, computationally efficient

tools to simulate nourishment evolution for long-term strategic planning under sea level rise.

1.4 Aim and scope of this thesis

The central aim of this thesis is to inform the sustainable and multifunctional design of coastal management strategies by developing, validating and applying a morphodynamic modelling framework that can simulate the multi-decadal evolution of nourished sandy coasts under varying design strategies and sea level rise rates. A key requirement is that the framework captures time- and depth-dependent cross-shore sand redistribution following nourishment, as this process governs both morphological and functional outcomes. To address this aim, this research is structured around five interlinked research components (schematized in Fig. 1.5.), presented as Chapters 2 through 6:

Chapter 2 - Sand nourishment for multifunctional coastal climate adaptation

This chapter presents a conceptual framework to understand the multifunctionality of sand nourishments. Through a combination of stakeholder workshops and literature review, it maps the links between nourishment design, morphology, and coastal functions such as safety, recreation, and nature. It emphasizes the trade-offs and synergies among these goals and outlines three key lessons to guide future multifunctional coastal adaptation. This sets the conceptual foundation for subsequent chapters, which aim to quantify and model the relevant morphodynamics.

Chapter 3 - Simulating decadal cross-shore dynamics at nourished coasts with Crocodile

This chapter introduces and validates Crocodile, a novel behavioural diffusion type cross-shore model designed to simulate sand nourishment evolution over decades. It fills a methodological gap between short-term process-based models and long-term empirical approaches, with a focus on predicting indicators useful to evaluating coastal functions such as beach width, coastal volume, and shoreline change. This model forms the basis for the morphologic modelling in the rest of the thesis.

Chapter 4 - Exploring decadal beach profile dynamics in response to nourishment strategies under accelerated sea level rise

This chapter applies Crocodile to assess nourishment strategy performance under different sea level rise scenarios. It compares two distinct strategic nourishment approaches, offering insights into their effectiveness and sustainability. The model results highlight the importance of depth-dependent morphodynamic analysis and morphologic feedbacks such as profile steepening. This chapter extends the modelling framework's relevance to nourishment planning for climate adaptation and links closely to multifunctionality by analyzing nourishment frequency, ecological disturbance, and nourishment lifetime.

Chapter 5 - The relevance of depth-dependent sand dispersion in long-term morphological development of mega nourishments

This chapter explores the evolution of larger-scale nourishments in both cross-shore and alongshore directions by applying a novel coupled modelling framework of Crocodile and ShorelineS. It quantifies the depth-dependent sand redistribution in gaussian shaped mega nourishments across time and space and identifies morphological phases related to profile equilibration and alongshore diffusion. This chapter complements earlier chapters by addressing alongshore sand dynamics and offering design recommendations for future large-scale interventions.

Chapter 6 - Synthesizing nourishment dynamics for coastal function delivery

The final chapter synthesizes insights from the earlier chapters by explicitly linking the simulated morphologic changes in to coastal functions introduced in Chapter 2. It evaluates how modelled physical indicators like beach width and nourishment lifetime influence key societal outcomes as recreation and ecological support. It also outlines a science-based approach for using morphological models to inform adaptive and multifunctional nourishment planning, and discusses future directions for integrating this work with ecosystem service modelling and stakeholder-driven coastal management.

The thesis focuses on open, sandy, wave-dominated coasts, using the Dutch coast for its primary case studies due to its good data availability and long nourishment history. The modelling framework is designed for simulating decadal-scale average morphological trends. To this end we use simplified forcing and do not resolve intra-annual variability such as storm events or complex feedbacks such as vegetation-morphology interactions. While the modelling tools are developed and validated using Dutch case studies, the analysis aims to extract transferable insights that can inform nourishment design and policy in other sandy, wave-dominated coastal settings worldwide. The scope bridges morphologic coastal modelling and functional assessment, laying the groundwork for more integrated, multifunctional nourishment planning. The findings aim to inform both scientific understanding and practical decision-making in coastal zone management.

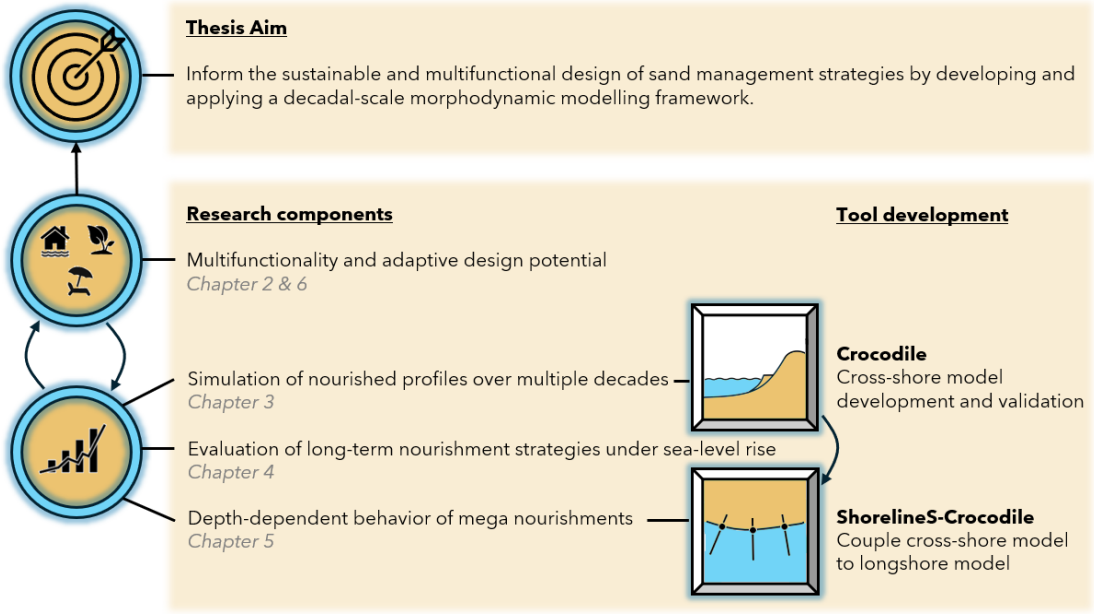

Figure 1.5 Schematic of aim and research components of this thesis.

2 Sand nourishment for multifunctional coastal climate adaptation

This chapter presents a conceptual framework to understand the multifunctionality of sand nourishments. Through a combination of stakeholder workshops and literature review, it maps the links between nourishment design, morphology, and coastal functions such as safety, recreation, and nature. It emphasizes the trade-offs and synergies among these goals and outlines three key lessons to guide future multifunctional coastal adaptation. This sets the conceptual foundation for subsequent chapters, which aim to quantify and model these dynamics.

This chapter is published as:

Geukes, H. H., Kettler, T. T., Lansu, E. M., Bax, V., Höfer, S., de Schipper, M. A., de Winter, R., Luijendijk, A. P., Reijers, V. C., van Bodegom, P. M., van de Lageweg, W. I., van der Heide, T., & van Oudenhoven, A. P. E. (2024). Sand nourishment for multifunctional coastal climate adaptation: three key implications for researchers. Nature-Based Solutions, 6(April), 100191. https://doi.org/10.1016/j.nbsj.2024.100191

2.1 Abstract

Increased climate impacts threaten coastal functions globally, highlighting the need for multifunctional coastal climate adaptation. Sand nourishment can adapt sandy coasts to sea level rise, mitigate erosion, increase flood safety, enhance ecological habitats and expand recreational space. Therefore, sand nourishment is increasingly regarded as a promising nature-based strategy for coastal climate adaptation. However, despite this growing recognition, the assessment of how sand nourishment design impacts multifunctional adaptation remains limited. In this perspective article, we argue for three key lessons for researchers to optimise assessing multifunctional coastal climate adaptation by sand nourishment. We conducted stakeholder workshops to scope and inform our perspective, performed semi-structured literature reviews to concretise and validate this for international applications, built a qualitative model to visualise our interdisciplinary overview of how nourishments impact coastal multifunctionality, reflected on this in expert workshops, and identified implications for researchers. In this manner, we assessed the effects of nourishment design on coastal morphology, ecology, socio-economics and ecosystem services in realising the key policy goals of flood safety, nature and recreation. We found that sand nourishment design can result in conflicts between policy goals, generate ambiguous outcomes and lead to system-wide feedback effects. As such, we identified three key lessons: (1) conflicts between policy goals require informing political decision-making

on prioritisation between coastal functions, (2) concreteness is needed on otherwise ambiguous functions, and (3) ongoing, multidisciplinary system-wide monitoring is essential. We thus call for a holistic approach to sand nourishment design and encourage researchers from diverse expertise and localities to expand on and adapt our findings to optimise informing sand nourishment design for delivering multifunctional coastal climate adaptation worldwide.

2.2 The need for understanding the multifunctionality of sand nourishments

Globally, there is an increasing need to develop strategies for multifunctional climate adaptation. Sandy coasts offer multiple societal functions but are under threat worldwide, with projections indicating that up to half of these coasts will face severe erosion by the end of the century (Vousdoukas et al., 2020b). Meanwhile, the natural capacity of these coasts to accommodate erosion is reduced, as their backshores are heavily occupied by human infrastructure, especially in densely populated areas (Lansu et al., 2024). Hence, adaptation strategies are called for that not only maintain coastal safety but also pursue the additional policy goals provided by sandy coasts, including, for instance, their benefits to biodiversity and cultural practices (IPCC, 2023). Traditionally, coastal flood safety was ensured by hard-engineered coastal infrastructure, such as dams and dikes, but this has shifted towards utilising sand nourishments. For sand nourishments, off-site sand is placed on the beach or shoreface to increase the volume in the coastal profile (Hanley et al., 2014). While compensating for erosion, this volume increase can also provide recreational space and enhance ecological habitats, thus benefitting the policy goals of flood safety, recreation and nature simultaneously (Schipper et al., 2021). Here, 'nature' should be understood broadly, including both ecological and cultural benefits (Díaz et al., 2018a). By supplying ecosystem services for multiple policy goals, sand nourishments can thus promote coastal multifunctionality (Manning et al., 2018).

Recognising these potentially multifunctional effects of sand nourishments, research has developed from focusing on morphology in the 1970s and 1980s (Dean, 2003) towards combining multiple perspectives, including ecological and socio-economic ones, at the beginning of the 21st century (Baptist et al., 2009). Recently, sand nourishments have been increasingly regarded as 'natural solutions' that deliver 'win-wins' for multiple functions (IPCC AR6 Working Group I, 2021). This optimistic multifunctional potential is also underlined in policy literature. For instance, sand nourishments are described as nature-based solutions (i.e., potentially providing multiple benefits) to combat increased climate impacts on coasts (IPCC, 2023).

While the multifunctional potential of sand nourishments has been recognised in policy and research, the academic assessment of how sand nourishments deliver multifunctional outcomes can still be improved. Sand nourishments are increasingly designed with multiple functions in mind (e.g., Rijkswaterstaat, 2020). However, research on sand nourishments and nature-based solutions has not yet fully captured how these interventions can lead to optimal multifunctional outcomes

(Bakhshianlamouki et al., 2023; Key et al., 2022; Kindeberg et al., 2023a). For instance, sand nourishments specifically designed to mitigate coastal erosion can have detrimental, unforeseen implications on the local landscape aesthetics and recreational quality (Chiva et al., 2018), and biodiversity (Speybroeck et al., 2006a; Staudt et al., 2021; Wooldridge et al., 2016). To promote multifunctional climate adaptation by sand nourishment, it is therefore essential to acknowledge the interconnections between their different functions (Schipper et al., 2021). Such knowledge provides insights into potential trade-offs, synergies and unintended consequences of an intervention (Haila and Levins, 1992), which allows coastal planners to better manage and optimise the outcomes of sand nourishments for multifunctional adaptation strategies (Nesshöver et al., 2017).

In this perspective paper, we aim to contribute to the ongoing dialogue about how sand nourishments can promote multifunctional coastal climate adaptation, by identifying key implications for researchers. To this end, we integrated our perspectives as researchers from several Dutch universities and research institutes on the impacts of sand nourishments on coastal geomorphology, socioeconomics, ecology and ecosystem services. Our perspective was informed and shaped by workshops with stakeholders and experts. We iteratively concretised and validated this perspective for international applications through semi-structured literature reviews. We visualised the impacts of sand nourishments on multiple functions in a qualitative model. In internal workshops, we reflected on the integrated effects of sand nourishments from an interdisciplinary system's perspective. As such, we identified three lessons and implications for researchers assessing the multifunctionality of sand nourishments for coastal climate adaptation worldwide.

Below, we firstly describe how we formed our perspective. Secondly, to clarify and communicate our understanding of the system's effects of sand nourishment, we show an overview of their integrated effects visually, after which we describe three key lessons for researchers. These lessons entail our perspective on how researchers can optimise assessing the multifunctional effects of sand nourishments for coastal climate adaptation.

2.3 Integrating and forming perspectives

Our perspective on optimising research on multifunctional sand nourishments was informed by workshops and ongoing dialogues with stakeholders. From 2020 to 2023, we conducted 4 workshops with 12 Dutch stakeholders involved in planning and managing sand nourishments, including policymakers, NGOs and executive organisations from local to national levels. In these workshops, we discussed how sand nourishments can deliver multifunctional climate adaptation and the potential implications for decision-making on sand nourishment design, planning, maintenance and evaluation. These workshops were performed in the context of the C-SCAPE research project, for which we investigate how sand nourishments can contribute to climate adaptation strategies that increase coastal multifunctionality. These discussions informed, enriched and scoped our perspective.

To validate our perspective for wider international application, we performed complementary semi-structured literature reviews (see the Appendix for their detailed outcomes). We refer to these reviews as 'semi-structured' as we searched for literature with a preset approach and subsequently applied expert reflection and interpretation to advance the reviews. This approach allowed us to follow emerging patterns, create shared definitions of variables, and integrate qualitative insights and perspectives from distinct areas of expertise (see Greenhalgh et al., 2018). The preset approach to our literature reviews followed the scoping obtained at the stakeholder workshops. It was structured by our expertise on four features of the coastal system: socioeconomics, geomorphology, ecology and ecosystem services, which together reflect the impacts of nourishment design on coastal multifunctionality. For these four features, we gathered information in the current academic literature on how sand nourishment design can impact the overarching goals of nature, recreation and flood safety by mitigating erosion and adapting coasts to increased climate impacts. These are the most commonly recurring policy goals for which sand nourishments are utilised (Hanson et al., 2002; Schipper et al., 2021). We ensured that the literature represented sand nourishment effects for a wide range of localities. As nourishment design variables, we considered cross-shore placement location, nourishment volume and nourishment frequency, since these variables are most frequently adjusted to generate multifunctionality. We thus did not include all potential design variables, e.g., leaving out sediment size, longitudinal nourishment location, sand colour and locally dependent elements such as the presence of coral reefs or seagrass. As these areas of expertise do not reflect all potentially relevant information on the impacts of nourishment design on coastal multifunctionality, these reviews present a subset of how the entire coastal system is impacted, and can be adjusted and expanded by researchers rooted in other localities and academic disciplines – which we strongly encourage.

To give an overview of the system effects of sand nourishments on coastal multifunctionality, we visualised and conceptualised these literature reviews iteratively into a qualitative model. A qualitative model is ideally suited to visualize and gain insight into a socioecological system's structure, dynamics and drivers. It allowed us to link diverse scientific disciplines, and bring together and evaluate variables that may otherwise be difficult to relate. We iteratively integrated and translated the knowledge of the literature reviews into the model (Fig. 2.1), following the methodology described by Haila & Levins (1992). The model consists of sand nourishment design options as input variables, the system effects as mediating variables and connections, impacts on the policy goals as output variables, and the general causal and directional relations as arrows between those. We included information as a mediating variable if it had a unique effect and was affected by another variable in the model. If two variables had the same relations to others or did not alter the model dynamics uniquely, we considered them as one overarching variable. We connected variables if there was a distinct increasing or decreasing causal relationship between them. If the effects could be both increasing and decreasing, we separated one of the two variables to distinctly show each effect. The arrows thus indicate the direction and general impact of this relationship – not our

view on the desirability of this impact. The effects can accumulate; if a variable with a decreasing effect on the next is increased, the net effect on the latter variable is a stronger decrease. The directions of the relationships reflect a generic pattern (based on literature) that may deviate locally, depending on, e.g., the environmental, policy and management context. This model construction followed the literature reviews and expert assessment iteratively, in which the authors had to be in agreement on the variables and their causal connections.

We performed several workshops among the co-authors during and after the development of literature reviews and the model. In these, we interpreted the system effects of sand nourishments to assess how sand nourishment design impacts nature, flood safety and recreation, and to identify implications for researchers. Classification of the elements in the model and relationships between the different elements were verified during these expert workshops, resulting in the visualization of the multifunctionality of sand nourishments as depicted in Fig. 2.1. We also reflected on how nourishment design could affect the drivers of the individual policy goals, how these drivers interrelate, and what conflicts and synergies result from those. We related this information to the current literature on multifunctional sand nourishments, and we analysed its implications for decision-making to optimise multifunctional sand nourishment design. This culminated in three key lessons for researchers on the multifunctional potential of sand nourishments for coastal climate adaptation worldwide.

2.4 Visualizing the multifunctionality of sand nourishments

Our qualitative model illustrates how sand nourishment design can affect the policy goals of recreation, flood safety and nature from the integrated perspectives of geomorphology, ecology, socioeconomics and ecosystem services (Fig. 2.1). The large number of relationships within and between the features of the coastal system is striking; many variables causally influence other variables in this system, connecting all features of the coastal system and policy goals considered in this study. This highlights how interdisciplinary and multifaceted the impacts of sand nourishments are. For definitions, detailed descriptions and references to literature for the variables and interactions shown, see the Appendix. Below, we highlight some key points of this model.

Geomorphological variables affect the system's outcomes in different ways, affecting both the system's socioeconomic and ecological components diversely (Fig. 2.1). Notably, the system's socioeconomic aspects predominantly influence the ecological components and do so mostly with a decreasing effect. Conversely, fewer effects lead from the system's ecology to its socioeconomics.

Zooming in on the role of distinct variables, at least two variables steer the multifunctional effects of sand nourishments: beach width and how coastal users perceive the area's naturalness. Beach width has the most diverse impact on the other variables and influences all policy goals. The perceived naturalness links the effects of sand nourishments on ecology to the socioeconomics of the coast.

Regarding nourishments' effects on the three policy goals, distinct aspects of the overarching policy goals are affected differently. More precisely, the sunbathing recreationist generally favours a narrower beach to be closer to the seashore, whereas the active recreationist utilises a wider beach for on-land activities (Broer et al., 2011; Cabezas-Rabadán et al., 2019a; Pinto et al., 2020). The presence and dynamics of sandbanks can decrease the swimmer safety in the water (De Zeeuw et al., 2012; Fletemeyer et al., 2018), but can also be considered necessary for water-based recreation such as surfing (Albada et al., 2007; Dally and Osiecki, 2018; Manero and Mach, 2023). While sand nourishments generally increase the flood safety of the coastline, they can decrease the local safety of the users, e.g., due to increased construction work and currents (Fletemeyer et al., 2018). Also, both the occurring biodiversity and how the naturalness of the area is perceived shape the benefits of nourishments to achieving the policy goal of nature, as an interplay between ecology and culture-specific socio-economic elements (Díaz et al., 2018a; Hattam et al., 2015a; Jacobs et al., 2020a; Rodrigues Garcia et al., 2017).

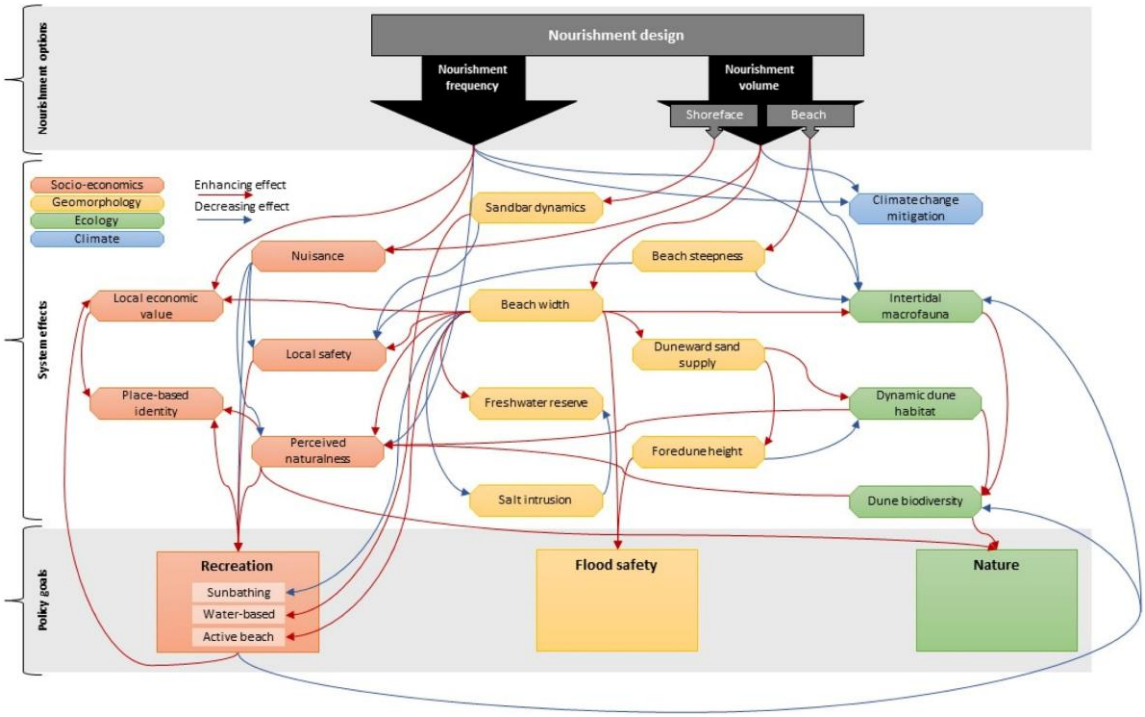

Figure 2.1 Qualitative model illustrating the potential processes and interactions following sand nourishment design. The nourishment design options are depicted at the top of the figure. The effects on the coastal system are displayed in the middle horizontal section. The policy goals most strived for in multifunctional coastal climate adaptation are depicted at the bottom of the figure. Arrows demonstrate increasing or decreasing general causal relations between the variables, which can be enhanced by previous effects.

2.5 Lessons learned to optimize the multifunctionality of sand nourishments

2.5.1 Lesson 1: Conflicts between policy goals require informing political decision-making on priorities

Through our workshops, reviews and discussions, we found that multifunctional sand nourishments are not only a clear win-win for nature, flood safety and other policy goals. This adds nuance to suggestions in academic literature (e.g., Borsje et al., 2011; van der Meulen et al., 2023) that illustrate sand nourishments as such. Synergies between policy goals can indeed occur, but conflicts between them must also be acknowledged. Recently, awareness of such potential conflicts has been growing (Kindeberg et al., 2023b; Schipper et al., 2021). Below, we illustrate these with one example of a potential synergy and two examples of potential conflicts.

A potential win-win design option involves enhancing beach width. This can increase recreational space and contribute to wave attenuation. It can also enhance dune-ward wind-driven sand supply, which, in turn, can lead to more dynamic foredunes, thus supporting more dune biodiversity (G. Baeyens and Martínez, 2008), and increases foredune volume and height, which also benefits flood safety (Liquete et al., 2013a). In contrast, increasing the nourishment volume over its frequency can lead to conflicting outcomes on the policy goals. Increased volume reduces the negative impact on intertidal macrofauna by allowing more recolonization time (van Egmond et al., 2018), thereby reducing the impact on local biodiversity and benefitting the policy goal of nature. However, larger volumes can also lead to restricted beach access and strong currents (De Zeeuw et al., 2012; Fletemeyer et al., 2018), hence reducing recreation potential. Another conflict between policy goals follows from placing a nourishment on the beach, instead of on the shoreface. Beach nourishment can create fewer sand banks and hazardous currents, benefiting the safety and recreational potential for swimmers. However, this placement location severely affects the intertidal macrofauna, reducing the coastal biodiversity and benefits to the policy goal of nature.

Researchers can improve purposeful multifunctionality by informing decision-makers of potential conflicts between policy goals (Fig. 2.2). Since conflicts between policy goals are likely to arise when applying sand nourishments, their multifunctionality can be improved by carefully and explicitly prioritising these goals, which opens up new research directions. Acknowledging the multifunctional effects of sand nourishment is the first step for this. However, conflicts between values are inherent in design choices, sand budgets will shrink, and emissions and costs will rise with increasing climate impacts (Haasnoot et al., 2021; Velpen et al., 2022). Hence, nourishment design becomes increasingly challenged and will entail more sensitive deliberations on which coastal functions to maintain. Such choices constitute political decision-making. Addressing the conflicts and synergies between climate adaptation goals is thus not merely a technical but also an inherently political choice, which should be taken together with decision-makers and society (Doorn, 2019). Even in cases where multifunctional outcomes are considered, not all stakeholders might agree on the

optimal or right prioritisation of the limited resources. Incorporating these perspectives fairly leads to more legitimate, better-informed and supported interventions (Rawls, 1971; Stirling, 2008; Taebi, 2017). Researching such political decisions on sand nourishment design entails, for instance, investigating which stakeholders are affected by implementing sand nourishments as climate adaptation, investigating how they would prioritise the potential outcomes and finding ways to incorporate these fairly (Rawls, 1971). The political nature of choosing the right manner of adaptation is increasingly acknowledged in research on multifunctional assessments (Manning et al., 2018) and nature-based solutions (Melanidis and Hagerman, 2022; Wijsman and Berbés-Blázquez, 2022). Yet, in assessing sand nourishment strategies for coastal climate adaptation specifically, this brings new directions for future research.

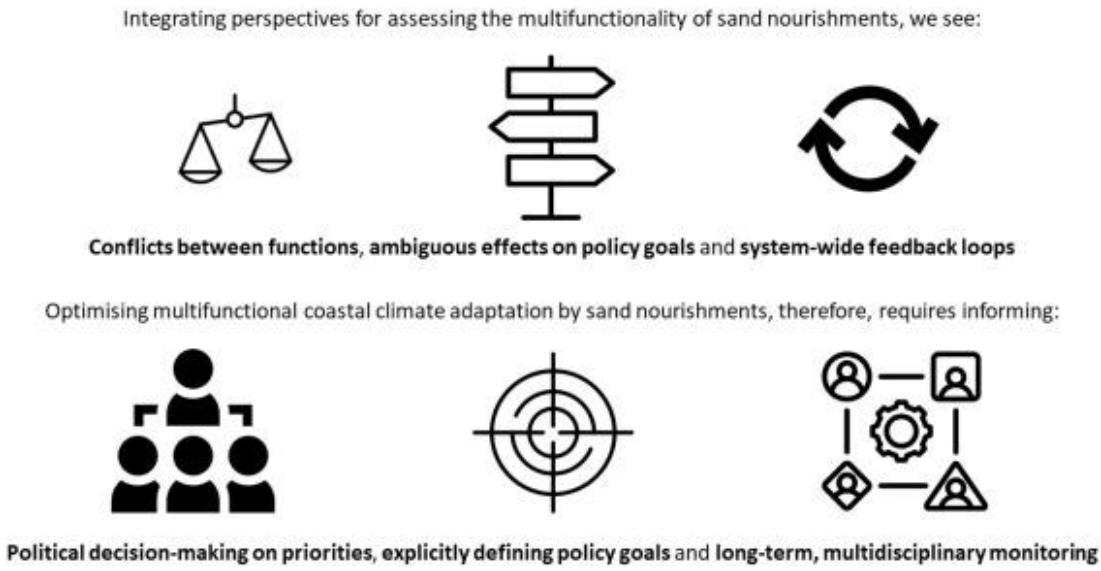

Figure 2.2 Lessons learned for optimising multifunctional coastal climate adaptation by sand nourishment.

2.5.2 Lesson 2: Concreteness is required on otherwise ambiguous functions

The outcomes of multifunctional sand nourishments may be ambiguous if the individual policy goals are not defined precisely. Distinct aspects of the policy goals can conflict, and if these broad goals are not legitimately specified, this can lead to undesired and unfair outcomes (Kaufmann et al., 2022; Thaler et al., 2018). For instance, if nourishments' effects on 'nature' or 'recreation' are measured by specific indicators without acknowledging that these reflect a particular understanding of these goals, the assessment may lead to ambiguity and conflicts with stakeholders (H. H. Geukes et al., 2024). While this gap between broad evaluation categories and specific indicators has been recognised in research on indicator development (Hinkel, 2011), we find that the policy goals are still often regarded as unitary terms when assessing sand nourishments.

We note that distinctive aspects of recreation, safety and nature are affected differently by sand nourishment design. For instance, active recreationists (e.g.,

runners and hikers) may profit from a wider beach, while sunbathing and water-based recreation may be negatively affected by the increased distance to the waterline. Sand nourishment design may also affect distinct aspects of safety differently. A large nourishment volume enhances flood safety, but can also increase beach steepness and currents, decreasing swimmer safety. Also, sand nourishments can harm intertidal macro-fauna and thereby the biodiversity of the beach in the short term. However, in the long term, they may increase the perceived naturalness, as they benefit the dune-ward sand supply, dune dynamics and dune biodiversity.

We stress the need for ongoing dialogue between researchers and decision-makers to formulate explicitly what outcomes could and should be delivered by multifunctional sand nourishments. While open terminology can be useful for gathering stakeholder support and collaboration, it contrasts with the need for concreteness in, for instance, goalsetting, assessing potential impacts, and evaluating and assessing performance (H. H. Geukes et al., 2024). This dichotomy between open terminology and concreteness for assessment has been described as a challenge in defining indicators for nature-based interventions (van Oudenhoven et al., 2018a). Specific indicators have been developed for applying and assessing sand nourishments, but, the 'right' indicator depends on the context it is used and the information available (van Oudenhoven et al., 2018b). Stakeholders might hold diverse perspectives on what achieving a policy goal might entail, and they might thereby disagree on whether an indicator reflects that performance (H. Geukes et al., 2021). Therefore, as nourishments are increasingly utilised to benefit multiple functions and impact more stakeholders, research can improve informed decision-making by developing indicators that explicitly inform on the status of achieving policy goals and the diverse perspectives thereon. Having an explicit view of what constitutes desired outcomes depends on effective and reciprocal communication with legitimate decision-makers (Hanson et al., 2020). In this communication, decision-makers with a democratic mandate may precisely define policy goals, while researchers provide insight into how nourishments may affect those goals. Furthermore, this communication should be iterative, to allow for adapting and adjusting the multifunctional design towards the outcomes that are both desired and feasible. Research that aims to inform optimising the multifunctional outcomes of sand nourishments could for instance investigate the interpretations and variability of these policy goals, as has been proposed for climate adaptation planning (Taebi et al., 2020).

2.5.3 Lesson 3: Monitor system-wide – and keep on doing so

Designing sand nourishments for a policy goal may lead to unforeseen feedback effects. For instance, a nourishment may be designed with a larger beach width to attract additional visitors. These extra visitors may, however, put pressure on biodiversity, by, for instance, harming dune vegetation (Hesp et al., 2011a). This may reduce the area's perceived naturalness, decrease the capacity of the foredunes to bind sediment or alter the identity visitors attach to the place. Such effects may decrease the area's attractiveness, resulting in fewer visitors – a negative feedback

loop for the recreational function of the beach. Nourishments with wider beaches may also increase the recreational potential of the coast, leading to increased identity building with the area and therefore increased societal pressure to sustain this recreational potential. The relationships in the coastal systems can be context-dependent and differ, for instance, in their temporal development, which leads to increased complexity of overseeing and monitoring multifunctional outcomes.

The presence of feedback loops and complex interactions demonstrates that the consequences of nourishment design may be dynamic and non-linear. This puts perspective to studies on multifunctional evaluation of sand nourishments that assume linear and static relations between the drivers of policy goals and their realisation, against which, for instance, the framework of ecosystem services has been cautioned (see, e.g., Norgaard, 2010). A common example involves assuming that the recreational value of the beach increases in line with its physical carrying capacity (e.g., Martino & Amos, 2015; McLachlan et al., 2013). Additionally, our observations align with the growing recognition of nature-based solutions in general as interventions with potentially complex outcomes (Dunlop et al., 2024), and coasts as complex socio-ecological systems (Refulio-Coronado et al., 2021), in which sand nourishments can lead to complex effects (Schipper et al., 2021). We, therefore, encourage further research on the variables that determine this complexity and its outcomes, their development over time, and the quantification of the non-linear outcomes of sand nourishment design. For instance, as has been suggested for decision-making under deep uncertainty, research assessing sand nourishments as adaptive and multifunctional nature-based adapatation strategies could focus on understanding what determines path dependencies (Haasnoot et al., 2013b).

Our findings strengthen the call for long-term, system-wide monitoring of multifunctional sand nourishments (Palinkas et al., 2022). This monitoring can consider temporal variations in the delivery of multifunctionality and reactions to perturbations, relating to potentially complex dynamics (Scheffer, 2010). Additionally, monitoring can focus on key variables that govern the system's multifunctionality – which include beach width and the perceived naturalness, given the policy goals of nature, flood safety and recreation. This monitoring can inform management with means to oversee and control the system's multifunctional outcomes. Moreover, as unforeseen feedback loops may occur, monitoring can consider that unexpected effects may arise, and appropriate resources should be reserved for adapting to these.

2.6 Towards an integrated design to optimize multifunctional sand nourishments

We identified three key implications for researchers to inform the design and evaluation of sand nourishments for multifunctional coastal climate adaptation. Contrary to literature suggesting clear win-win outcomes, we see that conflicts between policy goals also occur, specifically between flood safety and the other policy goals, and between nature and recreation. Moreover, relationships between these goals can be ambiguous, contain feedback loops and lead to conflicts within and

between functions. We, therefore, argue that decision-makers can carefully prioritise between functions and define these explicitly, as the optimal nourishment design depends on what outcomes are desired, being a political decision for society. Our findings also imply that the policy goals are not as clear as they initially may seem. Explicitness, achieved in communication between researchers and decision-makers, is thus required in designing for and evaluating otherwise ambiguous functions. To accommodate for the complex socio-ecological dynamics, system-wide monitoring is required, as a continuous effort. We thus found system behaviour that calls for researchers and decision-makers to carefully define and prioritise the desired nourishment outcomes and to be prepared for complex system behaviour when designing for multifunctional climate adaptation.

In this perspective, we thus call for a holistic approach to assessing multifunctional sand nourishment, urging researchers to consider the need for explicit political prioritisation among policy goals, clear and reciprocal communication to address ambiguous outcomes, ongoing, multidisciplinary monitoring, and research into potential feedback effects and path dependencies. As an invitation to researchers from diverse expertise and localities, we encourage the expansion and adjustment of the proposed model, to optimise sand nourishment design for delivering multifunctional coastal climate adaptation globally.

2.7 Appendix: Indicator–function relationships for sand nourishments

This appendix provides the results of the iterative semi-structured literature reviews. Four sub-chapters present the potential, general impacts of nourishment design (nourishment volume, frequency and cross-shore placement location) on the multifunctionality of the sandy coastal system (the delivery of the policy goals of recreation, flood safety and nature) in the features of the coastal system: geomorphology, socio-economy, ecology and ecosystem services. In these sub-chapters, we describe the effects of adjusting nourishment design on the variables in that feature of the coastal system, we define the variable and describe how these affect other variables in the coastal system. Variables displayed in Figure 1 are printed in bold to facilitate their identification.

2.7.1 Geomorphology

In nourishment design, we consider two key aspects: **nourishment frequency**, referring to how often sand is replenished, and **nourishment volume**, indicating the total quantity of sand placed. The placement of this sand can occur at two cross-shore locations: directly on the shore above the water line, which we term "**beach nourishment**", or onto the shoreface, known as "**shoreface nourishment**." Each of these locations has an increasing impact on **beach width**, although in different manners. Sand that is added to the beach directly enhances **beach steepness** and **beach width**. The beach narrows in the subsequent months to years as sand is redistributed from the initial placement area in both cross-shore and alongshore directions. This redistribution rate is generally the highest during the first large storms and decreases over time (Luijendijk et al., 2017; Seymour et al., 2005). Although more

moderate and gradual, volume placed on the **shoreface** also enhances **beach width** as sand is redistributed from the placement area onshore during calm wave conditions. Additionally, shoreface nourishments can provide a buffer against coastal erosion during storms resulting in decreased sand loss in the region landwards of the nourished area, thereby preserving beach width (M.J.P. van Duin et al., 2004).

Furthermore, widening the beach can lead to greater retention of precipitation and improved groundwater replenishment, ultimately causing an expansion of the **freshwater reserve** (Huizer et al., 2019, 2016). Moreover, sand nourishments may reduce the likelihood of land-surface inundation, seawater infiltration, and **salt intrusion**, so that it also contributes indirectly to the amount and quality of the **freshwater reserve** (Huizer et al., 2019, 2016). Nevertheless, these advantages may be restricted if the nourished sand erodes. Moreover, the impact of nourishment on groundwater behaviour and dynamics near the land-ocean interface varies depending on the specific site and remains challenging to predict due to their inherent complexity and variability.

Wider beaches generally lead to increased **dune-ward sand supply** (Davidson-Arnott and Law, 1996; De Vries et al., 2011). When wind velocity exceeds a certain threshold, it initiates the movement of sediment on the dry beach surface which can then be deposited or captured by vegetation on the foredunes. Thereby, generally, **foredune height** increases.

Another effect of nourishment placement is that **shoreface nourishments** can disrupt autonomous inter-annual **sandbar dynamics** (Ojeda and Ojeda, 2008; Van Der Spek and Elias, 2013). The nourishment can introduce alongshore variability in the position and depth of the outer bar, potentially impacting its cross-shore migration rate and direction. Moreover, Yates et al. (2009) reported exaggerated growth of sand bars after sand nourishment, related to offshore transport of nourishment sand.

The construction of a sand nourishment project results in significant carbon (CO_2) emissions due to the extraction and transportation of sand. If sediments from nearby marine sources are used, the emissions per cubic meter range from 2 to 5 kg of CO_2 (Vidal and Van Oord, 2010). This carbon footprint increases as the distance between the mining site and the beach increases. Additionally, fuel consumption and emission levels are influenced by the type of dredging vessel and the disposal method, such as pumping, spraying or dumping through bottom doors (Wilsoncroft, 2017). Determining and comparing the carbon footprint of sand nourishment projects is complex and site-specific. However, it can be inferred that **greater nourishment volume** and **return frequency** result in higher **greenhouse gas (GHG) emissions**. For a similar total amount of sand, increasing nourishment volume generally causes less emissions than increasing in nourishment frequency.

2.7.2 Socio-economics

The implementation of sand nourishment results in different types of **nuisances**, including beach access restrictions (Seekamp et al., 2019), drifting sand (Karalinas et al., 2020), and the presence of bulldozers, pipelines and other nourishment-related equipment on the beach (Usher, 2021). In this context, the **nourishment frequency**

determines how often beach users are confronted with a nuisance, whereas the **nourishment volume** influences the duration of the nuisance (i.e., more voluminous nourishments generally take longer to complete). Similarly, previous studies have associated nourished beaches and shorefaces with enhanced **local safety** risks and incidents, such as surf accidents (Muller, 2018), unsafe swimming conditions (Fletemeyer et al., 2018), and risks related to steepened beach profiles (**beach steepness**) and local sand subsidence (Fletemeyer et al., 2018; Hamza et al., 2018).

Beyond sustaining tourism and recreation, beaches need to be sufficiently wide to protect shore-front properties and coastal infrastructure from high-water risks (Mullin et al., 2019). Shore-front property values follow an increase in **beach width** (Catma, 2020). An increase in **nourishment frequency** for adapting to increased erosion rates due to sea level increases the local house prices, uplifting the **local economic value**; similarly, house prices drop significantly when nourishment subsidies and frequencies suddenly decrease (McNamara et al., 2015). Sand nourishments constitute an essential financial resource to the coastal economy at large and play into the **local economic value** by allowing for increased **recreational potential** (Houston, 2021; Klein and Osleeb, 2010).

The **local economic value** is fundamental to communal thriving and thereby to the local **place-based identity** (Akerlof and Kranton, 2010; Fiorentino et al., 2024). However, it should be noted that an increase in economic value may also lead to a decrease in the place-based identity of some, e.g., increased prices may force out previous inhabitants and visitors, which some critical studies have labelled as the 'green gentrification' effect of nature-based adaptation (Bauer, 2023) – but which have not been recorded for sand nourishments, yet.

Beach visitors and coastal inhabitants place significant value on their sense of place or their **place-based identity** (Blake, 1974; Carter et al., 2007). This identity is, amongst others, shaped by local culture, landscape aesthetics, the natural environment and the local coastal community(Carter et al., 2007; Stedman, 2002), which can be drastically altered by sand nourishment (Shivlani et al., 2003). Such identities are deeply formed by peoples' environment, how they behave in it and how they interact in it; these identities are shaped by continuity in their **perceived naturalness** of the place and the physical (e.g., **recreational**) **activities** they perform in it (Blake, 1974).

This **perceived naturalness** is generally increased by an increase in ecological elements, such as **biodiversity** (Cardinale et al., 2012). Ecological and perceived naturalness do generally correlate but can diverge (Lamb and Purcell, 1990). Their relation depends on people's perception of what nature is and should be, as a cultural or cognitive concept, which differs between people (Jacobs et al., 2020b; Van Den Berg et al., 1998). This perception of nature influences the actual benefits that nature brings, as, for instance, actual species richness contributes less to psychological human well-being than the perceived species richness or natural quality (Dallimer et al., 2012) and judgements of whether a policy goal is actually achieved (Geukes et al., 2021b). The perceived naturalness of a coast can decrease with increased displays of human interventions (i.e., the '**nuisance**' of nourishments), as seeing demonstrations

of human interventions in a coastal landscape can lead to it being considered unnatural (Gesing, 2019).

2.7.3 Ecology

Upscaling **nourishment frequency** or **volume on the beach** decreases the presence of **intertidal macrofauna**. In the intertidal area, macrofauna live within the top part of the sediment. Sudden deposits of large **nourishment volumes** that exceed the ability of macrofauna to burrow upward have fatal consequences. As a result, population numbers and species diversity are minimized on freshly nourished beaches (Schlacher et al., 2012; Speybroeck et al., 2006b), especially if nourishment layers exceed 1 meter . Over time, adults and juveniles from adjacent, unnourished areas migrate and larvae recolonize the nourished beach stretch, replenishing the local species pool (Leewis et al., 2012). Some intertidal macrofauna species' richness and abundance will take about one year to recover to their pre-nourishment levels, whereas other species did not after 1.5 years (Leewis et al., 2012). Thus, with increased **nourishment frequency**, species with a slower recovery rate will likely be lost, leading to a shift in the local population pool. **Beach width**, however, could enhance **intertidal macrofauna**, with wider beaches supporting species richness (Cardoso et al., 2012; Janssen and Mulder, 2005; Mclachlan and Dorvlo, 2007). Lastly, increased **beach steepness** due to nourishments might further decrease intertidal macrofauna communities, whose composition (Leewis et al., 2012; McLachlan and Dorvlo, 2005) and zonation (Cardoso et al., 2012) is, among others, strongly driven by local morphological conditions. For example, increased beach steepness is associated with a decrease in species richness and abundance (Cardoso et al., 2012), and can even inhibit the establishment of macrofauna (McLachlan et al., 1993).

Local **dune biodiversity** is generally negatively affected by increases in sand nourishment volume and frequency. **Dune biodiversity**, in our case, refers to the local pool of flora and all trophic levels of fauna. Naturally occurring macrofauna diversity is a key driver of beach secondary production, with higher diversity exponentially supporting higher secondary production rates (Rodil and Lastra, 2022). For example, beach macrofauna presents a major food source for secondary consumers (Rodil & Lastra, 2022), e.g. shore birds. If the abundance of **intertidal macrofauna** decreases, **dune biodiversity** generally declines as well. This could trigger trophic cascades with far-reaching implications for coastal food webs (Rodil & Lastra, 2022) and, thus, **dune biodiversity**.

The beach-dune bio-geomorphology is another factor influenced by nourishment. Specifically, nourishment can enhance the **dynamic dune habitat**. Here, we define **dynamic dune habitat** as the amount of sand-sharing capacity between the beach and the foredune system (Geelen et al., 2015; Martínez et al., 2008). Sand-sharing capacity depends on the presence of sand in this system and on its ability to be mobilised. First, sand accumulation requires **dune-ward sand supply**. This allows the development of incipient foredunes through an interplay between aeolian sand movement and sediment stabilization by plants (Bonte et al., 2021; Feagin et al., 2015; Hesp et al., 2011b; Martínez et al., 2008; van Puijenbroek et al., 2017). Incipient

foredunes are often short-lived (Hesp and Martínez, 2007), only temporarily stabilising sand. However, dune grasses on incipient dunes may accumulate enough sand to outgrow overwash levels and form established foredunes (Feagin et al., 2015; Hesp et al., 2011; Hesp & Martinez, 2007). Second, **dynamic dune habitats** require a balance between vegetated and bare surfaces (Bonte et al., 2021). As discussed by Hesp & Martinez (2007), enhanced **dune-ward sand supply** contributes to the presence of bare sandy areas and therefore ensures **dynamic foredune areas**. Both incipient- and established mobile foredunes provide habitat for an assemblage of specialized beach and dune flora (Feagin et al., 2015) and fauna (G Baeyens and Martínez, 2008). Thus, through the enhancing effect of **dune-ward sand supply** on **dynamic dune habitat, dune biodiversity** can be positively influenced.

Considering the effect socio-economics will likely have in the presented context, we find that once nourishment measures succeed in enhancing the policy goal **recreation**, the local **dune biodiversity** and **intertidal macrofauna** are likely to decrease due to a rise in undesirable cumulative effects including, (i) trampling of dunes and vegetation, leading to plant disruption (Hesp et al., 2011), and (enhanced) erosion (e.g., Bonte et al., 2021); (ii) beach clean-ups, destroying incipient foredunes, loss of habitat by wrack removal, killing of intertidal macrofauna by use of vehicles (Schlacher et al., 2012); (iii) habitat fragmentation caused by on-beach facilities like restaurants or beach huts (Jackson and Nordstrom, 2011).

2.7.4 Ecosystem Services

We define coastal ecosystem services as the benefits humans derive from the habitat, biological or system properties and processes of the coastal ecosystem (following Costanza et al. (1997). As sand nourishments alter these systems, they will affect the delivery of the coastal ecosystem services accordingly (De Schipper et al., 2021). We investigated the provisioning of ecosystem services that benefitted the policy goals of recreation, safety and nature. Note that ecosystem service information should be adapted to the decision-making process it is required. For instance, when advocating for maintaining natural coastal areas, decision-makers generally require broad information on the potential natural and recreational value of sand nourishments. However, when evaluating the project, they require concrete information that reflects a much narrower understanding of the advocated policy goal, e.g., on the occurrence of specific species or visitor numbers per recreational activity. For communication to be effective, this concretisation should be in line with the policy goals as perceived by the decision-makers (Geukes et al., 2024b).

2.7.5 Recreation

The approval and preference for **recreational activities** as coastal ecosystem services are strongly influenced by individuals' **place-based identity** (Akerlof and Kranton, 2010; Hynes et al., 2018). Also, people's experiences of the area's natural elements, compared to their expectations of what should be present, shape their views on the suitability of the area for recreation. As a result, the value of recreational coastal ecosystem services depends on the area's **perceived naturalness** (Blake, 1974;

Brambilla and Ronchi, 2020; Usher, 2021) and varies substantially across cultural differences between the coastal users (Hynes et al., 2018).

A prerequisite for performing **recreational activities** is **local safety** (McLachlan et al., 2013). This safety affects varying recreational activities differently. The activities involved in nourishing the beach (**nuisance**) can create local hazardous circumstances, decreasing **local safety** on the beach (Fletemeyer et al., 2018). Along the shore, the presence of **dynamic sandbanks** and a variable coastline can decrease **local safety** by creating strong currents that may cause drownings (De Zeeuw et al., 2012). This decreases the potential for '**sunbathing**' recreationists, who prefer easy and safe access to the waterfront. In contrast, **sandbank dynamics** can increase the potential for **water-based recreation** like surf sports, as, for instance, in Florida, an 'elbow' shaped nourishment was built that dynamically improved surfing conditions (Albada et al., 2007).

Recreational activities are differently affected by the **width of the beach**. For **sunbathing** and **water-based recreationists**, beaches from at least 15 to around 100 meters are considered optimal, studies in the Netherlands, Portugal and Spain found, as there should be some physical carrying capacity for the beach users, but they have to walk to the seashore – whereas **active recreation** such as hiking, running and dog walking benefit from a wider beach (Broer et al., 2011; Cabezas-Rabadán et al., 2019b; Pinto et al., 2020). This points to winners, losers and trade-offs associated with the expansion of the coastal strip and suggests that the effects of nourishments are location-specific, depending on which type of recreational activities are dominant on the beach in question.

As **beach width** and the **shoreface (sandbank) dynamics** affect the delivery of the coastal ecosystem service of recreation differently, we thus differentiate between different **types of recreation** delivered by different sand nourishments as coastal ecosystem services, in line with Lamb et al. (2014) and Van Oudenhoven et al. (2018). In South Florida, the Gold Coast of Australia and in Southern Sweden, it was indeed found that the recreational appreciation of sand nourishments depended on the type of beach user, which was acknowledged by decision-makers on sand nourishments in the Netherlands (Dhakal et al., 2016; Shivlani et al., 2003; van Oudenhoven et al., 2018a; Van Well et al., 2023).

2.7.6 Flood safety

Coastal safety consists of three components: preventing floods from occurring; if they are to occur, reducing society's vulnerability to them; and increasing the adaptability or resilience of society to such events (Correljé and Broekhans, 2015; Seddon et al., 2020). Coastal safety as an ecosystem service delivered by sandy beaches and affected by nourishment mainly relates to flood prevention (**flood safety**). Nourishments increase the geomorphological capacity of the sandy shores to combat the increased exposure due to sea level rise (Liquete et al., 2013), as increased **beach width** and **foredune height and volume** both increase the flood safety of the hinterland (Davidson-Arnott, 2005; de Winter and Ruessink, 2017; Hanson and Beach, 2003; Hattam et al., 2015b; Liquete et al., 2013b).

2.7.7 Nature

The policy goal of **nature** as an ecosystem service includes both ecological and cultural benefits to people (Díaz et al., 2018b). In sand nourishments, both these aspects of nature were reflected in policy goals that aimed to increase 'nature', as these goals focus both on expanding space predominantly meant for recreation and on enhancing benefits to biodiversity (Geukes et al., 2024; Van Oudenhoven et al., 2018).

An increase in **biodiversity** benefits the policy goal of nature in two ways. Regarding the ecosystem services of sandy shores that relate to nature as a policy goal, nature is often valued instrumentally. In this case, it is valued because of the biophysical functions the coastal ecosystem fulfils, such as primary production, maintaining food web dynamics, nutrient cycling, habitat provisioning, carbon storage and maintaining genetic variation (Hattam et al., 2015). These functions are labelled as **biodiversity**. Additionally, it is generally argued that all natural elements have an intrinsic value to people, which is oftentimes reflected in policy goals (Curry, 2011). So, in this manner, increasing **biodiversity** can also directly benefit the policy goal of nature.

Enhancing **nature** as an ecosystem service can also be a policy goal because of relational values, i.e., because it is required for social interactions that are valued by society (Chan et al., 2018; Schröter et al., 2020). This valuation of nature can include cultural ecosystem services of aesthetics, spiritual experience and place attachment that are related to the natural environment (Hattam et al., 2015). These types of valuation of coastal nature depend on the **perceived naturalness** of the area, which can have cognitive, cultural, spiritual or symbolic meanings that shape people's view of how this natural environment should be (Jacobs et al., 2020a; Rodrigues Garcia et al., 2017).

3 Simulating decadal cross-shore dynamics at nourished coasts with Crocodile

This chapter introduces and validates Crocodile, a novel behavioural diffusion type cross-shore model designed to simulate nourishment evolution over decades. It fills a methodological gap between short-term process-based models and long-term empirical approaches, with a focus on predicting indicators useful to evaluating coastal functions such as beach width, coastal volume, and shoreline change. This model forms the basis for the morphologic modelling in the rest of the thesis.

This chapter is published as:

Kettler, Tosca, Matthieu de Schipper, and Arjen Luijendijk. "Simulating decadal cross-shore dynamics at nourished coasts with Crocodile." Coastal Engineering 190 (2024): 104491.

3.1 Abstract

Projections of high rates of sea level rise have stimulated proposals for adaptation strategies with increasingly high nourishment volumes along sandy beaches. An underlying assumption is that coastal profiles respond rapidly to nourishments by redistributing sediments towards a (new) equilibrium shape. However, this perception may not be valid when high volumes of nourishment are applied, as the profile shape may then undergo significant deformation. Current state-of-the-art modelling techniques often concentrate on a single spatio-temporal scale, either lacking the necessary temporal horizon or failing to provide the required level of cross-shore detail. This article introduces Crocodile, a diffusion based cross-shore model designed to bridge the gap between short- and long-term nourishment modelling. The model simulates the effects of nourishment strategies on coastal volume, coastline position and beach width over a decadal timeframe. It incorporates different elements which compute cross-shore diffusion, sediment exchange with the dune and alongshore sediment losses. To test the model performance, a series of idealized nourishment scenarios are examined, along with three case studies along the Dutch coast with different nourishment strategies over the past few decades. The modelled coastal volume, shoreline position and beach width strongly resemble the observations with only a 12% overestimation in profile volume and 13% underestimation in beach width. Averaged over selected periods of nourishment, trends and trend reversals between different strategies are well replicated with slight overestimation for coastal volume trends by $1.5\,m^3/m/yr$ (10%), while beach width trends are underestimated by $0.2\,m/yr$ (15%). Given that the added nourishment

volumes are typically in the order of $100\ m^3/\mathrm{m}$, these model errors are considered sufficiently low to conclude that Crocodile effectively simulates variations in coastal volume, coastline position and beach width over a decadal timeframe in response to different nourishment strategies. Therefore, Crocodile can facilitate the evaluation of future nourishment strategies.

3.2 Introduction

At a time of accelerating sea level rise (IPCC AR6 Working Group I, 2021), growing coastal populations (IPCC AR6 Working Group II, 2022), and rising concerns about coastal squeeze (Doody, 2013), sustainable coastal management is one of the most important issues facing the world. One such solution is sand nourishment, which involves the placement of sand on the foreshore, beach, or dune to build up or maintain the coastal sediment budget as well as the position of the shoreline. Under the force of waves, winds and currents, the sand is dispersed in alongshore and cross-shore directions (M. J.P. van Duin et al., 2004). Over the coming decades, the anticipated acceleration of sea level rise is likely to shorten the lifespan of individual nourishments (Haasnoot et al., 2020) prompting proposals for adaptation strategies that involve higher nourishment volumes. These adaptation strategies involve various design considerations, such as the amount of sand volume applied, the expected frequency of nourishment, and the location of the nourishment along the cross-shore profile. The rationale behind these design choices follows from the accessibility of materials and knowledge and the objectives of coastal management, which may involve addressing coastal erosion, preserving a particular beach width, or stabilizing the coastline (Brand et al., 2022; Cooke et al., 2012; Defeo et al., 2009; Hanson et al., 2002). These objectives can be guided or evaluated by coastal state indicators such as coastline position, beach width and profile volume change, as they are closely linked to issues of coastal safety (e.g., Van Koningsveld and Mulder, 2004), ecology (e.g.,Schooler et al., 2019), and socioeconomics (e.g., Cabezas-Rabadán et al., 2019; McLachlan et al., 2013; Valdemoro and Jiménez, 2006). In the design phase of nourishment programs, it is therefore desirable to have prior knowledge of the corresponding response of these coastal state indicators to evaluate the effectiveness of nourishment programs. With this study, we aim to fulfil this need. We develop a tool to examine the decadal-scale response of coastal indicators to nourishment programs and test its performance at case study locations along the central Dutch coast.

3.2.1 Temporal evolution of nourishment across different timescales

An increasing number of nourishments has been executed and has been described in the scientific literature (De Schipper et al., 2014; Hamm et al., 2002; Luo et al., 2016; Stronkhorst et al., 2018; Valverde et al., 1999). However, quantifying the impacts of nourishment schemes is yet challenging because of the complexity and variability of the physical processes involved, acting within a broad spatiotemporal range. Consequently, most traditional methods that compute sediment transport and morphological behaviour in the coastal zone focus on a specific spatiotemporal scale and do not capture the broad temporal spectrum (~years-decades) required to offer

a holistic view on the effects of design choices in nourishment schemes. To illustrate the nature of the uncertain relation between coastal state indicators and nourishment, we examine it from multiple time perspectives.

Short-term (days to years) and small-scale (0.1-1 km) processes can be exemplified by the immediate impacts of storms on a nourished coastal profile, as well as the evolution of bays and lagoons that may be present. Directly after the placement of a beach nourishment, the beach is widened, and the volume of the coastal profile is increased. This sand is rapidly redistributed from the beach to the nearshore when storm frequency is high. This can result in a notable decrease in beach width and shoreline retreat over a short period of time. Despite of this redistribution, the sand often remains in the active profile region over this timeframe. In the case of shoreface nourishments, these short-term effects are typically less visible.

On the medium-term (months to years), changes in the local sediment budget typically become visible in the behaviour of profile volume, beach width and coastline. This sediment budget includes sediment supply and losses via gradients in alongshore transport by wind, waves, and tidal currents. A positive sediment budget is generally correlated to an increasing beach width and seaward shoreline migration, and a negative to the opposite. Nourishment adds to the total sediment budget and thereby impacts these trends. For example, a shoreline that was previously retreating may become stabilized. On these timescales, an increase in dune growth may also become noticeable. The impacts of nourishments decrease over time, as the deformation of the nourishment body occurs. Over sufficiently long temporal and spatial scales, the nourishment is diffused in cross-shore and alongshore directions. The rate and extent of this diffusion depend on the scale of the nourishment relative to its environment and the hydrodynamic climate. Diffusion is generally stronger when the vertical amplitude of the perturbation is higher, its horizontal wavelength is shorter, and under a highly energetic wave climate (Hamm et al., 2002).

A broad set of complex physics-based models has been applied to study nourishment impacts on the short and medium timescales, for example, XBeach (e.g., Baykal et al., 2017; Huisman et al., 2019), Unibest-TC (e.g., van Duin et al., 2004), Delft-3D (e.g., Giardino et al., 2010) and Cshore (e.g., Kalligeris et al., 2020)These models describe elementary basic processes of flow, waves, and sediment response and have been applied to study how the placement of a single nourishment changes topography, which in turn affects hydrodynamics and thereby morphological evolution. Recently, the timescales that can be reached with these models have increased, and examples exist of morphological forecasts spanning multiple years (Luijendijk et al., 2019; Ranasinghe, 2016a). However, their practicability to assess the decadal impacts of repeated nourishment is yet limited as extensive calibration is required. This calibration leads to site-specific parameter settings and process formulations, which in turn can result in inaccurate predictions beyond the calibration/validation period (Montaño et al., 2020; Ranasinghe, 2020). Additionally, the computational effort of process-based approaches is considerably large, further limiting their practicability to test multiple nourishment designs.

Long-term (decades to millennia) coastal behaviour is generally related to a large scale (~10-100 km). It is often described as the gradual adjustment of an entire coastal system to an equilibrium that matches the total sediment budget and (changed) climatic circumstances (Bruun, 1962, 1954). This includes relative sea level variation and changes in storm frequency and intensity. Nourishment programs commonly adopt an equilibrium perspective, wherein the focus lies on the long-term, large-scale viewpoint. In this perspective, the analysis of a nourishment strategy primarily considers the sediment volume added, irrespective of the specific placement location (e.g., McCarroll et al., 2021). Coastal profiles are herein assumed to respond to nourishment by rapid equilibration to a new shape after sand nourishment, suggesting a direct correlation between the amount of nourishment applied, the profile volume, and the coastline. Thus, any short- and medium-term impacts of nourishment on coastal indicators are not covered by this approach. However, when large volumes of sand are added to account for the anticipated acceleration of sea level rise, the shape of the profile can deform substantially. In such instances, equilibrium-type approaches may provide erroneous information regarding the evolution of the shoreline and offer no insight into the beach width variability.

3.2.2 Problem statement

Understanding the time-varying deformation of the coastal profile is essential for gaining insights into coastal state indicators that are closely associated with nourishment objectives. Such insights can inform strategic decisions pertaining to nourishment projects, including the appropriate volume of sediment to be applied, the expected frequency of nourishment cycles, and the optimal cross-shore location. These considerations encompass not only the direct impacts immediately following nourishment placement but also the long-lasting effects that persist over multiple decades. Nevertheless, currently used modelling techniques fail to effectively integrate the necessary spatial resolution with the required decadal time horizon for conducting such an analysis. Process-based approaches are yet impractical due to demanding computational efforts and extensive calibration needs, while equilibrium-type approaches miss the required level of detail. What we seek is a middle ground, a method that bridges the gap between short- and long-term nourishment modelling. How can we effectively address this gap and comprehend the combined influence of multiple nourishment interventions in a slowly changing environment?

3.2.3 Bridging the gap between short and long-term nourishment modelling

The answer may lie in an alternative viewpoint that has yet been little explored in the context of nourishment programmes. Given the ever-changing nature of boundary conditions and significant profile deformation due to nourishment on shorter timescales, it becomes evident that a state of static equilibrium is never truly attained in practical scenarios. Instead, a continuous and gradual adaptation takes place towards a 'dynamic equilibrium'. This 'dynamic equilibrium' then refers to a normative average morphology that matches the instantaneous sediment budget and climatologic circumstances and can serve as a reference around which the actual morphology fluctuates. The duration of this adaptation depends on profile depth,

ranging from hours in the vicinity of the waterline (e.g., Lippmann et al., 1989) to millennia in the proximity of the inner shelf (e.g., Stive and de Vriend, 1995). To what extent the average morphology resembles a dynamic equilibrium relies on this timescale of morphological response with respect to the timescale and magnitude of the changing boundary conditions. In this context, nourishment acts as one such dynamic boundary condition.

A limited set of models have been built upon this philosophy, that the introduction of a nourishment essentially constitutes a perturbation to a coast, having a particular dynamic state (Chen and Dodd, 2021, 2019; Coelho et al., 2017; Marinho et al., 2017; Stive et al., 1991). Over sufficiently long temporal and spatial scales, this perturbation is diffused in cross-shore and alongshore directions. Such an approach was developed by Stive et al. (1991), who used a generic combination of physical inductive concepts and a detailed process-based model to simulate cross-shore dynamics resulting from repetitive beach- and nearshore nourishment. Work building forth on this approach was mostly data-driven (as by Baramiya et al., 2019; Capobianco et al., 1994; Lavrentiev, 2015), resulting in parameter settings and process formulations that limit the forecast horizon to a single nourishment cycle in a specific setting. Examples of other diffusion-type applications are the work of (Chen and Dodd, 2021, 2019), wherein the nourishment dispersion has been calculated based on physics-based equations including wave, tide, and sediment dynamics, or a data-driven sediment-budgeting method applied to a nourishment (Marinho et al., 2017).

To establish a foundation for our study, we build forth on the inductive assumptions on dynamic profile response proposed by Stive et al. (1991). With the execution of more nourishments and the availability of bathymetric profile datasets spanning multiple decades and various sites, there is now an opportunity to combine Stive's methodology with the latest knowledge on long-term nourishment behaviour in a predictive model. To this end, we are introducing a diffusion-type behavioural model named Crocodile (**Cro**ss-shore **Co**astal **Di**ffusion **L**ong-term **E**volution model).

The novelty in our approach is the specification and quantification of the model terms and parameters through the use of inductive ideas inferred from observed or expected behaviour, on the grounds of long-term records of bed level data at nourished coasts. With Crocodile, we present a tool that is simple, robust and computationally efficient, designed explicitly to examine the decadal-scale behaviour of coastal indicators previously used to guide or evaluate nourishment programmes, i.e., coastal volume, coastline position (Brand et al., 2022; Hanson et al., 2002) and beach width (Cabezas-Rabadán et al., 2019b; McLachlan et al., 2013; Valdemoro and Jiménez, 2006).

3.3 Paper outline

The paper starts by presenting the theoretical frame of reference for Crocodile (2.1), followed by a model description that details its specific design and implementation (2.2). In this paper, Crocodile is applied on the central Holland coast. We included a description of the relevant morphological and hydrodynamical details of the region and the local nourishment policy (3.1). The model set-up for all simulations is

described (3.2), along with varied parameter settings per simulation (3.3). Crocodile is then applied to simulate idealized nourishment strategies (4.1) and to hindcast cross-shore coastal evolution at case study locations with varying nourishment histories (4.2) over a couple of decades. Finally, we discuss the total performance of Crocodile in different cases (4.3) and discuss strengths, limits, and potential applications (5). Finally, the paper concludes (6) by evaluating Crocodile's ability to simulate the temporal evolution of coastal indicators under various nourishment programmes.

3.4 Methods

3.4.1 Model philosophy

The present modelling framework builds forth on principles proposed by Stive et al. (1991), wherein the reshaping of the cross-shore profile depend on the vertical magnitude of perturbations to the long-term equilibrium profile as well as the hydrodynamic climate. The novelty in our approach lies in the definition and quantification of the model terms and parameters based on inductive insights as well as decadal records of bathymetry and topography along nourished coasts. Crocodile computes the evolution of the cross-shore profile shape which is then translated to the coastal indicators of interest. The model is behaviour-oriented, meaning that the model components are formulated to optimally simulate the evolution of these indicators without aiming to resolve the underlying physics other than mass-conservation.

We consider sandy beaches with lengths in the order of kilometres, wherein the alongshore variation of the coastal profile and hydrodynamic processes can be neglected. As we consider the nourishment as a profile perturbation and assume a 'dynamic equilibrium' background profile, any autonomous (nourishment-independent) profile development affecting the profile shape is not resolved. This means that cycles of storm and recovery, cyclic bar behaviour and the passage of alongshore shoreline undulations are not included.

3.4.2 Model description

In this section, we present a summary of the mathematical equations that comprise the model. Every timestep t, Crocodile computes the 'instantaneous' bed level $Z\ (x,t)$ being the time-dependent profile approaching a dynamic equilibrium profile

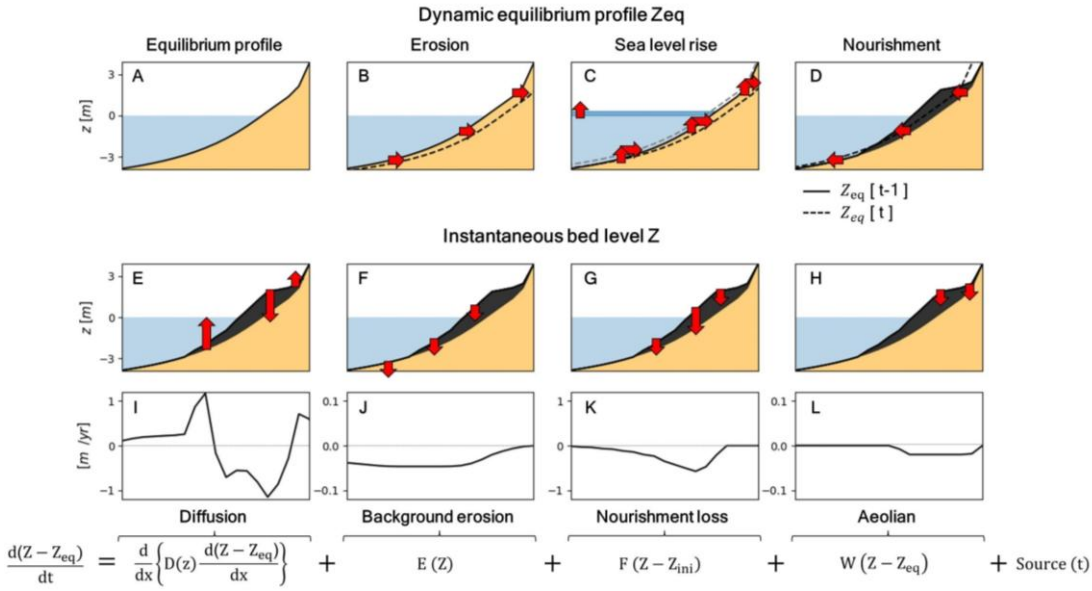

Figure 3.1 Schematic overview of Crocodile. Upper row: Translation of the dynamic equilibrium profile (A) as a response to erosion (B), sea level rise (C) and nourishment (D). Red arrows indicate the direction of translation. Middle row: Instantaneous bed level response to nourishment per model subcomponents diffusion (E), background erosion by existing alongshore gradients in transport (F), enhanced alongshore losses at the nourishment (G) and aeolian losses (H). Direction and magnitude of bed level change are indicated by red arrows.

Lower row: Magnitude of model subcomponents as function of the cross-shore position: diffusion (I), background erosion (J), nourishment erosion (K) and aeolian (L) directly after nourishment implementation. Note the different scales.

$Z_{eq}\ (x,t)$. The horizontal coordinate system x is defined positively offshore from the landward model boundary. Two vertical coordinate systems denoted as z and z' are utilized, which are both defined positively upwards from the mean water level (MWL) but originated from different points. While z refers to a vertical position with reference to $MWL(t=0)$, z' is anchored at $MWL(t)$. Both Z and Z_{eq} are defined within the z coordinate system. Changes in the coastal system (e.g., sea level rise, alongshore transport gradients, or the implementation of nourishments) lead to horizontal and vertical translation of $Z_{eq}\ (x,t)$ as given by a sediment volume balance (see Fig. 1a-d). The translation component of sea level rise is modelled based on the principles established by Bruun (1954, 1962), whereby the equilibrium profile is raised by the change in sea level and shifted onshore to balance total sediment volume.

At its core, the model computes the rate and extent of sediment dispersion as the sum of five components:

$$\frac{\mathrm{d}(\mathrm{Z}-\mathrm{Z_{eq}})}{\mathrm{dt}} = \frac{\mathrm{d}}{\mathrm{dx}}\left\{\mathrm{D(z')}\frac{\mathrm{d}(\mathrm{Z}-\mathrm{Z_{eq}})}{\mathrm{dx}}\right\} + \varepsilon_{\mathrm{D}}(\mathrm{z}) + \mathrm{E(z')} + \mathrm{F}(\mathrm{Z}-\mathrm{Z_{ini}}) + \mathrm{W}\left(\mathrm{Z}-\mathrm{Z_{eq}}\right) + \mathrm{Source(z',t)} \quad (3.1)$$

Cross-shore diffusion

The first and second RHS components of Eq. *(3.1* describe cross-shore diffusion. The first term is a diffusion term that redistributes any perturbation from Z_{eq} in time and space. It resembles the diffusion term by Stive et al. (1991), and similar diffusion terms have been incorporated in other cross-shore modelling approaches (e.g., Baramiya et al., 2019; Capobianco et al., 1994; Davidson, 2021; Lavrentiev, 2015). It includes the depth-dependent coefficient $D(z')$ (with the physical dimension of m^2/day), which represents the average sediment redistribution capacity along the profile and thereby regulates the morphological timescale of response (Fig. 3.2). Stive et al. (1991) originally derived the shape and magnitude of $D(z')$ by fitting $D(z')$ to approximate nourished and unnourished runs using a process-based profile model (Unibest-TC), covering timeframes ranging from seasons to decades. In Crocodile, we deviate from this approach by adding a formulation for the subaerial losses and by connecting the shape of the diffusivity profile to the local wave climate. As a result, the submerged part of $D(z')$ closely resembles Stive et al. (1991). The shape of the diffusivity profile $D(z')$ is prescribe ed as a function of boundary conditions and the local hydrodynamic climate, facilitating easy implementation of locations with different hydrodynamic characteristics in Crocodile.

We consider the following morphological zones in the cross-shore profile for defining $D(z')$:

The upper part of the active zone (Z1 in Fig. 3.2C), extending from the low waterline Z_{LW} to the maximum elevation reached by wave runup over a decadal timeframe. This zone includes the intertidal area and the subaerial beach, being only recurrently mobilized by wave runup. In this zone, we assume the morphological timescale of diffusion to linearly depend on the frequency that an elevation is reached by wave runup. To estimate this frequency, we adopt a linear relation defined by Ruggiero et al. (1997) between exceedance elevation for runup maxima $R_{2\%}$ and offshore significant wave height H_s:

$$R_{2\%} = \begin{cases} 0 & for\ H_s < 0.44 \\ 0.5\,H_s - 0.22 & for\ H_s \geq 0.44 \end{cases} \quad (3.2)$$

With this relation, we translate a multi-decadal record of the sum of the offshore water level WL (including tide and surge) and offshore significant wave height to a survival function (i.e., $1 - Cumulative\ Distribution\ Function$, as visualized in Fig. 3.2A) that represents the shape of $D(z')$ in this upper zone Z1:

$$\mathrm{D}(z') = D_{MAX} * \Big(\big(1 - CDF(WL + R_{2\%})\big) + Z_{LW}\Big)\ for\ (Z_{LW} - 1) < \mathrm{z}' \tag{3.3}$$

Consequently, the diffusion coefficient in the highest zone Z1 is maximum (D_{MAX}) around the (average) low waterline Z_{LW} and decreases to almost zero at the elevation of the extreme total water level. Note that the zone extends 1m below Z_{LW} to include all area exceeding extreme low water levels.

A zone of constant maximum sediment diffusivity (Z2 in Fig. 3.2C) is applied between the low waterline Z_{LW} and the edge of the surf zone during average wave conditions Z_E. This roughly corresponds to the zone of maximum sediment transport identified by de Vriend (1992):

$$\mathrm{D}(z') = D_{MAX}\ for\ Z_E < \mathrm{z}' < (\mathrm{Z_{LW}} - 1)\mathrm{D}(z') \tag{3.4}$$

The lower part of the active zone or surf zone (Z3 in Fig. 3.2C) where sediment is intermittently mobilized depending on the hydrodynamic conditions. This zone stretches from the average edge of the surf zone Z_E to depth of closure Z_{DOC}. In this zone, we assume wave height to be the primary controlling parameter for the variations in sediment flux over depth (Battjes et al., 1991; Chen, 2021). We assume the morphological timescale at profile elevation Z here to linearly depend on the water depth of wave breaking $Z_B = -\gamma \mathrm{Z}$, whereby γ is set 0.44 (Miche, 1954). To this end, a multi-decadal record survival function of wave height is translated to a survival function and $D(z')$ (as visualized in Fig. 3.2B), and $D(z')$ is calculated as:

$$\mathrm{D}(z) = D_{MAX} * \Big(\big(1 - CDF(H_B)\big) + Z_E\Big)\ for\ Z_{DOC} < \mathrm{z}' < Z_E \tag{3.5}$$

Consequently, the diffusion coefficient is large in the active zone (zone of maximum wave breaking) and decreases to almost zero at the shoreface (Fig. 3.2B).

The lower part of the shoreface (Z4 in Fig. 3.2C), which is dominated by wave shoaling and tidal currents which is only active at decadal to century timescales. This zone extends from the depth of closure Z_{DOC} to a user defined maximum depth of significant sediment transport Z_{min}. Diffusivity in the lower zone is described as $D(Z_{min}) = D_{dw}/dz' * D(Z_{DOC})$, whereby a gradient of diffusion coefficient in deep water D_{dw}/dz must be estimated. $D(z')$ is assumed to decrease exponentially in between:

$$\mathrm{D}(z') = D(Z_{DOC}) * 10^{\frac{dD_{dw}}{dz} * (z' + Z_{DOC})}\ for\ Z_{min} < \mathrm{z}' < \mathrm{Z_{DOC}}\mathrm{D}(z') \tag{3.6}$$

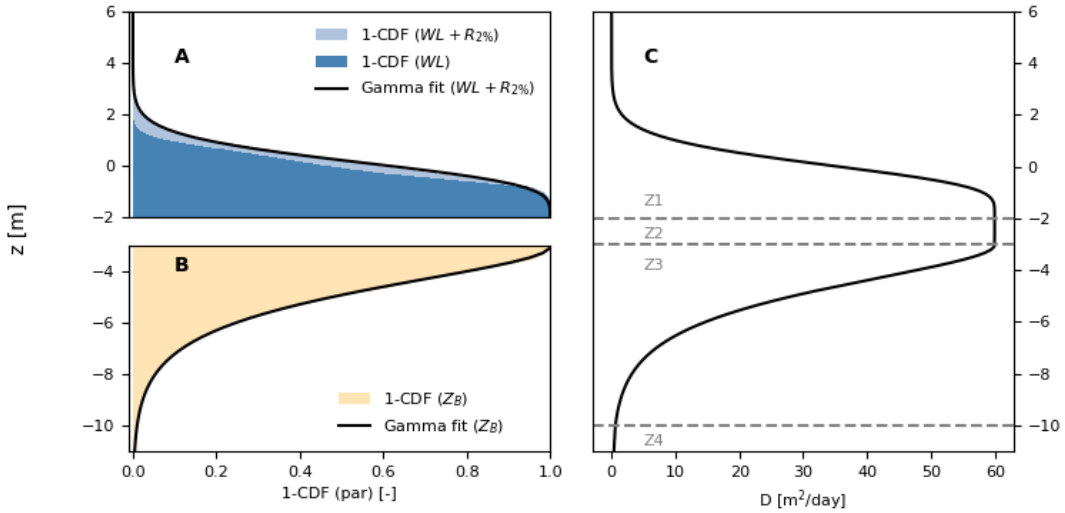

Figure 3.2 A) Example survival functions of WL (water level and surge) and $WL + R_{2\%}$ (water level, surge, and wave runup). B) Example survival function of Z_B whereby breaker index γ is set 0.44 (Miche, 1954). C) Resulting diffusion coefficient $D(z')$ with $D_{MAX} = 60\ m^2/day$ as adopted from de Vriend et al. (1993). Z1, Z2, Z3 and Z4 indicate zones as referred to in the main text, divided by the grey dashed lines. The CDFs and zonation in this example are based on the hydrodynamic data of 1985 to 2018 at the Dutch IJmuiden measuring station.

Although many forces and factors that affect morphology and drive morphological change (i.e., bed composition, tidal currents) are not included within these definitions, the most important cross-shore variations in sediment response over the profile are captured within $D(z')$. Key aspects of the formulations are that the morphological timescale is shortest in the zone of maximum wave breaking, and that the edge of the active zone moves seawards if the timescale increases.

Since the diffusion component varies over depth the volume conservation of sand is not guaranteed. To ensure volume conservation, a correction term $\varepsilon_D(z)$ is applied wherein the difference in integrated profile volume ΔVp is redistributed. Hereby, the amount of redistribution per location is weighted by the relative elevation change $dz[t,x] - min(dz[t])$ at that location, whereby parts of the profile that are inactive (i.e., $dZ = 0$) are excluded:

$$\Delta Vp(t) = \int_{t=t-1}^{t=t} \int_{\mathrm{X=0}}^{\mathrm{X=Xmax}} \left(\frac{\mathrm{d}}{\mathrm{dx}} \left\{ \mathrm{D(z)} \frac{\mathrm{d(Z - Z_{eq})}}{\mathrm{dx}} \right\} \right) dx\ dt \tag{3.7}$$

$$\varepsilon_D(z) = -dt * \frac{\Delta Vp[t]}{dx} * \frac{dZ[t,x] - min(dZ[t])}{\sum(dZ[t,x] - \min(dZ[t]))}\ where\ dZ[t,z] > 0 \tag{3.8}$$

Background erosion

The background erosion term $E(z)$ represents sediment supply and losses to the profile through gradients in alongshore transport independent of the implementation of any nourishments, with the physical dimension $m^3/m/yr$. Gradients can originate from natural processes and human activities such as engineering works at adjacent beaches. For the sake of simplicity, we keep $E(z)$ constant over time throughout the simulations. Given that the alongshore gradients predominantly occur within the active profile zone, we distribute the volume change over the profile with the shape of $D(z)$:

$$E[z] = E_{tot} * \frac{D(z')}{\int_{Xmin}^{Xmax}(D(z'))\,dx} \tag{3.9}$$

In the current application the magnitude of sediment changes due to ambient alongshore gradients is obtained from a multi-year record of profile elevation changes $dZ_{obs}(x)$:

$$E_{tot} = \int_{Xmin}^{Xmax} \frac{dZ_{obs}}{dt}\,dx \tag{3.10}$$

Alternatively, E_{tot} could also be estimated using a alongshore transport model or coastline data.

Nourishment loss

The third RHS element in Eq. 3.1, $F(Z - Z_{eq})$, represents the enhanced sediment losses following the implementation of a nourishment. These losses stem from the increased exposure of the new coastline to waves and currents, compared to its neighbouring profiles (Verhagen, 1993). As described by Verhagen (1996) enhanced sediment loss dV_f from initial beach nourishment volume V_{ini} can be described with an exponential decay function:

$$dV_f[t] = -P * V_{ini} * e^{-\frac{t}{\Phi}} \tag{3.11}$$

Whereby P represents the fraction of V_{ini} that is dispersed over the nourishment lifespan and Φ represents a nourishment loss exponent. This means that fraction $(1 - P)$ is covered by the other terms on the RHS of Eq. 3.1.

The magnitude of the enhanced sediment losses following the implementation of a nourishment has been linked to the wave climate, profile steepness, the active height of the zone with alongshore transport and the extent of the nourishment (Arriaga et al., 2017; Huisman et al., 2013). Considering these dependencies, we assume that Φ increases with depth and we assume that P decreases with depth. This depth-dependency offers an advantage, as it allows us to incorporate shoreface nourishments, which were not considered in the analysis by Verhagen (1996). To this end, we define the depth-dependent nourishment loss $dV_{f,Z}(t,z)$ at timestep $(t - t_n)$ after nourishment:

$$dV_{f,Z}[t,z] = -\mathrm{p(z)} * (\mathrm{Z} - \mathrm{Z_{ini}}) * e^{-\frac{t-t_n}{\Phi(z)}} \tag{3.12}$$

Herein, $p(z)$ and $\phi(z)$ are the vertically varying counterparts to P and Φ from Eq. 3.11. V_{ini} has been replaced by $(Z - Z_{ini})$ to account for multiple successive nourishments as well as contemporary profile evolution resulting from the other terms on the RHS of Eq. 3.1.

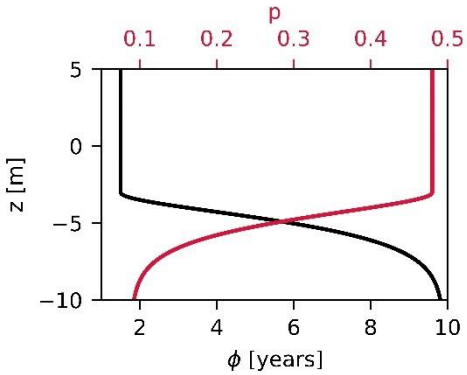

Figure 3.3 Variation of p(z) and $\phi(z)$ with profile elevation z.

In the definition of $\phi(z)$ we follow the shape of $D(z)$, assuming that the timescale of enhanced nourishment losses in the region permanently submerged ($Z < Z_{LW} - 1$) is linearly dependent on the relative sediment redistribution capacity along the profile (Fig. 3.3):

$$\mathrm{D}(z') = D_{MAX} * \Big(\big(1 - CDF(WL + R_{2\%})\big) + Z_{LW}\Big) \; for \; (Z_{LW} - 1) < \mathrm{z}' \tag{3.13}$$

$$\phi(z) = \begin{cases} \phi_B & for \; Z \geq \mathrm{Z_{LW}} - 1 \\ \phi_B + \dfrac{d\phi}{dD} * \dfrac{\mathrm{D_{max}} - \mathrm{D(z)}}{\mathrm{D_{max}}} & for \; Z < \mathrm{Z_{LW}} - 1 \end{cases} \tag{3.14}$$

Thereby, ϕ_B represents the nourishment loss exponent for beach nourishments and $d\phi/dD$ its increase relative to $D(z')$. Likewise, we assume that the fraction of enhanced nourishment loss is linearly dependent on the relative sediment redistribution capacity along the profile:

$$p(z) = \begin{cases} p_B & for \; Z \geq \mathrm{Z_{LW}} - 1 \\ p_B + \dfrac{dp}{dD} * \dfrac{\mathrm{D_{max}} - \mathrm{D(z)}}{\mathrm{D_{max}}} & for \; Z < \mathrm{Z_{LW}} - 1 \end{cases} \tag{3.15}$$

Estimations of both terms can be obtained from either observations or an analytical approach. $F(Z - Z_{eq})$ in Eq. 3.1, being the rate the enhanced sediment losses following the implementation of a nourishment, is then given by the time derivative of $dV_{f,Z}[t,z]$:

$$F(Z - Z_{ini}) = \frac{dV_{f,Z}}{dt} \tag{3.16}$$

Due to the volume dependency, $F(Z - Z_{eq})$ is largest directly after nourishment placement and decreases gradually over time.

$F(Z - Z_{eq})$ is particularly large when a nourishment has a feeder-type function. For feeder-type nourishments where planform coastline curvature drives substantial lateral losses, we propose an alternative approach to determine nourishment loss exponent ϕ following Tonnon et al. (2018). Essential herein is the definition of a alongshore transport intensity parameter ($\partial \mathrm{Qs}/\delta\theta$), defined as the variation of the net alongshore transport $\mathrm{Qs}[m^3/\mathrm{yr}]$ for a small change of the coastline orientation $\theta[°]$:

$$\frac{\partial \mathrm{Qs}}{\delta\theta} = \frac{\mathrm{Qs}}{\Delta\theta} * \cos(2\Delta\theta) \tag{3.17}$$

wherein $\Delta\theta[°]$ is the relative difference between the local coastline orientation and the coastline orientation that yields net zero sand transport. Tonnon et al. (2018) propose that ϕ relates to nourishment design parameters $V_{ini}[m]$ (initial nourishment volume), $L_{ini}[m]$ (initial nourishment length) and $W_{ini}[m]$ (initial nourishment cross-shore width):

$$\phi = 1.91 * 10^{-2} * V_{ini} * \left(0.2 * \frac{L_{ini}}{W_{ini}} + 1\right)\left(\frac{\partial \mathrm{Qs}}{\delta\theta}\right)^{-1} \tag{3.18}$$

The constant $1.91 * 10^{-2}$ scales with $\partial \mathrm{Qs}/\delta\theta$ ($30.000\ m^3/\mathrm{yr}/°$ in Tonnon et al. (2018)) and includes the impact of the wave climate, cross-shore profile, and sediment. This ϕ can be adjusted to other locations by recalculating $\partial \mathrm{Qs}/\delta\theta$ and scaling the constant in Eq. 3.18. $F(Z - Z_{ini})$ can then be calculated by substituting ϕ in Eq. 3.12 with p(z)=1 and subsequently substituting $dV_{f,Z}$ in Eq. 3.16.

Sediment exchange with the dune area

The fourth RHS component of Eq. 3.1, $W(Z - Z_{eq})$, describes variations in sediment exchange from the subaerial beach and the intertidal zone to the dune area (Fig. 3.1 h, I). If the profile is equal to the equilibrium profile ($Z = Z_{eq}$) the subaerial beach and the intertidal zone are, by definition, in morphodynamic balance. In other words, for $\mathrm{Z} = \mathrm{Z_{eq}}$, the volume of sediment transferred from deep water to the beach balances the long-term landward sediment transfer from the beach towards the dune area. However, this balance does not imply zero dune growth, as a net landward sediment supply can exist within the equilibrium profile (i.e., the equilibrium concept does not include the dune area). $\mathrm{W}\left(\mathrm{Z} - \mathrm{Z_{eq}}\right)$ thus only represents the change in dune growth with respect to an initial situation. Total dune growth can then be computed by adding $\mathrm{W}(\mathrm{Z} - \mathrm{Z_{eq}})$ to the initial net landward sediment supply.

On a decadal timescale, dunes evolve in a variety of ways dependent on biological, geological, and physical factors (Carter, 1991). Hence, it is difficult to quantify and predict the impact of nourishment on duneward sediment exchange. However, we can simplify the depiction to highlight some primary anticipated impacts. Several studies have shown that wider beaches may lead to higher sediment supply (Davidson-Arnott and Law, 1996; De Vries et al., 2011) and increased protection against storm wave

attack (Davidson-Arnott, 2005). Therefore, we confine our definition of W $(Z - Z_{eq})$ to the critical fetch theory, whereby the amount of aeolian sediment transport linearly scales with fetch length until a certain limit is reached (Bauer et al., 1996). If the beach width exceeds its initial value BW_0, it results in an additional net transport of sediment towards the dune, while a beach width narrower than BW_0 causes the dunes to supply sediment to the beach. The dune area is modelled as a source or sink of sediment, i.e., its type, shape and evolution are not modelled.

We adopt a linear relation between beach width and dune growth in m^3 per m alongshore whereby linear coefficient α must be estimated:

$$W_{calc} = \frac{\alpha}{dt} * (BW - BW_0) \tag{3.19}$$

Following the critical fetch theory, we assume that dune growth reaches a constant maximum value W_{Max} when a certain critical beach width BW_c is exceeded:

$$W_{total} = \min (W_{calc}, W_{max}) \tag{3.20}$$

Whereby,

$$W_{max} = \frac{\alpha}{dt} * (BW_c - BW_0) \tag{3.21}$$

Sediment that is used to adjust the dune growth is subtracted from (or added to) the intertidal zone and subaerial beach.

$W[Z - Z_{eq}]$ is then subtracted from the intertidal area and subaerial beach:

$$W[Z - Zeq] = \frac{-W_{total}}{X[Z_{df}] - X[Z_{\mathrm{LW}}]} \; for \; Z_{LW} \leq Z \leq Z_{df} \tag{3.22}$$

Reported relations between beach width and dune growth are highly variable over time and space, as noted by de Vries et al., (2011). The same applies to the magnitude of a critical beach width or a maximum dune growth rate. Nevertheless, the presented approach provides a system description with a sufficient scientific basis to depict the major aspects of dune growth impacts related to nourishment, wherein dune growth at recently nourished beaches increases with beach width until a certain maximum. In the context of the current application, this comprehensive system description provides an adequate basis to differentiate between nourishment scenarios.

Nourishment implementation

Nourishments are added into dynamic profile Z using the $Source\ (z, t)$ term. For the current study we avoid intricate designs and instead employ triangular cross shore designs, comprising a near horizontal platform and a linear slope towards the nourishment toe (Fig. 3.1D). The cross-shore added volume V_n and design height H_n (upper connection point to profile Z), landward slope S_{lw} and seaward slope S_{sw} are pre-defined. Crocodile then computes a shape that matches these four design characteristics.

Computed coastal state indicators

Crocodile returns the 'instantaneous' bed level $Z\ (x,t)$. Bed level data are translated to three coastal state indicators: the temporal evolution of profile volume change ΔV_p, beach width BW and shoreline migration ΔCL.

$$\Delta V_p = \int_{X_{min}}^{X_{max}} \big(Z(x,t) - Z(x,t=t_0)\big)\, dx \tag{3.23}$$

The position of the coastline X_{cl} is determined by calculating a volumetric weighted average between the horizontal positions of high (X_{HW}) and low water (X_{LW}). This involves integrating $Z(x,t)$ between X_{HW} and X_{LW} to obtain the sand volume above the level Z_{LW} in this section. The adoption of this volume-based approach aims to avoid that local small-scale variations in profile height, such as intertidal sand bars, result in large fluctuations in X_{cl}:

$$X_{cl} = X_{HW} + \frac{\int_{X_{HW}}^{X_{LW}} \big(Z(x,t) - Z(X_{LW},t)\big)\, dx}{2 * (Z_{HW} - Z_{LW})} \tag{3.24}$$

X_{cl} is used to compute BW and ΔCL, whereby the landward limit of the beach width is positioned at the initial horizontal location of the dune foot $X_{df}(t=0)$.

$$BW = X_{cl}(t) - X_{df}(t=0) \tag{3.25}$$

$$\Delta CL = X_{cl}(t) - X_{cl}(t=0) \tag{3.26}$$

BW and ΔCL only differ by their point of reference. We chose to include both variables in our analysis, as ΔCL depicts absolute changes while BW offers insights from a relative perspective.

3.5 Model application: the Holland coast

The Crocodile model is applied to the central Dutch coast in two ways. Firstly, we examine idealized nourishment scenarios to analyse whether Crocodile can replicate corresponding behaviour of coastal indicators (Section 3.6.1). Moving from this conceptual application, we transition to nourished case study sites along the central Dutch coast to examine Crocodile's performance reproducing site-specific behaviour resulting from diverse nourishment strategies using measured profiles (Section 3.6.2).

3.5.1 The Holland coast: site description and nourishment strategy

The Holland coast consists of sandy beaches and dunes with an average tidal range of about 1.6 m (Wijnberg, 1995). These beaches are interrupted by various structures, including harbour moles (IJmuiden, Scheveningen, and Hoek van Holland), discharge locks (Katwijk aan Zee), and a sea dike (Hondsbossche and Pettemer Zeewering). The nearshore zone is characterized by a roughly uniform, gradual sloping beach profile, occasionally interspersed with periodic nearshore bars. The shoreface slopes vary

alongshore between 1:400 and 1:160, and slopes in the breaker zone vary from about 1:50 to 1:150 (Wijnberg 1995).

The primary concern driving the current nourishment strategy the Netherlands is safety against flooding. Over time, the total volume of nourished sand has increased to a current level of about 12 million m3 of sand per year. The sand is mainly supplied to the shallow zone (shallower than NAP -8 m) and is not spreading (yet) or only slowly to the deeper coastal zone. This leads to an increase in the average sediment volume in the shallow zone compared to the deeper zone. As a result, the profile of the Dutch coast becomes relatively steeper (Van der Spek & Lodder, 2014). The quantity and type of nourishment supplied vary per location and depend on various factors such as the current condition of the beach and dune system, anticipated future changes, and the preferences of local stakeholders. Additionally, some locations receive additional sand to maintain sufficient sediment supply for areas that cannot be nourished. As a result, different nourishment strategies are employed in different locations along the central Dutch coast. For the purposes of this study, three locations have been chosen, each with varying coastal profiles and nourishment histories. From North to South: Egmond, Katwijk, and Monster (Fig. 3.4).

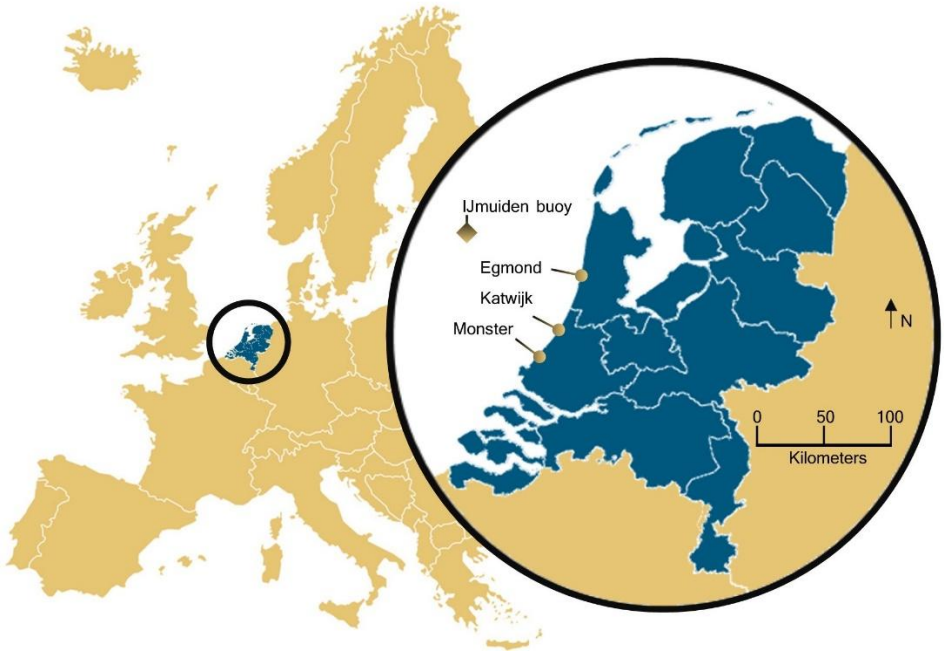

Figure 3.4 Locations of case study sites along the sandy Dutch coast and the IJmuiden wave buoy used for the long-term wave data.

3.5.2 Model set-up for all simulations

Profile schematization

This section introduces the profile schematization and sums the parameters used for all simulations. Both $Z(x, \mathrm{t} = 0)$ and $Z_{eq}(x, t = 0)$ are derived from a smoothened multi-year average measured profile obtained from the JARKUS dataset (Wijnberg and Terwindt, 1995a). The smoothening and averaging ensure that such that the dynamics of the nourishment are isolated from concurrent coastal behaviour (e.g., cyclic bar

behaviour). The beach is extended linearly from the dune foot Z_{df} to the upper model boundary Z_{max}, with the slope equal to the dune slope observed between +4 and +6 m above sea level. The temporal resolution in the numerical scheme dt is 1/10 year, the spatial resolution in the cross-shore dx is 20 m. The mean water level is set $MWL(t = 0) = 0\ \mathrm{m}\ NAP$, NAP being the local Dutch vertical datum, approximately equal to mean sea level. MWL rises linearly throughout all simulations with $SLR = 1.7\ mm/yr$, equal to the average observed relative sea level rise along the Dutch coast over the past century (Drijfhout and Le Bars, 2021).

Parametrization

All hydrodynamic and morphodynamic parameter values are obtained from literature concerning the central Dutch coast (Table 3.1). Elevations that mark the zonation in the diffusion curve $D(z')$ are based on Wijnberg and Kroon (2002), rounded to $Z_{HW} = 1m\ NAP$, $Z_{LW} = -1m\ NAP$, $Z_{df} = 3m\ NAP$ and $Z_B = -3m\ NAP$. The maximum diffusion coefficient D_{max} is adopted from De Vriend et al. (1993), who estimated that $D_{max} = 60\ m^2/day$ for the central Dutch coast. Offshore wave height and water level statistics used to define the shape of $D(z)$ are obtained from the IJmuiden station of the Dutch Ministry of Public Works, located 35 km offshore (Fig. 3.4). The gradient of diffusion coefficient in deep water dD_{dw}/dz is taken $1/100$ following estimates of morphological timescales for the Dutch coastal shelf from numerical model experiments (Boers, 2005). Any estimate for this gradient is site-specific and arbitrary, however the model results show little sensitivity to this deepest part of the $D(z)$ curve within the current application. A common value for wave breaker index $\gamma = 0.44$ is adopted from Miche (1954). For the Holland coast, Tonnon et al. (2018) estimated $\partial \mathrm{Qs}/\delta\theta = 30.000\ m^3/yr/°$ (i.e., $\mathrm{Q_s} = 200.000\ m^3/yr$ and θ=6.6°). The linear relation between beach width and dune growth is adopted from de Vries et al. (2012) as $\alpha = 0.1475$, and based on 10-year observations of beach width and dune growth along the Holland coast. Additional dune volume growth W_{Max} is based on the maximum dune growth that has been measured at a mega nourishment in the Netherlands which was $60\ m^3/m/yr$ (Kroon et al., 2022b). As the dune growth at adjacent beaches was $15\ m^3/m/yr$, we reason that $W_{Max} = 60 - 15 = 45\ m^3/m/yr$.

Parameters related to $F(Z - Z_{ini})$ are established through observations of nourishment lifespans based on yearly surveys conducted at multiple nourished locations along the central Dutch coast. These lifespans are defined here as the time that an excess of sand is present in the initial nourishment area compared to the pre-nourished situation. For beach nourishments, we adopt the parameterization of (Verhagen, 1996) who proposed that $p_b = 0.48$ and $\phi_b = 1.5\ yr$. To define $d\phi/dD$ and dp/dD we use observed nourishment lifespans of shoreface nourishments by Huisman et al. (2019), who studied the cross-shore profile change and alongshore redistribution of 19 shoreface nourishments along alongshore uniform sections of the Dutch coast. On average, 40% (+/-20% standard deviation) of the initial nourishment volume was eroded from the initial nourishment region after 3 years. From numerical model calculations of initial erosion and accretion rates over these nourishments, Huisman et al. (2019) estimated that on average 27.5% of the eroded sand was redistributed alongshore (+/-12.5% standard deviation). Based on these values, we

assume that $p[z=-5m]=0.275$ and $\phi[z=-6m]=-\frac{3}{\ln(1-0.4)}=5.87\,yr$. As $D[z=-2]=D_{max}=60\,m^2/day$ and $D[z=-6]=20.7\,m^2/day$, we calculate $d\phi/dD=\frac{1.5-5.87}{60-20.7}=-0.11\,yr\,m^{-2}day$ and $dp/dD=\frac{0.48-0.275}{60-20.7}=0.0052\,m^{-2}day$.

Nourishment design parameters

The design height, landward slope, and seaward slope of the implemented nourishments are based on prevalent Dutch values as described by Brand et al. (2022). Hereby we discriminate between beach nourishments, shoreface nourishments and mega nourishments. All have triangular cross shore shapes, comprising a near horizontal platform and a linear slope towards the nourishment toe. For beach nourishments the platform connects with the original profile at $H_n=MSL+2\,m\,NAP$. The landward slope is $S_{lw}=1:200$ and the seaward slope S_{sw} is taken equal to the intertidal slope of $Z_{eq}(x,t=0)$:

$$S_{sw}=\frac{Z_{HW}-Z_{LW}}{X[Z_{HW}]-X[Z_{LW}]}\;for\;Z_{LW}\leq Z\leq Z_{df} \tag{3.27}$$

We depart from the latter definition when it becomes impractical to achieve the combination of all four design characteristics. This occurs specifically when there is a combination of a low intertidal slope and low nourishment volume (roughly $V_n\leq 150\,m3/m$). In such situations, we opt for a steeper seaward slope $S_{sw}=1:20$. Shoreface nourishments are implemented with $H_n=MSL-4\,m$, $S_{lw}=1:10000$ and $S_{sw}=1:50$. Mega nourishments, here defined as nourishment with $V_n\geq 2000\,m3/m$, are implemented with $H_n=MSL+7\,m$ with S_{lw} and S_{sw} defined similar to those used for beach nourishments.

Model input per site

Site-specific modifications in the model setup include the record of profile surveys to define the initial profile shapes $Z(x,t=0)$ and $Z_{eq}(x,t=0)$ and total background erosion E_{tot}. The nourishment implementation, including its timing, volume, and cross-shore location, can either be predefined or based on certain conditions. For the generic scenarios, nourishments with a predefined volume and cross-shore location are implemented when the shoreline passes landwards of a reference point. For the case studies, all nourishment parameters are predefined according to the local nourishment history.

Parameter	Description	Value	Source
dt	Temporal resolution	$0.1\ yr$	-
dx	Horizontal grid resolution	$20\ m$	-
Z_{min}	Elevation of lower model boundary	$-20\ m$ NAP	-
Z_{max}	Elevation of upper model boundary	$20\ m$ NAP	-
$MWL(t=0)$	Mean water level at t=0	$0\ m$ NAP	-
SLR	Sea level rise	$1.7\ mm/yr$	(Drijfhout and Le Bars, 2021)
Z_{HW}	Elevation of high water	$1\ m$	Wijnberg (2002)
Z_{LW}	Elevation of low water	$-1\ m$	Wijnberg (2002)
Z_{df}	Elevation of dune foot	$3\ m$	Wijnberg (2002)
Z_E	Elevation of lower limit of the surf zone during average wave conditions	$-3\ m$	Wijnberg (2002)
Z_{DOC}	Depth of closure	$-10\ m$	Hinton and Nicholls (1998)
D_{max}	Maximum diffusion coefficient	$60\ m^2/day$	Stive (1991)
$\frac{dD_{dw}}{dz}$	Gradient of diffusion coefficient in deep water	$1/100$	Boers (2005)
γ	Wave breaker index	0.44	Miche (1954)
$\frac{\partial Qs}{\delta \theta}$	Longshore transport intensity parameter	$30.000\ m^3/yr/°$	Tonnon et al. (2015)
p_b	Fraction of enhanced nourishment loss	0.48	Verhagen (1995)
ϕ_b	Nourishment loss exponent	$1.5\ yr$	Verhagen (1995)
$\frac{dp}{dD}$	Gradient of fraction of enhanced nourishment loss	$0.0052\ m^2 day^{-1}$	See par. 3.2.2.
$\frac{d\phi}{dD}$	Gradient of nourishment loss exponent	$-0.11\ yr\ m^2 day^{-1}$	See par. 3.2.2.
α	Coefficient of linear relation between beach width and dune growth	0.1475	de Vries (2011)
W_{Max}	Maximum dune growth	$45\ m^3/m/yr$	Kroon (2022)

Table 3.1 Parameters that are fixed for all simulations in this research paper.

3.6 Results

3.6.1 Idealized nourishment simulations

For our initial analysis, we establish three simulations with nourishment strategies in a Dutch coastal setting. In all simulations, we follow a 'reactive' shoreline maintenance policy. Thereby, a new nourishment is placed when the coastline migrates landward of its initial value, i.e., when ΔCL is negative. The three simulations vary in the cross-shore position and volume of the nourishments applied, with the simulated scenarios being regular beach nourishment, regular shoreface nourishment and mega nourishment. The initial profile and morphological and hydrodynamic model set-up are equal for the three simulations to isolate the impact of the nourishment strategy.

The initial profile applied is a median, smoothened profile based on bathymetric measurements from the unnourished years (1956-1997) at Katwijk beach, the Netherlands. As described by Huisman et al. (2019), an average observed background erosion rate in the Netherlands is $E_{tot} = -28\ m^3/m/yr$, which is adopted

in these generic simulations. The design height and cross-shore shape of the applied nourishments resemble the standard formulations for the different nourishment types described in section 3.2.3. The applied cross-shore nourishment volumes are based on average volumes applied along the central Dutch coast over the past couple of decades as described by Brand et al. (2022), which is $V_n = 200\ m^3/m$ for regular beach nourishments and $V_n = 450\ m^3/m$ for shoreface nourishments. Design dimensions adopted for the scenario with mega nourishments are adopted from Tonnon et al. (2018), reflecting the design of the Sand Engine; $V_n = 9000\ m^3/m$ and $L_{ini} = 1333$. The total simulation duration is 40 years.

The target of the modelling exercise is to analyse whether Crocodile reproduces the evolution ΔV, ΔCl and BW as we expect based on observations. For the beach nourishment scenario, we expect the beach to widen each time a nourishment is implemented followed by rapid erosion, with ΔCl and BW returning to their initial values after about 3 years (Brand et al., 2022). Furthermore, we anticipate observing a disparity in sediment transport rates along the profile, whereby the middle and lower shoreface cannot keep in pace with the upper part of the profile (as observed by van der Spek & Lodder, 2014). This leads to a volume deficit compared to Z_{eq} in these regions. Consequently, ΔV averaged over a nourishment lifetime is expected to decrease progressively. For the shoreface nourishment scenario, the influence of shoreface nourishments on ΔCl and BW is anticipated to have a delayed effect compared to the time of nourishment application. In an evaluation of shoreface nourishments for the central Dutch, Witteveen&Bos (2006) found that the volume in the beach and upper nearshore zone is increased by approximately 10% of the nourished volume after one year and this will further increase up to 20–30% in the years after. After 4-10 years, the nourishment has no effect anymore. The mega nourishment is expected to show similar, but extended characteristics as the beach nourishment scenario with a volume deficit compared to Z_{eq} around the depth of closure.

In all scenarios (Fig. 3.5), the features described in section 3.4.1 are generally well reproduced, indicating that Crocodile can effectively simulate profile responses characterizing nourishment application. For the beach nourishment scenario, ΔCl and BW return to their initial values after 3.5 years on average. This return period gradually increases over the simulation from 2.5 to 3.9 years due to sediment piling up on the subaerial beach area. As expected for this scenario, ΔV averaged over a nourishment lifetime decreases over time. By the dissipation of the 9th beach nourishment after 32 years, ΔV has decreased by $-48\ m^3/m$ compared to the initial situation. For the shoreface nourishment scenario, we observe delayed and less distinct effects of the nourishment on ΔCl and BW, aligning with our initial expectations. Both fluctuate with only a $10\ m$ amplitude, reaching maxima at 2.3 years after nourishment implementation. Throughout the simulation, ΔCl and BW take on average 10.8 years to revert to their initial values, which is somewhat slower than the timeframe of 4-10 years reported by Witteveen&Bos (2006). The mega nourishment scenario shows similar characteristics as the beach nourishment scenario but with extended spatial and temporal scales. ΔCl and BW increase by $840\ m$ after implementation and return to their initial values after 40 years.

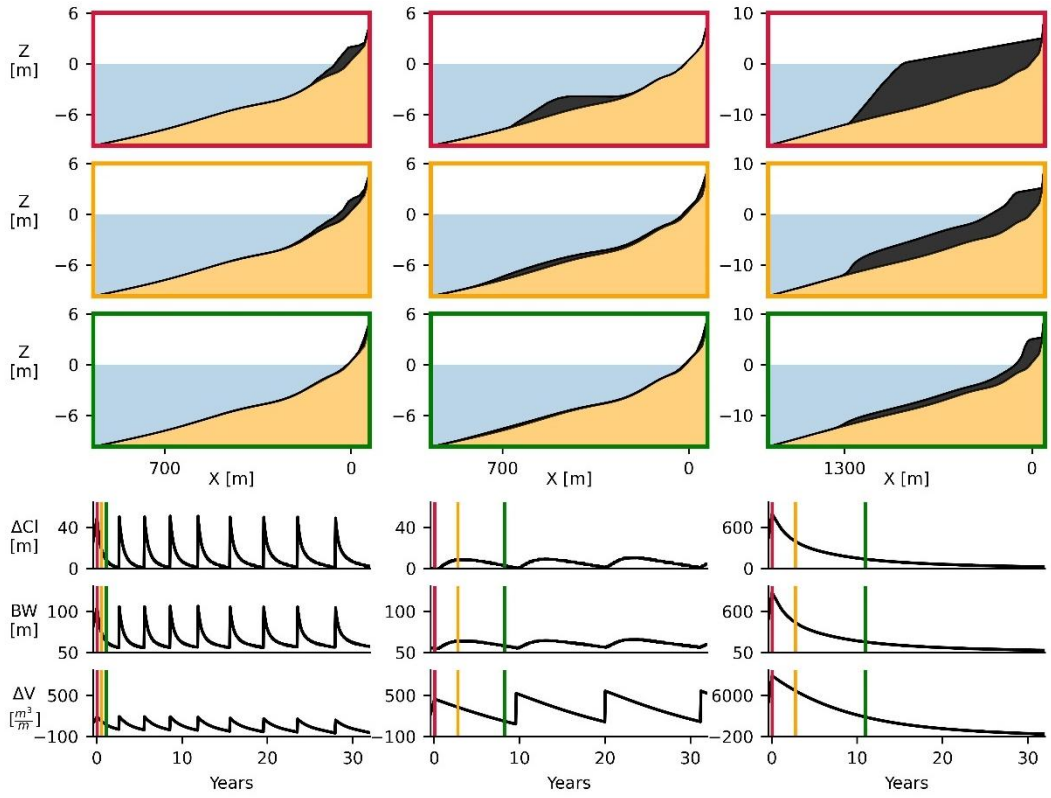

Figure 3.5 Demonstration of simulated nourishment scenarios, whereby beach (left), shoreface (centre) or mega (right) nourishments were reactively implemented when ΔCl passed its initial position. The upper three rows display the simulated nourishment evolution at timesteps indicated by the colour of the frames in the lower three rows, that show the temporal evolution of ΔCl, BW and ΔV. The peaks in ΔV and the corresponding responses in other indicators arise from the implementations of individual nourishments.

3.6.2 Case studies

The model is applied to three case study sites along the central Dutch coast that vary in coastal profile and nourishment history. For case study site #1 Monster beach we demonstrate the workflow in detail, the other two are presented more concisely. The transect near Monster Beach is examined because it has been subjected to different nourishment strategies, which have resulted in distinct responses of the coastal state indicators. The second case study, Egmond, adopted a strategy of frequent regular small-scale beach nourishments, while the third site, Katwijk, employed a strategy with solely shoreface nourishments.

For each case study, the initial profile shape and total background erosion E_{tot} are obtained from JARKUS profile bathymetric measurements over an unnourished period. As the wave climate shows little spatial variation along the central Dutch coast, hydrodynamic parameter settings are identical. Nourishment application in the model matches the nourishment history of the case study location in volume, timing, and cross-shore position. The objective of the modelling exercise is to analyse to what extent Crocodile replicates observed site-specific morphological responses to

nourishment application. The comparison includes not only absolute values but also trends and trend reversals in these indicators. By focusing on trends, the comparison becomes more straightforward as observations reflect stochastic aspects of hydroclimatic forcing that are not reproduced by the model, which is stationary forced.

Monster beach case study

The transect near Monster beach is examined because it has been subjected to diverse nourishment strategies, The first nourishment conducted in the selected transect was a beach nourishment in 1986. This nourishment was followed by beach nourishments in 1993 and 1997, with the primary objective of preserving the coastline seaward from its 1990s location. From 2001 onwards, it was decided that also sand loss lower in the profile was to be compensated. Consequently, the total nourished volume increased from about $40\ m^3/m/yr$ between 1986 and 2001 to $230\ m^3/m/yr$ between 2001 and 2011 (Fig. 3.6C). Shoreface nourishments were also introduced during this period. In the JARKUS annual profile measurements, we observe a significant increase ΔV of $108\ m^3/m/yr$ and seaward coastline migration with $6\ m/yr$ between 2001 and 2011 (Fig. 3.6F). In 2011, a 21.5 Mm3 mega nourishment known as the Sand Engine was implemented as a pilot project to test the effectiveness of mega feeder nourishments (Stive et al., 2013) (Fig. 3.6B).

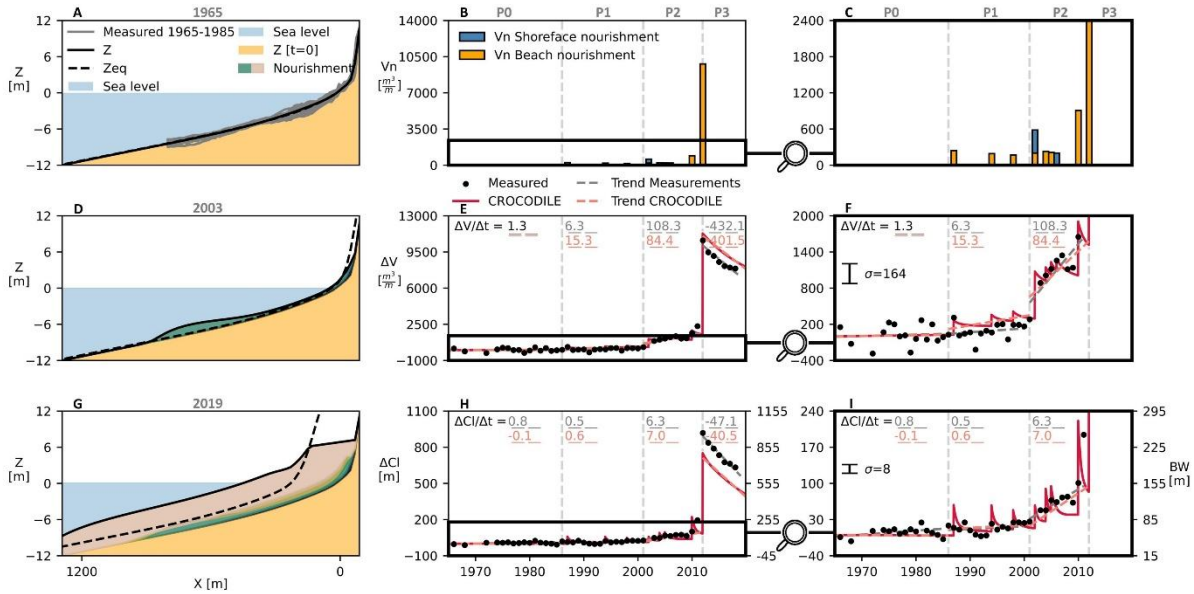

Figure 3.6 Left) Snapshots of simulations at the Monster transect. Centre and right) Applied nourishment volume over time, and coastal indicator response, whereby the right plots are a vertical stretch from the black square in the centre plots. Grey dashed lines indicate measurement trendlines, red dashed lines indicate simulation trendlines with rates displayed on top. Trendlines are calculated over the different subperiods (P0-P3), which are indicated on top of 6B and 6C. A standard deviation for the measurements is indicated with σ.

In our analysis we divide the nourished period in three subperiods; a period of beach nourishment between 1986 and 2001 (P1), followed by a period with more volume supplied in both beach and shoreface nourishment (P2) and the period after the construction of the Sand Engine in 2011 (P3). Crocodile accurately reproduces the long-term pattern of coastal indicators observed during both the nourished and unnourished periods, as depicted in Fig. 3.6. In the pre-nourished period (P0), both ΔV and ΔCl exhibit relative stability, aligning well with the observed data. It is worth noting that the model simulates a minor retreat of the coastline, which can be attributed to the slight rise in sea level. Between 1986 and 2001 (P1) ΔCl remains stable conform to observations, while the increase in ΔV is overestimated by $9\ m^3/m/yr$. In contrast, the accretion between 2001 and 2011 (P2) by $108\ m^3/m/yr$ was underestimated by 12%, and contemporary coastline accretion is accurately reproduced. Thus, regarding the reversal in volume trends following the shift in nourishment strategy, the transition from P0 to P1 was overestimated by $9\ m^3/m/yr$, whereas the transition from P1 to P2 was underestimated by $33\ m^3/m/yr$ (Table 3.2). Additionally, the reversal in coastline trends after both transitions was well reproduces, with a slight overestimation of $1\ m/yr$.

The Sand Engine implementation results in a modelled overestimation of ΔV by 6% and underestimated in ΔCl by 17%. The volume discrepancy results from a disparity between the reported nourishment volume ($8995\ m^3/m$) and the actual volume increase ($8306\ m^3/m$) at the location during the initial JARKUS measurement, which occurred 8 months after the Sand Engine construction. Over this period, approximately $800\ m^3/m$ of nourishment had already eroded from the transect (De Schipper et al., 2014). The smaller beach width observed can be attributed to the simplified geometry of the Sand Engine in the simulation compared to its real-world counterpart. In reality, a small lake is present at the location of the transect. As we chose to adhere to the reported nourishment volumes and a simplified geometry, the omission of this lake resulted in a narrower beach width. Lastly, the erosion of the Sand Engine is slightly underestimated in both ΔV by $31\ m^3/m/yr$ and ΔCl by $7\ m/yr$.

Egmond aan Zee beach case study

The Egmond aan Zee case study (Egmond from hereon) was examined due to its exceptionally high frequency of (16) nourishments since 1991 (Fig. 3.7A). We analyse if the effects of a short nourishment return period could be replicated using Crocodile. The major reason for the high nourishment frequency in Egmond is the maintenance of a coastline that is placed seawards compared to adjacent regions, in order to protect the local boulevard. Between 1991 and 1998, six beach nourishments ranging from 120 to $300\ m^3/m$ were carried out. It has been reported that the accumulation of sand from these consecutive nourishments led to relatively fast dissipation of the nourished sand (van der Spek et al., 2007). For this reason, a combination of a shoreface nourishment and a beach nourishment was implemented in 1999 to extend the required return period. As this was successful, in the years hereafter more combinations of beach and shoreface nourishments were implemented with return periods ranging from 3 to 5 years.

A summary of the case study observations and simulated coastal indicators at Egmond is given in Fig. 3.7C and 3.7E. During the unnourished period (P0), $\Delta V/\Delta t$ is by definition reproduced. Over the nourished period (P1), $\Delta V/\Delta t$ increased by $42.5\ m^3/m/yr$ according to JARKUS measurements. This increase is closely replicated with the model, as it was estimated only 4% too high ($+44.5\ m^3/m/yr$), The simulated individual nourishment responses to ΔV after 1999 exhibit a sawtooth-shaped pattern resembling the observed data. Over the unnourished period, Egmond showed minimal coastline migration which aligns closely with the observed data (Fig. 3.7E). During the frequently nourished period from 1991 to 1998, we observe that the seaward migration of the coastline is overestimated (Fig. 3.7C). Despite ΔV being consistent with observations, Crocodile underestimates the redistribution of the nourished sand in the cross-shore direction, resulting in an excess of sand remaining in the initial nourished area. However, from 1999 onwards, the simulated coastline aligns more closely with the observations. Overall, the rate of change in coastline position ($\Delta Cl/\Delta t$) is underestimated by 56% over the entire period P1, with the sidenote that the overall change in coastline position (ΔCl) is well reproduced.

Katwijk beach case study

As an example of a shoreface nourishment strategy, the Katwijk aan Zee case study (Katwijk from hereon) is examined. At the examined transect both the coastal volume and the coastline were fairly stable ($< -1\ m^3/m/yr$ and $< 1\ m/yr$ respectively) until the first nourishment in 1999 (Fig. 3.7D, F). Nevertheless, the desired coastline was then decided to be shifted seawards to increase protection, as the hinterland has an important societal and economical value. Therefore, the total applied nourishment volume was larger than the local sediment demand. In total, three shoreface nourishment projects were carried out at the Katwijk transect (Fig. 3.7B). For all projects, we observe that the volume increase measured over the active profile is equal or larger than the volume of nourishment administered. The coastline has moved gradually seawards during the nourished period at a rate of $0.7\ m/yr$. In 2019, a beach nourishment was placed in the area until 250 m North of the investigated transect was placed to mitigate erosion of the coastline. It is unclear whether this adjacent nourishment affected the coastal indicators in the transect, and the period after 2019 is therefore not considered in the analysis.

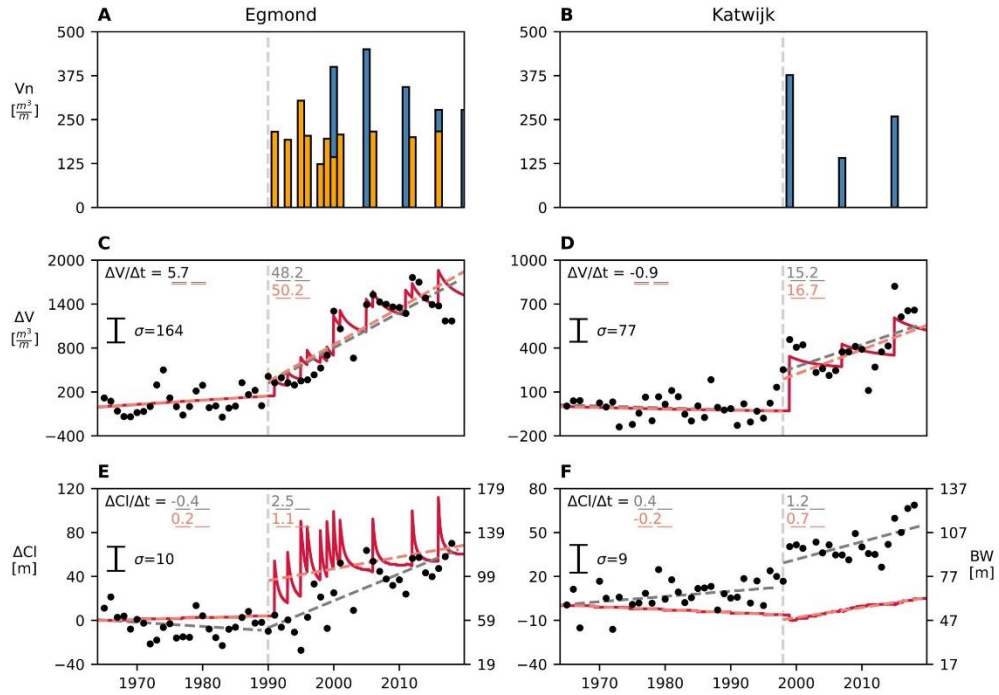

Figure 3.7 Observations and Crocodile simulations and at (left) Egmond and (right) Katwijk. A/B) Applied nourishment volume over time. Beach nourishments are orange, shoreface nourishments are blue. C/D) Profile volume. E/F) Coastline migration and beach width. Grey dashed lines indicate measurement trendlines, red dashed lines indicate simulation trendlines with rates displayed on top. A standard deviation for the measurements is indicated with σ.

A summary of the case study observations and simulated coastal indicators at Katwijk is given in Fig. 3.7. During the unnourished period (P0) $\Delta V/\Delta t$ is again reproduced (Fig. 3.7D). Over the nourished period (P1), the increase in $\Delta V/\Delta t$ is closely replicated, whereby it was estimated 9% too high. However, the simulations show sawtooth-shaped responses in ΔV following shoreface nourishments, although such behaviour is not clearly discernible in the observations. This demonstrates the nature of Crocodile, where the absence of stochastics leads to an overestimation of the distinctiveness of a nourishment response. Therefore, it can be concluded that while the trend $\Delta V/\Delta t$ is well represented for shoreface nourishment scenarios, the individual response of ΔV per nourishment is overestimated in the model.

Over the unnourished period, our simulation indicates a marginal shoreline retreat of $-0.2\ m/yr$ during the unnourished period, in contrast to the slight accretion observed in the measurements (Fig. 3.7F). Presently, the formulation used in Crocodile is unable to account for the combination of background erosion and an advancing shoreline. As a result, ΔCl is underestimated over the nourished period at Katwijk. Although the trend reversal as a response to shoreface nourishment is replicated in the simulation, it is underestimated by 42%.

3.6.3 Combined results

Our objective was to present a model approach to evaluate nourishment strategies by simulating the decadal-scale response of repetitive nourishments to key coastal indicators. In this section, we combine the findings of application of Crocodile to Egmond, Katwijk, and Monster to evaluate whether the model successfully simulated these indicators, including trends and trend reversals that coincided with the timing and magnitude of changes in nourishment strategy. Firstly, we examine yearly averages of the simulated coastal indicators and compare these to the yearly observations, as presented in Fig. 3.8. The modelled and observed coastal indicators show overall good agreement. Specifically, on average (median), the model overestimates ΔV compared to the measurements by 12% (Fig. 3.8A), while ΔCl and BW are underestimated by 13% (Fig. 3.8C). These findings validate that the reproduced coastal indicators fall within the appropriate range, which is essential for employing the model as an investigative tool to explore nourishment responses at these sites.

To explicitly assess whether we can simulate coastal response to changes in nourishment strategies, we conduct a comparative analysis of the simulated and measured trends between the specified nourishment timeframes. Within these timeframes, observed $\Delta V/\Delta t$ ranges from -432 to $108\, m^3/m/yr$, and observed $\Delta BW/\Delta t$ ranges from -47 to $6.3\, m/yr$. On average, modelled $\Delta V/\Delta t$ is found to be $1.5\, m^3/m/yr$ (7%) higher than the actual value (Fig. 3.8B), while modelled $\Delta BW/\Delta t$ is $0.2\, m/yr$ (15%) lower (Fig. 3.8D). The median reversals in these trends between these intervals are slightly better replicated than the absolute trends. Specifically, we observed a median $2.0\, m^3/m/yr$ (4%) overestimation in trend reversals for $\Delta V/\Delta t$, and a $0.6\, m/yr$ (9%) overestimation in trend reversals for $\Delta BW/\Delta t$.

We consider the trend reversals as indicative of the dynamic profile response to different nourishment periods. Their magnitude can therefore serve as a reference for interpreting the significance of the error in trends between simulation and measurement. This allows us to gauge the relevance of the error when utilizing the model for nourishment strategy evaluations within a specific case study. For instance, in Egmond we observed a volumetric trend of $5.7\, m^3/m/yr$ over an unnourished period, which was increased to $48\, m^3/m/yr$ over the nourished period (Table 3.2). The model predicted an increase in volumetric trend of $50\, m^3/m/yr$. Comparing the difference between these two to the difference between the observed trends in the two periods shows that the model error is small enough to replicate the response to nourishment. By comparing the difference between these two values ($2\, m^3/m/yr$) to the difference between the observed trends in the two periods ($42\, m^3/m/yr$), we can deduce that the model error is sufficiently small to discriminate the profile response to nourishment.

When we extend this comparison to encompass all chosen subperiods and various study sites, we consistently observe that all trend reversals exhibit the correct direction (positive/negative). Furthermore, for all but one of the selected subperiods, the magnitude of the trend reversal between a period and the preceding one exceeds

the margin of error between simulation and measurement. In Table 3.2, this comparison is illustrated by the grey arrows accompanied by the percentage of the magnitude of error compared to the preceding trend reversal. This can also be seen in Fig. 3.8 B/D, by comparing the difference in trend between the subperiods with the distance to the 1:1 grey line. The exception where the error exceeds the trend reversal is the trend change between time period P0 and P1 at Monster beach. In this period, the total amount of nourishment applied was relatively modest, and it is reasonable to deduce that the corresponding minor trend reversal predominantly signifies natural variability rather than being attributable to a response to nourishment. This underlines that Crocodile is able to replicate coastal response to changes in nourishment strategies if this response is large enough and thereby clearly discernible in the observations. Overall, these findings suggest that the model's error is acceptably small compared to the response of the indicators to nourishment, allowing us to confidently assert that the model performs satisfactory for the chosen cases.

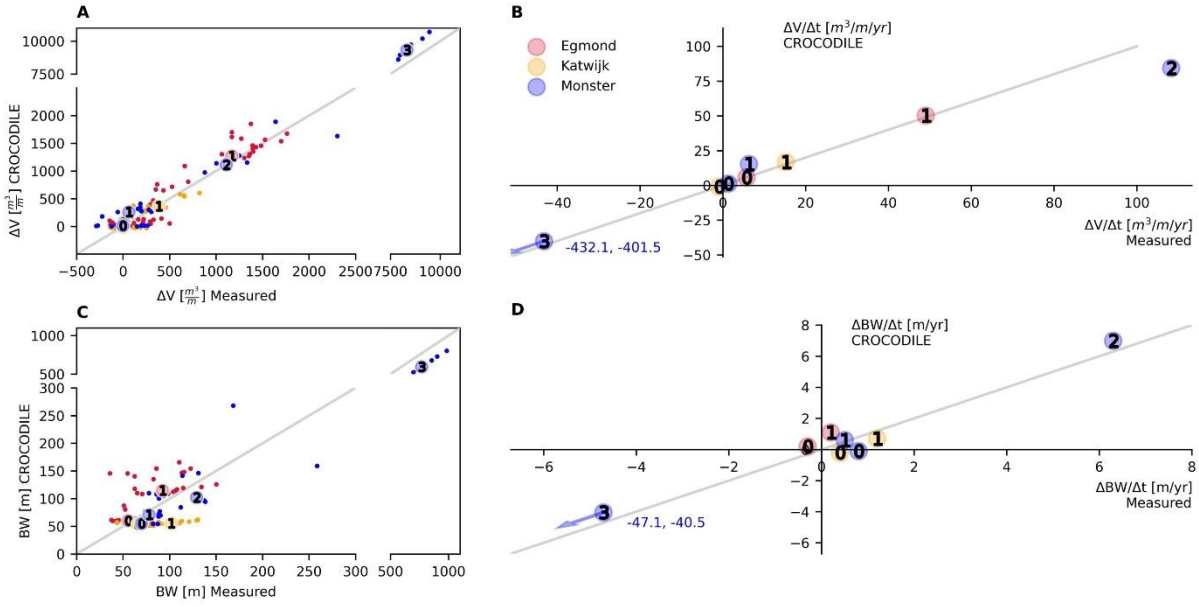

Figure 3.8 A/C Measured coastal indicators versus simulated coastal indicators. B/D Temporal trends in measured coastal indicators versus trends in simulated coastal indicators. The big dots show averages over specified nourishment timeframes, whereby the period succession (as displayed in Fig. 3.6 and 3.7) is noted by the number in the dot. The blue arrows in panel B/D indicate the direction of the last period at Monster, which lies beyond the plotting area. For all panels, the grey line indicates where these relations fit 1:1. Note that the axes in panels A/C are split to show both beach/shoreface datapoints and mega nourishment datapoints.

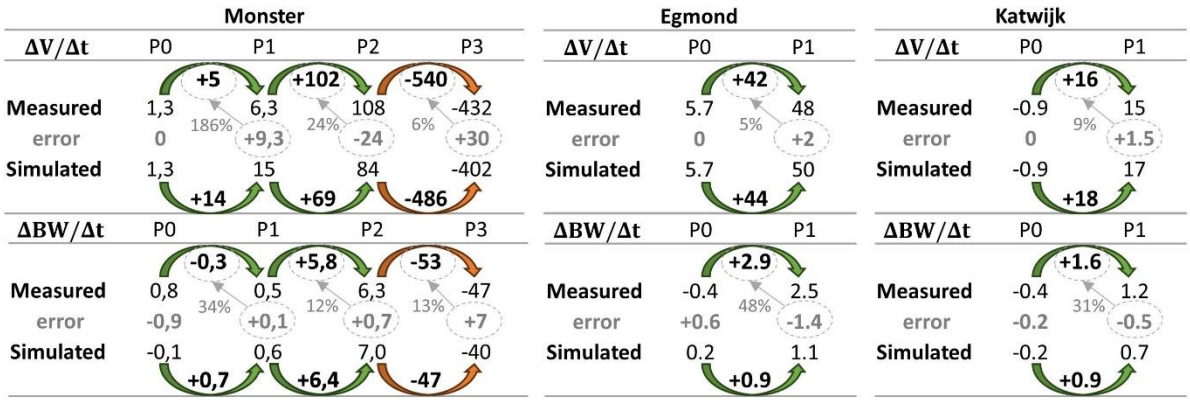

Table 3.2 Measured and simulated trends and trend reversals (noted in the bold arrows) over the specified nourishment timeframes. The error (modelled trends extracted from observed trends) is given in grey. The values under comparison are enclosed in grey dashed circles, accompanied by the percentage of the error relative to the preceding trend reversal (in absolute terms).

3.7 Discussion

Our objective was to present a model approach to evaluate nourishment strategies by simulating the decadal-scale response of repetitive nourishments to coastal volume, shoreline position and beach width. The model is behaviour-oriented, meaning that the model components are formulated to optimally simulate the evolution of these indicators without delving into the intricacies of underlying physics. Thereby, we intentionally designed the model with simple formulations to enable the decadal simulation of nourishment strategies without extensive calibration efforts. We opted for a purely cross-shore approach, simplifying our analysis by assuming that alongshore variations in coastal profiles and hydrodynamic processes along the shoreline can be disregarded for our current purpose.

While Crocodile's strength lies in its simplicity, it also serves as the primary source of its constraints. As we consider the nourishment as a profile perturbation and assume a 'dynamic equilibrium' background profile, any autonomous (nourishment-independent) profile development affecting the profile shape is not resolved. This means that cycles of storm and recovery, cyclic bar behaviour and the passage of alongshore shoreline undulations are not included in the model. In many instances, it can be challenging to discern the effects of nourishment in the observations, especially when there are substantial autonomous coastal developments. Additionally, the observations reflect stochastic aspects of hydroclimatic influences (e.g., energetic vs moderate years) that the model, being stationary forced, cannot replicate. In other words, the model's outcomes represent the 'climatology' of the simulated coast and provide the anticipated 'annual average' value for a given coastal indicator at a particular time. Consequently, the model cannot be utilized as a predictor or compute specific details of the cross-shore profile shape on short

timescales. Instead, its primary capability lies in comparing the long-term profile responses between periods with and without nourishment.

Our study confirmed that the model was able to accomplish this task, as evidenced by the accurate reproduction of trends and trend reversals between the observations and simulations. By focusing on these trends, we effectively bridged the inherent disparity between the observations and simulation results. We selected case study locations for our analysis where we did not anticipate autonomous (longshore) profile development to overshadow the response to nourishment. For future applications, the model formulations (Eq. 3.2 to 3.18) can be refined by using more complex formulations including additional hydrodynamical and morphological processes, if either the study site or modelling exercise requires this. Additionally, we anticipate that integrating Crocodile with an alongshore model could facilitate the analysis nourishment applications in alongshore non-uniform coastal settings.

Some considerations should be made regarding the selection of input parameters. The parameter values chosen for this study serve as an initial approximation for the Dutch coast. Parameter values (Table 3.1) are not universally applicable or may change in the future. When applying Crocodile in a different coastal setting, careful evaluation of these parameters is necessary. Furthermore, it is important to acknowledge that the input parameters specific to the case study are sensitive to errors in cross-shore measurements. In the present application, the temporal and spatial resolution were relatively high, but this sensitivity may become more significant when limited measurements are available. Although Crocodile is thought to be transferable to other sandy coastal environments with varying cross-shore profiles and wave climates, it is worth mentiong that this assumption is yet to be verified.

3.8 Conclusions

A diffusion based cross-shore model, Crocodile, has been developed to simulate the effects of nourishment strategies on coastal indicators such as coastal volume, coastline position and beach width over a decadal timeframe. The model contains elements to compute cross-shore diffusion, sediment exchange with the dune and alongshore sediment losses, whereby enhanced lateral loss after implementation of the nourishment is discriminated from ‘background erosion’. Crocodile was applied to a series of idealized nourishment scenarios, showing that the model can simulate expected profile responses that characterize nourishment application. Moreover, the model was applied to multiple case study locations along the Dutch coast that have undergone different nourishment strategies over the past decades. Our analysis involved a comparison between annual field measurements at these locations and the model's outcomes, demonstrating a strong alignment. Specifically, the model exhibited a 12% overestimation in profile volume compared to the measurements, while it underestimated beach width by 13%. These findings validate that the reproduced coastal indicators fall within a small range, essential for employing the model as an investigative tool to explore nourishment responses at these sites.

To assess the impact of nourishment strategies on coastal indicators in these case studies, we segmented the observation timeframe into subperiods characterized by variations in nourishment strategies (i.e. nourishment type and volumes applied). Within these subperiods, we computed trends in total profile volume and beach width for both the field measurements and simulation results. Considering all subperiods, observed volume trends ranged from -432 to $108\ m^3/m/yr$ and observed trends in beach width ranged from -47 to $6.3\ m/yr$. The median simulated volume trend was found to be $1.5\ m^3/m/yr$ (7%) higher than the measured value, while median temporal beach width trend is $0.2\ m/yr$ (15%) lower. We considered the reversals in these trends between subperiods as indicative of the dynamic profile response to different nourishment periods. These were slightly better replicated than the absolute trends. Specifically, we observed a median $2.0\ m^3/m/yr$ (4%) overestimation in volume trend reversals, and a $0.6\ m/yr$ (9%) overestimation in beach width trend reversals. Thereby, we consistently observed that all modelled trend reversals exhibit the correct sign (positive/negative). We used the magnitude of these trend reversals as a reference for interpreting the significance of the error in trends between simulation and observations. Doing so, we observed that for most of the selected subperiods, the magnitude of the trend reversal between a period and the preceding one exceeded the margin of error between simulation and measurement. This indicates that the model's error is small enough to discriminate the response of the coastal indicators to the different nourishment periods.

These results show that Crocodile successfully simulated the magnitude of key coastal indicators, as well as their temporal trend and trend reversals that coincided with the timing and magnitude of changes in nourishment strategy. Thereby, Crocodile fills a gap left by previous modelling techniques, which often focus on a single spatio-temporal scale and fail to capture the combined effects of cross-shore deformation over a decadal timeframe. Crocodile is relatively simple, robust, and computationally efficient, allowing for multiple (stochastic) simulations to be conducted within a short timeframe. Therefore, Crocodile can facilitate the evaluation of future nourishment strategies, steered by different sea level rise scenarios.

4 Exploring decadal beach profile dynamics in response to nourishment strategies under accelerated sea level rise

This chapter applies Crocodile to assess nourishment strategy performance under different sea level rise scenarios. It compares two distinct strategic nourishment approaches, offering insights into their effectiveness and sustainability. The model results highlight the importance of depth-dependent morphodynamic analysis and morphologic feedbacks such as profile steepening. This chapter extends the modelling framework's relevance to nourishment planning for climate adaptation and links closely to multifunctionality by analyzing nourishment frequency, ecological disturbance, and nourishment lifetime.

This chapter is published as:

Kettler, Tosca, Matthieu de Schipper, and Arjen Luijendijk. "Exploring decadal beach profile dynamics in response to nourishment strategies under accelerated sea level rise." Ocean & Coastal Management 260 (2025): 107477.

4.1 Abstract

Accelerated sea level rise prompts the upscaling of nourishment strategies, either through larger individual nourishment volumes or increased frequency of implementation. In such strategies, the nourished sand may lack time to effectively redistribute in the designated timeframe, leading to significant deformation of the profile over multiple nourishment cycles. This study quantifies subsequent effects, focusing on profile steepening, nourishment lifetimes, and the feasibility of operational objectives. We simulated two common nourishment strategies at a Dutch case study location using the cross-shore morphological model Crocodile over a 50-year timespan under sea level rise rates of 2 to 32 mm/year. The choice of strategy led to a variation up to 75% in the total amount of sand used. Our results show increasing profile deformation with nourishment volume applied and duration of the nourishment strategy, with sand accumulating in the nourished section and little dissipation to the lower shoreface. The consequent profile steepening leads to reduced nourishment lifetimes by up to 30%. Additionally, under high sea level rise rates, more erosive coasts experience a reduction in nourishment lifetimes down to annual intervals, while less erosive areas require up to four times more sand than currently needed. These findings illustrate key dilemmas in the formulation of future

nourishment strategies and highlight the importance of optimizing these strategies to account for sea level rise.

4.2 Introduction

The use of nourishments is widely adopted to protect low-lying coastal areas from coastal erosion and sea level rise. Planning of longer-term programs involving nourishment application encompasses various design considerations, including the volume of sand applied, the anticipated return period between nourishments, and the depth at which sand is added to the cross-shore profile. There are notable variations among countries in their coastal management practices concerning nourishment (Brand et al., 2022; Cooke et al., 2012; Defeo et al., 2009; Hanson et al., 2002). Some countries, such as Italy and France, apply nourishment mostly in a reactive strategy in response to local requirements. Typically, the need for nourishment revolves around mitigating erosion at the local scale to prevent coastline retreat, but it may also include creating space for recreation. Long-term planning, an overarching strategy, or regular monitoring of the coastline may not always be present in these cases. Other countries, such as Germany and the Netherlands, established proactive long-term nourishment programs that involve operational objectives on factors such as the volume of sand applied and coastal state indicators such as coastline position, beach width and sand volume in the profile (Brand et al., 2022; Hanson et al., 2002). For example, the Netherlands has established a strategic goal to "sustainably maintain flood protection levels and sustainably preserve functions of dune areas" (Lodder et al., 2020). This goal translates into a tactical approach to keep the sediment budget in the coastal system, extending from MSL-20 m (mean sea level, referred to as NAP (Normaal Amsterdams Peil) in Dutch studies) up to the inner dune row, in equilibrium with sea level rise. The operational objectives of this approach include guidelines on the position of the coast and the annual volume of sand to be nourished. The design and assessment of such a nourishment program necessitate regular monitoring of the bathymetry and a thorough understanding of the coastal system. Also, sand volumes applied are generally higher and therefore this approach is only feasible if sufficient sand and the financial resources required for the execution of the program are available (Hanson et al., 2002).

Presently, adapted long-term nourishment programs to mitigate higher rates of sea level rise are formulated and explored (Haasnoot et al., 2020; Rijkswaterstaat, 2020). These programs often involve significantly greater volumes of sand compared to present-day practices. For instance, Haasnoot et al. (2020) estimated that nourishment volumes up to 20 times larger than those currently employed may be necessary to address extreme sea level rise rates of 60 mm per year at the Dutch coast. Achieving this could involve upscaling either the individual nourishment volume, the frequency of return, or both. A widely accepted assumption in formulating such nourishment programs is that coastal profiles respond to nourishment by rapid adjustment to a (new) equilibrium shape incorporating the added sand volume (Bruun, 1962, 1954; McCarroll et al., 2021a). From this viewpoint, the total amount of added sand is the primary concern for profile evolution, while specific design elements like cross-shore

location, frequency of return, and individual nourishment volumes are considered less critical. The validity of this perspective hinges on the timescale of equilibration of the coastal profile in relation to the timescale and extent of profile deformation caused by nourishment. Such profile equilibration is realized under the force of waves, wind, and tidal currents, which do not uniformly affect the profile. The upper profile experiences higher energy levels compared to the lower part, resulting in varying rates of sand redistribution along the profile. Consequently, timescales for morphological adaptation in response to altered boundary conditions such as nourishment implementation range from hours around the waterline to millennia near the inner shelf (Stive and de Vriend, 1995).

Therefore, it can take several decades for nourished sand to reach slower responding (lower-elevation, more seaward) areas in the profile (Hands and Allison, 1991). In the same rationale, nourishments placed lower in the profile typically redistribute slower (Beck et al., 2012), requiring shoreface nourishment to be about 25% larger than beach nourishment volumes for similar impact (Stive et al., 1991). The rate and extent of nourishment redistribution increase with larger nourishment volumes (Gijsman et al., 2018), with finer nourishment grain sizes (Ludka et al., 2016), and may be influenced by the presence of geological or man-made structures (Faraci et al., 2013). Additional factors influencing sand redistribution are, amongst others, the profile shape(e.g. de Schipper et al., 2015; Liu et al., 2024), the wave climate and surf zone processes (Pang et al., 2021, 2020), the sand's mineralogical composition (Yao et al., 2024) and sorting processes (Duan et al., 2020).

In future nourishment scenarios involving higher nourishment volumes we hypothesize that the nourished sand may lack time to effectively redistribute in the designated timeframe. Over multiple nourishment cycles this can lead to significant deformation of the profile shape, such as widening of beaches and the steepening of the profile when nourished sand accumulates in the nourished profile section. Observations of such profile deformation effects have already been documented in the Netherlands, where several decades of nourishment have resulted in notable steepening of the profile (Rijkswaterstaat, 2020; van der Spek and Lodder, 2015).

Profile steepening has been suggested to shorten the lifespan of individual nourishments, as it can lead to increased wave energy levels higher in the profile, inducing accelerated sand dispersion from the active zone to the lower shoreface (Stive et al., 1991). However, no such acceleration was observed after implementing a mega nourishment, despite a 50% increase in submerged profile slope between MSL-3 and MSL-19 m (Taal et al., 2023). As repeated upper profile nourishment may at most cause a similar effect, it can be deduced that the dissipation of nourished sand to the lower shoreface will have a minor impact on nourishment feasibility. Therefore, there is little reason to require the lower shoreface to grow along with sea level rise for coastal safety purposes. For the Netherlands, which maintains a tactical approach of keeping the sediment budget in the coastal system with a lower limit at MSL-20 m, this lower limit could be adjusted to a shallower depth. This knowledge is relevant as a future concern in high-volume nourishment scenarios is the extensive usage of sand. The seabed of the North Sea might in high-volume nourishment scenarios lack

sufficient mineable sand volumes for nourishment, and socio-economic developments may compete for sand as a resource, such as for constructing infrastructure (Bendixen et al., 2019; Torres et al., 2017).

Yet, the extent to which future upscaled nourishment volumes disperse and their effects - such as profile steepening, reduced nourishment return periods, and challenges in achieving strategic goals - are minimally quantified in present-day literature. The recently developed cross-shore morphological model Crocodile (Chapter 3) is specifically designed to simulate decadal profile responses to repeated nourishment, providing an opportunity to quantify these effects. In this study, we use this model to explore the physical feasibility of nourishment strategies involving larger sand volumes. To this end, two nourishment strategies are formulated that represent two outer ends within the spectrum of nourishment programs currently deployed in different countries; a hold-the-line strategy as reactive approach with minimal sand usage, and a sand balance strategy as proactive option aiming to elevate the coastal system, stretching seaward as deep as MSL-20 m, along with sea level rise. With Crocodile, 50-year morphological simulations are performed wherein these strategies are applied at a Dutch case study location, under sea level rise rates ranging from 2 to 32 mm/yr.

Based on the simulations conducted, we explore the solution space to mitigate accelerated sea level rise within the boundaries of laterally uniform nourishment strategies. Our goal is to establish explicit time-dependent relationships between nourishment strategy, sea level rise, and nourishment dispersion, with a specific focus on quantifying how much sand reaches the lower shoreface and addressing concerns about coastal steepening and reduced nourishment lifespan. We also simulate how different tactical approaches affect the volume of sand used. The insights gained aim to inform strategic decisions for nourishment programs, including the appropriate volume of sand to be applied as formulated within operational objectives.

This paper begins by detailing the relevant morphological and hydrodynamical characteristics of the central Holland coast, along with a description of the Dutch present-day operational nourishment programme (2.1). Hereafter, the numerical diffusion-based model Crocodile is briefly described (2.2), followed by an outline of the simulations performed which differ in rate of sea level rise and nourishment strategy (2.3). For all simulations, we explore the cross-shore profile dynamics and nourishment efficiency (3) and discuss insights and implications that can be drawn from the results (4). Finally, the paper concludes (5) by summarizing the main findings and evaluating the effectiveness of the simulated nourishment scenarios under different rates of sea level rise.

4.3 Methods

4.3.1 Case study

Our case study location is located along the Dutch sandy coast, a densely populated delta region where protection against relative sea level rise is crucial to prevent socio-economic disasters. A central region, the Holland Coast, was selected because of its

well-documented and intensive local nourishment policy, and the extensive monitoring program providing yearly altimetric and bathymetric profile measurements (Wijnberg and Terwindt, 1995a). Within this region, we adopt an unnourished coastal profile at the beach town called Monster (Fig. 4.1) as initial profile for our simulations.

Site description

The Holland coast consists of sandy beaches and dunes with an average tidal range of about 1.6 m (Wijnberg and Terwindt, 1995a). The nearshore zone is characterized by a gradual sloping beach profile, occasionally interspersed with periodic nearshore bars. The shoreface slopes vary alongshore between 1:160 and 1:400, and slopes in the breaker zone vary from about 1:50 to 1:150 (Wijnberg and Terwindt, 1995a).

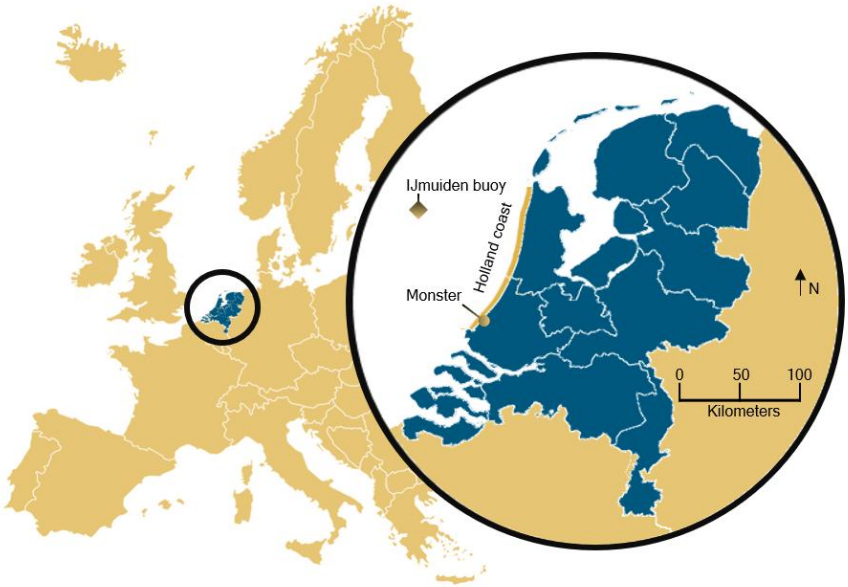

Figure 4.1 Location of case study site along the sandy Dutch coast and the IJmuiden wave station used for the long-term wave data.

Due to the rising sea level, soil subsidence and a declining sedimentary input from marine and riverine sources this coastal area has an erosive character. Therefore, the Dutch government executes a proactive nourishment program, wherein the main strategic goal is to maintain sustainable flood protection (Lodder et al., 2020). This program locally adheres to a hold-the-line approach, where the primary objective is to maintain the coastline seaward from a reference line (Van Koningsveld and Mulder, 2004). This reference line, known as the basal coastline 'BCL', has been determined based on the coastline position between 1980 and 1990. The momentary coastline 'MCL' serves as a volume-based proxy for the current shoreline position and is to be preserved seaward from the BCL. The position of the MCL is determined by calculating a weighted average of the cross-sectional profile volume A (in m3/m alongshore) between the horizontal dune foot position (X_{df}) and the low water line plus the same elevation (h) below the low water line (Fig. 4.3D). It is expressed in meters relative to the BCL:

$$MCL = \frac{A}{2h} + X_{df} \tag{4.1}$$

The adoption of this volume-based approach aims to avoid that local small-scale variations in profile height, such as intertidal sand bars, result in large fluctuations in MCL (Van Koningsveld and Mulder, 2004). The MCL position is evaluated each year, and nourishments are carried out when it is landward of the BCL or anticipated to cross the BCL in the following year (Brand et al., 2022).

Since 2000, a second criterium has been used to maintain the sediment budget in the coastal system in equilibrium with sea level rise (SLR). Based on Mulder (2000) estimates of regarding the annual sediment demand in the coastal system, this is realized by the operational objective to annually nourish 12 million m^3 sand. For future sea level rise scenarios, the annual sediment demand V_{sd} is calculated as follows (Lodder and Slinger, 2022):

$$V_{sd} = A_{cf} * SLRr + V_{sub} + V_e \tag{4.2}$$

In this equation, A_{cf} represents the planform surface area of the coastal foundation (in m^2) which is the coastal area that is wished to grow along with sea level rise, defined as the area between MSL -20 m up to the inner dune row. Thereby, A_{cf} is regarded as the active profile on multiple-decadal timescales. $SLRr$ denotes the local relative sea level rise rate, expressed in m/yr. V_{sub} includes the local sediment demand (in m^3/yr) caused by sand extraction and anthropogenically induced subsidence due to the extraction of gas, oil, and salt. Both are not accounted for in the definition of relative sea level rise. V_e includes the net export of sand (in m^3/yr) from the coastal foundation area over its boundaries. This includes the sand export to the tidal inlets along the Dutch coast (Wadden sea, Western Scheldt) and the potential net export over the Dutch borders.

It is not established in the operational objectives how and where the added volume V_{sd} should be nourished. Typically, sand is added to depths shallower than MSL - 8 m, either directly onto the beach for beach nourishment or between MSL-4 and MSL-8 m for shoreface nourishment. The quantity and type of nourishment supplied vary per location and depend on various factors such as the current condition of the beach and dune system, anticipated future changes, and the preferences of local stakeholders. As not every location is suitable or desirable for nourishment, some nourishment locations receive additional sand to ensure that the volumetric target, annual nourishing V_{sd}, is reached.

4.3.2 The model: Crocodile

With the numerical diffusion-based model Crocodile (Chapter 3), we conduct 50-year morphological simulations of a coastal transect with bed level $Z\ (x, t)$, with x referring to the horizontal coordinate and t referring to time. This model has specifically been developed to simulate effects of nourishment strategies on coastal profile evolution over a multiple-decadal timeframe (e.g. Fig. 4.2). Crocodile has been built upon the philosophy that the introduction of a nourishment essentially constitutes a

perturbation to a coast, having a particular dynamic state (similar to models developed by e.g. Chen and Dodd, 2021, 2019; Coelho et al., 2017; Marinho et al., 2017; Stive et al., 1991). Over sufficiently long temporal and spatial scales, this perturbation is diffused in cross-shore and alongshore directions. Thereby, a continuous and gradual adaptation of the coastal profile takes place towards a 'dynamic equilibrium' profile $Z_{eq}\ (x,t)$. This profile represents the theoretical shape and position the coastal profile would attain if all physical forces (waves, winds and tidal currents) and boundary conditions (sea level elevation and sand budget) in the coastal system remained constant with time. Changes in these boundary conditions (e.g., sea level rise, alongshore transport gradients, or the implementation of nourishments) lead to horizontal and vertical translation of $Z_{eq}\ (x,t)$ as given by a sediment volume balance. The translation of the profile due to sea level rise is modelled based on the principles established by Bruun (1954, 1962), whereby $Z_{eq}\ (x,t)$ is raised by the change in sea level and shifted onshore to balance total sediment volume.

Every timestep t, Crocodile computes the 'instantaneous' bed level $Z\ (x,t)$ being the time-dependent profile approaching the dynamic equilibrium profile $Z_{eq}\ (x,t)$. The rate and extent of sand dispersion in $Z\ (x,t)$ depend on the vertical difference between $Z\ (x,t)$ and $Z_{eq}\ (x,t)$ as well as z', being the profile depth relative to the mean sea level MSL:

$$\frac{\mathrm{d}(\mathrm{Z}-\mathrm{Z_{eq}})}{\mathrm{dt}}=\frac{\mathrm{d}}{\mathrm{dx}}\left\{\mathrm{D}(\mathrm{z}')\frac{\mathrm{d}(\mathrm{Z}-\mathrm{Z_{eq}})}{\mathrm{dx}}\right\}+\varepsilon_{\mathrm{D}}(\mathrm{z})+\mathrm{E}(\mathrm{z}')+\mathrm{F}(\mathrm{Z}-\mathrm{Z_{ini}})+\mathrm{W}\left(\mathrm{Z}-\mathrm{Z_{eq}}\right)+\mathrm{Source}(\mathrm{z}',\mathrm{t}) \tag{4.3}$$

The first and second RHS components of Eq. 4.3 describe cross-shore diffusion, with $\varepsilon_{\mathrm{D}}(\mathrm{z})$ being a correction term for volume conservation. These elements have varying time-dependent effects on cross-shore development (Chapter 3, Fig. 3.1). By inclusion of a diffusion coefficient, $D(z')$, the dependency of time-dependent profile dynamics on water depth z' is incorporated. $D(z')$ represents the average sediment redistribution capacity along the profile and thereby regulates the morphological timescale of response. It determines the rate and extent of cross-shore sand diffusion and thereby has a key role in both the time-dependent nourishment dispersion, as well as the depth-dependent coastal adaptation to sea level rise. The shape of $D(z')$ is prescribed as a function of boundary conditions and the local hydrodynamic climate, facilitating easy implementation of locations with different hydrodynamic characteristics in Crocodile. The third and fourth components on the RHS of eq. 4.3 represent alongshore sand losses, the fifth component describes sand exchange with the dune, and nourishments are incorporated as a source term.

The model is behaviour-oriented, meaning that the model components are formulated to optimally simulate the evolution of the cross-shore profile without aiming to resolve the underlying physics other than mass-conservation. As we consider a nourishment as a profile perturbation and assume a 'dynamic equilibrium' background profile, any autonomous (nourishment-independent) profile

development affecting the profile shape is not resolved. This means that cycles of storm and recovery, cyclic bar behaviour and the passage of alongshore shoreline undulations are not included. The model was validated using three Dutch case study locations in Kettler et al. (2024), reproducing the decadal evolution of bulk parameters such as beach width, shoreline position, and coastal volume for nourishment strategies with varying nourishment volumes and cross-shore placement. On average, volumetric trends were overestimated by 1.5 m3/m/yr (7%), while modelled coastline trends were 0.2 m/yr (15%) lower than observed. A more detailed description of the model and the validation study is available in Kettler et al. (2024).

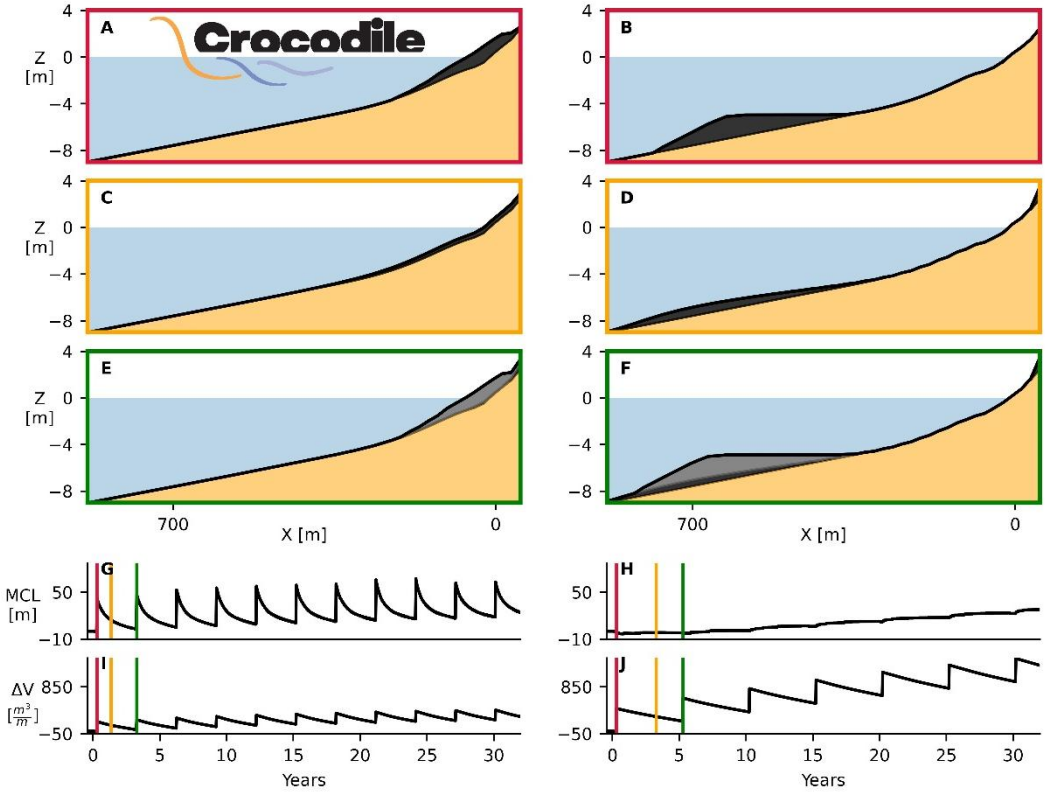

Figure 4.2 Simulated profile behaviour for 2 nourishment strategies by Crocodile. Left: $200\ m^3/m$ beach nourishment is applied every 3 years. Right: $450\ m^3/m$ shoreface nourishments every 5 years. The upper three rows display the evolution of bed level $Z(x,t)$ at different times in a nourishment cycle (times are indicated by the coloured lines in the timeseries in the lower panels). Bottom two rows show the temporal evolution of shoreline position MCL-BCL and profile cross-sectional volume ΔV. The peaks in ΔV and the corresponding responses in MCL-BCL arise from the implementations of individual nourishments.

Profile schematization

All simulations start from the same initial profile, which is derived from a set of yearly alti- and bathymetric surveys at Monster over an unnourished period (1966-1979), obtained from the JARKUS dataset (Wijnberg and Terwindt, 1995a). The initial profile (both

$Z\ (x, t = 0)$ and $Z_{eq}\ (x, t = 0)$) is a smoothened multi-year average from these surveys, such that sub-decadal autonomous coastal behaviour (e.g., storm cycles, cyclic bar behaviour) is excluded. This approach allows us to avoid selecting a theoretical definition of Z_{eq}, which would otherwise necessitate making assumptions about hydrodynamic conditions (Dean, 1991), sediment characteristics (Yao et al., 2024), and other environmental factors that could introduce uncertainties into determining the equilibrium profile.

The slope of the resulting initial profile in the 'active' zone between MSL - 10 m and the dune foot (MSL + 3 m) is 1:115. The dune front is represented by a linear slope extending from the dune foot Z_{df} to the upper model boundary Z_{max}, with the slope equal to the dune slope observed between MSL + 4 and MSL + 6 m, which was 1:3.875 at Monster.

Parametrization

The temporal resolution in the numerical scheme dt is 1/10 year, the spatial resolution in the cross-shore dx is 20 m. The mean water level is set $MWL(t = 0) = \mathrm{MSL} + 0\ \mathrm{m}$. All hydrodynamic and morphodynamic parameter values are obtained from literature concerning the central Dutch coast, equal to Kettler et al. (2024). Because of its importance for the outcomes, we highlight the key parameter related to cross-shore diffusion and erosion, diffusion coefficient $D(z')$. To define $D(z')$, both a maximum value D_{max} is required, as well as hydrodynamic statistics to define its depth-dependency. The maximum of $D(z')$, D_{max}, is adopted from De Vriend et al. (1993), who estimated that $D_{max} = 60\ m^2/day$ for the central Dutch coast. $D(z')$ has this maximum value in the surf zone, and its magnitude over the remainder of the profile is a fraction of D_{max} based on offshore wave height and water level statistics obtained from the IJmuiden wave station located 35 km offshore (Fig. 4.1). Total background erosion rate $E_{longshore}$ is fixed at 40 $m^3/m/yr$ in our simulations. During the period from 1750 to 1980, the coastline retreat near Monster was about 300 m (Dillingh and Stolk, 1989). Assuming an active profile height of 30 m (from -20 MSL to +10 MSL), it can be inferred that a representative long-term total background erosion is approximately $300 * 30/230 \approx 40\ m^3/m/yr$.

Nourishment design parameters

The design height, landward slope, and seaward slope of the implemented nourishments are based on prevalent Dutch values as described by Brand et al. (2022). Hereby we discriminate between beach nourishments and shoreface nourishments. Both are implemented with triangular cross shore shapes, comprising a near horizontal platform and a linear slope towards the nourishment toe. For beach nourishments the platform connects with the original profile at elevation $H_n = MSL + 2\ m$. The landward slope is $S_{lw} = 1{:}200$ and the seaward slope S_{sw} is taken equal to the intertidal slope of $Z_{eq}(x, t = 0)$ between high water level $z'_{HW} = MSL + 1\ m$ and low water level $z'_{LW} = MSL - 1\ m$:

$$S_{sw} = \frac{Z'_{HW} - Z'_{LW}}{X_{eq}[Z'_{HW}] - X_{eq}[Z'_{LW}]} \tag{4.4}$$

Whereby $X_{eq}[z']$ refers to the horizontal position of the equilibrium profile intersecting with depth z'. For the profile at Monster S_{sw} = 1:40. Shoreface nourishments are implemented with $H_n = MSL - 5\ m$, $S_{lw} = 1{:}10000$ and $S_{sw} = 1{:}50$.

Evaluated coastal indicators

Crocodile computes the evolution of instantaneous bed level elevation $Z(x,t)$, which is translated into a set of coastal indicators. To analyse the dispersion of the nourished sand in our simulation, we examine changes in the volume of sand stored in two vertically constrained profile sections (Fig. 4.3A). The lowest section represents the volume of the lower shoreface and its change ΔV_{ls} is given by integrating the change in $Z(x,t)$ over this section:

$$\Delta V_{ls} = \int_{X_{min}}^{X_{doc}} \big(Z(x,t) - Z(x,t=t_0)\big)\, dx \tag{4.5}$$

The upper section represents the active profile and its change ΔV_{ap} is given by:

$$\Delta V_{ap} = \int_{X_{doc}}^{X_{max}} \big(Z(x,t) - Z(x,t=t_0)\big)\, dx \tag{4.6}$$

The change in total profile volume ΔV_p is then equal to the sum of ΔV_{ls} and ΔV_{ap}:

$$\Delta V_p = \Delta V_{ls} + \Delta V_{ap} \tag{4.7}$$

In these definitions, X_{min} is the seaward model boundary, positioned at $Z(X_{min}, t = 0) = NAP - 20\ m$ in this work. The horizontal position X_{doc} represents the depth of closure in the initial profile, serving as a boundary between the active profile and lower shoreface. We approximate its depth at $Z(X_{doc}, t = 0) = NAP - 10\ m$ in this application (Hinton and Nicholls, 1998). X_{max} is the landward horizontal position where $\frac{dZ}{dt} = 0$ throughout the simulations, approximately positioned at $Z\big(X_{df}, t = 0\big) = NAP + 6\ m$. Two sinks of sand outside the modelled profile exist, which are direct outputs from the model. These are ΔV_{dune}, which is the cumulative volume of sand transported towards the dunes, and the volume that has eroded alongshore $E_{longshore}$. We compare ΔV_{ls}, ΔV_{ap}, ΔV_{dune} and $E_{longshore}$ to the cumulative total nourished volume ΣV_N:

$$\Sigma V_N = \sum_{t=0}^{t} V_N\, dt \tag{4.8}$$

Wherein V_N is the individual nourishment volume. Additionally, we compute the required profile volume change ΔV_{L_p*SLR} to elevate the profile with sea level rise (SLR) (Fig. 4.3B):

$$\Delta V_{L_p*SLR} = L_p * SLR \tag{4.9}$$

With L_p being the profile length between X_{min} and X_{max}. Comparing V_{L_p*SLR} to the sum of ΔV_{ls} and ΔV_{ap} shows how the sand budget in the profile evolves with respect to sea level rise. If these two are equal, the sand budget is sufficient for this profile to grow along. Additionally, we analyse the position of the MCL with respect to BCL, which is determined as $BCL = MCL(t = 0)$ in the current analysis. Herein X_{df} is positioned at $Z(x, t = 0) = 3m$. Moreover, the submerged profile slope S_p between $z' = MSL(t) - 19$ and $z' = MSL(t) - 3$ is evaluated to quantify profile steepening (Fig. 4.3C):

$$S_p = 16/(X[z' = MSL(t) - 19, t] - X[z' = MSL(t) - 3, t] \tag{4.10}$$

The slope of the initial profile $Z(x, t = 0)$ is given by:

$$S_{ini} = S_p(t = 0) \tag{4.11}$$

(10)

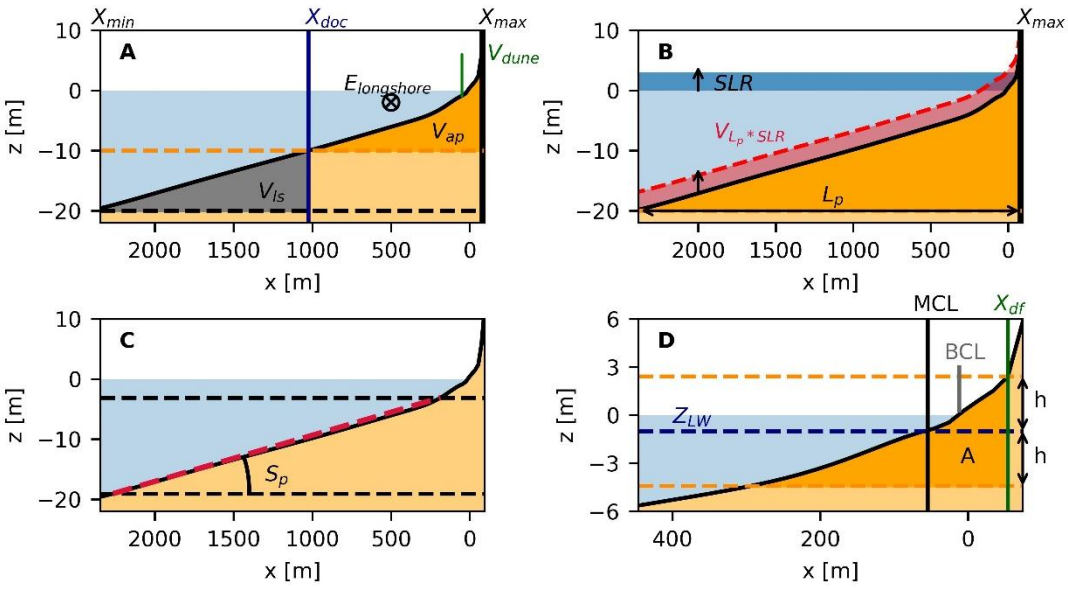

Figure 4.3 Overview of evaluated parameters. A) Two volumetric profile sections V_{ap} (in orange) and V_{ls} (in grey), which are horizontally constrained by the horizontal positions X_{min}, X_{doc} and X_{max} in the initial profile. Sand fluxes $E_{longshore}$ and V_{dune} are indicated with arrows. B) The required volume to elevate the profile with sea level rise V_{L_p*SLR} for profile length L_p. C) Submerged profile slope S_p. D) Momentary coastline MCL and basis

coastline BCL. The profile section between the orange dashed lines is utilised to compute MCL and is also referred to as the MCL zone.

4.3.3 Scenarios

Sea level rise scenarios

We consider a set of stationary sea level rise rates ($SLRr$): 2, 4, 8, 16 and 32 mm/yr, which is hereafter referred to as $SLRr2, SLRr4, SLRr8, SLRr16$ and $SLRr32$. These rates remain constant throughout the simulation for simplicity. Thereby, we avoid specifying when in time this occurs, which is inherently uncertain. The sea level rise rates are based on expected sea level rise rates in the Netherlands over the next century, estimated by KNMI (2023) (see appendix A1). The KNMI scenarios provide the context for the sea level rise rates adopted in this research. $SLRr2$ reflects conditions over the past decades, $SLRr4$ serves as an estimate for the next decade, $SLRr8$ is anticipated several decades from now, and $SLRr16$ may be approached near the end of this century under high emissions. $SLRr32$ is included to explore extremities, without pretending high likelihood of occurrence.

Nourishment scenarios

We established conceptual nourishment scenarios, categorized in two subsets based on different operational objectives. The first subset follows a 'proactive sand balance strategy' with predefined nourishment volumes inspired by the present-day Dutch nourishment program (Fig. 4.4 – left column). The second subset of conceptual nourishment scenarios adopts a 'reactive hold-the-line strategy' (Fig. 4.4 – right column). Both subsets are simulated twice under all different sea level rise rates (2.3.1.), whereby nourishments are either repeatedly placed directly on the beach or as shoreface nourishment.

2.3.2.1 Proactive sand balance strategy

The first subset of conceptual nourishment scenarios follows a 'proactive sand balance strategy', where nourishments are planned based on expected sand losses and sea level rise. The modelled scenarios use predefined nourishment volumes in line with the present-day Dutch nourishment program (depicted in Fig. 4.4A,B). Presently, adapted proactive sand-balance strategies are formulated to define the coastal zone management of the Netherlands under climate change (Haasnoot et al. 2020, RWS kustgenese2.0). These strategies estimate future annual nourishment volumes required to elevate the coastal foundation zone, stretching seaward as deep as MSL-20 m, along with sea level rise. By simulating such scenarios, we aim to study potential constraints when upscaling the current Dutch nourishment program with larger volumes of sand.

We hypothesized earlier that sand may accumulate in the nourished area if the nourished sand does not effectively redistribute within the designated timeframe, leading to beach widening and profile steepening. Therefore, we evaluate to what extent the upscaled nourishment volumes spread over the whole design area (i.e. the coastal foundation zone over its full depth). Moreover, if the nourishment accumulates high in the profile, we assess how much the beach widens over time ($MCL - BCL$) and

how much the profile steepens (ΔS_p). Furthermore, by comparing $V_{L_{p*SLR}}$ to the sum of ΔV_{ls} and ΔV_{ap} we assess whether the sediment budget in the profile balances with sea level rise, and thereby whether the design objective is fulfilled.

We follow a top-down methodology, where the local nourishment volume in the considered transect is determined based on the sediment demand in the coastal foundation area (A_{cf}). The strategic goal is to raise A_{cf} in response to sea level rise. The required volume of sand for this purpose, sediment demand V_{sd}, is defined using Eq. 4.2 for the different rates of sea level rise. We base the equation components on (Rijkswaterstaat, 2020), with the adoption of $A_{cf} = 702\ km^2$ (Rijkswaterstaat, 2020 Table 6-2) for the central Dutch coast, and $V_e + V_{sub} = 2.568\ mln\ m^3/yr$. Consequently, V_{sd} amounts to 3.972 $mln\ m^3/yr$ for $SLRr2$, approximately doubling for $SLRr8$, and escalating to over six times as large for $SLRr32$ (Table 4.1).

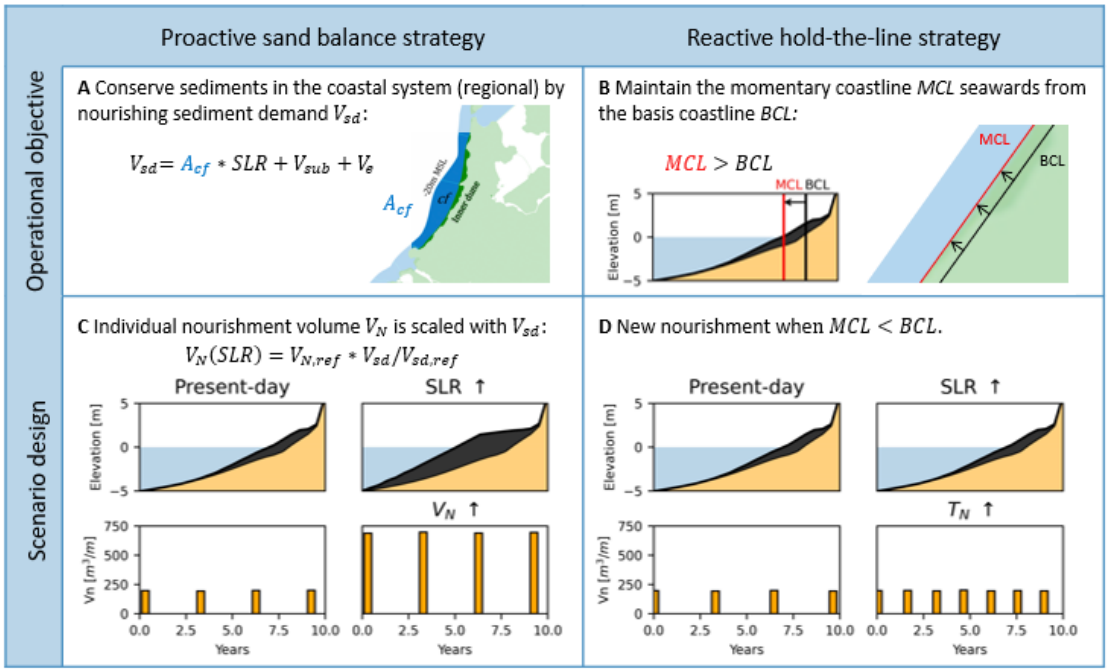

Figure 4.4 Schematic illustration of the operational objectives and scenario design for the nourishment *scenarios established in this research. (A) The operational objective for the proactive sand balance strategy is to conserve sediments in the regional coastal system by nourishing sediment demand V_{sd}. This includes the volume of sand required to elevate the coastal foundation area A_{cf}, stretching seaward as deep as MSL-20 m, along with sea level rise, and compensate for subsidence V_e and sand loss due to erosion V_e. (B) The operational objective for the reactive hold-the-line strategy is to maintain the momentary coastline MCL seawards from the basis coastline BCL. (C) The scenario design adopted in the proactive sand balance strategy is to upscale individual nourishment volume V_N proportionally in relation to V_{sd} under accelerated sea level rise. (D) The scenario design adopted in the reactive hold-the-line strategy is to place a new nourishment when the MCL crosses landwards from the BCL.*

To design nourishment scenarios at our case study site, we must make assumptions about the distribution of V_{sd} along the coast. In the Netherlands, nourishment is typically concentrated in specific locations known as erosional hotspots, characterized by higher erosion rates compared to the surrounding areas. Conversely, other locations are not suitable or desirable to receive nourishment. Additional nourishments are occasionally placed at the erosional hotspots to ensure that the volumetric target of annual nourishing V_{sd}, is reached. We presume our case study transect to be one such location, and we assume the continuity of this policy.

As a result, our scenarios incorporate nourishment volumes that surpass the average sediment demand per meter alongshore in the region. This demand can be computed by dividing V_{sd} by the total length of the central Dutch coast L_c (V_{sd}/L_c wherein $L_c = 107\ km$). For $SLRr2$, V_{sd}/L_c is $37\ m^3/m/yr$, equivalent to beach nourishment volumes of $121\ m^3/m$ every $3\ yr$ or shoreface nourishments of $185\ m^3/m$ every $5\ yr$. These values are notably smaller than the average nourishment applications at nourished sites in the Netherlands over the past few decades. As reported by Brand et al. (2022), beach nourishments in the Netherlands have an average individual volume of $200\ m^3/m/yr$ with a $3-yr$ return period and shoreface nourishments have average volumes of $450\ m^3/m/yr$ with a $5-yr$ return period. This disparity between the average sediment demand and actual nourishment volumes arises from the uneven distribution of nourishments along the Dutch coast.

We formulate two conceptual present-day strategies for our case study site grounded in the findings of Brand et al. (2022). One involves beach nourishment of $200\ m^3/m/yr$ every $3\ yr$, and the other involves shoreface nourishment of $450\ m^3/m/yr$ every $5\ yr$. Recalculated to yearly sand usage, the applied beach nourishment amounts to $66\ m^3/m/yr$, and the applied shoreface nourishment is higher with $90\ m^3/m/yr$. These values can be adjusted for different sea level rise while maintaining a constant frequency of nourishment. Then the individual nourishment volume V_N is proportionally upscaled in relation to V_{sd}:

$$V_N(SLR) = V_{N,ref} * V_{sd}/V_{sd,ref} \tag{4.12}$$

Here, $V_{N,ref}$ and $V_{sd,ref}$ respectively represent the nourishment volumes and sediment demand under $SLRr2$. With Eq. 4.12, individual nourishment volumes are, similar to V_{sd}, doubled for $SLRr8$, and sixfold for $SLRr32$ (Table 4.1). While such large cross-sectional nourishment volumes have been implemented before (Brand et al., 2022; Valloni et al., 2007), there are no known locations where such large volumes have been consistently nourished at 3- or 5-year intervals.

It should be kept in mind that upscaling V_{sd} for sea level rise mitigation could also be realized by increasing the frequency of nourishment, instead of increasing individual nourishment volumes. Nevertheless, for the computed sediment demand opting for an increase in frequency is anticipated to be an unfavourable strategy for ecological and socio-economic reasons (Schipper et al., 2021). The sediment demand under high sea level rise namely demands a significantly shortened return period T_N. For example, under $SLRr8$, T_N decreases to approximately 1.5 years for beach

nourishment and 2.4 years for shoreface nourishment (Table 4.1, 2 lowest rows). Moreover, adjusting frequency shows similar outcomes as increasing individual nourishment volume for the evaluated coastal indicators within the presented approach. Therefore, only the volume upscaled scenarios are presented hereafter.

Table 4.1 Nourishment options for different $SLRr$ scenarios. From top to bottom: $\boldsymbol{SLRr}$ - rate of sea level rise; $\boldsymbol{V_e + V_{sub}}$- volumes of exported sand $\boldsymbol{V_e}$ and anthropogenically induced subsidence $\boldsymbol{V_{sub}}$; $\boldsymbol{A_{cf} * SLR}$ - volume of sand needed to elevate the coastal foundation zone $\boldsymbol{A_{cf}}$ with sea level rise; $\boldsymbol{V_{sd}}$ - total sediment demand; $\boldsymbol{V_{sd}/V_{sd,ref}}$ - nourishment upscaling ratio; $\boldsymbol{V_N\ Beach}$ - beach nourishment volume (for a constant return period of 3 yr.); $\boldsymbol{V_N\ Shoreface}$ - shoreface nourishment volume (for a constant return period of 5 yr.); $\boldsymbol{T_N\ Beach}$ - beach nourishment return period (for a constant nourishment volume of $200\ m^3/m$); $\boldsymbol{T_N\ Shoreface}$ - shoreface nourishment return period (for a constant nourishment volume of $450\ m^3/m$).

$\boldsymbol{SLRr}\ (mm/yr)$	**2**	**4**	**8**	**16**	**32**
$\boldsymbol{V_e + V_{sub}}\ (mln\ m^3/yr)$	2,6	2,6	2,6	2,6	2,6
$\boldsymbol{A_{cf} * SLRr}\ (mln\ m^3/yr)$	1,4	2,8	5,6	11,2	22,5
$\boldsymbol{V_{sd}}\ (mln\ m^3/yr)$	4,0	5,4	8,1	13,8	25,0
$\boldsymbol{V_{sd}/V_{sd,ref}}$	1,0	1,4	2,1	3,5	6,3
$\boldsymbol{V_N\ Beach}\ (m^3/m),\ T_N = 3\ yr$	**200**	**271**	**412**	**695**	**1260**
$\boldsymbol{V_N\ Shoreface}\ (m^3/m),\ T_N = 5\ yr$	**450**	**609**	**927**	**1563**	**2836**
$\boldsymbol{T_N\ Beach}\ (yr),\ V_N = 200\ m^3/m$	3,0	2,2	1,5	0,9	0,5
$\boldsymbol{T_N\ Shoreface}\ (yr),\ V_N = 450\ m^3/m$	5,0	3,7	2,4	1,4	0,8

Reactive hold-the-line strategy

The alternative nourishment strategy explored is the commonly employed hold-the-line approach (Fig. 4.4 – right column). In contrast to what we refer to as a 'proactive strategy', the frequency of nourishment is not predetermined in this case. The individual nourishment volumes for this approach remain at $200\ m^3/m$ for beach nourishments and $450\ m^3/m$ for shoreface nourishments through all simulations. In the hold-the-line simulations, we stipulate that, within the nourished transect, the MCL should remain seawards from the BCL. To this end, a new nourishment is placed directly before the coastline crosses landwards from its initial position. Although this approach could as well be classified as a proactive strategy, a key difference is that regularly bed level observations determine the implementation of nourishments. This approach aligns with common coastal management policies in, for example, Italy and France (Hanson et al., 2002).

The cumulative total nourished volume, ΣV_N, employed during these simulations is typically much lower than in the proactive scenarios, thereby representing a minimum amount of sand to keep the coastline 'in place' under a specific rate of sea level rise. By comparing ΣV_N between the two scenarios, we highlight the extent of this difference. Moreover, it is acknowledged that accelerated sea level rise increases the

rate of coastline regression, which in this approach results in a reduction of the nourishment return period, T_N, as the volume of nourishment remains constant. This study contributes to understanding of this issue by quantifying reductions in T_N under accelerated sea level rise. Additionally, from these simulations we examine how the profile steepens and T_N evolves with scenario duration.

Background erosion by gradients in alongshore transport

Within a hold-the-line strategy, T_N varies significantly over different locations (e.g. Brand et al., 2022). In addition to sea level rise, T_N is influenced by factors such as the local hydrodynamic climate, sediment characteristics, tidal currents and the background erosion, i.e. the supply and loss of sediment through existing gradients in alongshore transport (Nederbragt, 2006). Additionally, within the same location, nourishment return periods fluctuate over time due to temporal variability in these factors. This variability may stem from natural sources like variations in storminess and sediment supply from rivers. Furthermore, human interventions can induce more permanent changes in sediment supply (e.g. Almar et al., 2015).

We investigate one of these dependencies; the variation in supply and loss of sediment through gradients in alongshore transport $E_{longshore}$, defined as the amount of sand loss in cubic meter per alongshore meter, with units of $m^3/m/yr$. To investigate the relation between T_N and $E_{longshore}$, we perform additional 50-year simulations with alongshore erosion rates $E_{longshore}$ ranging from -10 to -70 $m^3/m/yr$ under the same set of $SLRr$ scenarios.

4.4 Results

4.4.1 Proactive sand balance strategy

Simulated behaviour for beach nourishment scenarios

The simulations with a duration of fifty years show sand accumulation in the nourished section, resulting in a growing deformation of the cross-shore profile that increases with both scenario duration and the rate of sea level rise (Fig. 4.5A-E). In the proactive beach nourishment scenario under $SLRr2$, the beach is nourished with $200\ m^3/m$ every 3 years, resulting in stepwise 200 m^3/m increases in ΔV_{ap} (Fig. 4.5F). The major portion (90%) of this added sand disperses in the subsequent years, spreading either in alongshore direction ($\Delta E_{longshore}$ in Fig. 4.5F) or beyond the landward boundary of the profile (ΔV_{dune} in Fig. 4.5F). Throughout the simulation no sand reaches the lower shoreface in this scenario, as $\Delta V_{ls} = 0$. The average annual volumetric increase in ΔV_{ap} over the successive nourishment cycles amounts to $6\ m^3/m/yr$, closely aligning with ΔV_{lp*SLR}, which is $8\ m^3/m/yr$. The MCL thereby migrates hardly seawards (appr. 20 m, Fig. 4.5K).

For the simulations wherein $SLRr$ exceeds $4\ mm/yr$, the increase in ΔV_p (Eq. 4.6) is larger than V_{lp*SLR}, exceeding the necessary volume to elevate the profile with sea level rise (Fig. 4.5G-J). In addition, the profile gradually steepens (Fig. 4.5P-T) and the MCL migrates seaward with each nourishment over the successive nourishment cycles (Fig. 4.5K-O). These trends are more pronounced at higher $SLRr$, indicating that the

lateral sand dispersion does not proportionally increase with the larger nourishment volumes. While under $SLRr2$ only 10% of ΣV_N remains in ΔV_p, this increases to 20% ($SLRr4$), 40% ($SLRr8$), 60% ($SLRr16$) and 80% ($SLRr32$). As the simulations mainly differ in the volume of nourishment applied, we find a non-linear, decreasing relationship between nourishment volume ΣV_N and sand dispersion rates ΔV_p.

The phenomenon of profile steepening and seaward MCL migration due to the accumulation of nourishments high in the profile is subsequently referred to as 'upper profile obesity' (best visible in Fig. 4.5D-E). The extent of profile steepening under present-day sea level rise rates ($SLRr2/SLRr4$) is moderate, but under higher $SLRr$ the profile steepening increases when larger volumes of nourishment are applied in a shorter timeframe, whereby the profile slope increases with scenario duration. For example, in 50 years under $SLR8$ the initial submerged profile slope S_p of 1:133 increases to 1:108 (+23%, Fig. 4.6R).

The upper profile obesity leads to increased dispersion rates, resulting in reduced annual growth of ΔV_{ap} as the scenario duration increases. We observe minimal influx of sand into the lower shoreface. Although ΔV_p exceeds V_{lp*SLR}, this sand is stored in ΔV_{ap} and ΔV_{ls} does not grow along with SLR, a phenomenon we term 'lower shoreface starvation' hereafter. If the predetermined nourishment volumes are adhered to when upper profile obesity develops, nourishments are positioned further seaward due to constraints on available space within the initial active profile. After several decades of beach nourishment under $SLRr16$ and $SLRr32$, nourishments are ultimately placed beyond the seaward boundary of the initial active profile. The latter can be observed in Fig. 4.5d-e, where the expansion of ΔV_{ls} aligns with ΣV_N.

Simulated behaviour for shoreface nourishment scenarios

The simulations with shoreface nourishments show sand accumulation in the nourished section, resulting in a growing deformation of the cross-shore profile that escalates with both scenario duration and the rate of sea level rise (Fig. 4.6A-E). In the proactive scenario involving repeated shoreface nourishment under $SLRr2$, the shoreface is nourished with $450\ m^3/m$ every 5 years, resulting in stepwise $450\ m^3/m$ increases in ΔV_{ap} (Fig. 4.6F). The sand reaches the beach as it redistributes along the profile, with a portion dispersing alongshore and over the landward boundary. The portion of ΣV_N that remains in the profile after 45 years is 32%. This translates to an average annual increase in ΔV_p by $28\ m^3/m/yr$, approximately 4.5 times more than in the beach nourishment scenario, and much more than ΔV_{lp*SLR} (Fig. 4.6F). The remaining 68% of ΣV_N is transported either alongshore or beyond landward boundary of the profile. As the nourishments are placed outside the MCL zone (Fig. 4.3C), their individual effect on the MCL is lagging the nourishment implementation. In this scenario, the MCL is relatively stable, with 20 m seaward migration (Fig. 4.6K).

For the scenarios with $SLRr$ exceeding $4\ mm/yr$, we see how the nourishment strategies become affected by the sand redistribution capacity along the profile. While under $SLRr2$ only 32% of ΣV_N remains in ΔV_p, this increases to 44% ($SLRr4$), 59% ($SLRr8$), 74% ($SLRr16$) and 86% ($SLRr32$) (Fig. 4.6F-J). In the scenarios with $SLRr$

exceeding $8\,mm/yr$, this accumulation becomes so substantial that the available space for placing nourishments becomes limited and nourishments are being placed outside the initial active profile. This can be observed in Fig. 4.6H-J by the stepwise growing ΔV_{ls}. Nevertheless, the larger nourishments still induce larger onshore sand fluxes. The MCL migration 50 years is $46\,m$ under $SLRr2$ and increases to $66\,m$ ($SLRr4$), $98\,m$ ($SLRr8$), $128\,m$ ($SLRr16$) and $210\,m$ ($SLRr32$) (Fig. 4.6K-O).

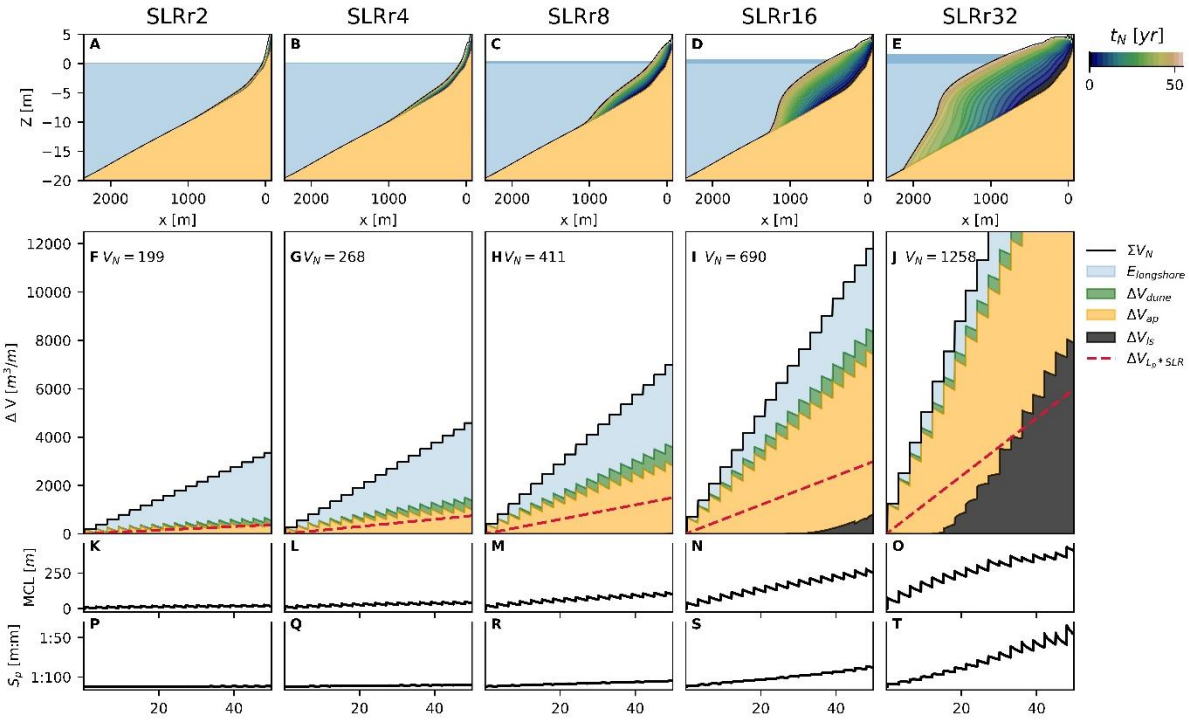

Figure 4.5 Proactive beach nourishment scenarios. Each column represents a scenario with the rate of sea level rise indicated by "SLRr" + the head number (in mm/yr). Panels A-E show the profile shape and sea level after 50 years whereby the sand-coloured profile represents the initial profile and the blue/green colours the sand from successive individual nourishments placed at year t_N indicated by the colour bar on the right. Panels F-J represent the cumulative nourished volume ΣV_n and shows the part of it that is eroded ($E_{longshore}$) and the part that is stored in different profile sections. The latter is subdivided in the dune volume (ΔV_{dune}), the active profile volume (ΔV_{ap}) and the lower shoreface volume (ΔV_{ls}). The red dashed line represents the volume required to elevate the total profile with SLR (V_{lp*SLR}). If this line equals $\Delta V_{ap} + \Delta V_{ls}$ ($= \Delta V_p, see\ Eq. 6$), there is sufficient sand in the profile to grow along with SLR. Panel K-O represent the MCL compared to the BCL (positioned at x=0 m). Panel P-T show the submerged profile slope S_p, measured between MSL-3 and MSL-19 m.

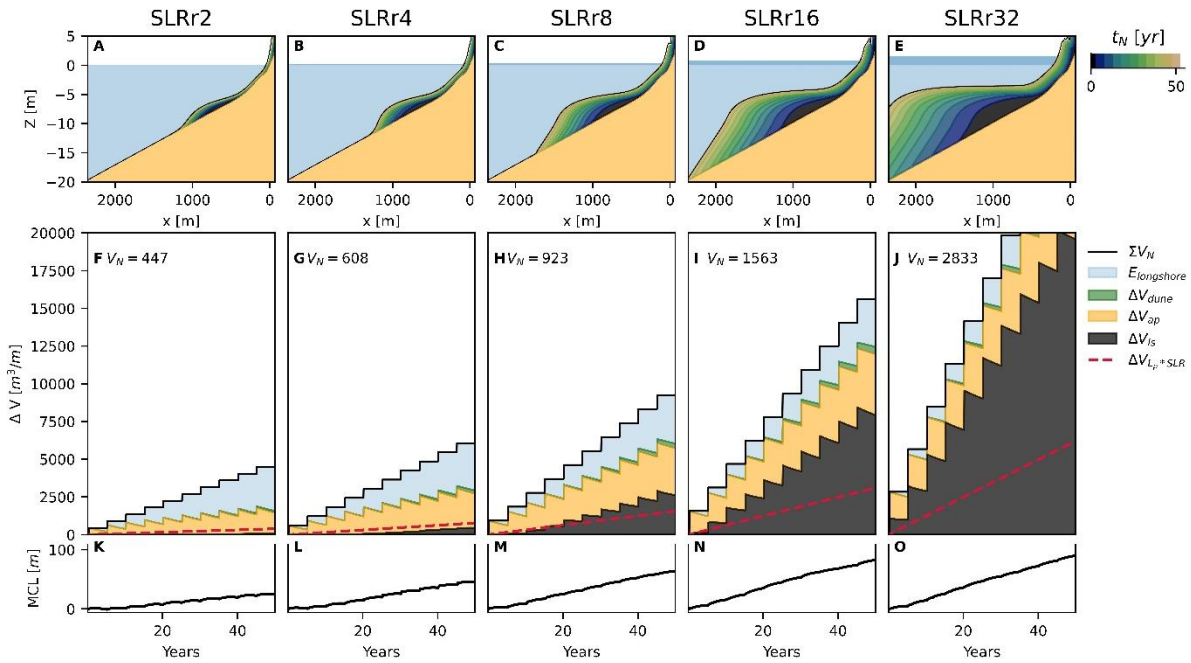

Figure 4.6 Proactive shoreface nourishment scenarios. For descriptions of panel contents, the reader is referred to Fig. 4.4.5.

4.4.2 Reactive hold-the-line strategy

Simulated behaviour for beach nourishment scenarios

The beach nourishment scenarios following a reactive hold-the-line strategy prove highly cost-effective concerning the volume of sand used to counteract MCL retreat. Total nourished volume ΣV_N in these scenarios is considerably smaller than in the proactive scenarios. Under $SLRr2$, it is roughly one third smaller, and under $SLRr8$, ΣV_N is half as large, and under $SLRr32$ scenario, it diminishes to a quarter (Fig. 4.11A). We observe that this is an insufficient amount of sand for ΔV_p to grow along with ΔV_{LP*SLR} for all scenarios. While ΔV_{ap} fluctuates around its initial value for $SLRr2$ and $SLRr4$ and grows slightly with scenario duration under higher $SLRr$, there is no growth of the lower part of the profile ($\Delta V_{ls} = 0$) across all scenarios (Fig. 4.7F-J).

The impact on the profile shape induced by the nourishments is consequently less pronounced than in the proactive beach nourishment scenarios (compare Fig. 4.7A-E to Fig. 4.7A-E). Under $SLRr2$ and $SLRr4$, the profile returns to its initial shape after each nourishment cycle. As a result, the return period T_N between the nourishments is stable over these scenarios (Fig. 4.7U,V). In $SLRr2$ scenario, T_N is approximately 4 years. In contrast, under $SLRr8$ and higher $SLRr$, sand accumulates in the nourished section and the profile steepens (Fig. 4.7R-T). In scenarios $SLRr8, SLRr16$ and $SLRr32$, S_p respectively increases from the initial value 1:129 to 1:126 (3%), 1:122 (6%), and 1:112 (15%) over the 50 years of simulation. This leads to an increase in alongshore and cross-shore sand dispersion with scenario duration inducing a gradual reduction of T_N. In the case of $SLRr32$, this results in a decrease in T_N from about 3 to under 2 years, equivalent to a 25% to 50% reduction compared to $SLRr2$ (Fig. 4.7Y). In section 3.2.3 we delve further into this profile steepening and subsequent reduction in T_N.

Simulated behaviour for shoreface nourishment scenarios

In the shoreface nourishment scenarios following a reactive hold-the-line strategy, the nourishments are positioned seawards from the MCL zone. Compared to the proactive approach, ΣV_N is reduced by approximately equivalent proportions as for the reactive versus proactive beach nourishment scenarios (Fig. 4.11B). Consequently, the growth of ΔV_p is slower than $\Delta V_{L_p * SLR}$, as the sand does not reach the lowest parts of the profile sufficiently to elevate with SLR (Fig. 4.8I-J). As shoreface nourishments enhance the sand budget in the MCL zone with a time delay, the first nourishment is relatively less effective counteracting MCL retreat (Fig. 4.9F-J). The resulting landward sand supply is then insufficient to counteract SLRr and alongshore erosion, which drive the MCL inland. Therefore, shortly after the first nourishment, a second one is implemented to preserve the coastline.

Both for the first nourishment as for the remainder of the simulation T_N reduces significantly with increasing SLRr (Fig. 4.9P-T). While the average T_N under SLRr2 is 7.4 years, the average T_N in $SLRr32$ is 4 years (55%) shorter. T_N roughly stabilizes after the second nourishment in simulations with the lowest SLRr, once dispersion rates reach their maximum. In $SLRr16$ and $SLRr32$, sand accumulates in the nourished area over the course of the simulation. Similar to the proactive shoreface nourishment scenarios, the accommodation space of nourishment then declines in these scenarios with largest SLR rates. Therefore, the nourishments are placed further seawards, leading to a reduction of effectiveness as cross- and alongshore sand redistribution is slower. Consequently, T_N slightly declines over the successive nourishment cycles (Fig. 4.9S,T).

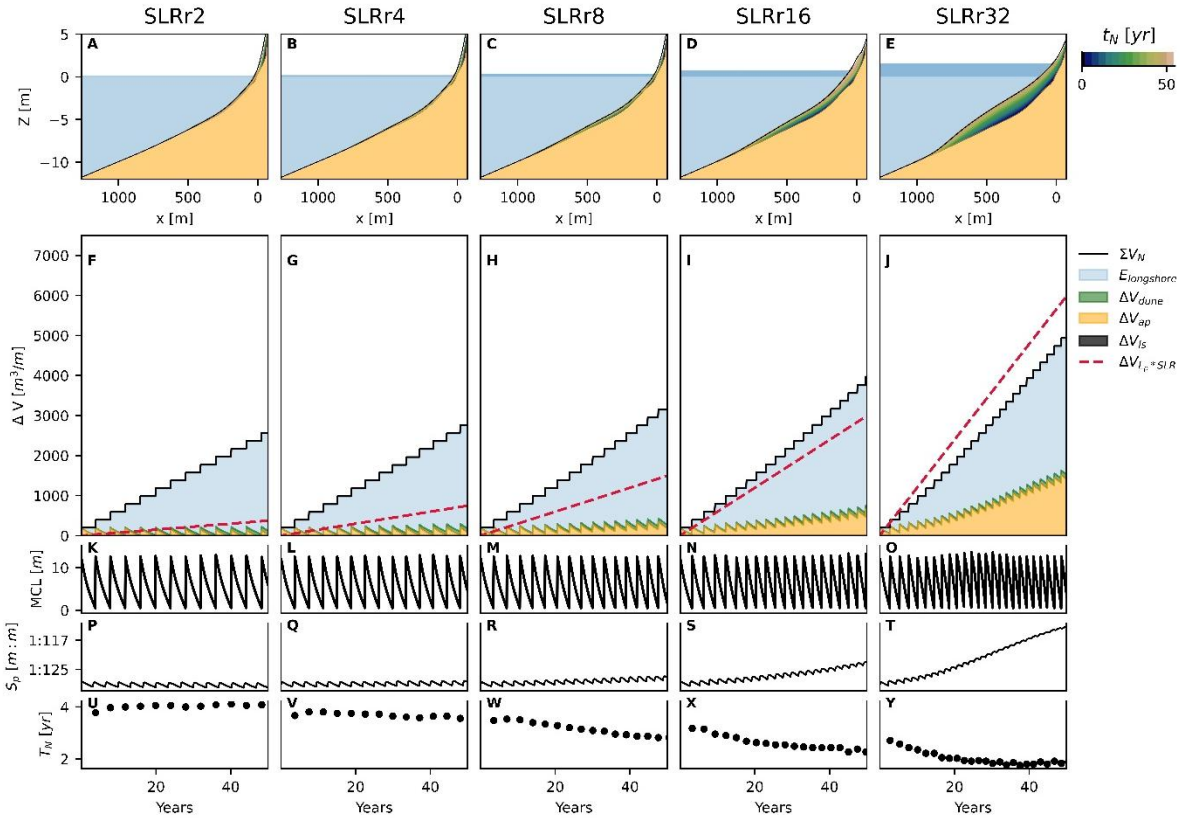

Figure 4.7 Reactive hold-the-line beach nourishment scenarios. Each column represents a scenario with the rate of sea level rise indicated by "SLRr"+the head number (in mm/yr). Panels A-E show the profile shape and sea level at the end of each simulation whereby the sand-coloured profile represents the initial profile and the blue/green colours the successive individual nourishments. Panels F-J represent the cumulative nourished volume ΣV_n and shows the part of it that is eroded ($E_{longshore}$) and the part that is stored in different profile sections. The latter is subdivided in the dune volume (ΔV_{dune}), the active profile volume (ΔV_{ap}) and the lower shoreface volume (ΔV_{ls}). The red dashed line represents the volume required to elevate the total profile with SLR (V_{lp*SLR}). If this line equals $\Delta V_{ap} + \Delta V_{ls}$ ($= \Delta V_p, see\ Eq. 6$), there is sufficient sand in the profile to grow along with SLR. Panel K-O represent the MCL compared to the BCL. Panel P-T show the submerged profile slope S_p, measured between MSL-3 and MSL-19 m. Panel U-Y show the nourishment return period T_N.

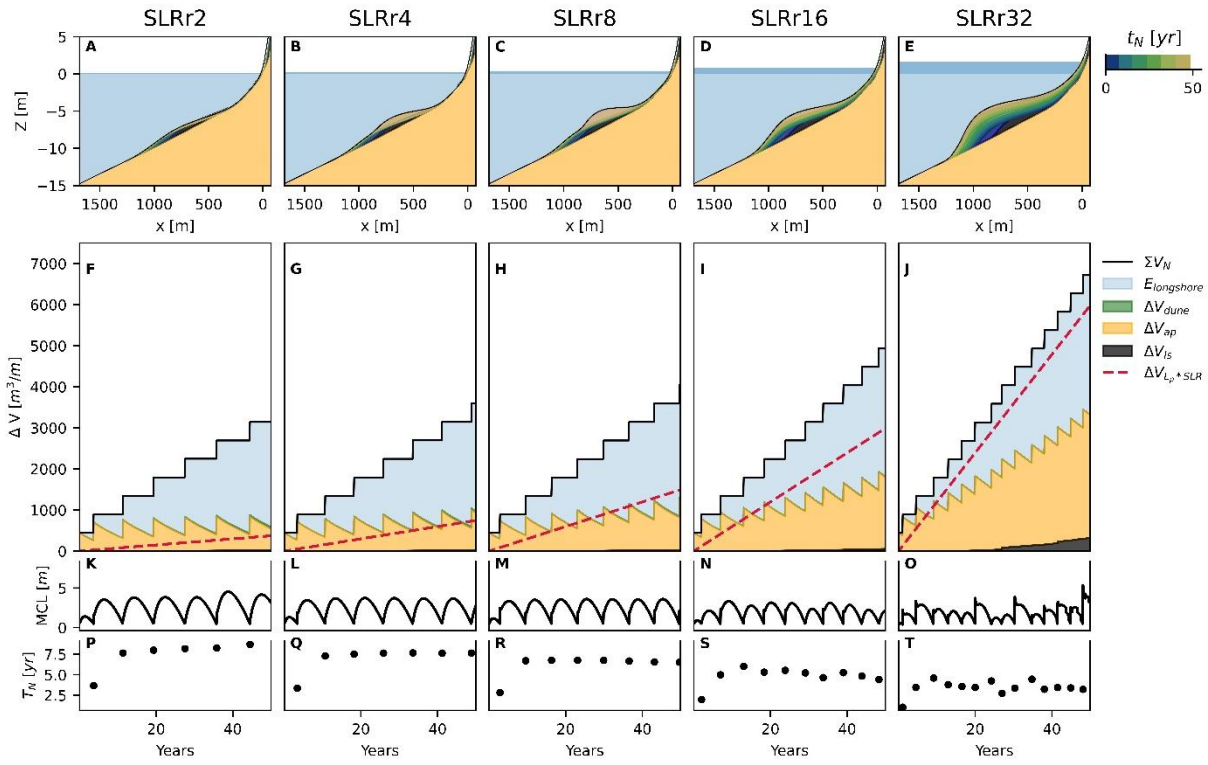

Figure 4.8 Reactive hold-the-line shoreface nourishment scenarios. For descriptions of panel A-O contents the reader is referred to Fig. 4.7. Panel P-T show the nourishment return period T_N.

4.4.3 Profile steepening and nourishment lifetime reduction

Earlier, we briefly addressed the degree of profile steepening in the proactive (Fig. 4.5 P-T) and reactive (Fig 8 P-T) beach nourishment scenarios. In both cases, the steepening leads to increased rates of alongshore and cross-shore nourishment dispersion. In the reactive case this is most evident as it results in a subsequent reduction in nourishment lifetime T_N. Therefore, we use reactive simulations to further explore this relation. To this end, we extend the reactive beach nourishment strategy simulations to 200 years or until MSL surpasses $NAP + 2m$. Profile steepening is expressed as the change in submerged profile slope $(S_p - S_{ini})$. The relative reduction in T_N compared to lifetime of the first nourishment in the simulation, $T_{N,first\ nourishment}$ is given by:

$$\Delta T_N[\%] = 100 * T_N(t)/T_{N,first\ nourishment} \tag{4.13}$$

We analyse the relationships between the value of $(S_p - S_{ini})$ at the last timestep before nourishment placement and $\Delta T_N[\%]$ of that nourishment. Under various $SLRr$, these relationships are similar, whereby $\Delta T_N[\%]$ declines as $(S_p - S_{ini})$ increases (Fig. 4.9A). We note an asymptotic trend around a 30% reduction in T_N under the higher $SLRr$. This point is reached after 100 years under $SLRr8$ or after 50 years for $SLRr16$, when the profile has steepened by about 8% (from 1:129 to 1:120). However, under $SLRr2$ and $SLRr4$, this asymptote remains elusive within the 200-year timeframe.

To extrapolate this finding into a broader context, we fit an exponential curve between S_{ini}, the profile slope increase $(S_p - S_{ini})$, and $\Delta T_N[\%]$:

$$\Delta T_N[\%] = a * (\exp\left(-\left(\frac{b}{S_{ini}}\right) * (S_p - S_{ini})\right) - 1) \quad (4.14)$$

Utilizing a non-linear least squares algorithm to minimize the variance between Eq. 4.13 and the simulation data, we determine the parameters as $a = 32$ and $b = 34$, yielding an R^2 value of 0.64.

To explore the sensitivity of this relationship to different sites with S_{ini}, we analyse an alternate set of beach nourishment simulations, this time over a less steep profile characterized by an initial slope $S_{ini} = 1{:}201$. This profile is derived from a set of yearly alti- and bathymetric surveys at the Dutch coastal town Katwijk over an unnourished period (1966-1998), sourced from the JARKUS dataset (Wijnberg and Terwindt, 1995a). The simulations with this profile reveal similar T_N reductions over time, albeit with a more moderate degree of profile steepening (Fig. 4.9B). Nevertheless, in percentages compared to the initial profile slope, the profile steepening is similar. Repeating the fitting procedure for the Katwijk data with Eq. 4.13 yields parameters $a = 34$ and $b = 28$ with an R^2 value of 0.72. Given that a and b are of comparable magnitude for both the initial profiles at Monster and Katwijk, we infer that Eq. 4.13, with approximate values $a \approx 33$ and $b \approx 31$, can effectively estimate the anticipated reduction in T_N attributed to profile steepening for the range of slopes evaluated.

These findings confirm that steepening of the coastal profile leads to faster beach nourishment redistribution and a reduction in T_N over time, but suggest that it becomes significant only after several decades of frequent nourishment and under sea level rise rates exceeding 8 mm/yr. In these scenarios, our simulations show a reduction in return periods over time by up to 30% due to coastal steepening, in addition to the reduction caused by increased sea level rise rates. Under low $SLRr$, T_N is sufficiently long to allow the profile to roughly return to its original shape. Thereof, we conclude that at present, profile steepening is unlikely to significantly decrease T_N.

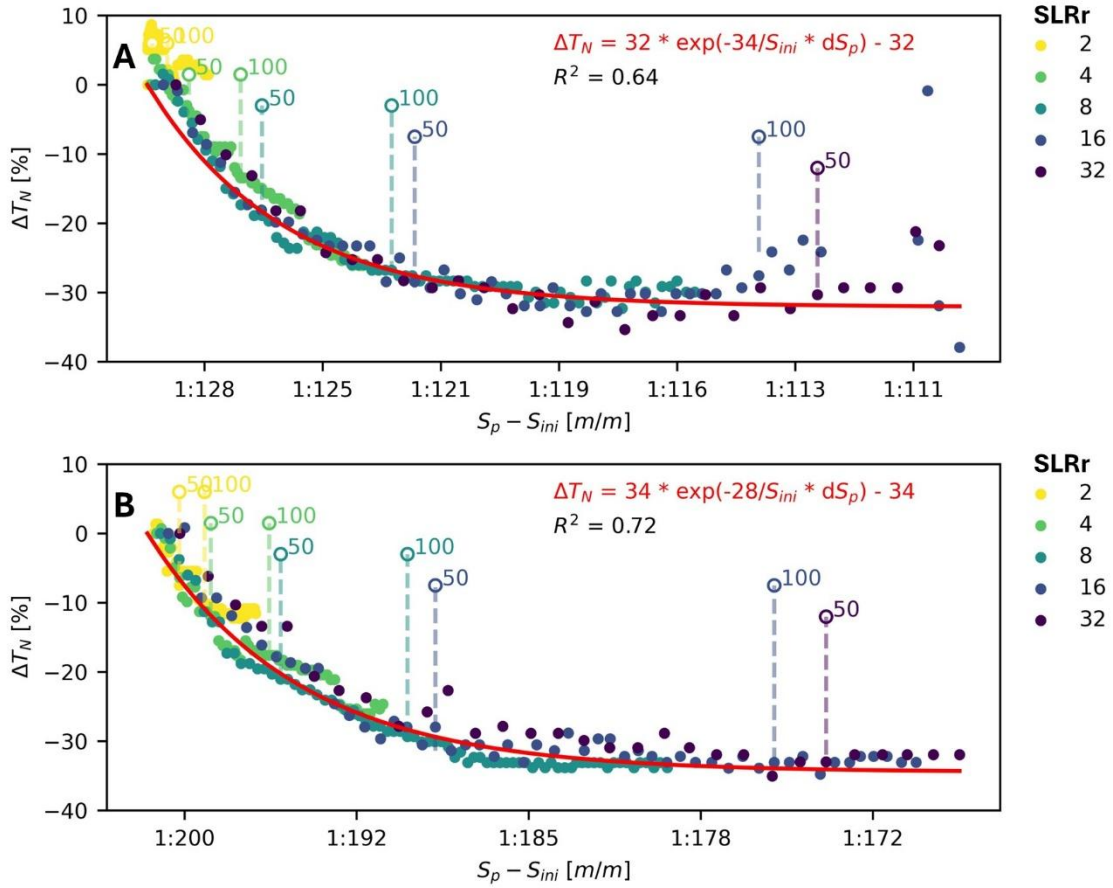

Figure 4.9 Change in beach nourishment return period ΔT_N reduction as a function of increase in submerged profile slope $S_p - S_{ini}$ under various SLR rates distinguished by different colors. The scattered data points are derived from the reactive hold-the-line beach nourishment simulations at (A) Monster and (B) Katwijk, where each dot indicates the T_N and pre-placement ($S_p - S_{ini}$) of an individual beach nourishment. Nourishments placed approximately 50 and 100 years into the simulation timeframe are indicated by the dashed lines. The nonlinear least-squares fit, minimizing the difference between the data and Eq. 4.13, is depicted in red.

4.4.4 Impact of the existing gradients in alongshore transport

Nourishment efforts are generally focused on locations where a negative alongshore gradient in sand transport is present. Model results presented in the previous sections included this alongshore effect with a magnitude of $E_{longshore}$ = -40 $m^3/m/yr$. In this section we research the influence of $E_{longhsore}$ on nourishment dissipation. We adopt the reactive hold-the-line strategy for this analysis, as the nourishment dissipation in this strategy is quantifiable through a subsequent reduction in nourishment lifetime T_N. To evaluate the influence of $E_{longhsore}$ on T_N, we present the results of an alternate set of reactive hold-the-line simulations with alongshore erosion rates $E_{longshore}$ varying from -10 to -70 $m^3/m/yr$. As T_N varies over a single simulation, we evaluate the average T_N of all nourishments implemented within the 50-year timeframe.

We observe that T_N decreases for both increasing $SLRr$ and increasing $E_{longshore}$, as illustrated in Fig. 4.10. The influence of $E_{longshore}$ is largest for low $SLRr$; for beach nourishments under $SLRr2$, the average T_N decreases significantly from 4 to 2.5 year (-38 %) if $E_{longshore}$ is increased from $-40\ m^3/m/yr$ to $-70\ m^3/m/yr$ (Fig. 4.10A, left column). Such dependence of T_N on $E_{longshore}$ is less prominent for larger $SLRr$. Under $SLRr32$, T_N is reduced from 2 to 1.5 year (-25%) when comparing $E_{longshore} = -70\ m^3/m/yr$ to $-40\ m^3/m/yr$ (Fig. 4.10A, right column). Shoreface nourishments exhibit similar relationships between $E_{longshore}$ and T_N. Comparing shoreface nourishments under $E_{longshore} = -70\ m^3/m/yr$ to $-40\ m^3/m/yr$, T_N is reduced from 7.5 to 4.3 year (-43%) under $SLRr2$ (Fig. 4.10B, left column), and from 3.4 to 2.5 year (-26%) under $SLRr32$ (Fig. 4.10B, right column). These results highlight the dependency of T_N on the$E_{longshore}$, recognizing it as another major contributor to long-term coastline retreat, alongside sea level rise. Moreover, the results underline that T_N may vary over time due to temporal variability in $E_{longshore}$.

Additionally, we compare how the simulated T_N responds to accelerated SLR among locations with a given $E_{longshore}$ for $SLRr2$ versus $SLRr32$. In a highly erosive profile ($E_{longshore} = -70$ m³/m/year), the average return period decreases by 35% (from 2 to 1.3 years - Fig. 4.10A, lower row), while it decreases by 50% (from 4 to 2 years - Fig. 4.10A, centre row) under moderate $E_{longshore}$ =-40 m³/m/year, and by 75% (from 11.3 to 2.8 years - Fig. 4.10A, upper row) under a very low $E_{longshore}$ of -10 m³/m/year. Thus, we observe that the difference in T_N between simulations with different $E_{longshore}$ diminishes with increasing $SLRr$. This shift occurs because, with increasing $SLRr$, the primary purpose to place nourishments shifts from counteracting structural erosion to mitigating sea level rise. This finding may be even more important for low-erosive beaches than for beaches under high erosion rates. Although return periods become shortest for highly erosive settings, the reduction in return period and subsequent increase in sand demand for nourishment is largest for less erosive coasts. These coasts are likely less well-monitored because there is little need at present, so for coastal management this may be a factor to consider in future.

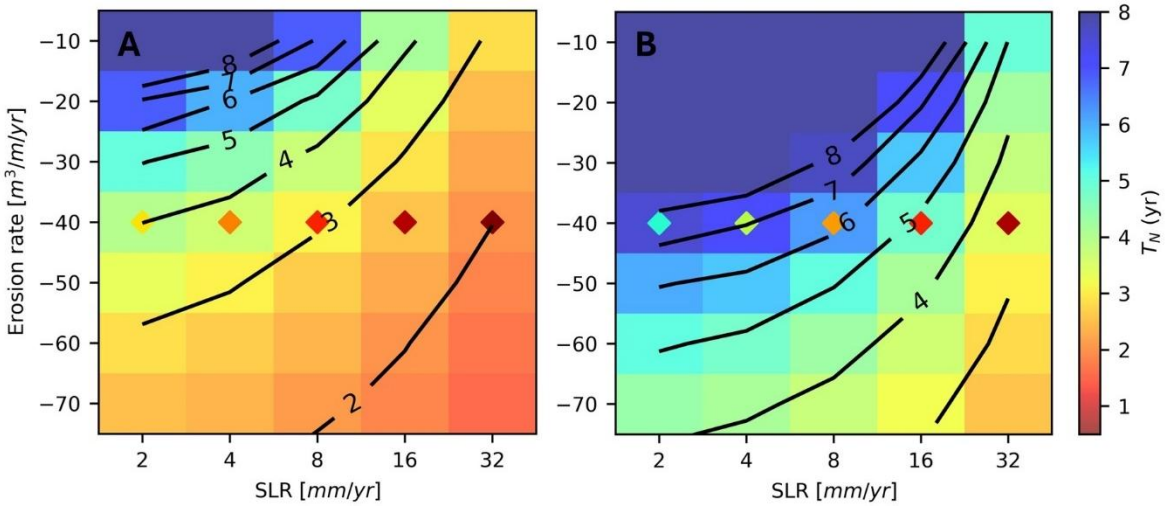

Figure 4.10 Nourishment return period T_N under reactive hold-the-line (A) beach and (B) shoreface nourishment scenarios, as a function of sea level rise rate SLRr and

alongshore erosion rate $E_{longshore}$. T_N is defined as the time between nourishment implementation and the moment the MCL retreats landwards from the BCL. The coloured diamonds refer to computed T_N (Table 4.1) in proactive scenarios with increased frequency and present-day nourishment volumes.

4.5 Discussion

4.5.1 Considerations in selecting a nourishment strategy

In this section, we delve into the practical considerations of selecting an appropriate nourishment strategy in light of accelerated sea level rise. Our discussion is based on the findings from Chapter 3, and we aim to contextualize our points by directly linking them to the results and observations detailed in that chapter.

Comparison of sand volumes between strategies

To mitigate accelerated sea level rise, nourishment programs can increase the volume or frequency of nourishments (or a combination of both). Our study demonstrates that magnitude of the increase strongly depends on the operational objectives adopted in a nourishment program. In the pro-active sand balance nourishment approach presented, the total nourishment volume over a 50-year timespan doubles for $SLRr8$, and escalates over sixfold for $SLRr32$ (Fig 11, blue bars marked "P"). Conversely, the reactive hold-the-line strategy involves considerably smaller sand volumes and raises, amounting to roughly two thirds under $SLRr2$ to a quarter under $SLRr32$ compared to the proactive approach (Fig. 4.11, blue bars marked "R"). Thus, the difference between these approaches increases as sea level rise accelerates, underscoring the importance of sand availability and economic considerations in strategy selection.

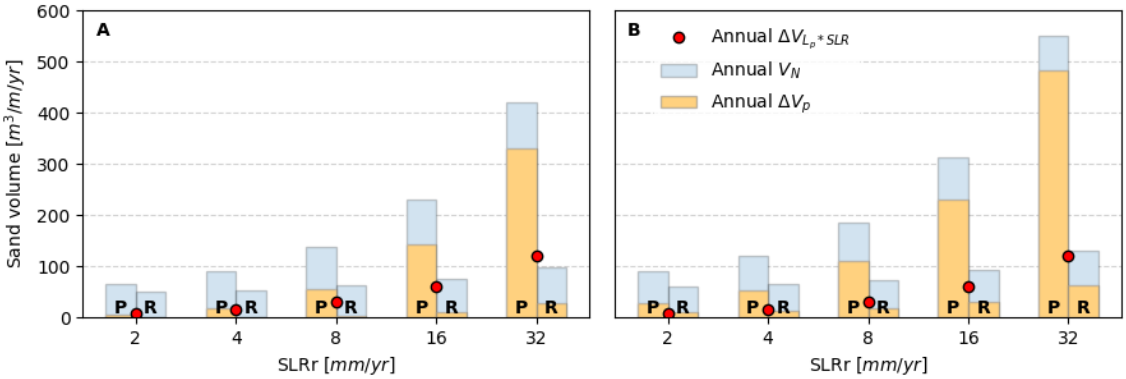

Figure 4.11 A volumetric comparison between the (A) beach and (B) shoreface nourishment for various SLRr scenarios as simulated. The P refers to the proactive sand balance scenarios, the R to the reactive hold-the-line scenarios. All volumes are averaged over 50 years of simulation. The graph includes annual nourished sand volume V_N and annual profile volume change ΔV_p. The red dots represent the volumes required to elevate the total profile with SLR (V_{lp*SLR}). If these equal ΔV_p, there is sufficient sand in the profile to grow along with SLR.

Feasibility of operational objectives

We observe a limitation in achieving the operational objective of elevating large areas along with sea level rise by nourishment concentrated in specific locations, such as in the proactive strategy presented. Our results indicate that as nourishment volumes increase, sand dispersion rates do not keep pace, leading to accumulation in the nourished profile section. In case of beach nourishment, 'upper profile obesity' develops whereby the coast steepens and the lower shoreface remains largely unaffected. This is consistent with bathymetric studies in the Netherlands indicating limited dissipation of nourishments to the lower shoreface in recent decades resulting in a relatively steeper profile (van der Spek and Lodder, 2015). We add to these findings that this remains the case under large nourishment volumes, confirming that the lower shoreface adaptation occurs over a considerably longer timescale compared to the application of nourishment. Consequently, it is not required that the lower shoreface grows along with sea level rise for coastal safety purposes.

In addition to the increased nourishment volumes, the insufficient nourishment redistribution under accelerated sea level rise is also partly attributable to a shift in the distribution of sand demand across the profile. With increasing sea level rise, the reason to place nourishments shifts from primarily counteracting structural erosion to primarily mitigating sea level rise. Both erosion and sea level rise increase the sediment demand of the profile, but the distribution of this demand across the profile differs. Structural erosion acts upon the profile according to the acting forces, with higher sand losses in the zone of wave breaking and along the coastline, and lesser impact on the lower shoreface. In contrast, sea level rise essentially reframes the profile, resulting in a profile-uniform 'apparent' loss of volume. In the context of structural erosion, it is logic to compensate for the total volumetric loss over the profile. However, under sea level rise, a computed sediment demand in a volume-based proactive strategy is contingent upon the profile length desired to grow along. Consequently, we anticipate that under severe rates of sea level rise, a revision of either the tactical goal or the nourishment design in such volume-based proactive strategies is inevitable.

Such a revision may include a thorough examination of the lowest elevation of the profile that is desired to grow with sea level rise. In line with this rationale, it has recently been proposed to restrict the seaward limit adopted within sand balance computations (A_{cf} in Eq. 4.2) to MSL-8 instead of MSL-20 m, significantly reducing the required nourishment volumes as the area to be elevated is over five times smaller (Taal et al., 2023). Our study supports this proposal. If maintaining the current tactical goals is preferred, alternative nourishment approaches or sites for nourishment could be explored. Possible locations could involve neighbouring places that are not yet intensively nourished. Alternative methods might encompass mega nourishment projects (e.g. De Schipper et al., 2014), outer delta nourishment or pipeline nourishment. Taking a broader perspective, the proactive volume-based scenario simulations presented in this study highlight that an effective present-day nourishment policy may not necessarily be the optimal approach under accelerated

sea level rise due to differences in sand demand, both in volume and distribution over the profile.

Sea level rise and nourishment lifetime reduction

We assessed how much the nourishment return frequency increases as a function of sea level rise and coastal erosion. Comparing hold-the-line simulations under $SLRr32$ to $SLRr2$ at our case study with moderate erosion rate (~40 m³/m/yr), the average nourishment return period reduces by about 50% for both beach and shoreface nourishment (from 4 to 2 years and from 7.4 to 3.4 years respectively) when individual nourishment volumes are unaltered. Coastal areas with higher erosion rates (~70 m³/m/yr) see return periods drop to annual intervals, while less erosive coasts face the largest reduction in return periods and require up to four times more sand than at present under $SLRr32$. To prevent the future shortening of nourishment lifespans in hold-the-line policies, increasing individual nourishment volumes may be advantageous.

Coastal steepening and nourishment lifetime reduction

Steepening of the profile occurs when beach nourishment accumulates in the upper profile section due to incomplete redistribution over the profile. The extent of profile steepening under present-day sea level rise rates ($SLRr2$ *or* $SLRr4$) simulated in both strategies presented was moderate, aligning with observations in the Netherlands (Rijkswaterstaat, 2020; van der Spek and Lodder, 2015). Under higher $SLRr$ the profile steepening increases when larger volumes of nourishment are applied in a shorter timeframe, whereby the profile slope increases with scenario duration. This steepening is consequently larger in the proactive than in the reactive strategy, due to the difference in sand volumes are applied. For example, in 50 years under $SLR8$ the initial submerged profile slope S_p of 1:133 increases to 1:108 (+23%) in the proactive scenario and to 1:115 (+16%) in the reactive case. Profile steepening has been raised as a concern, as has been suggested to shorten the lifespan of individual nourishments due increased wave energy levels higher in the profile leading to increased dune erosion (Stive et al., 1991). Our findings confirm this effect, but suggest that it becomes significant only after several decades of frequent nourishment and under sea level rise rates exceeding 8 mm/yr. In these scenarios, our simulations show a reduction in return periods over time by up to 30% due to coastal steepening, in addition to the reduction caused by increased sea level rise rates.

4.5.2 Reflection on methods

In interpreting the outcomes of this study, it is crucial to recognize that our objective is to simulate expected coastal responses to decadal nourishment programmes, not to predict the actual coastal evolution on a day to day basis. As we consider the nourishments as profile perturbations and assume a 'dynamic equilibrium' background profile, any autonomous (nourishment-independent) profile development affecting the profile shape is not resolved. This means that cycles of storm and recovery, cyclic bar behaviour and the passage of alongshore shoreline undulations are not included in the model. Additionally, there are stochastic aspects of hydroclimatic influences (e.g., energetic vs moderate years) that the model, being

stationary forced, cannot replicate. In many real-world scenarios, autonomous coastal developments often overshadow the effects of nourishment observed on short timescales. Consequently, the model cannot be utilized as a predictor or compute specific details of the cross-shore profile shape on short timescales. Instead, its primary capability lies in comparing the long-term profile responses between periods with different strategies of nourishment.

We acknowledge that the high rates of sea level rise and nourishment volumes used in this research exceed the conditions in the case studies used for model validation (Chapter 3). This discrepancy arises because no existing sites currently experience these conditions - which was also a key motivator for the present study. The gap between the validation cases and the modelled scenarios introduces significant uncertainty into the model's outcomes, and we emphasize that the quantitative results should only be interpreted as indicative. However, we are confident that our model reliably captures the timescale of response, and therefore, despite uncertainties in the exact timing and magnitude, the predicted sediment patterns are expected under large-scale nourishment scenarios.

Within the work presented, our exclusive focus on two locations (Monster and Katwijk) was intentional to maintain conciseness in the results. The model used requires input parameters that are tuned for these locations. Other regions will react differently to nourishment, influenced by factors such as sediment type, the local wave climate and erosion rate. Although outcomes are expected to be qualitatively similar with a comparable methodology, the timing and extent of profile changes are likely to differ. In cases of similar nourishment design, the dispersion of nourished sand is generally faster when the sediment used is finer (Ludka et al., 2016), when the hydrodynamic climate is more energetic (Hamm et al., 2002) and when alongshore erosion rates are larger. Moreover, if the nourished stretch of coast is bounded in either alongshore or cross-shore directions, either naturally or by man-made structures, this may reduce the strength or limit of sand dispersion.

The strategies presented in this study serve as a framework for the current analysis, rather than a definitive set of options. Our scenarios assume the continuation of a chosen policy over half a century, revealing disproportionate outcomes such as the accumulation of large volumes of sand in the proactive scenarios. In real-world coastal management, any strategy leading to such undesirable changes would almost certainly be subject to revision along the way. Moreover, while our exploration is confined to the boundaries of laterally uniform nourishment strategies, there are numerous other options for coastal protection to consider. These alternatives may include different sandy approaches, such as pipeline or feeder nourishments, as well as 'hard' protection measures such as seawalls and dikes. The selection of a particular strategy in practice will include the morphological effects outlined in this work as well as socio-economic and ecologic aspects (Hanson et al., 2002). Taking a step further, the inquiry into how the coast shall be protected may extend to more fundamental considerations, such as determining the threshold of sea level rise under which our coast can and should be maintained in its present form (Haasnoot et al., 2020) and when a retreat or managed realignment policy is to be favoured.

4.6 Conclusions

In the face of accelerated sea level rise, policymakers may consider different nourishment strategies involving larger sand volumes. High individual nourishment volumes or short return periods can lead to ineffective sand redistribution, whereby it may take decades for sand to reach slower-responding areas, typically farther from the nourishment site and at greater depths. The present study quantifies subsequent effects, including profile steepening, reduced nourishment lifetimes, and challenges in achieving strategic operational objectives, which are minimally addressed in current literature. Two common nourishment strategies were simulated with the cross-shore morphological model Crocodile over a 50-year timespan under different rates of sea level rise; the hold-the-line approach as reactive approach with minimal sand usage, and the sand balance approach as proactive option to elevate the coastal system, stretching seaward as deep as MSL-20 m, along with sea level rise.

An intercomparison between these strategies highlights the impact of strategy selection on sand volume usage. In the coming 50 years, the proactive strategy requires up to 6 times more sand than present-day volumes ($SLRr2$) to mitigate high sea level rise rates ($SLRr32$). The reactive hold-the-line strategy, in contrast, uses much less sand, requiring 30% less sand under low sea level rise rates ($SLRr2$) and 75% times less under high sea level rise rates ($SLRr32$). This underscores the importance of sand availability and economic considerations in strategy selection.

The simulations show that when high volumes of sand are applied, sand dispersion rates prove too slow for complete redistribution across the profile, leading to sand accumulation in the upper, nourished part of the profile over time. This effect increases with nourishment volume and duration of the nourishment strategy. In particular, the lower shoreface is hardly influenced by nourishments placed in the active profile. For example, a 50-year beach nourishment strategy under $SLRr8$ leads to profile steepening by 23% in the proactive simulation and 16% in the reactive case. This profile steepening highlights a limitation in achieving the proactive strategy's operational objective of elevating large areas, stretching seaward as deep as MSL-20 m, along with sea level rise. Under high rates of sea level rise, it may be necessary to reconsider operational objectives or nourishment design in such strategies, for instance by decreasing the profile depth to grow along with sea level rise.

The reactive hold-the-line simulations quantify how nourishment return periods reduce under accelerated sea level rise for coasts subject to varying erosion rates. Coastal areas with higher erosion rates see return periods drop to annual intervals, while less erosive coasts face the largest reduction in return periods and require up to four times more sand than at present under high sea level rise rates ($SLRr32$). The profile steepening leads to a supplementary reduction in return periods over the 50-year simulations by up to 30%. For the tested Dutch case this becomes significant after several decades of frequent nourishment and under sea level rise rates exceeding 8 mm/yr.

The projections of nourishment strategies discussed in this study provide insights into the relationships between man-made alterations to the sand budget and cross-shore

dynamics. These relationships are instrumental in the formulation of future nourishment strategies and highlight the importance of optimizing these strategies to account for sea level rise.

5 Numerical assessment of decadal redistribution and profile equilibration at mega nourishments

This chapter explores the decadal evolution of feeder-type mega nourishments through the coupled modelling framework Crocodile–ShorelineS. It quantifies the depth-dependent redistribution in gaussian shaped mega nourishments across time and space and identifies morphological phases related to profile equilibration and alongshore diffusion. This chapter complements earlier chapters by addressing alongshore sand dynamics and offering design recommendations for future large-scale interventions.

This chapter is submitted as:

Kettler, Tosca, Matthieu de Schipper, Bas Huisman and Arjen Luijendijk. " Numerical assessment of decadal redistribution and profile equilibration at mega nourishments." Coastal Engineering, submitted.

5.1 Abstract

Feeder-type mega nourishments are postulated to offer a more durable and eco-friendlier alternative to frequent small-scale beach nourishments. Understanding decadal-scale morphological evolution of mega nourishments is essential for strategic coastal management, yet current models often fail to fully capture the coupled alongshore and cross-shore sediment redistribution processes that govern their performance. This study presents and applies a coupled modelling framework, integrating the cross-shore model Crocodile with the alongshore shoreline evolution model ShorelineS, to simulate the long-term morphological development of Gaussian-shaped mega-nourishments over a 50-year period. The Crocodile model represents the wave climate-aggregated, long-term response of cross-shore profiles, omitting short-term event-driven variability (e.g. individual storms) that is of limited relevance for long-term nourishment assessment, which enables highly efficient simulations. Model calibration and validation were performed using 15-year monitoring data from a Dutch mega-nourishment. Results reveal a two-phase long-term behaviour: an initial ~10-year equilibration phase during which sand redistributes through both cross-shore profile adjustment and alongshore dispersion, followed by a long-term phase of predominant alongshore sand dispersion. Sand placed near or below the closure depth remains largely immobile for over 50 years, even for high-volume nourishment scenarios. While increasing nourishment volume

enhances redistribution, efficiency per unit volume therefore declines as more sediment needs to be placed in deeper water, where it is less mobile. These results underscore the importance of accounting for depth-dependent dispersion when estimating nourishment lifetimes and provide a practical framework for evaluating large-scale nourishment designs. The proposed framework provides a pathway for flexible and efficient long-term coastal morphological modelling which includes the long-term cross-shore profile changes. This improves predictive accuracy, particularly in areas experiencing significant accretion or erosion such as at large-scale nourishments.

5.2 Introduction

Coastal regions worldwide face growing pressures from climate change and intensive human activity, raising concerns about significant socio-economic and environmental losses in coming decades (Brown et al., 2016; Hinkel et al., 2014; Luijendijk et al., 2018; Ranasinghe, 2016b; Wong et al., 2022). To prevent such losses, strategic planning of coastal zones is essential. Over recent decades, sand nourishments have emerged as a widely used and flexible strategy for beach preservation (Brown et al., 2016; Cooke et al., 2012; Elko et al., 2021; Hanson et al., 2002), offering a potentially more environmentally friendly alternative to hard protection measures (Hanson et al., 2002). Nourishing sandy coastlines not only mitigates erosion and shoreline retreat due to sea level rise, but it can also increase opportunities for recreation, the size and quality of ecological habitats, and support dune systems through aeolian transport (de Vriend et al., 2015; Hanson et al., 2002; van Westen et al., 2024).

Traditional beach nourishments include frequent, moderate-scale sand placements which gradually disperse over a typical individual lifespan on the order of 1–8 years (Brand et al., 2022; Pinto et al., 2020). Despite its relatively eco- and socio-friendly image, the implementation of sand nourishment can result in different types of nuisances, including temporary beach access restrictions (Seekamp et al., 2019) and the visual and physical intrusion of heavy machinery and equipment such as bulldozers and pipelines on the beach (Usher, 2021). Ecologically, frequent nourishments can disrupt benthic communities, as construction activities bury or kill benthic organisms, may alter sediment characteristics (Karalinas et al., 2020), and disrupt prey availability for shorebirds and other species (Gittman et al., 2016; De Schipper et al., 2021; Schlacher et al., 2012; González & Holtmann-Ahumada, 2017). Recovery times vary; some species recolonize within a year, while slowly reproducing or site-dependent species may take decades or never fully return (Hanley et al., 2014; Leewis et al., 2012).

In response, at some locations larger-scale mega nourishments have been implemented; the Netherlands pioneered herein with the Sand Engine project, a concentrated nourishment designed to disperse and feed adjacent coasts over decadal timescales (de Schipper et al., 2016; Stive et al., 2013). The United Kingdom followed with the Sandscaping feeder nourishment at Bacton in 2019 (Lorenzoni et al., 2024), and a sandy mega nourishment was recently built in Benin, West Africa, as

part of a climate adaptation program (Alves et al., 2020). These mega nourishments are intended to last significantly longer and may also feed adjacent shores for decades (de Schipper et al., 2016). Due to their increased longevity, they are postulated to be more environmentally friendly and less disturbing than recurrent traditional beach nourishments (Stive et al., 2013).

Coastal adaptation plans to mitigate higher rates of sea level rise explore significantly greater volumes of sand compared to present-day practices (Amrouni et al., 2024; Haasnoot et al., 2020; Rijkswaterstaat, 2020), amplifying both socio-economic and ecological pressures. The potential role of mega nourishments herein remains under investigation, but if a conventional nourishment program requires very frequent (annual, or biannual) return, the option of concentrated mega nourishments with a feeding function might deliver more societal and environmental benefits and fewer adverse side effects.

While mega nourishments offer the potential to reduce ecological and societal disturbance compared to frequent smaller interventions, their multifunctional effects remain uncertain and highly context-specific. They require substantial up-front investment, yet the long-term benefits – particularly over long time horizons – can be difficult to predict (Brière et al., 2018). For instance regarding the delivery of environmental benefits, Herman et al. (2021) observed that the long-term burial impact of the Sand Engine on fast-recovering benthic species under the Sand Engine was evenly severe as that of smaller, more frequent nourishments. On the other hand, the Sand Engine introduced greater landscape heterogeneity by introducing spatial variability in sediment types, hydrodynamic conditions, and landform development (Hulskamp et al., 2025). This enhanced environmental diversity was linked to increases in regional benthic biodiversity, suggesting that ecological outcomes may not only depend on disturbance, but also on the creation of new niches.

Mega nourishments thus shape the coastal landscape in ways that influence long-term flood safety, dune development, and recreational potential. These outcomes depend strongly on how sand redistributes over time and space, both cross- and alongshore. As a result, the uncertainty in multifunctional effects of mega nourishments highlights the importance of predicting the long-term evolution of key morphodynamic indicators—such as shoreline position, beach width, and profile volume—over decadal timescales. Understanding the influence of strategic choices, such as placement location and nourishment dimensions, on the expected alongshore and cross-shore sand dispersion is essential to inform potential mega nourishment projects. These dispersion patterns result in nourishment lifetime, beach width and sand volume per location of a strategy, which in turn can inform the potential of a coast to deliver socio-economic and ecologic functions (see Chapter 2).

5.2.1 Morphological development of mega nourishments

Sand nourishments are observed to undergo a two-phase morphological development following implementation. In the initial phase, lasting seasons to years, sand redistributes both by cross-shore equilibration and alongshore dispersion. This phase is characterized by rapid reshaping of the nourishment body as wave action

redistributes sand both seaward and along the coast, transforming the manmade planform and cross-shore profile shape toward a more natural shape (de Schipper et al., 2016; Stive et al., 2013; Willson et al., 2017). For instance, at the Sand Engine, within five months after implementation the profile slope between + 1 m and − 4 m reduced from 1:32 to 1:45. After 18 months, the mean sea level isobath had retreated by approximately 150 m, and the profile slope approached 1:53, closely matching the local pre-nourishment slope of 1:55 (de Schipper et al., 2016). As the profile equilibrates, the system transitions into a second, longer-term morphological phase in which development is increasingly governed by alongshore transport, gradually dispersing sediment laterally to adjacent coastlines (Luijendijk et al., 2017).

This phased, depth-dependent sand dispersion is realized under the force of waves, wind, and tidal currents, each exerting varying influence depending on elevation. As Roest et al. (2021) postulate, wave- and current-driven processes are dominant between the wave run-up limit and the depth of closure, below which sand mobility is limited. Above the wave run-up level, in the supratidal zone, aeolian forces are dominant. This results in varying rates of sand redistribution along the profile. Consequently, timescales for morphological adaptation in response to changed boundary conditions, such as nourishment, range from hours around the waterline to millennia near the inner shelf (Stive and de Vriend, 1995). It can therefore take several decades for nourished sand to reach slower responding (lower-elevation, more seaward) areas in the profile (Hands and Allison, 1991). In the same rationale, nourishments placed lower in the profile typically redistribute slower (Beck et al., 2012), requiring shoreface nourishment to be about 25% larger than beach nourishment volumes for similar impact (Stive et al., 1991).

In addition to placement elevation, the rate and extent of nourishment dispersion depends, amongst others, on the wave climate and surf zone processes (Pang et al., 2020, 2021), the nourishment's shape (e.g. de Schipper et al., 2015; Liu et al., 2024), nourishment grain sizes (Ludka et al., 2016), the presence of geological or man-made structures (Faraci et al., 2013), the sand's mineralogical composition (Yao et al., 2024) and sorting processes (Duan et al., 2020). Larger nourishments generally exhibit longer lifespans, not only because more sand is placed at morphodynamically less active depths, but also because the rate at which wave-driven transport can mobilize and redistribute sediment is inherently constrained (Hanson et al., 2002). This limits the relative erosion rate per cubic meter as nourishment volume increases (Tonnon et al., 2018; Arriaga et al., 2020).

Observations from the Sand Engine confirm that cross-shore and alongshore redistribution of the nourished sand strongly varies on depth, with the strongest morphological response around the waterline and limited morphodynamic activity at lower-elevation, more seaward parts of the profile, around the depth of closure (Roest et al., 2021). In their five-year post-construction data analysis of the Sand Engine, Roest et al. (2021) investigated sediment mobility at various depths and mapped the temporal evolution of both cross-shore and alongshore extents. At the nourishment centre, a retreat of 400 m at a rate of ~80 m/year was observed, while the shape of the MSL - 10 m contour over the 17 km alongshore domain did not translate

significantly over time. Their work suggests limiting cross-shore extent in a mega nourishment design, since it is uncertain whether nourished sediment in lower-elevation, more seaward parts of the profile will become active in the coastal system.

However, a few years of post-nourishment monitoring may be insufficient to capture the mobilization of sand placed in lower-elevation, seaward areas, and it remains uncertain whether such sand will actively contribute to the coastal sediment budget over longer timescales. This uncertainty is particularly relevant for the design and evaluation of (future) mega nourishments, which may involve substantial volumes may be placed at depth. The present study addresses this knowledge gap by investigating depth-dependent sand redistribution of mega nourishments, including the timescales of profile equilibration and the mobility of sand across different elevations.

5.2.2 Morphological modelling of mega nourishments

Existing engineering tools are limited in their ability to simulate the coupled alongshore and cross-shore dynamics at appropriate scales. Process-based models like Delft-3D (Luijendijk et al., 2017) can resolve detailed hydrodynamic and sediment transport processes, including wave-driven transport and cross-shore profile change. However, their high computational demand renders them impractical for simulating long-term (e.g., 50-year) scenarios over large spatial domains (O~10 km). Conversely, one-line shoreline models - such as GENESIS (Whitley 2020), UNIBEST-CL (Deltares, 2025), LONGMOR (Tonnon et al., 2018) and ShorelineS (Roelvink et al., 2020) - efficiently solve diffusion equations for shoreline evolution (Pelnard-Considere,1956), but they typically assume a constant beach profile and focus only on alongshore gradients. They are based on the premise that coastal profiles respond to nourishment by rapid adjustment to a (new) equilibrium shape incorporating the added sand volume (Bruun, 1954, 1962). From this viewpoint, the total amount of added sand is the primary concern for profile evolution, while specific design elements like cross-shore location and placement depth are considered less critical. The validity of this perspective hinges on the timescale of equilibration of the coastal profile in relation to the timescale and extent of profile deformation caused by the nourishment. However, for mega nourishments, equilibration can take a decade or more, and profile deformation is substantial. In such cases, the assumption of rapid adjustment fails, limiting the predictive accuracy of one-line models.

Classic one-line models indeed often underestimate nourishment lifetimes and over-predict erosion rates for mega nourishments, because they ignore the initial cross-shore adjustment phase. For instance, parametrizations of Dean and Yoo (1992) on nourishment lifetime projected on the Sand Engine dimensions projects 30% of nourished sand remaining after 3 years in the Sand Engine, while in reality about 82.5% of the volume remained after 3 years (Tonnon et al., 2018). Similarly, in monitoring and design documentation, the Sand Engine's effective lifetime was estimated at around 20 years - a value derived from model-based expectations during the design phase and early observations (Stive et al., 2013). The one-line models treat shoreline changes as a purely alongshore diffusion process whereby they overestimate diffusion of large coastal perturbations, leading to faster predicted

erosion of nourishments. Cross-shore transport gradients are neglected, while these may be relatively large during the initial years as the man-made beach profiles are relatively steep (e.g. 1:32 for the zone + 1 m to − 4 m at the Sand Engine versus 1:55 pre-nourishment). Tonnon et al. (2018) estimated that the Sand Engines effective lifetime could reach 40–50 years when accounting for the initial cross-shore adjustment phase. Similar prolonged mega-nourishments lifetimes were estimated by Arriaga et al., (2017) and Kroon et al., (2015).

5.2.3 Approach of present study

The decadal evolution of mega nourishments includes depth-dependent aspects – sand placed at different elevations redistributes at different rates - that have not yet been systematically addressed in decadal-term modelling studies. This study addresses this gap by explicitly simulating cross-shore heterogeneity, aiming to enable simulating depth-dependent sand redistribution of mega nourishments, focusing on the timescales of profile equilibration and the mobility of sand across different isobaths.

To do so, a coupling of two diffusion-type models was developed: ShorelineS (Roelvink et al., 2020), which simulates complex one-dimensional coastline shapes, and Crocodile (Chapter 3) developed to predict decadal-scale evolution of profile metrics such as shoreline position and coastal volume. The resulting model framework allows for simulation of alongshore and cross-shore sand redistribution of nourished sites without relying on computationally intensive 2D/3D process-based approaches. An important advantage of this approach is computational efficiency: by using simplified physics (diffusion-based transport) and avoiding wave-by-wave time stepping, the model can simulate in the order of 10 years of evolution in roughly an hour wall time on a standard laptop (with a 1.9 GHz processor and 32 GB of RAM). This efficiency makes it feasible to run many scenarios, such as testing different nourishment sizes or placement locations, which is valuable for long-term coastal management under uncertainty.

In this study, we simulate Gaussian-shaped mega nourishments of varying volumes to investigate depth-dependent sand redistribution, focusing on the timescales of profile equilibration and the mobility of sand across different isobaths. One of the simulated nourishments was designed with dimensions comparable to the Dutch Sand Engine, enabling evaluation of model performance against field measurements. The results are discussed in a broader context, highlighting their implications for morphodynamic modeling, and to inform the design, spatial configuration and volume planning of future mega nourishments.

5.2.4 Outline

This chapter starts with by describing the new coupled model framework and case study location, as well as design of 50-year simulation scenarios (section 5.3). We present the model outcomes for both the validation case and scenario simulations, focusing on shoreline change, isobath migration and volume redistribution (section 5.4). Subsequently, these findings, their implications for coastal engineering practice and their transferability to other nourishment projects and settings are discussed

(section 5.5). We conclude by summarising the main outcomes of the study (section 5.6).

5.3 Modeling approach

To investigate the depth-dependent redistribution of sand after implementation of mega nourishments, we use a new coupled modeling framework that integrates shoreline and cross-shore profile evolution. The ShorelineS model represents longshore sediment transport and subsequent translation of the shoreline, while the cross-shore profile model Crocodile simulates gradual profile equilibration. These models are dynamically coupled to capture both alongshore spreading and depth-dependent cross-shore adjustment simultaneously. This section outlines the model components, coupling procedure, simulation setup, and key parameters used in the validation case study and volume-upscaled scenarios.

5.3.1 Model description

ShorelineS (Roelvink et al., 2020) is a model for coastal planform evolution that uses, similar to most coastline models, a one-line (i.e. shoreline) approach based on one dimensional equations for alongshore sand transport due to oblique wave incidence and mass conservation (Pelnard-Considère, 1957). It operates on a freeform grid that consists of one or multiple coastal sections represented as strings of coastline points. The coastline sections can evolve freely and may include complex shapes such as undulations, island and spits. While most 1D models assume a small wave angle (in many cases maximum 45˚, e.g. Hanson & Kraus, 1989; Kristensen et al., 2016; Tonnon et al., 2018), ShorelineS is capable of describing complex coastal transformations such as the splitting and merging of coastline sections. A first hindcast of the Sand Engine (Roelvink et al., 2020) shows the ability of a tuned ShorelineS simulation to reproduce both the observed erosion patterns and the large-scale reshaping of the nourishment.

In ShorelineS, the coastline points are assumed to be representative of the translation of the active coastal profile, and hence are situated at the MSL (Mean Sea Level) contour. The basic equation for the updating of the coastline position is based on the conservation of sediment:

$$\frac{\partial n}{\partial t} = -\frac{1}{D_c}\frac{\partial Q_s}{\partial s} - \frac{\text{RSLR}}{\tan\beta} + \frac{1}{D_c}\sum q_i \qquad (5.1)$$

where n represents the cross-shore shoreline position, s the alongshore coordinate (Fig. 5.1), t is time, D_c is the active profile height (m), Q_s is the alongshore transport (m^3/yr), tan β is the average profile slope between the dune or barrier crest and the depth of closure, $RSLR$ is the relative sea level rise (m/yr) and q_i are the source/sink terms ($m^3/m/yr$) due to cross-shore transport, overwash, nourishments, sand mining and exchanges with rivers and tidal inlet.

Once the alongshore sediment transport is computed, the gained/lost sediment is assumed to redistribute instantly in the cross-shore direction over the active profile height h_a, maintaining a constant shape of the cross-shore profile. In case of $RSLR = 0$

and $q_i = 0$, the shoreline change here thus linearly depends on the alongshore transport gradient $\frac{\partial Q_s}{\partial s}$ and on the active height D_c. Typically, the active height is defined from the inner depth-of-closure (Hallermeijer, 1981) to the berm height or dune toe.

Longshore sediment transport

The gradient in alongshore transport $\frac{\partial Q_s}{\partial s}$ can be computed in ShorelineS in several ways. We opt for transport formula 'VR14', which is a parameterization derived from the TRANSPOR2004 model and presented in van Rijn (2015). Hereby sediment transport Q_s depends on the local wave climate, shoreline orientation and bathymetry:

$$\mathrm{Q_s} = 0.0006 * \ q_{scal} * t_{sc} * \ K_4 * \ K_{swell} * \rho_s * tan\beta^{0.4} * {D_{50}}^{0.6} * {H_{s,br}}^{2.6} * v_{total} \quad (5.2)$$

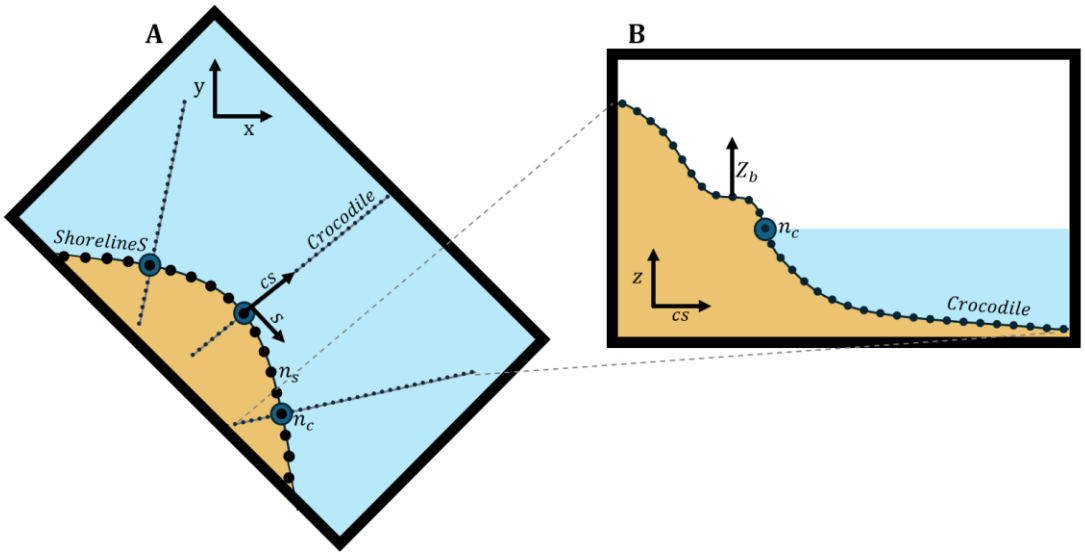

Figure 5.1 Schematic overview grid domains included in the ShorelineS-Crocodile framework. A) Coastline-following coordinate system in the x (North) – y (South)domain, where s represents the alongshore coordinate, and n represents the cross-shore shoreline position, with n_c referring to grid points with a Crocodile profile and n_s without. B) Cross-shore coordinate system with cross-shore coordinate cs (with its origin following cross-shore position n_c), elevation coordinate z and bed level Z_b.

Wherein q_{scal} is a calibration factor of the transport, t_{sc} = 365·24·60·60 is the conversion from seconds to a yearly sediment transport rate to obtain Q_s as $[m^3/yr]$. K_4 is a coefficient that adjusts the sediment transport based on the sediment's density $\rho_s[kg/m3]$ and porosity p:

$$K_4 = 1/\big(\rho_s * (1-p)\big) \quad (5.3)$$

The VR14 bulk transport formulation is similar to Mil-Homens (2013) and Kamphuis (1991) in its main assumptions but differs due to its additional factor to capture the

presence of swell wave conditions through a swell wave parameter K_{swell}, which depends on the occurrence of the swell conditions (P_{swell} in percentage of the year):

$$K_{swell} = 0.015 * P_{swell}(1 - 0.01 * P_{swell}) \quad (5.4)$$

The β in the VR14 formulation represents the slope of the coastal profile. Steeper slopes amplify transport rates, while flatter slopes reduce them. D_{50} represents the sediment grain size. $H_{s,br}$ is the refracted wave height at the point-of-breaking (in [m]). v_{total} represents the alongshore currents due to waves (v_{wave}) and due to tide-driven flow (v_{curr}).

$$\mathrm{v_{total}} = \mathrm{v_{wave}} + v_{curr} \quad (5.5)$$

Herein, v_{wave} is calculated based on the significant wave height at breaking $H_{s,br}$ and the breaking wave angle ϕ_{br}. It is largest for large waves and angles ~45˚.

$$v_{wave} = 0.3 * \left(g * H_{s,br}\right)^{0.5} \sin(2 * \phi_{br}) \quad (5.6)$$

Data required for the ShorelineS model are 1) measured coastlines, 2) wave climate conditions, 3) sediment parameters and 4) transport boundary conditions at the edge of the model. For further information we refer to the ShorelineS manual (Huisman et al., 2024).

Profile change computation

In this research, we couple ShorelineS to the diffusion-type profile evolution model Crocodile (Chapter 3) (Fig. 5.2). Crocodile has been built upon the philosophy that the introduction of a nourishment essentially constitutes a perturbation to the coastal cross shore profile, which tends to evolve to a particular dynamic state (similar to models developed by e.g. Chen and Dodd, 2021, 2019; Coelho et al., 2017; Marinho et al., 2017; Stive et al., 1991). Over sufficiently long temporal and spatial scales, perturbations like nourishments are assumed to diffuse in cross-shore and alongshore directions. Thereby, a continuous and gradual adaptation of the coastal profile $Zb\ (cs, t)$ takes place towards a 'dynamic equilibrium' profile $Zb_{eq}\ (cs, t)$, where cs denotes the cross-shore direction. The latter represents the theoretical average shape and position the coastal profile would attain if all physical forces (waves, winds and tidal currents) and boundary conditions (sea level elevation and sand budget) in the coastal system remained constant with time. Changes in these boundary conditions (e.g., sea level rise, alongshore transport gradients, or the implementation of nourishments) lead to horizontal and vertical translation of $Zb_{eq}\ (cs, t)$ as given by a sediment volume balance. The translation of $Zb_{eq}\ (cs, t)$ due to sea level rise is modelled based on the principles established by Bruun (1954, 1962), whereby $Zb_{eq}\ (cs, t)$ is raised by the change in sea level and shifted onshore to balance total sediment volume.

For the present application, the elements of Crocodile coupled to ShorelineS include its computation of cross-shore sand redistribution, and a depth-dependent term for

sand gain or losses over the cross-shore profile. These elements have varying time-dependent effects on cross-shore profile shape development (Chapter 3, Fig. 5.1). The diffusion term forces gradual cross-shore dispersion towards equilibrium shape on timescales dependent on the wave climate and the size of the (man-made) perturbation. The erosion and deposition term removes or adds sand from the cross-shore profile volume corresponding to the alongshore transport gradient $\frac{\partial Q_s}{\partial s}$ computed by ShorelineS.

Every timestep t, Crocodile computes the 'instantaneous' bed level $Zb\,(cs,t)$ being the time-dependent profile approaching the dynamic equilibrium profile $Zb_{eq}\,(cs,t)$. The rate and extent of sand dispersion in $Zb\,(cs,t)$ depend on the vertical difference between $Zb\,(cs,t)$ and $Zb_{eq}\,(cs,t)$ as well as z', being the profile depth relative to the mean sea level MSL:

$$\frac{\mathrm{d(Zb-Zb_{eq})}}{\mathrm{dt}} = \frac{\mathrm{d}}{\mathrm{dcs}}\left\{\mathrm{D(z')}\frac{\mathrm{d(Zb-Zb_{eq})}}{\mathrm{dcs}}\right\} + \mathrm{E(z')} + \mathrm{Source(z',t)} \tag{5.7}$$

The first right-hand side component of Eq. 5.7 describes cross-shore diffusion. By inclusion of a diffusion coefficient, $D(z')$, the dependency of time-dependent profile dynamics on water depth z' is incorporated. $D(z')$ represents the average sediment redistribution capacity along the profile and thereby regulates the morphological timescale of response. It determines the rate and extent of cross-shore sand diffusion and thereby has a key role in both the time-dependent nourishment dispersion, as well as the depth-dependent coastal adaptation to sea level rise. The shape of $D(z')$ is prescribed as a function of boundary conditions and the local hydrodynamic climate (see Chapter 3), facilitating easy implementation of locations with different hydrodynamic characteristics in Crocodile.

The second component on the right-hand side of Eq. 5.7 represents alongshore sand gain or losses from the cross-shore profile. Hereby we assume erosional/depositional patterns to mirror the wave climate as well. The (depth-integrated) alongshore transport gradient $\frac{\partial Q_s}{\partial s}$ is computed by ShorelineS and used here.

$$E(z') = \frac{\partial Q_s}{\partial s} * \frac{D(z')}{\int_{Zmin}^{Zmax}\big(D(z')\big)\,dz} \tag{5.8}$$

Lastly, the source term in Eq. 5.7 may be used to represent additional nourishment.

The Crocodile model is behaviour-oriented, meaning that the model components are formulated to optimally simulate the evolution of the cross-shore profile without aiming to resolve the underlying physics other than mass-conservation. As we consider a nourishment as a profile perturbation and assume a 'dynamic equilibrium' background profile, any autonomous (nourishment-independent) profile development affecting the profile shape is not resolved. This means that cycles of storm and recovery, cyclic bar behaviour and the passage of alongshore shoreline undulations are not included. The model was validated using three Dutch case study

locations in Chapter 3, reproducing the decadal evolution of bulk parameters such as beach width, shoreline position, and coastal volume for nourishment strategies with varying nourishment volumes and cross-shore placement. On average, volumetric trends were overestimated by $1.5\ m^3/m/yr$ (7%), while modelled coastline trends were $0.2\ m/yr$ (15%) lower than observed. A more detailed description of the model and the validation study is available in Chapter 3 in this thesis.

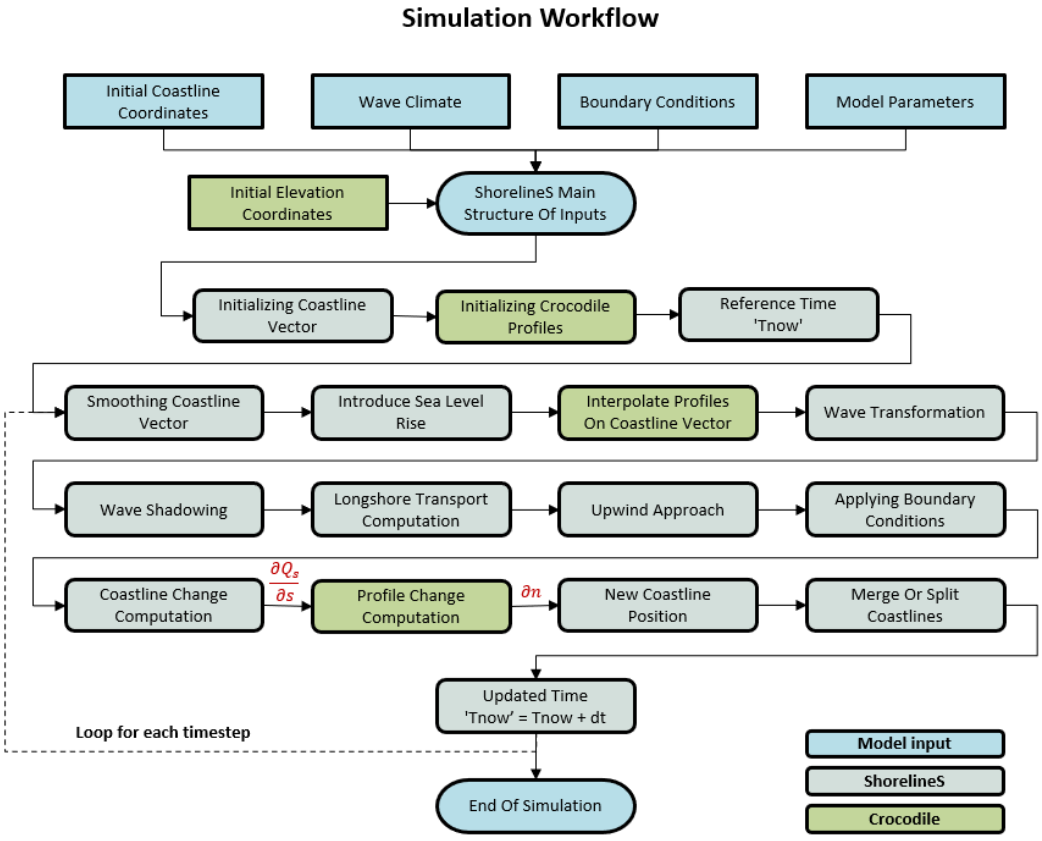

Figure 5.2 Schematic overview of all components included in the ShorelineS-Crocodile framework with exchange of parameters for coupling in red.

Interpolating profiles on Coastline grid

At the start of the simulation, the indices of grid points where $Zb(x,t)$ is computed using Crocodile, P_i, are determined based on a regular spacing interval P_{int} starting from P_{start} to P_{end}. These grid points correspond to coastline positions (x, y) adopted from ShorelineS. Thereby, P_i where the shore-normal either has a landward orientation, or is sheltered (e.g. in a lagoon) are excluded as these locations are not represented by Crocodile, which is designed to simulate open coastal behaviour. The cross-shore coordinate cs over which the profile develops is oriented tangent to the coastline with local coastal orientation ϕ, with its origin cs_0 located at $\big(x(P_i,t), y(P_i,t)\big)$ stretching landward to seaward from CS_{min} to CS_{max}, and corresponding planform location of cs grid points (x_{cs}, y_{cs}). This means that cs_0 changes every timestep along with shoreline movement dn.

The data required for the Crocodile model consist of (x, y, z) point data for both the instantaneous bed level Zb and the dynamic equilibrium profile Zb_{eq} (Fig. 5.1), that cover the domain of all transects. $Zb(P_i, t = t_0)$ and $Zb_{eq}(P_i, t = t_0)$ are extracted from these files for z corresponding to $\mathrm{x,y} = (x_{cs}, y_{cs})$. And wave climate parameters to define $D(z)$.

Each simulation timestep after alongshore transport gradient computation (Eq. 5.1) Crocodile receives the updated grid points (x, y), and all transect location indices P_i are re-determined the location where $\big(x(P_i, t), y(P_i, t)\big)$, is closest to $\big(x(P_i, t-1), y(P_i, t-1)\big)$. After this, we eliminate P_i where the coastline either has a landward orientation, or is sheltered. Cross-shore grid $cs(P_i, t)$ moves along with local coastal orientation ϕ, with its origin cs_0 located at $\big(x(P_i, t), y(P_i, t)\big)$ stretching landward to seaward from CS_{min} to CS_{max}.

For small changes in planform position $\big(x(P_i, t), y(P_i, t)\big)$, we assume the cross-shore profiles are alongshore uniform, and only their cross-shore position and orientation affect Zb and Zb_{eq}. Changes in cross-shore distance, i.e. over coordinate cs, and local profile orientation (ϕ) are accounted for as follows; if ϕ has deviated more than 1° from the configuration at the time of the last interpolation (or the simulation start), timestep t_{ref}, i.e.,

$$| \phi(P_i, t) - \phi\big(P_i, t_{ref}\big) | \geq 1^{\circ} \tag{5.9}$$

the profile is re-aligned by comparing the origin position of cs (x_{cs0}, y_{cs0}) to its position at t_{ref}, and the orientation $\phi\big(P_i, t_{ref}\big)$, is projected onto the new orientation $\phi(P_i, t)$ to yield a transformed coordinate cs_{proj} that remains consistent with the direction of profile development tangent to the shoreline. This projection accounts for the angular difference with respect to the average orientation of the coastal section ϕ_{coast} and is given by:

$$cs_{proj} = \frac{cs}{\cos\big(\phi\big(P_i, t_{ref}\big) - \phi_{coast}\big)} * \cos(\phi(P_i, t) - \phi_{coast}) \tag{5.10}$$

Zb and Zb_{eq} are then linearly interpolated onto cs_{proj}, producing re-aligned profiles consistent with the updated orientation. This framework enables the model to dynamically follow the evolving coastline while preserving valid cross-shore profile shapes under gradual rotation or migration of the shoreline.

From the profile change computed in the Crocodile model, we determine the coastline cross-shore position $n_c(t)$ as a weighted average method to extract the coastline between high water level Zb_{HW} and low water level Zb_{LW}, as follows:

$$n_c(t) = CS_{HW} + \frac{\int_{CS_{HW}}^{CS_{LW}} \big(Zb(cs, t) - Zb(cs = CS_{LW}, t)\big)\, dcs}{2 * (Z_{HW} - Z_{LW})} \tag{5.11}$$

Wherein CS_{HW} and CS_{LW} are the cross-shore positions where $Zb = Zb_{HW}$ and $Zb = Zb_{LW}$ respectively. We compute the coastline change $\frac{\partial n_c}{\partial t}$ due to cross-shore redistribution as:

$$\frac{\partial n_c}{\partial t} = n_c(t) - n_c(t-1) \tag{5.12}$$

wherein $n_c(t)$ and $n_c(t-1)$ represent the coastline at two consecutive iteration timesteps.

Adjusting the shoreline position for cross shore profile changes

After the shoreline change $\frac{\partial n_s}{\partial t}$ is computed in ShorelineS (Eq. 5.1, Fig. 5.3 step 2), profile change is computed (Eq. 5.3, Fig. 5.3 step 3) and the corresponding shoreline change $\frac{\partial n_c}{\partial t}$ (Fig. 5.3 step 4), and $\frac{\partial n}{\partial t}$ is corrected for cross-shore adaptation using the Crocodile model (Fig. 5.3 step 5). This adjustment is performed by linearly interpolating the difference between $\frac{\partial n_c}{\partial t}$ and $\frac{\partial n_s}{\partial t}$ at all P_i and adding this to ShorelineS at all grid points n_s. To ensure that $\frac{\partial n_c(P_i)}{\partial t}$ is not extrapolated to locations that are too far away, an additional point is inserted into the $\frac{\partial n_c}{\partial t}$ array whenever the distance between two P_i exceeds 1.5*P_{int}. For this additional point, $\frac{\partial n_c}{\partial t}$ is set equal to $\frac{\partial n}{\partial t}$. This is for instance the case when a large, sheltered area is present in the simulation.

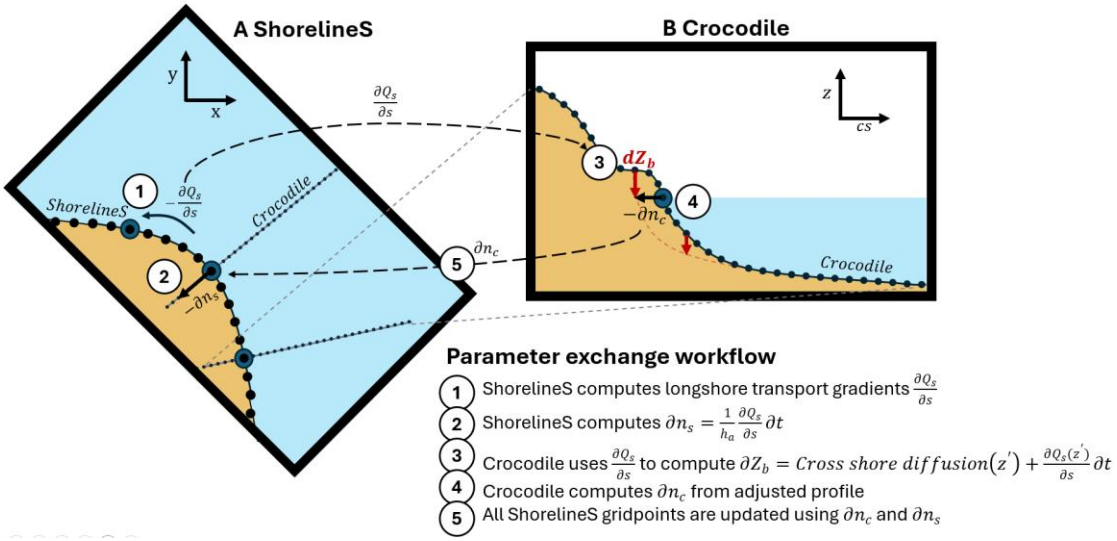

Figure 5.3 Workflow for parameter exchange in shoreline and profile change modeling in ShorelineS-Crocodile. Figure numbers are referred to in the main text.

The merger of Crocodile in ShorelineS can be understood as the combination of two key components: (1) a time-dependent, dynamic active height D_c in Eq. 5.1, which influences coastline changes caused by erosion and deposition (corresponding to the

second term on the right-hand side of Eq. 5.7); and (2) a source/sink term in Eq. 5.1, representing the effects of cross-shore redistribution (corresponding to the first term on the right-hand side of Eq. 5.7). Both terms have important implications for the conservation of sediment within the simulation framework. While ShorelineS-Crocodile conserves volume over the combined cross-shore and alongshore domain, the implementation of cross-shore processes causes volume to be redistributed across elevation, rather than remaining strictly within the horizontal planform. As a result, planform area is no longer conserved, which contrasts with the behaviour of standalone ShorelineS for cases without sources or sinks.

5.3.2 Model calibration and validation approach

Case study location

The Sand Engine, or "Zand Motor", is a large-scale nourishment project located along the Delfland coast in the Netherlands (Fig. 1.2). It was designed as a pioneering solution to address long-term coastal erosion while supporting ecological and recreational benefits. To this end, 17 million m³ of sand was placed with the shape of a hook-shaped peninsula with about 2.4 km alongshore length, extending the shoreline about one km seaward (Stive et al., 2013). To evaluate the performance of our coupled shoreline-profile model, a schematized nourishment is used with dimensions comparable to the Sand Engine, enabling model validation against observed shoreline positions, isobath migration, and profile volume evolution over a 12-year period following implementation.

Wave data

The wave climate is represented in the model as a probability distribution divided into 50 wave direction bins, each associated with an equal total energy flux and a single wave height class (Fig. 5.4). This distribution stays consistent over time, and at each time step, the model randomly selects one wave condition from these 50 options. The same probability distribution is utilized to define the shape of diffusion coefficient $D(z)$ in Crocodile. To this end, the probability that a given wave height is exceeded is described by the survival function (i.e., 1 − cumulative distribution function), as shown in Fig. 5.4. We use a wave climate computed with SWAN (Booij et al., 1997) at 10 m water depth similar to the approach of van Rijn and Huisman (2025).

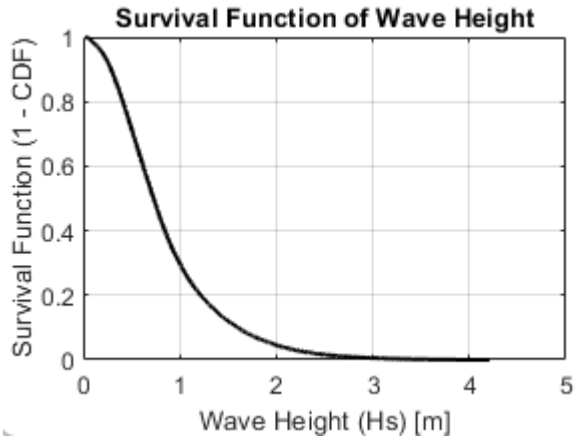

Figure 5.4 Survival function of significant wave height (Hs), defined as one minus the cumulative distribution function ($1 - CDF$), representing the probability that a given wave height is exceeded , as used in the simulation setup.

Model grids

We adopt a simplified geometry for the Sand Engine, using a Gaussian planform fitted to its August 2011 post-construction shape. We define $Zb_{eq,grid}(x,y)$ as a alongshore-uniform grid with cross-shore elevation Zb_{av} (Fig. 5.5A). Zb_{av} is an average profile derived from a set of yearly alti- and bathymetric surveys at the nearby beach of the town Monster over an unnourished period (1966-1979), obtained from the JARKUS dataset (Wijnberg and Terwindt, 1995a), such that sub-decadal autonomous coastal behaviour (e.g., storm cycles, cyclic bar behaviour) is excluded. This cross-shore shape is smoothened with a Gaussian smoothing filter with a kernel size of 30 points, to reduce the impact of small-scale features on the simulation results. This approach avoids the need to adopt a theoretical definition for an equilibrium profile Zb_{eq}, which requires assumptions about hydrodynamic conditions (Dean, 1991), sediment characteristics (Yao et al., 2024), and other environmental factors that could introduce uncertainties. For each individual Crocodile transect P_i, $Zb_{eq}(Pi, cs)$ is derived by interpolating $Zb_{eq,grid}$ on the initial coordinates $\big(x(P_i, t = t_0), y(P_i, t = t_0)\big)$ corresponding to that transect. As a result, the slope and position of Zb_{eq} vary for each transect, depending on its orientation and location. This method ensures that non-shore-perpendicular transects adjust to a slope consistent with the larger-scale coastal system.

To arrive at $Zb_{grid}(x,y)$ a rotated anisotropic Gaussian shape function is added to $Zb_{eq,grid}(x,y)$ which represents a simplified mega-nourishment shape based on the LIDAR alti- and bathymetric measurements at the Sand Engine just after implementation (Fig. 5.5). The Gaussian function is defined by amplitude A, spatial spreads σ_x (cross-shore) and σ_y (longshore), and rotated by coastal orientation angle θ, centred at (x_0, y_0).

$$Zb_{gaussian}(x,y) = \tag{5.13}$$

$$A \cdot \exp(-[\, a * (x - x_0)^2 + 2b * (x - x_0)(y - y_0) + c) * (y - y_0)^2])$$

With

$$a = (cos(\theta))^2 / (2 * \sigma_x^2) + (sin(\theta))^2 / (2 * \sigma_y^2) \quad (5.14)$$

$$b = -sin(2\theta) / (4 * \sigma_x^2) + sin(2\theta) / (4 * \sigma_y^2) \quad (5.15)$$

$$c = (sin(\theta))^2 / (2 * \sigma_x^2) + (cos(\theta))^2 / (2 * \sigma_y^2)(z') \quad (5.16)$$

The final bathymetry, $Zb_{grid}(x, y)$, is constrained with maximum elevation $Zb_{max} = 4\ m$ which represents the elevation of the top dry area of the Sand Engine:

$$Zb_{grid}(x, y) = \min\Big(\max\Big(Z_{beq,grid}(x, y) + Zb_{gaussian}(x, y), Zb_{eq,grid}(x, y)\Big), Zb_{max}\Big) \quad (5.17)$$

We fit this shape to resemble the coastline and bathymetric contours of the centre transect, arriving at $A = 6000\ m$, $\sigma_x = 440$ and $\sigma_y = 690$. Integrating the elevation difference between $Zb_{grid}(x, y)$ and $Zb_{eq,grid}(x, y)$ over the grid domain yields the nourishment volume added, $V_N = 20668522\ m^3$. This is slightly higher than the volume in the real-world Sand Engine, mainly because of absence of the lagoon and lake in the schematized nourishment (de Schipper et al., 2016).

To create a ShorelineS input shoreline grid, the MSL elevation contour is extracted from the $Zb_{grid}(x, y)$ and $Zb_{eq,grid}(x, y)$, whereby a spatially uniform grid is defined in the *x* (east-west) and *y* (north-south) directions using a base cell size $ds_0 = 100\ m$. The model adaptively updates this grid during simulation, keeping cell sizes between 70% and 140% of ds_0. Points with location (x_s, y_s) are added when spacing exceeds $2 * ds_0$, and removed when it drops below 70% of ds_0. Tangent to (x_s, y_s) cross-shore transects are defined with uniform cross-shore intervals $dcs = 20\ m$ and horizontal grid cell coordinates (x_c, y_c), where Zb and Zb_{eq} are extracted for each Crocodile transect.

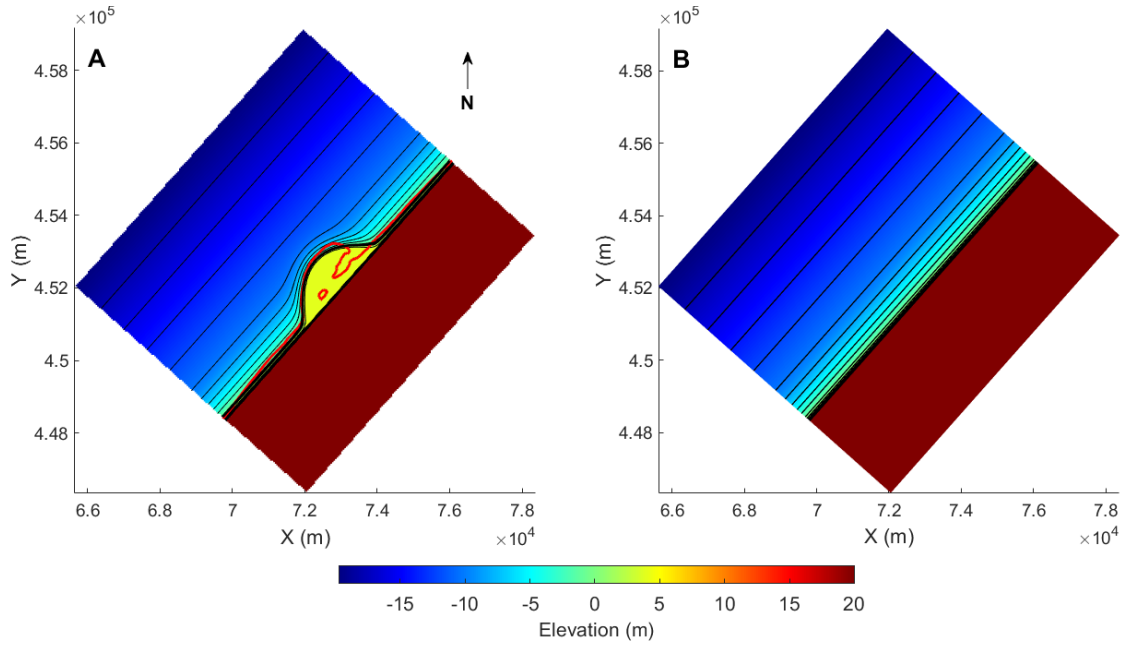

Figure 5.5 A) Initial profile elevation $Zb_{grid}(x,y)$, B) initial equilibrium profile elevation $Zb_{eq,grid}(x,y)$. Colors indicate elevation relative to mean sea level. The coastline of the Sand Engine (red) is shown for scale reference.

Parameter settings

In the simulations performed in this research we use a fixed coastal timestep $dt = 6\ hours$. Sediment transport in ShorelineS is modelled using the VR14 formulation, with a median grain size of $d50 = 0.2\ mm$, roughness height $ks = 0.05\ m$, and active profile height $h_0 = 10\ m$.

Extraction of coastal state indicators

We extract several coastal state indicators from the simulations and JARKUS measurements. Parameters from the ShorelineS-Crocodile simulation are denoted with a subscript $\_c$, while parameters from the ShorelineS standalone simulation are denoted with subscript $\_s$ and JARKUS measurements with subscript $\_m$.

The first coastal state indicator is the evolution of shoreline $(x(t), y(t))$ over time. For each measured transect, we compute the cross-shore shoreline position n_m as:

$$n_m(t) = CS_{HW} + \frac{\int_{CS_{HW}}^{CS_{LW}} \left(Zb(cs,t) - Zb(cs = CS_{LW}, t)\right) dcs}{2 * (Z_{HW} - Z_{LW})} \tag{5.18}$$

where CS_{LW} and CS_{HW} denote the cross-shore positions of the mean low- and high-water elevations Z_{LW} and Z_{HW}, respectively, and dcs is the cross-shore integration variable. The adoption of this centre of mass-based approach aims to mitigate local variations and thereby achieve more consistent outcomes. We then interpolate the corresponding measured planform coordinates $(x_m(t), y_m(t))$ at this cross-shore location.

The change in coastline position is then given by:

$$\Delta n_m(t) = n_m(t) - n_m(t_{ref}) \tag{5.19}$$

The second coastal state indicator is the temporal evolution of profile volume change ΔV_p. For JARKUS measurements we compute this as:

$$\Delta V_{p,m} = \int_{cs_{min}}^{cs_{max}} \left(Zb(cs,t) - Zb(cs, t = t_{ref})\right) dcs \tag{5.20}$$

Whereby cs_{max} and cs_{min} are the cross-shore coordinates where $Zb(cs, t = t_{ref})$ is below 10 and above -20 m respectively. In ShorelineS-Crocodile the $cs - z$ transect orientation changes along with coastline orientation. In this case, we use a similar formula to obtain ΔV_p but with a correction to project on the tangent axis:

$$\Delta V_{p,c} = \int_{cs_{min}}^{cs_{max}} \left(Zb(cs,t) - Zb(cs, t = t_{ref})\right) dcs * \cos\left(\phi_{xy} - 270 - \theta\right) \tag{5.21}$$

Whereby ϕ_{xy} represents the orientation of the transect at its coastline point (x_0, y_0), which we compare to coastal orientation angle θ.These angles are defined clockwise from the north, i.e. $\phi_{xy} = 270$ would represent an east-west transect with the sea to the west an d land to the right.

For ShorelineS standalone we build upon its intrinsic assumption that volume and coastline position are linearly coupled by multiplying the coastline position $n_S(t)$ with active profile height h_0:

$$\Delta V_{p,s} = (n_S(t) - n_S(t_{ref})) * h_0 \tag{5.22}$$

Whereby shoreline movement directly translates to a corresponding volumetric change, uniformly distributed over the active profile height.

Also, we consider changes in position in different depth contours. In the measurements we compute the cross-shore elevation contour position $\Delta cs_{contour}$ as:

$$CS_{contour}(t) = CS_{(Z_b = z_{contour}+1)} + \frac{\int_{CS_{(Z_b = z_{contour}+1)}}^{CS_{(Z_b = z_{contour}-1)}} (Zb(cs,t) - z_{contour} - 1)\, dcs}{2} \tag{5.23}$$

And for ShorelineS-Crocodile similarly to volume with a correction for the rotating transect orientation:

$$CS_{contour}(t) = CS_{(Z_b=z_{contour}+1)} + \frac{\int_{CS_{(Z_b=z_{contour}+1)}}^{CS_{(Z_b=z_{contour}-1)}} (Zb(cs,t) - z_{contour} - 1)\, dcs}{2} * \cos(\phi_{xy}(t) - 270 - \theta) \quad (5.24)$$

And its change as:

$$\Delta CS_{contour}(t) = CS_{contour}(t_{ref}) - CS_{contour}(t) \quad (5.25)$$

For ShorelineS we assume the depth contours to move parallel along with the coastline, thus;

$$\Delta CS_{contour,s}(t) = CS_{Zb_{eq},contour,s}(t_{ref}) - \Delta n_s(t) \quad (5.26)$$

A last metric we consider is a ratio between the centre transect profile volume and its alongshore component:

$$R_{cs}(t) = \frac{dV_p(t)}{dn(t) * h_0} \quad (5.27)$$

This is inspired by the ratio between nourishment volume and planform area proposed by Dean (2002), but reformed to only consider the central nourishment transect to avoid the need to interpolate to obtain a alongshore integrated total nourishment volume and area. It describes the progression of profile equilibration after nourishment. During equilibration, $dV_p(t)$ stays constant while $dn(t) * h_0$ decreases. The function approaches unity when equilibration progresses.

Similarly, we compute the percentage of shoreline change driven by alongshore sand dispersion (% dn_{ls}) as:

$$\%\, dn_{ls} = \frac{R_{cs}(t)}{R_{cs}(t_{end})} * 100\% \quad (5.28)$$

and cross-shore sand dispersion (% dn_{cs}) as:

$$\%\, dn_{cs} = (1 - \frac{R_{cs}(t)}{R_{cs}(t_{end})}) * 100\% \quad (5.29)$$

Calibration

We calibrate transport calibration factor q_{scal} in Eq. 5.2 to match changes in profile volume V_p observed at the centre transect of the Sand Engine during two years shortly after implementation (August 2012 – August 2014). The lowest root mean square error (RMSE) between observed and modelled V_p is found for transport calibration factor q_{scal}=0.24. Note this q_{scal} value only influences the rate of alongshore developments, not the shape. This q_{scal} value is relatively low and implies that, at this site, only 24% of the alongshore sediment transport is effectively generated compared to what could be expected from the van Rijn formula under default conditions.

The low value may be explained by the wave focusing due to refraction of the shallow, wide and gently sloping foreshore in front of the peninsula. This leads to early wave breaking and strong refraction, resulting in waves arriving more shore-normal than expected, lowering the wave-driven alongshore transport. As shown in Tonnon et al. (2018), the inclusion or exclusion of this shallow zone (between -10 m and -6 m elevation) can change estimated transport by a factor of 2, or even more. The calibrated q_{scal} compensates for this physical mechanism that is not reproduced in ShorelineS.

5.3.3 Simulation set-up for volume-upscaled mega nourishments

To evaluate the impact of nourishment volume on cross-shore and alongshore redistribution, we evaluate two volume-upscaled 'future' nourishment solutions. We follow a top-down methodology to determine the size of mega nourishments under elevated sea level rise, whereby the local nourishment application in the simulated transect is determined based on the sediment demand in the area. In the Netherlands. The annual sediment demand V_{sd} for the coastal zone is computed as follows (Lodder and Slinger, 2022):

$$V_{sd} = A * SLRr + V_{sub} + V_e \tag{5.30}$$

The nourishment strategies assume that area A, here defined as the region between closure depth x_{doc} and the seaward first dunetop $x_{dunetop}$, shall grow along with the rate of sea level rise $SLRr$ with a 'basis' amount of sand (V_e) needed to account for erosion due to alongshore transport gradients. No volume changes to account for subsidence are used here ($V_{sub} = 0\ m^3$).

While the need for this research is partially motivated from the foreseen acceleration in sea level rise over the coming century, we chose not to explicitly include many scenarios with different rates of sea level rise ($SLRr$). Rather, we choose two distinct $SLRr$ scenarios to define volumes of sand applied per nourishment event V_N; with Eq. 5.1 it can then be deduced what return period T_N is required to adhere to nourishing V_{sd} under a particular $SLRr$. This is motivated by the fact that the impact of scenario choices such as V_N, T_N and nourishment placement location on nourishment dynamics dominate the effect of rising sea levels on morphologic changes. V_N is thereby chosen such that we adhere to V_{sd} under either $SLRr = 8\ mm/yr$ or $SLRr = 16\ mm/yr$ for the nourishment design similar to the Sand Engine; thus

$$V_{N,SLRr} = \mathrm{V_{N,Sand\ Engine}} + A * (\mathrm{SLRr} - 0.002) * T_N \tag{5.31}$$

Whereby we use $\mathrm{V_{N,Sand\ Engine}} = 20.7 * 10^6\ \mathrm{m^3}$ (similar to our schematized Sand Engine) for $SLRr = 2\ mm/yr$ over the original design timespan of $T_N = 20\ years$, for an area obtained by multiplying the alongshore stretch of coast between the harbour entrances of Scheveningen and Rotterdam with an estimate of the cross-shore profile extent $A = 17\ km\ (longshore) * 5km\ (cross-shore) = 85\ km^2$. Under $SLRr = 8\ mm/yr$ we arrive at $V_N = 31\ 000\ 000$, and under $SLRr = 16\ mm/yr$ $V_N = 44\ 000\ 000$

(Fig. 5.6). These nourishments are designed by stretching the Gaussian shape in cross-shore direction by increasing σ_x (Eq. 5.13-5.18).

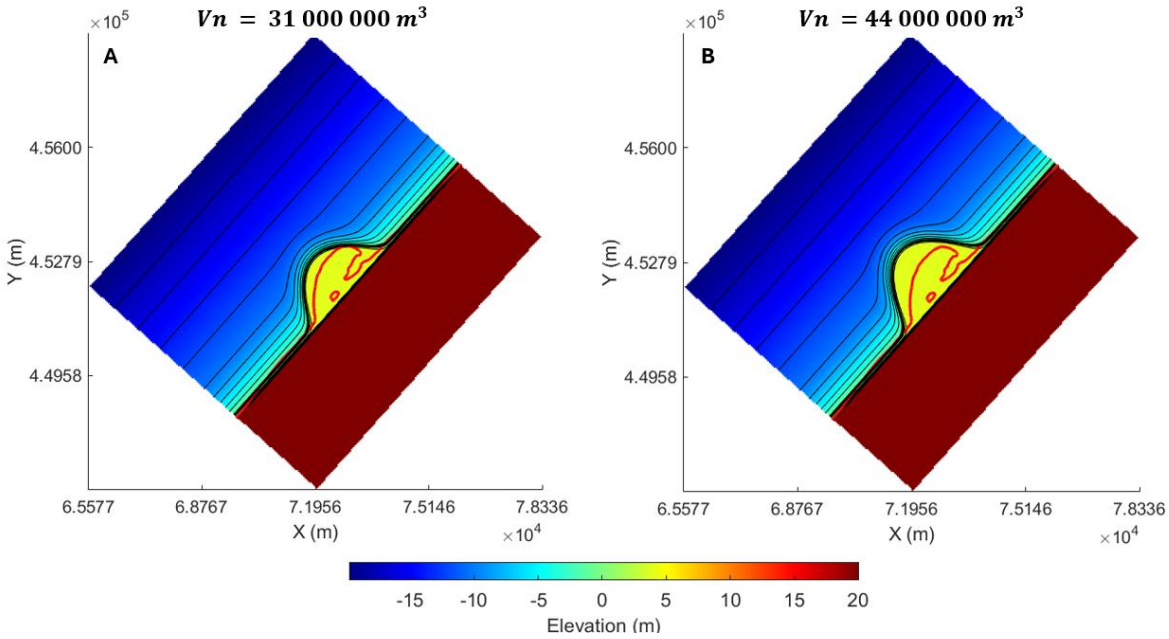

Figure 5.6 Initial elevation grid Zb_{grid} for simulations with gaussian-shaped mega nourishments with initial volumes of A) $V_N = 31\,000\,000\,m^3$, and B) $V_N = 44\,000\,000\,m^3$. The coastline of the Sand Engine (red) is shown for scale reference.

5.4 Results

5.4.1 Model-observation comparison

To assess the validity of the coupled Crocodile–ShorelineS model for simulating shoreline, volumetric and isobath evolution following mega nourishment, simulation outputs are compared against 10-year observational data from the Sand Engine case study. The following section focuses on the model's ability to reproduce the key morphological changes in volume and shoreline position over the first decade following implementation.

The coupled model, calibrated on two years of data, successfully reproduces the main patterns of shoreline change over the 10-year timespan (Fig. 5.7). It replicates the rate of fast shoreline retreat that decelerates with time at the peninsula centre, and the gradual accretion in adjacent beaches. Across the 10-year validation period (2014-2024) the root mean square error (RMSE) is below 55 m, whereby ShorelineS-Crocodile slightly overestimates the overall coastline retreat and underestimates coastline accretion across the domain (Fig. 5.7). This error could be reduced by calibrating the model over the entire coastal stretch rather than just the central transect, or by extending the 2-year calibration period.

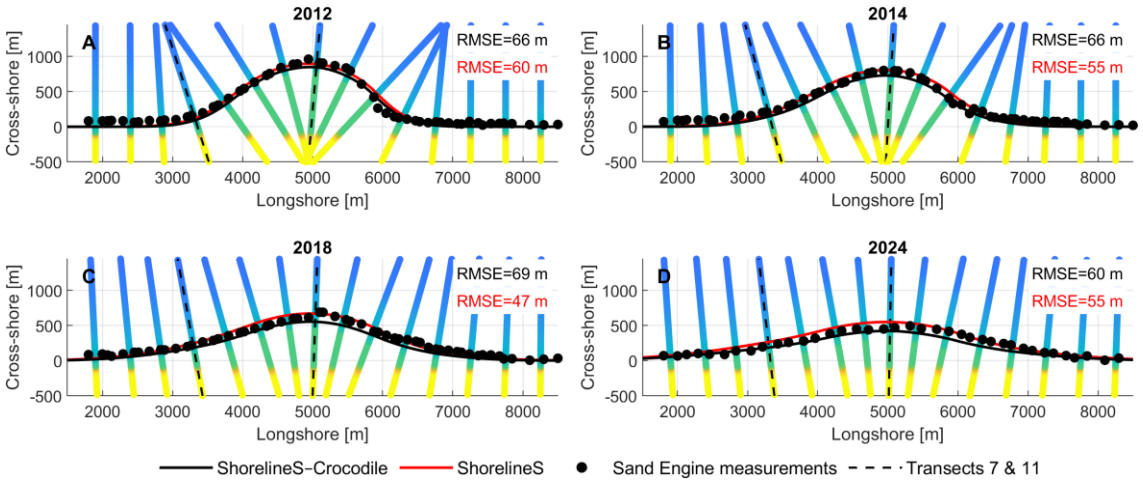

Figure 5.7 Evolution of the shoreline modelled with ShorelineS-Crocodile (black line) against observed shoreline (most seaward MSL + 0 m contour from JARKUS measurements in black dots). The red line shows the modelled shoreline from standalone ShorelineS for reference. Colored lines represent the Crocodile transects with colors according to the colorbar in Fig. 5.6.

Focusing on the central peninsula transect (dashed line at alongshore position 5000 m in Fig 5.7), it becomes evident that the evolving cross-shore dynamic profile, $Zb(t)$, drives the rapid initial shoreline retreat at this point (Fig. 5.8A). This retreat is primarily due to the initially steep profile (1:32 for the zone $MSL + 1$ to $MSL - 4\,m$) near the shoreline and within the upper surf zone after implementation of the Sand Engine - significantly steeper than the equilibrium profile $Zb_{eq}(t)$ (1:55 for the zone $MSL + 1$ to $MSL - 4\,m$). This steepness causes net cross-shore sand transport to lower elevations, resulting in retreat around the MSL 0 m isobath and slight offshore shift of the profile between $MSL - 6$ and $MSL - 10\,m$. Because this sand remains within the defined seaward and landward boundaries of the cross-shore profile (as per Eq. 5.21), it does not contribute to net profile volume loss. Instead, the volume change reflects the lateral (alongshore) redistribution of sediment. Both the modelled shoreline retreat and the calculated volumetric change at the centre transect are consistent with Sand Engine observations, yielding root mean square errors (RMSE) of 12 m for shoreline position and 139 m³/m for cross-shore volume change (Fig. 5.8C).

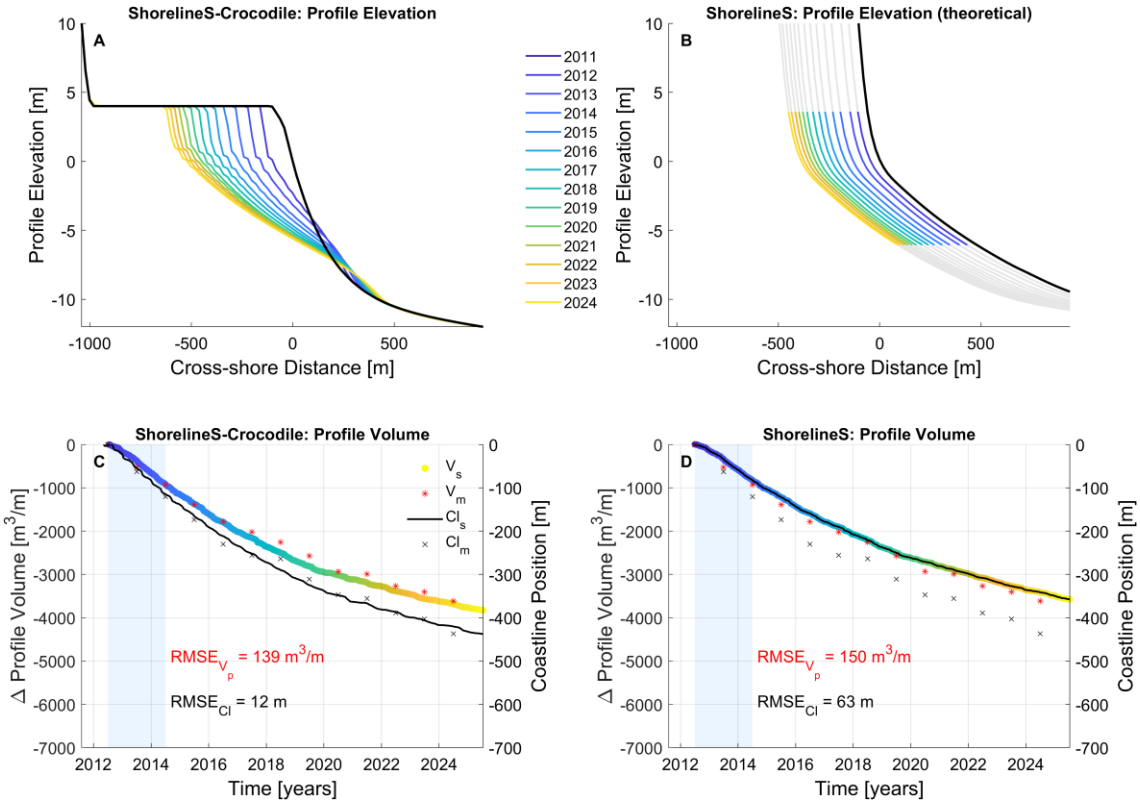

Figure 5.8 A,B) Evolution of Sand Engine profile elevation in the central nourished transect simulated with ShorelineS-Crocodile (A) and deduced from a standalone ShorelineS simulation (B). The black line in A and B shows the initial profile. C,D) Evolution of profile volume (coloured) and coastline position (black) in the central nourished transect simulated with ShorelineS-Crocodile (C) and with ShorelineS (D), along with JARKUS observations. The blue area shows the calibration period. Profile colours in A and B match with the volume data within the same year in C and D respectively.

Accretion along the lateral flanks of the peninsula occurs between $MSL - 9\,m$ and $MSL + 4\,m$, with the overall profile shape and slope within this range remaining largely unchanged (Fig. 5.9A). A data-model comparison at $1\,km$ north of the peninsula centre (indicated in Fig 5.7 with a dashed line), yields an $RMSE$ of $201\,m^3/m$ for profile volume change and $30\,m$ for shoreline change (Fig. 5.9C). These skill metrics are lower than those for the peninsula centre transect, which is expected given that the model was calibrated specifically for volume changes at the peninsula head. Additionally, morphological changes at this flank location are less influenced by the nourishment compared to the central area, contributing to the reduced model performance.

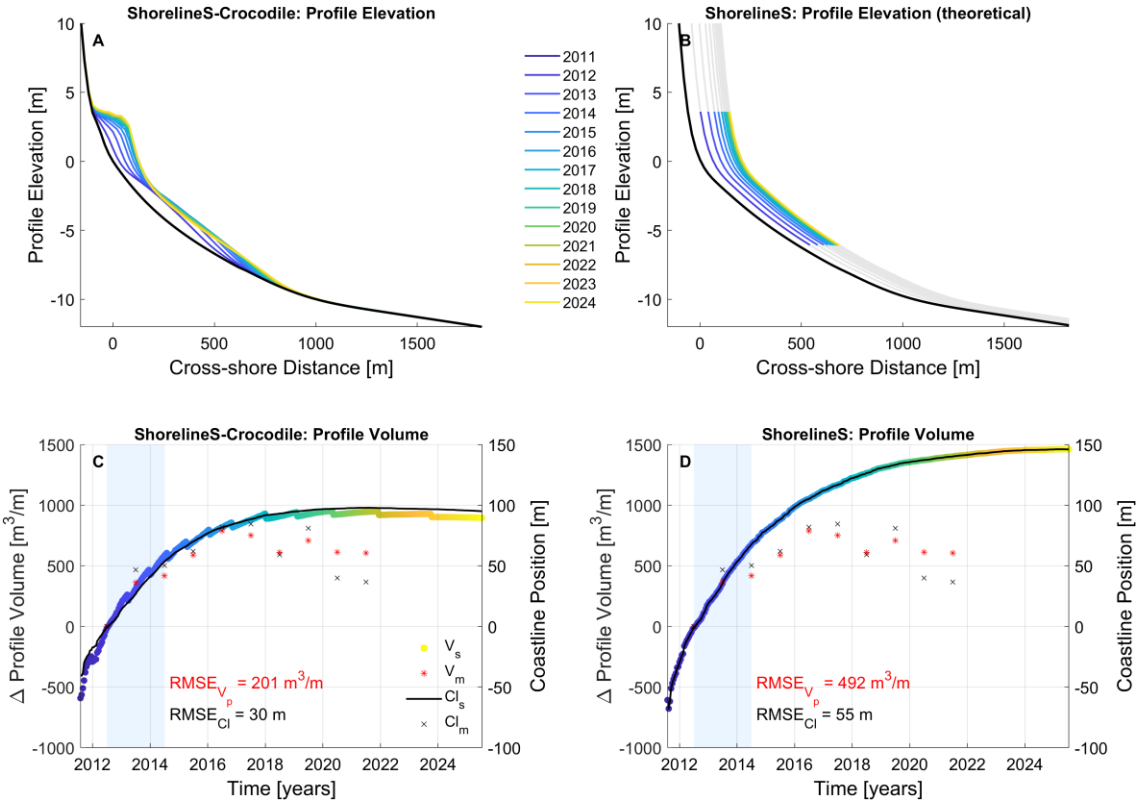

Figure 5.9 A,B) Evolution of Sand Engine bed elevation profile in a transect northwards of the Sand Engine simulated with ShorelineS-Crocodile (A) and deduced from a standalone ShorelineS simulation (B). The black line in A and B shows the initial profile. C,D) Evolution of profile volume (coloured) and coastline position (black) in a transect northwards of the Sand Engine simulated with ShorelineS-Crocodile (C) and with ShorelineS (D), along with JARKUS observations. The blue area shows the calibration period. Profile colours in A and B match with the volume data within the same year in C and D respectively.

5.4.2 Influence of cross-shore profile evolution on model results

To isolate the impact of including cross-shore dynamics, shoreline evolution predicted by the coupled ShorelineS-Crocodile model is compared to results from the standalone ShorelineS. While both models are calibrated on profile volume using the same boundary conditions and forcing, only the coupled version accounts for depth-dependent cross-shore redistribution (Fig. 5.8 A vs. B).

Notable differences arise during the early years after Sand Engine implementation, particularly at the most seaward part of the peninsula. ShorelineS-Crocodile simulates more pronounced initial shoreline retreat than the standalone ShorelineS, driven by the steeper post-nourishment profile and associated cross-shore sediment transport to lower elevations. In contrast, ShorelineS relies on a fixed relationship between volume change and shoreline position (Eq. 5.22), resulting in a more uniform retreat across time. At the central transect, the coupled model reproduces the measured 255 m retreat within 1% (254 m) by year 5 (2012–2017), a clear improvement over the 192

m retreat simulated by ShorelineS alone (–24%, difference of 62 m; Fig. 5.8C,D). In the subsequent years, the absolute difference between the models continues to grow, but at a slower rate as the Crocodile profile evolves toward equilibrium: by year 12 (2024), the gap has widened to 79 m. ShorelineS–Crocodile then predicts 421 m retreat, only 2% below the observed 431 m, whereas ShorelineS alone underestimates retreat by 21% (342 m). This reflects a 19% improvement in predictive skill after 10 years through coupling.

Overall, ShorelineS-Crocodile slightly overestimates the overall coastline retreat across the 12 years, while ShorelineS tends to underestimate it (Fig. 5.7). Compared to JARKUS measurements, this faster shoreline retreat in ShorelineS-Crocodile is more accurate, with a significantly lower $RMSE = 11\,m$ compared to $RMSE = 59\,m$ for ShorelineS.

Volumetric changes and their predictive accuracy are roughly similar across both simulations. However, the coupled model redistributes the volume lost at the shoreline to lower-elevation, more seaward layers, effectively capturing the decoupling between volumetric and shoreline change. This enhances its ability to represent coastline dynamics resulting from contemporary cross- and alongshore processes, compared to the fixed linear relationship between dV_p/dt and dn/dt in ShorelineS.

Accretion patterns along the flanks of the peninsula are more similar, with both models producing a comparable seaward shift of the shoreline. This consistency is expected, as the volume of sand added in these areas is relatively small. As a result, the local profiles are already close to the dynamic equilibrium, and the Crocodile model's profile redistribution results in a very similar depth-dependent pattern as a shifting equilibrium profile (Fig. 5.9A,B). However, three years after nourishment implementation, ShorelineS predicts slightly larger accretion in the lateral areas. This is driven by larger alongshore transport gradients, as the shoreline at the nourishment centre remains further seaward for a longer period - a direct result of the absence of cross-shore equilibration in ShorelineS standalone. Including the cross-shore model improves the model skill with RMSE values decreasing from $RMSE = 492$ to $201\,m^3/m$ for profile volume change, and from $RMSE = 55$ to $30\,m$ for shoreline change.

5.4.3 Depth dependency of sand redistribution

The coupling of ShorelineS with the Crocodile model provides additional insight beyond shoreline position alone by resolving depth-specific sediment redistribution. To explore this layer-specific behaviour, we analyze the evolution of various depth contours in simulations and measurements, focusing on the central nourished transect, where the morphological response is most pronounced.

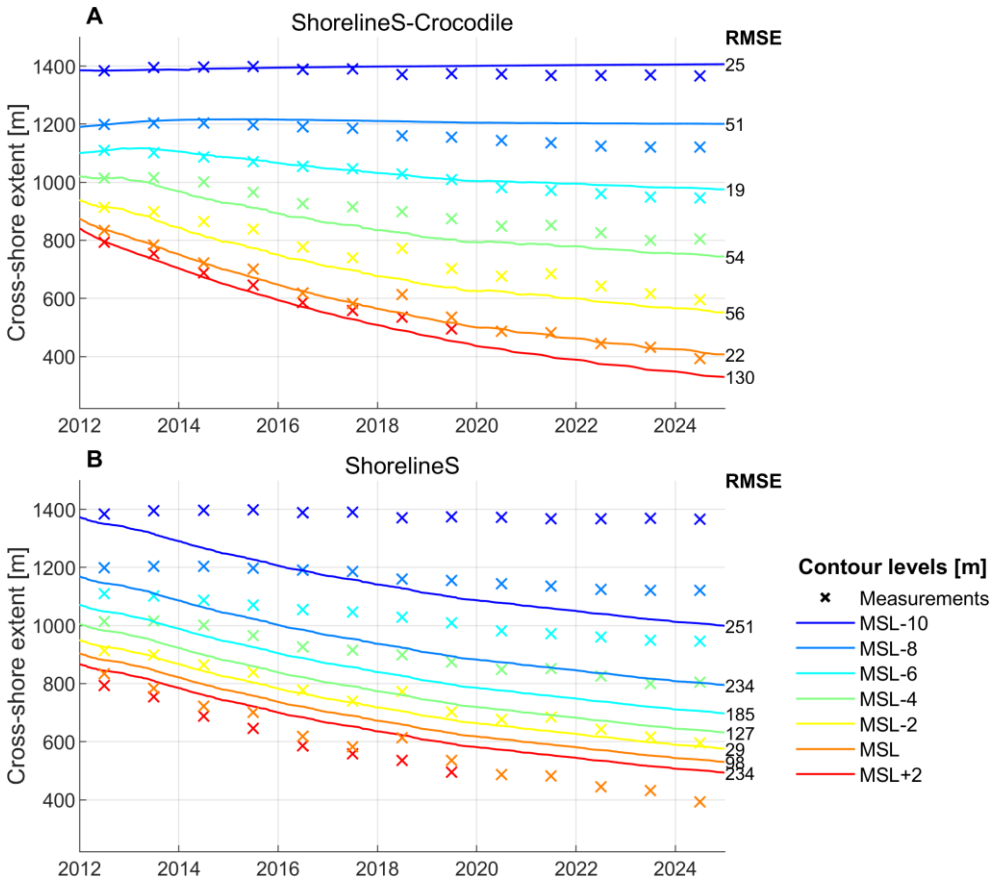

Figure 5.10 Evolution of depth contour levels in the central nourished transect simulated with ShorelineS-Crocodile (A) and deduced from ShorelineS simulation (B). The post-2020 measurements at $MSL + 2\,m$ were excluded due to the Sand Engine lake presence affecting this contour.

Modelled isobaths clearly show the impact of merging the two models (Fig. 5.10) ShorelineS-Crocodile shows good agreement with observations across different depth contours (Fig. 5.10A). It accurately reproduces the minimal contour movement at $MSL - 8$ and $MSL - 10\,m$, the initial accretion followed by erosion around $MSL - 6$ and $MSL - 4\,m$ and the previously discussed shoreline retreat at $MSL - 2$, MSL and $MSL + 2\,m$ contours. It is worth emphasizing that the cross-shore model was not explicitly calibrated to match the depth contour evolution at this site - indicating that the vertical variation in the diffusion coefficient is already physically meaningful and could further improve with optimization. Across all contours, ShorelineS-Crocodile achieves an average RMSE of 48 m, reflecting a strong agreement with the JARKUS measurements and validating the model's ability to simulate depth-dependent alongshore redistribution.

Although deducing depth contour behaviour from ShorelineS standalone (Fig. 5.10B) extends beyond its intended application, we include this comparison to illustrate that the equilibrium profile assumption performs poorly particularly for the lower-elevation, more seaward contours. On average, the $RMSE$ is $175\,m$. We thereby

conclude that the inclusion of Crocodile improves layer-specific lateral diffusivity of the nourishment shape.

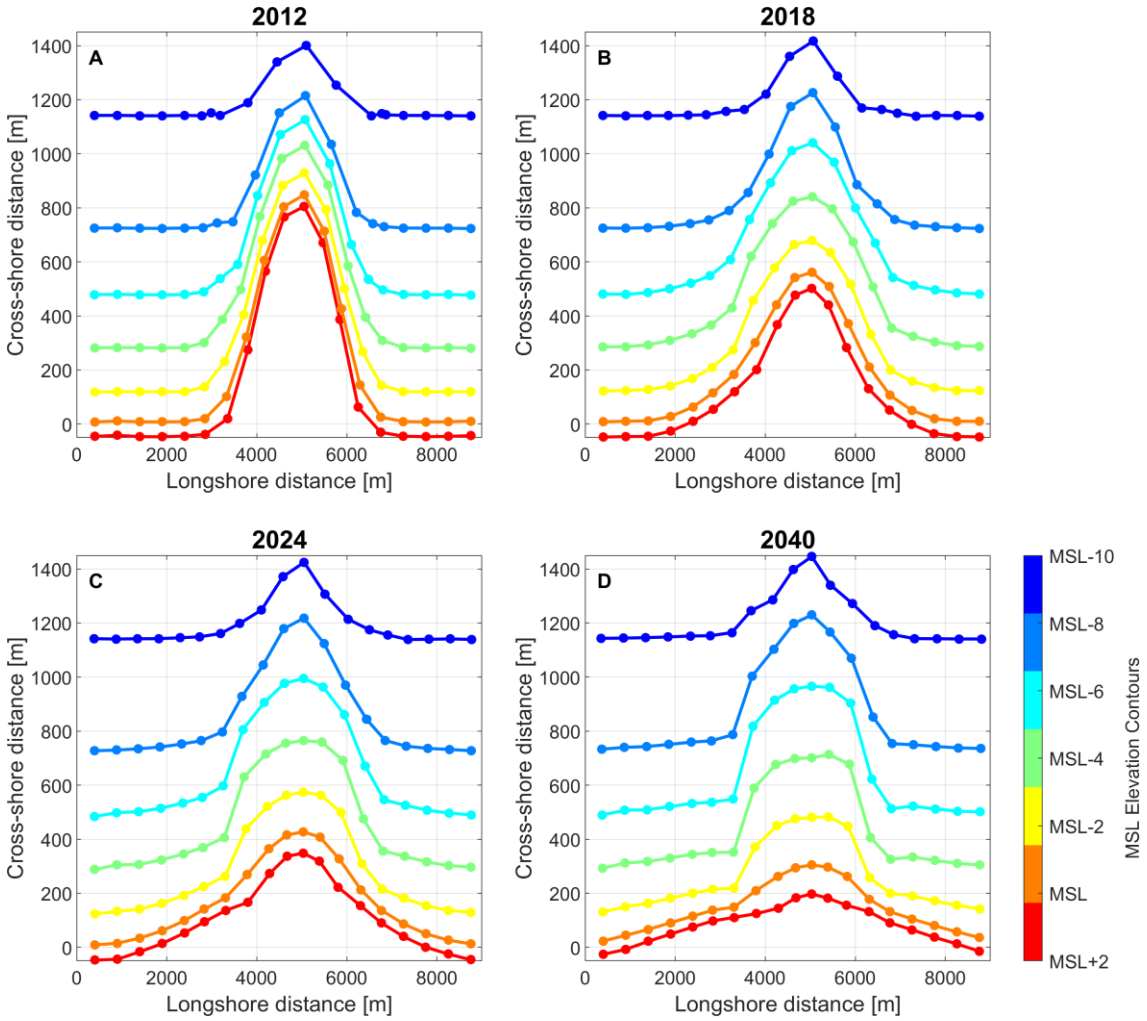

Figure 5.11 Evolution of depth contour levels in top view with ShorelineS-Crocodile. The cross-shore scale is stretched to enhance detail.

5.4.4 Impacts of cross-shore nourishment development on long-term nourishment forecasting

By extending the simulations over a 50-year period we examine how depth-dependent diffusivity influences computed long-term coastal change. The initial cross-shore redistribution resulting in more pronounced initial shoreline retreat at the peninsula head results in faster reduction of alongshore coastline curvature, which in turn reduces alongshore sediment transport gradients and long-term volumetric loss. Over the 50-year period, the coupled model simulates a total central profile volume loss of $5498\frac{m^3}{m}$, which is $444\frac{m^3}{m}$ (8%) more than in the uncoupled model (Fig. 5.8C). Given an initial nourishment profile volume of 10,875 m³/m at the central transect, and with more than half of that volume remaining after 50 years, the estimated lifetime of the Sand Engine in this study is relatively long. However, it is important to note that

ShorelineS computes $\frac{dQ_s}{dt}$ based on coastline position only, also in the coupled version. This simplification may underestimate the alongshore transport, as the seaward extent of lower depth contours, that retreat slower than the shoreline contour (Fig. 5.10), is not taken into account. While reduced alongshore transport may be realistic given the faster retreat, the actual effect is likely smaller than what the model suggests. Furthermore, this 8% difference in central profile volume loss falls well within the broader uncertainties of the modeling framework, leading to the conclusion that total volumetric losses are minimally affected by the inclusion of Crocodile.

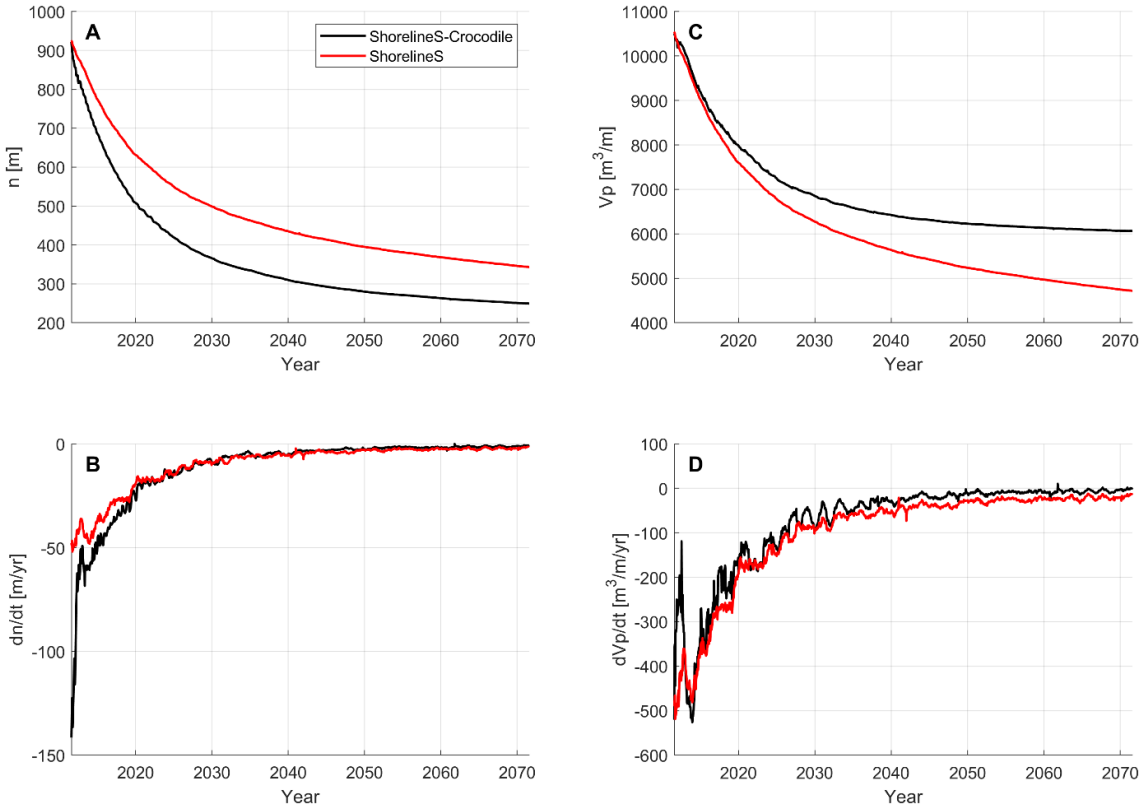

Figure 5.12 Evolution of A) coastline, B) profile volume, C) rate of coastline change and D) rate of volume change in the central nourished transect for a 60-year timespan. Note the larger differences compared to Fig. 5.7, as the reference point is now the start of the simulation rather than the first JARKUS measurement. Substantial changes occur within the first year, influencing the overall trends.

Our results show that cross-shore equilibration significantly affects shoreline retreat over the first decade, after which its influence diminishes considerably. In the coupled model, the shoreline retreats by 694 m over 50 years - 104 m (15%) more than in the uncoupled model (Fig. 5.12A). This difference develops almost entirely during cross-shore equilibration in the first 10 years; after that, the shoreline retreat rate dn/dt is approximately similar for the two (Fig. 5.12B). This pattern confirms that cross-shore processes have large influence in early shoreline evolution but exert limited influence in the longer term.

Further evidence of this early equilibration is provided by the Dean ratio (Eq. 5.27), which is levelling of approximately by 2020 (Fig. 5.13A), indicating that the profile has largely equilibrated by then. The asymptote is 0.8, and as active height $h_0 = 10\,m$ (chosen to match ShorelineS model settings), this means that the representative height of the active layer in the coupled model is about 8 meters. We observe that just after implementation, the percentage of shoreline change driven by cross-shore processes is 73%, and by alongshore processes 27% (Fig. 5.13B). After five years this ratio shifts to roughly 10% cross-shore versus 90% alongshore, and after ten years further to 100% alongshore.

Analysis of depth contours show how different layers begin responding to shoreline changes at different times. While shallower contours adjust relatively quickly, offshore contours around the closure depth remain largely immobile also over extended periods. At the nourishment head transect, the lower portion of the nourishment volume remains in place throughout the simulation (Fig. 5.10A). Similarly, in the lateral areas, minimal movement is observed around the MSL–8 m and MSL–10 m contours over the entire 50-year period, whereas higher-elevation contours continue to shift seaward even after 30 years (Fig. 5.11). These patterns indicate that a substantial fraction of the nourished sand, especially in lower-elevation offshore parts of the cross-shore profile, remains largely inactive within the coastal system over the 50-year analysis period.

The model in this study was calibrated based on volumetric change, whereas traditional shoreline models are often calibrated using shoreline position data (e.g., from historical aerial imagery, lidar, or satellite) under the assumption of equilibrium behaviour. Our results demonstrate that if ShorelineS had been calibrated solely on shoreline movement, it would have required a 50% higher q_{scal}, leading to 50% faster shoreline retreat and a correspondingly 50% shorter estimated lifetime for the Sand Engine. Since the model equations for alongshore transport (Eq. 5.2-5.6) compute volumetric change, calibration should be volume-based. However, if calibration is performed after the initial few years the assumption of purely alongshore transport becomes reasonably valid. This highlights a critical consideration that traditional shoreline models may misrepresent early behaviour. If a model is tuned to match the rapid initial shoreline response, which is largely affected by cross-shore equilibration, it will tend to overestimate long-term volumetric loss. Conversely, calibrating for longer-term shoreline retreat will likely underestimate the initial adjustment.

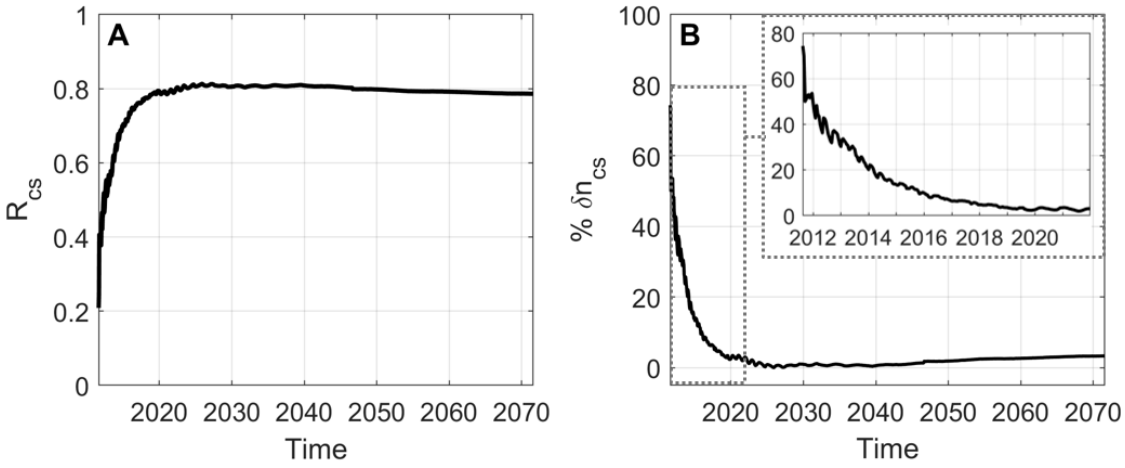

Figure 5.13 A) Dean ratio R_{cs} *computed for the central transect and B) percentage of shoreline change driven by cross-shore processes* % δn_{cs}.

5.4.5 Impacts of upscaling on cross-shore nourishment development

Our additional simulations with increased nourishment volumes show that larger nourishment volumes lead to mobilization of sand to lower-elevation, more seaward parts of the cross-shore profile and to enhanced alongshore sand dispersion, albeit at a lower rate per unit of nourished volume. We observe both faster shoreline retreat as well as increased volumetric loss (Fig. 5.14). Compared to the Sand Engine simulation where $Vn = 20\,000\,000\,m^3$ (V_n20), the total volume is 1.55 and 2.2 times larger in these upscaled mega nourishments with $Vn = 31\,000\,000\,m^3$ (V_n31) and $Vn = 44\,000\,000\,m^3$ (V_n44) respectively, and the initial cross-shore shoreline displacement in the central transect is 1.4 and 1.8 times larger (Table 5.1).

Over the 50-year simulations, we see that central transect shoreline retreat is 1.38 and 1.76 times faster for V_n31 and V_n44 respectively. Over the 50-year timespan, the total loss of volume from this transect was, for V_n31, 6898 m^3 (1.44 x more than V_n20) and for V_n44, 8570 m^3 (1.79 x more than V_n20). Thus, we see that the upscaling from V_n20 to V_n31 delivers more extra 'feeding volume' per volume extra nourished than the upscaling from V_n31 to V_n44. This results from the increasing seaward extent of the nourishments, which places a larger fraction of the volume at lower-elevation offshore locations. In these scenarios we furthermore observe slightly more movement in the lowest depth contours (Fig. 5.15) as well as a prolonged period of cross-shore adaptation before the shoreline and profile volume start to evolve in a linear relationship.

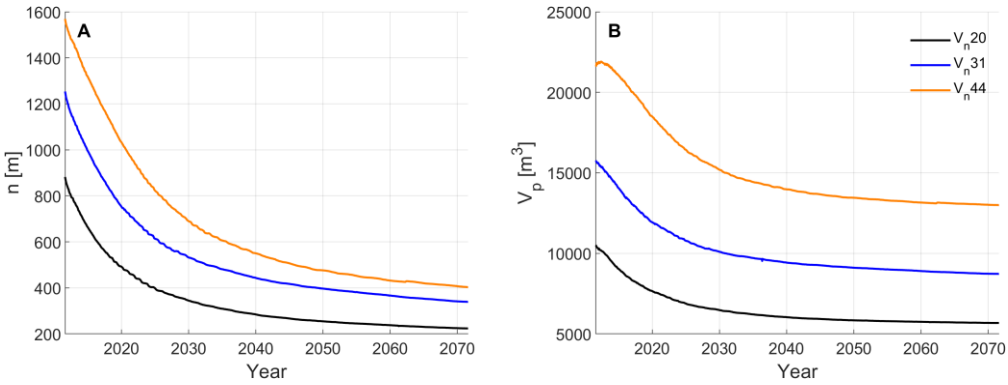

Figure 5.14 Evolution of A) coastline n and B) profile volume V_p in the central nourished transect for the different ShorelineS-Crocodile simulations.

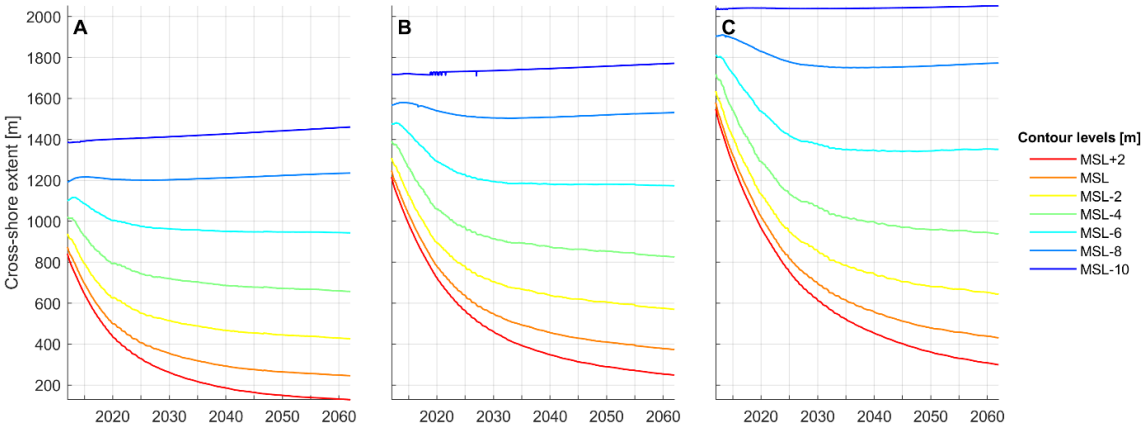

Figure 5.15 Depth contour evolution over time for the central transect for A) $V_N = 20\,000\,000\ m^3$, B) $V_N = 31\,000\,000\ m^3$, and C) $V_N = 44\,000\,000\ m^3$.

Table 5.1 Comparison of retreat and volume changes for different mega nourishments representing upscaling for sea level rise rates of 2, 8, and 16 mm/yr. Shown are approximated total nourishment demand (V_N), modelled shoreline position (n), and modelled profile volume (V_p) at $t = t_0$ and $t = 50$ $years$, and their changes over 50 years. Percentages in brackets denote relative values with respect to the V_{20} scenario.

$SLRr\ (mm/yr)$	**2**	**8**	**16**
Scenario	V_{20}	V_{31}	V_{44}
$V_N\ (m^3)$	20 000 000	31 000 000 (155%)	44 000 000 (220%)
$n\ [t = t_0]\ (m)$	882	1254 (142%)	1569 (178%)
$n\ [t = 50\ yr]\ (m)$	235	361 (154%)	427 (182%)
$\Delta n\ [\Delta t = 50\ yr]\ (m)$	-647	-893 (138%)	-1142 (176%)
$V_p\ [t = t_0]\ (m^3/m)$	10 506	15 759 (150%)	21 689 (206%)
$V_p\ [t = 50\ yr]\ (m^3/m)$	5731	8861 (155%)	13 119 (229%)
$\Delta V_p\ [\Delta t = 50\ yr]\ (m^3/m)$	-4775	-6898 (144%)	-8570 (179%)

5.5 Discussion

5.5.1 Implications of including cross-shore heterogeneity on decadal nourishment behaviour modelling

The decadal evolution of mega nourishments shows a clear depth-dependency: sand placed at different cross-shore elevations redistributes alongshore at different rates and over different timescales. This study addresses a key gap in nourishment modelling by explicitly incorporating cross-shore heterogeneity, enabling the simulation of depth-dependent sand redistribution at mega nourishments.

Traditional shoreline evolution models, based on the classical one-line theory (Pelnard-Considère, 1956), assume coastal profile with a time-invariant shape that shifts horizontally in response to net alongshore sediment transport. While this abstraction facilitates computational efficiency, it assumes that the three-dimensional morphological development can be represented by a single contour—the shoreline—and assumes a linear relationship between shoreline change and volumetric sediment loss or gain within the active profile. This assumption limits the model's capacity to represent vertical redistribution processes that are critical to nourishment evolution, especially for high-volume, large-scale interventions such as mega nourishments.

In our 12-year simulation of the Sand Engine, incorporating cross-shore deformation within the coupled ShorelineS-Crocodile framework significantly improved predictive performance. Compared to the uncoupled ShorelineS model, the coupled approach reduced the $RMSE$ for shoreline position ($30\,m$ vs. $55\,m$), depth contour migration ($48\,m$ vs. $175\,m$), and profile volume change ($201\,m^3/m$ vs. $492\,m^3/m$). The most substantial improvement stems from the ability to decouple shoreline retreat from volumetric loss. In the early years following nourishment implementation, the upper profile adjusts dynamically, resulting in rapid shoreline retreat as a large portion of the added sand is redistributed cross-shore to lower elevations, rather than transported laterally. Our simulations indicate that roughly the first decade is influenced by this cross-shore equilibration for a mega nourishment with Sand Engine dimensions. Just after implementation, the percentage of shoreline change driven by cross-shore processes is 73%, and by alongshore processes 27% (Fig. 5.13). After five years this ratio shifts to roughly 10% cross-shore versus 90% alongshore. After a 10-year equilibration phase, the influence of cross-shore deformation diminishes to less than 5%, and alongshore redistribution is the primary driver of morphological change. Consequently, assuming a fixed, linear relationship between shoreline displacement and volumetric change – as typically done in one-line models - can introduce biases in estimating sand dispersion and thereby nourishment longevity. Specifically, such models either underestimate the initial shoreline retreat or erroneously attribute it to alongshore sediment transport, thereby overestimating both the erosion rate and the volume of sand delivered to adjacent coastlines.

Essentially, we predict the mega nourishment eroding and feeding the adjacent coasts slower than a one-line diffusion model would predict. In our 50-year simulation, about half of the nourished sand volume remained in the vicinity of the peninsula, even as the shoreline shifted landward by on the order of 700 m (reducing the

peninsula's width to ~18% of its initial extent) (Fig. 5.12). This divergence between shoreline form and sediment volume highlights that nourishment lifetime is not a single, fixed quantity. Instead, nourishment longevity must be evaluated using multiple indicators, depending on the functional objective: volumetric retention for sediment budgeting, beach width for recreation, or shoreline position for infrastructure protection.

Our findings highlight that sand at different vertical levels of the profile disperse over different timescales. For the Sand Engine size mega nourishment, our simulation showed virtually no migration of the –10 m elevation contour over five decades, indicating that sand placed below the typical closure depth (~5–9 m below mean sea level for Dutch coasts (Hallermeijer, 1981) remained essentially immobile over the simulation period (Fig. 5.15A). This aligns with Dutch field observations that sand placed at lower elevations offshore does not significantly contribute to functional beach or dune development within management-relevant timeframes (Taal et al., 2023). Even under upscaled nourishment volumes, sand placed below the closure depth exhibited low mobility (Fig. 5.15B, C). This finding has important implications: nourishment depth distribution critically influences the effective sediment feeding rate, and sediment placed too deep may not serve any functional purpose within the planning horizon. This should be explicitly accounted for when estimating nourishment demand via volumetric balance models (e.g., Eq. 5.29).

This depth-dependent behaviour underscores the limitations of using single-indicator models or strategies when evaluating nourishment outcomes. Shoreline retreat in particular may not reflect true sediment loss but rather internal redistribution. For strategy design, this means that reliance on one-line or shoreline-only models could lead to misguided planning decisions. This is particularly the case when specific socio-economic or ecological functions are tied to indicators of the cross-shore profile such as beach width, dune growth, or sand availability. As highlighted by Geukes et al. (2024), different functionalities correlate with different morphological indicators; therefore, multi-indicator evaluation is essential for multifunctional, adaptive nourishment strategies.

5.5.2 Transferability of results to different nourishment projects

The magnitude of temporal and bathymetric scales of profile adjustment identified in this study are location- and project dependent. Previous studies have shown the dependence of (mega) nourishment dispersion on the nourishments initial geometry (e.g. Tonnon et al., 2018; Ribas et al., 2020). Also, the location of placement is of major influence, with dispersion rates depending on the profile shape (e.g. de Schipper et al., 2015; Liu et al., 2024), on wave climate intensity (e.g. Tonnon et al, Arriaga 2017, Arriaga 2020), on nourishment grain sizes (Ludka et al., 2016), mineralogical composition (Yao et al., 2024) and sorting processes (Duan et al., 2020). Thirdly, the observed adjustment rates and equilibrium timescales are influenced by the adopted modelling approach, which represents a long-term, climate-averaged response of an equilibrium cross-shore profile and therefore does not explicitly resolve seasonal variability or extreme wave conditions. As a result, sediment mobility at greater depths

may be underestimated, particularly in environments where episodic high-energy events or additional processes such as tides contribute to morphological change.

For these reasons, the equilibrium timescales and spatial extents reported here should not be regarded as universally applicable; rather, they illustrate how cross-shore adaptation can play a significant role in the evolution of mega nourishments. The present modelling framework demonstrates that incorporating a simple cross-shore diffusion component into a one-line approach can enhance both the detail and accuracy of predicted nourishment behaviour, while retaining the ease of application and computational efficiency of traditional one-line models.

The ShorelineS–Crocodile framework advances beyond traditional one-line models by explicitly including cross-shore processes, yet it also provides opportunities for further development. At present, the framework simulates a multi-year average coastal profile based on the prevailing wave climate, producing a gradual, smoothed erosion trend over time. This focus provides valuable insight into long-term equilibration and alongshore dispersion, but also highlights opportunities for extension. Incorporating short-term processes such as storm cycles, bar migration, or sand wave passage could enrich the simulations, revealing how episodic events temporarily accelerate or reverse sediment redistribution. Likewise, coupling with a storm-impact model such as XBeach would allow time-varying wave climates and extreme events to be represented, showing how they interact with long-term equilibration and potentially alter the decadal trends in profile volume, shape, and shoreline position.

Calibrating the diffusion coefficient in Crocodile offers a promising avenue for advancing the framework. The coefficient is presently defined from the local wave climate and observations of sand mobility across the profile, including the shoreface. Extending this basis with empirical datasets from diverse coastal settings and hydrodynamic regimes would allow systematic links to be established between diffusion coefficients and measurable site characteristics such as wave climate, sediment size, and profile slope. Such relationships would enhance the robustness and transferability of the ShorelineS–Crocodile framework, enabling broader application across a wide range of coastal environments.

The coupled model approach provides a valuable step towards more realistic long-term mega nourishment evolution forecasting. By capturing the vertical dimension of change with minimal added complexity, the model offers richer information to coastal planners.

5.6 Conclusions

Mega nourishments are proposed as a promising strategy for decadal-scale coastal protection, but their functional success depends on their morphodynamic evolution. For these large interventions the morphological evolution is depth-dependent: sand placed at different elevations in the profile redistributes at different rates. This study sets out to improve the modelling of long-term mega nourishment evolution by addressing a key gap in existing approaches: the lack of explicit representation of

cross-shore processes in traditionally alongshore-focused, one-line shoreline models. Using the Sand Engine as a case study, we developed and applied a coupled ShorelineS–Crocodile framework to investigate how depth-dependent sediment mobility influences nourishment behaviour over decadal timescales, and to assess the implications for predicting of key morphological indicators, such as coastline and isobath migration and profile volume changes, which can inform coastal nourishment strategy design and management.

Our results show that explicitly including cross-shore deformation significantly improves model skill compared to an uncoupled, cross-shore static approach. The coupled model reproduces observed changes slightly better in profile volume while it even more improves depth-dependent accuracy: at the nourishment centre, the RMSE of shoreline position decreases by 19% over a 10-year period, while the RMSE of depth-contour migration decreases by 73%. The model thereby shows that the initial decade is influenced by both cross-shore equilibration and alongshore dispersion, during which rapid shoreline retreat occurs. Immediately after nourishment implementation, about 73% of shoreline change is driven by cross-shore processes and 27% by alongshore processes. As equilibration progresses, the cross-shore contribution rapidly diminishes, and alongshore dispersion becomes the primary driver of shoreline change in the subsequent phase.

The simulations demonstrate the importance of depth-dependent sediment mobility. Sand placed below the closure depth is forecasted to remain largely inactive over five decades, highlighting that the vertical distribution of nourishment volume affects alongshore feeding rates and, therefore, effective nourishment lifetime. Our model shows that about half of the volume of sand nourished in the centre of the peninsula head is expected to remain in place throughout the 50-year simulation timespan. The coastline, however, is projected to retreat by 700 m, thereby only remaining 18% of the initial cross-shore extent. This finding underscores the need to evaluate nourishment performance using multiple indicators - such as shoreline position, profile volume, and depth contour change - rather than relying on a single metric.

These findings imply two design implications. The first is that mega-nourishments can leave a multi-decadal morphological footprint, particularly in lower-elevation offshore parts of the profile, in line with Tonnon et al. (2018). Sand deposited in these zones contributes little to protective or multifunctional outcomes due to its low mobility. Second, the feeding function does not scale linearly with nourishment volume or cross-shore extent. By retaining much of the simplicity and computational efficiency of a one-line model while adding the ability to represent vertical profile adjustment, the ShorelineS–Crocodile framework provides a practical, higher-fidelity tool for scenario testing in nourishment strategy. We hope our work can help coastal engineers design sustainable nourishment interventions that are both effective and efficient.

Synthesizing nourishment dynamics for coastal function delivery

6

This chapter synthesizes insights from the previous chapters by explicitly linking the simulated morphologic changes from Chapter 3,4 and 5 to coastal functions introduced in Chapter 2. It evaluates how modelled physical indicators like beach width and nourishment lifetime influence key societal outcomes as recreation and ecological support. This work thereby exemplifies quantification of trade-offs and synergies in multifunctional nourishment strategy design. It also discusses future directions for integrating this work with ecosystem service modelling and adaptive coastal management.

6.1 Introduction

Sandy shores globally provide vital functions, such as flood protection, ecological habitat, and recreational space, but face increasing pressure due to accelerating sea level rise and coastal squeeze (Barbier et al., 2011; Lansu et al., 2023). Sand nourishment has emerged as a nature-based solution for coastal protection while preserving or enhancing natural and recreational values (Hanson et al., 2002; De Vriend et al., 2015). Nourishments are often expected to deliver multifunctionality, contributing not only to shoreline stabilization but also to habitat creation, dune development, and recreation (Borsje et al., 2011; Manning et al., 2018). These may include supporting coastal habitats, facilitating dune development, and maintaining recreational beach width alongside flood protection. Yet, despite widespread adoption, the long-term system-wide effects of nourishment remain insufficiently understood, particularly regarding how design parameters - nourishment volume, placement depth, and frequency of return - influence morphological evolution and potential trade-offs, such as beach profile steepening, habitat disruption, or reduced recreational quality (Stive et al., 1991; Ludka et al., 2016; van Egmond et al., 2018; Cabezas-Rabadán et al., 2019).

To structure and interpret these effects, the thesis began by developing a conceptual framework (Chapter 2) based on a literature review of socio-economic, geomorphological, ecological, and ecosystem service dimensions. This framework clarified how nourishment-induced morphological change propagates through the coastal system to shape multiple, often competing, functions. This served as a conceptual foundation for the design of the morphological research in this thesis Recognizing the nonlinearity and complexity of coastal evolution, the research focused on long-term average behaviour - what might be called the morphological

climatology - to assess how nourishment strategic decisions influence key indicators like beach width and coastal volume over decades, rather than attempting to reproduce short-term or event-scale variability. In this chapter, we synthesize morphodynamic outcomes of simulated nourishment strategies across the different chapters (Section 6.2) and exemplify how this can be translated into coastal function delivery (Section 6.3) to support informed, adaptive multifunctional nourishment strategy planning (Section 6.4).

6.2 Morphodynamic outcomes of nourishment strategies

A central contribution of this thesis is to bridge a temporal and spatial gap in morphodynamic modelling. Most existing tools either simulate short-term dynamics in high detail (e.g., XBeach, Delft-3D) but lack feasibility for decadal applications (Giardino et al., 2010; Montaño et al., 2020), or rely on long-term empirical formulations (e.g., Bruun Rule, ShoreTrans) that fail to capture depth- and time-dependent sand redistribution (McCarroll et al., 2021; Bruun, 1962). This thesis addresses this gap through the development and validation of Crocodile, a behavioural cross-shore model designed to simulate decadal-scale profile evolution under nourishment based on diffusion-type equations. Grounded in long-term JARKUS bathymetric data from Dutch nourished sites, Crocodile was shown to reproduce key morphologic trends in shoreline migration, beach width, and coastal volume, with sufficient fidelity for strategic planning. In parallel, a novel model coupling between Crocodile and ShorelineS was developed to simulate depth-dependent behaviour of mega-nourishments, capturing both cross-shore equilibration and alongshore sand dispersion. This was tested on a Gaussian-shaped mega-nourishment resembling the Dutch Sand Engine showing that the depth-dependent sand redistribution was well replicated.

Beyond technical validation, the research yielded several overarching findings:

- **Morphological response to nourishment is nonlinear, path-dependent, and controlled by cross-shore placement.** In Chapters 3 and 4, we showed that large nourishment volumes can lead to significant profile deformation, with sand accumulating in the nourished section and little dissipation to the lower shoreface, especially when sand lacks time to redistribute between successive nourishments. Thereby, large sand volumes placed high in the profile steepen the coast over successive interventions, reducing nourishment lifetime. Conversely, sand placed close to the closure depth remains largely immobile. The latter also applies to mega nourishments which show marginal migration of lowest isobaths. These dynamics are often underrepresented in planning tools but may affect considerations in sand budgeting.
- **Nourishment effectiveness declines under accelerating sea level rise unless design adapts in frequency and volume.** In our scenario studies (Chapter 4), hold-the-line scenarios under high sea level rise led to annual nourishments in erosive zones – compromising ecological recovery - and fourfold increases in sand demand in little erosive zones, which at present may

lack nourishment planning. This highlights the importance of strategy flexibility and site-specific evaluation, especially as present-day decisions increasingly may constrain future options (Haasnoot et al., 2020).

- **Key indicators for nourishment effectiveness should reflect more than just volume, incorporating also frequency and spatial position** (Chapter 4 and 5). Profile simulations show that large nourishment volumes or short return intervals can lead to profile deformation, which may, for instance, include increases in beach width (Chapter 4). Simulations with the coupled ShorelineS–Crocodile model revealed a two-phase response for mega nourishments: an initial phase of roughly a decade during which sand redistributes both by cross-shore equilibration and alongshore dispersion, followed by a longer phase dominated by alongshore dispersion. Sand deposited in lower-elevation, offshore parts of the profile remained largely immobile over 50 years, implying that while mega-nourishments have a long-lasting morphological footprint, their functional efficiency does not scale proportionally with volume or cross-shore extent. Our simulations thereby showed limitations in scalability of nourishment, as more sand needs relatively more time to redistribute (Chapter 4 and 5).

To summarize, by modelling sand nourishment strategies including depth- and time-dependent sand redistribution over decadal timescales, this work can provide additional insights in coastal morphodynamic evolution. In the following section, we exemplify how these morphodynamic outcomes can be translated to a coast's potential to deliver diverse coastal functions.

6.3 Connecting morphodynamic outcomes to coastal functions

The morphodynamic outcomes from simulated nourishment strategies can serve as proxies for the potential delivery of coastal functions. Our analysis (Chapter 2) exemplifies how specific morphodynamic indicators translate to functional outcomes, and how the morphological outcomes of a nourishment can be mapped onto ecosystem service proxies: flood protection rises with increased dune and beach volume, recreation opportunities correlate with horizontal beach area, and ecological value increases with habitat area (dunes, intertidal) and with longer nourishment return periods. By understanding how the volume, location, and frequency of nourishment affect these indicators, we can evaluate trade-offs and make informed strategy selections.

The connection between these abiotic and functional metrics is explored in Geukes et al. (2025), a study developed in parallel with this thesis. In that study, morphological indicators were modelled at transects of the central Holland coast using Crocodile and systematically linked to coastal functions using the typology proposed by Manning et al. (2018). In this framework (Table 6.1), each indicator–function relationship was categorized into one of several response types - linear, threshold, threshold-plus, or combined threshold-plus - describing how changes in an indicator affect the level of function provided. Furthermore, each indicator was normalized on a 0–1 scale, where

1 represents the most favourable condition for supporting a given function. This approach allows different nourishment designs to be compared on a common basis for their ability to provide multiple functions. It is important to note, however, that these functional scores are inherently normative and context-specific: the relative importance and definition of each function may vary depending on location, time, and stakeholder perspective. The examples shown in this section offer a science-based example to illustrate how one can provide quantitative data to discuss possible trade-offs, rather than prescriptive design values.

In Geukes et al. (2025), recreational value was linked to beach width using a combined threshold-plus relationship, reflecting the empirical finding that user satisfaction increases with width up to an optimal range of approximately 30 to 120 meters (Broer et al., 2011; Cabezas-Rabadán et al., 2019a) beyond which returns diminish due to increased walking distance to the waterline (Fig. 6.1A). Moreover, wider beaches could facilitate onshore sand transport, enabling dune buildup, which in turn enhances coastal safety by reducing overtopping risk and expands habitat area for dune-dependent species. Site-specific literature shows that the presence of marram grass and dune volume show a positive relationship with beach width up to approximately 300 meters (Keijsers et al., 2014; Puijenbroek et al., 2017; Silva et al., 2019) (Fig. 6.1B), serving as an example of how morphology can support ecological and protective functions (Van der Biest et al., 2017a).

Thirdly, ecological value was linked to nourishment frequency through a threshold relationship, where high-frequency nourishment events depress the benthic community thereby reduce ecological value (Fig. 6.1C) based on work by González & Holtmann-Ahumada (2017), Hanley et al. (2014), Ocaña et al. (2022) and Speybroeck et al., (2006). Benthic organisms are sensitive to disturbance and killed during nourishment events but their abundance typically recovers within one year if no further disturbance occurs (Leewis et al., 2012). These benthos are critical to nutrient cycling, food webs, and coastal biodiversity. Assuming a roughly linear recovery, the ecological index in this framework is set near zero for nourishment return periods shorter than one year, reflecting chronic disturbance with little opportunity for recovery. It approaches its maximum value at return periods longer than five years, consistent with field-based evidence showing multi-year recovery times and cumulative effects of repeated nourishments on benthic communities (Leewis et al., 2012; Ocaña et al., 2022; Herman et al., 2022). A side note is that some benthic species (such as sand-dwelling amphipod crustaceans Bathyporeia and Haustorius) recolonize much more slowly after a nourishment event (Speybroeck et al., 2006), meaning frequent nourishments could greatly diminish those populations. Long-lived animal species that do not reproduce often, such as Pismo clams, may take decades to recover. The choice of this index thus also strongly depends on what species are evaluated. Table 6.1 displays additional examples of indicator–function relationships beyond those discussed above.

Function	Indicator	Range	Rationale	Indicator-Function Relationship
RECREATION	**Beach Width (Recreation)** Distance between average waterline and dune foot	30 -120 m	Indicates the dry beach space for (sunbathing) recreation. A minimum ensures adequate carrying capacity; a maximum limits distance to the sea. Thresholds are site-specific. [1]	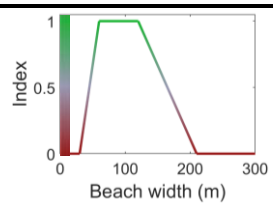
	Beach Face Angle Slope from high waterline to 1.5 m below the low waterline	0-5%	A flatter beach face enhances recreational safety. Slopes above 5% may lead to unstable or unsafe areas. Thresholds are site-dependent. [2]	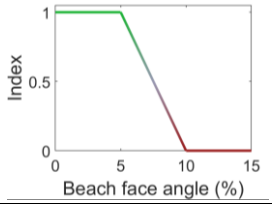
FLOOD SAFETY	**Beach Width** Distance between average waterline and dune foot	> Initial beach width	Greater width reduces wave energy that reaches the dunes during storms, erosion, and overtopping. Minimum threshold is site-dependent. [3]	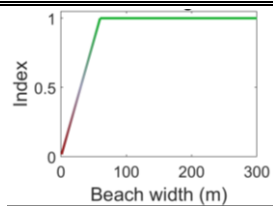
	Beach Width (Dune Building) Distance between average waterline and dune foot	> 300 m	Supports aeolian sand transport for dune growth. Dunes reduce flooding by trapping sand and buffering surges. Minimum threshold is site-dependent. [4]	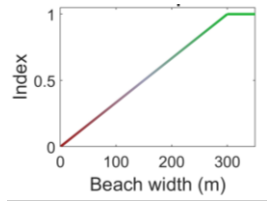
ECOLOGY	**Nourishment Frequency** Frequency of nourishment implementation	< 1 per 5 years	Frequent nourishments harm intertidal macrofauna, essential for coastal food webs. Recovery generally occurs within a year but varies by species. To maintain optimal ecosystem functioning, nourishment frequency should be minimized. [5]	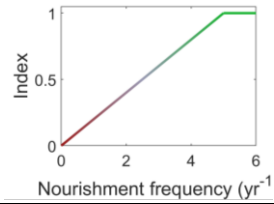
	Intertidal Zone Angle Slope from high to low tide	0-3%	Dissipative slopes (<3%) provide stable, moist, and food-rich conditions that support intertidal macrofauna. [6]	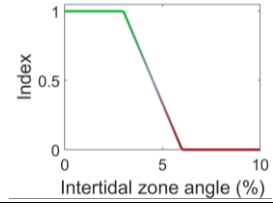
	Beach Width (Dune Building) Distance between average waterline and dune foot	> 300 m	Supports aeolian sand supply to dunes for marram grass and microhabitat development critical to biodiversity.[7]	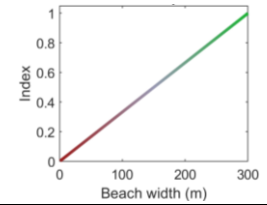

Table 6.1 Overview of selected coastal indicators, their optimal threshold ranges, and functional relationships. The Indicator-Function relationships presented were selected based on those most generically applicable across sandy beach systems. Where multiple threshold options existed in literature, we prioritized values most relevant to the central Dutch coast, aligned with our morphodynamic analysis. These functional scores are inherently normative and context-specific: the relative importance and definition of each function may vary depending on location, time, and stakeholder perspective.

1 (Ariza et al., 2010; Broer et al., 2011; Cabezas-Rabadán et al., 2019; De Souza Filho et al., 2014; García-Morales et al., 2017; González & Holtmann-Ahumada, 2017; Ocaña et al., 2022) **2** (Ariza et al., 2010; Chen et al., 2022; De Souza Filho et al., 2014; García-Morales et al., 2017; González & Holtmann-Ahumada, 2017; Lucrezi et al., 2016; Rijkswaterstaat, 2020; Van Ettinger & De Zeeuw, 2010; Wienhoven et al., 2020) **3** (Ariza et al., 2010; González & Holtmann-Ahumada, 2017; Larson & Kraus, 1989; Toimil et al., 2023; Venkatachalam et al., 2012) **4** (Galiforni Silva et al., 2019; González & Holtmann-Ahumada, 2017; Hanley et al., 2014; Van der Biest et al., 2017; Venkatachalam et al., 2012) **5** (González & Holtmann-Ahumada, 2017; Hanley et al., 2014; Leewis et al., 2012; Ocaña et al., 2022) **6** (Bosboom & Stive, 2023; González & Holtmann-Ahumada, 2017; Kelly, 2016; Mclachlan, 1990; Ocaña et al., 2022; Short & Wright, 1983) **7** (Galiforni Silva et al., 2019; González & Holtmann-Ahumada, 2017; Hanley et al., 2014; Keijsers et al., 2014; Kelly, 2016; Ocaña et al., 2022; Van der Biest et al., 2017; van Puijenbroek et al., 2017; Venkatachalam et al., 2012)

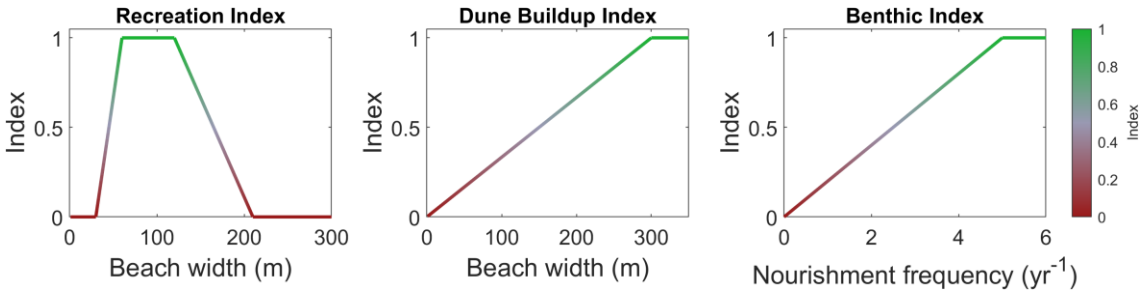

Figure 6.1 Example Manning Index scores for A) Recreation, B) Dune buildup and C) Benthic community. Colors refer to index values.

To illustrate the utility of these indicator–function relationships, we apply them to nourishment scenarios examined in this thesis. Consider a hold-the-line strategy under two sea level rise conditions (from Chapter 4): one with a present-day sea level rise rate of 4 mm/yr ($SLRr4$) and one with a potential future rate of 16 mm/yr ($SLRr16$). In both scenarios, a beach nourishment of 200 m³/m is implemented whenever the coastline retreats landward of its initial position, maintaining a consistent shoreline position. The modelled beach width in these cases fluctuates in a sawtooth pattern: immediately after nourishment the beach is about 100 m wide, then it gradually erodes back to around 60 m just before the next nourishment. This 60–100 m width range lies near the defined example optimal zone for recreation (maximizing the recreational index, see Fig 6.2A), and the upper end of this range provides some benefit for dune building, though dune growth could, according to this classification, be enhanced further by even wider beaches (see Fig. 6.2B). Under the higher SLRr16 scenario, the required nourishment frequency accelerates to roughly once every 3 years, and this frequency increases further over time due to coastal profile steepening (as shown in Chapter 4). The corresponding benthic (ecology) index under SLRr16 is therefore much lower (Fig. 6.2C) than under SLRr4, reflecting that the increased nourishment frequency may leave insufficient time for benthic communities to recover, thereby compromising ecological value in the area.

For comparison, we can evaluate these indices for a mega nourishment scenario as modelled in Chapter 5 using the coupled Crocodile-ShorelineS model. In this scenario, a concentrated gaussian shape comprising 20 million m^3 of sand is placed once (Fig. 6.3A), which gradually redistributes over the surrounding coast over multiple decades. Because the nourishment frequency is minimized to one major intervention in multiple decades, this strategy is less disruptive to benthic ecosystems than frequent small nourishments (and thereby the ecological index is 1). As the placement is concentrated alongshore, surrounding coastal areas are undisturbed assuming that these do not need supplementary nourishment. Having nearby areas remain undisturbed provides refuges and source populations for recolonization – organisms from these patches can migrate or disperse into the nourished zone, helping to restore the ecosystem's biodiversity (Diaz et al., 2004).

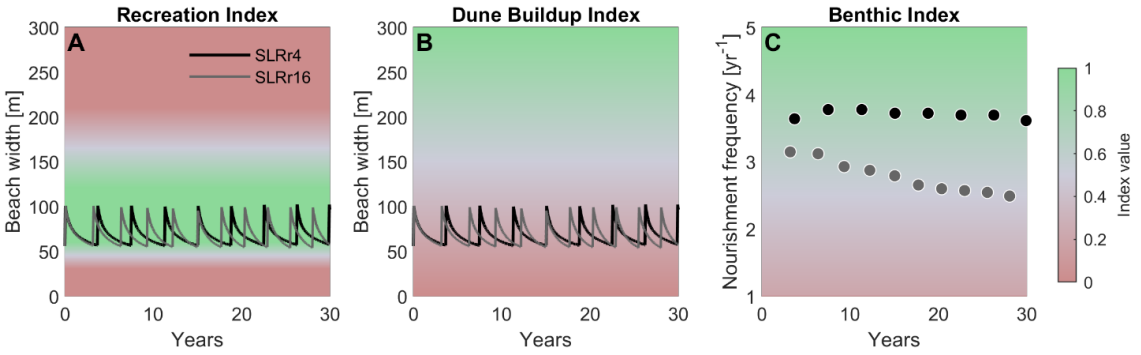

Figure 6.2 Example of the translation of morphological indices to ecosystem services. A) Beach width evolution and recreation index, B) beach width evolution and dune buildup index, C) Nourishment frequency evolution and benthic index, based on modeled outcomes of a 200 m³/m hold-the-line beach nourishment program under sea level rise scenarios of 4 mm/yr and 16 mm/yr. Background shading indicates relative index values (0–1), representing functional suitability. Index values are illustrative and context-dependent, influenced by local morphological, ecological, and stakeholder-specific considerations.

The beach width in the nourishment's centre is initially about a kilometre, thereby exceeding the typical optimal width for sunbathing recreation for many years (Fig. 6.3B). However, along the adjacent areas that gradually receive sand from the mega-nourishment, the beach width remains within or near the optimal range for recreation for much of this 30-year period. In fact, as the nourishment redistributes over time, these neighbouring beaches widen progressively, which contributes to dune development, yielding a higher dune-build up index compared to the regular, frequent nourishment strategy. This suggests that a mega-nourishment can offer long-term advantages for both coastal safety through sustained dune growth and dune habitat expansion. We note, however, that this analysis can be expanded with other forms of recreation that might actually benefit from an exceptionally wide beach (e.g. kite surfing, beach sports or events), partly offsetting the perceived recreational drawbacks in the nourishment centre.

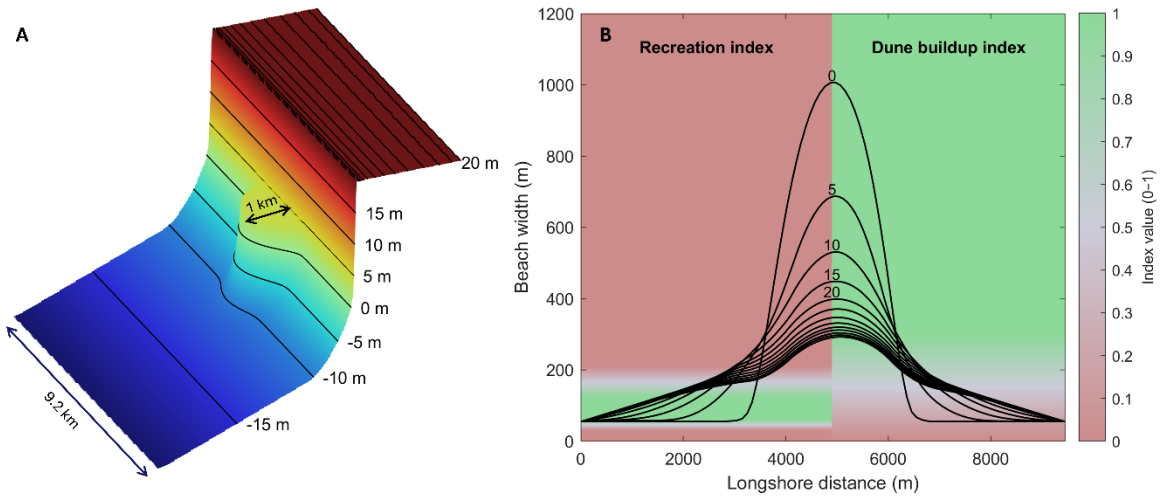

Figure 6.3 A) Initial configuration of a 20 million m³ mega beach nourishment placed with its crest at MSL + 4 m. B) Beach width change over time, with contour lines indicating 5-year intervals. Background shading illustrates the resulting (left) recreation index and (right) dune buildup index as functions of beach width. I Index values are indicative and context-dependent, and may vary with site-specific ecological and stakeholder priorities.

As a further exploration, we consider a third solution: a mega shoreface nourishment of similar scale and shape as the Gaussian mega-nourishment from Chapter 4, but fully placed in the subaqueous part of the profile, i.e. a shallow platform placed at approximately MSL - 4 m (Fig. 6.4A). The anticipated advantage of this design lies in its more gradual influence on beach width and shoreline position. After implementation, the shoreface mega nourishment slowly transfers sand onshore, causing the beach to widen incrementally over time rather than immediately. As a result, the beach width increases gradually, staying below about 200 m for many years and thereby remaining within a range favourable for recreation (Fig. 6.4B). The prolonged sand supply from the shoreface also elevates the dune growth index compared to the regular (smaller-scale) nourishment scenario, as a steady supply of sand continues to feed the dunes. Importantly, like the beach mega-nourishment, the shoreface mega-nourishment is a single intervention that leaves a large stretch of coast undisturbed for a long period, which could be beneficial for benthic recovery and overall ecological value. This example shows that, even though the approach is very schematized, one can use these models to support decision making on strategic choices.

While these functional indices provide valuable insight into how different nourishment designs may support or hinder various coastal functions, it is important to combine these with knowledge of the complexity and context of the real-world. The actual delivery of coastal functions is often influenced as much (or more) by external boundary conditions and site-specific factors as by morphology alone (Kindeberg et al., 2023; Stronkhorst et al., 2018; Temmerman et al., 2013a). Moreover, the relative importance of functions (safety, ecology, recreation, etc.) varies by location and

stakeholder priorities, meaning that what is "optimal" in one context may not be in another. Nevertheless, our results demonstrate that nourishment design choices (in terms of sand volume, placement, and frequency) often lead to sufficiently distinct morphodynamic trajectories that meaningful differences in functional delivery – whether in terms of flood protection, ecological health, or recreational space – can be expected. In this way, our research contributes guidance for the sustainable and multifunctional design of coastal sand nourishments, by showing how deliberate choices in nourishment strategy can align morphological outcomes with desired coastal functions.

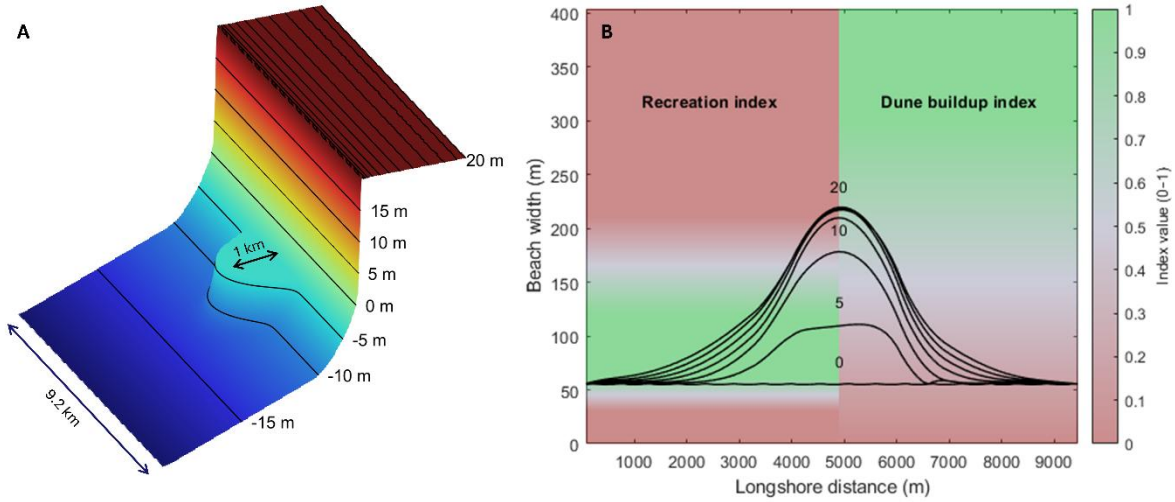

Figure 6.4 A) Initial shoreface nourishment configuration for a 20 million m³ mega shoreface nourishment placed with its crest at MSL – 4 m B) Beach width change over time following a. Contour lines represent 5-year time intervals of shoreline evolution. Background shading shows the corresponding (left) recreation index and (right) dune buildup index as functions of beach width. Index values are indicative and context-dependent, and may vary with site-specific ecological and stakeholder priorities.

6.4 Implications for adaptive nourishment strategy design

Nourishment offers strategic potential as a flexible, nature-based solution, but optimal implementation accounts for sand redistribution scaling across space and time, and for the diverse functions it is expected to support. While previous sections addressed long-term morphodynamic and functional implications of sand nourishment strategies, this section synthesizes the thesis findings into practical design considerations that support long-term adaptability and multifunctionality.

The findings across modelling experiments in this thesis suggest several key design parameters that influence nourishment outcomes: nourishment sand volume, frequency of application, vertical positioning (beach versus shoreface nourishment) and concentrated versus alongshore uniform. This section translates these findings into practical design lessons.

- **Account for timescales of morphologic response**. Coastal profiles respond non-linearly to nourishment, with timescales for sand redistribution increasing with both depth and volume (Chapters 4 and 5). An implication is that nourishment strategies effective for current sea level conditions may underperform when volumes are increased for higher sea level rise scenarios (Chapter 4). Larger volumes redistribute more slowly and can lead to unintended profile steepening or sediment accumulation. Strategic planning can benefit from morphologic models like Crocodile and the coupled ShorelineS–Crocodile model, which allow mapping of such outcomes. A second implication of depth-dependent morphologic timescales concerns cross-shore placement height, which plays a critical role in shaping coastal profiles over successive nourishment cycles. Repeatedly placing sand high on the profile was shown to steepen the beach, while sand deposited too deep - particularly below the active zone - tends to remain largely immobile, even over decadal timescales (Chapter 4 and 5). These outcomes underscore that the cross-shore position of nourishment controls alongshore redistribution rates and morphological outcomes, reinforcing the need to account for depth-dependent equilibration in strategic design.
- **Recognise - or preferably quantify - profile equilibration during mega nourishment design**. Mega nourishments, as examined in Chapter 5, typically exhibit a two-phase morphodynamic response: an initial phase during which sand redistributes both by cross-shore equilibration and alongshore dispersion, followed by longer-term phase dominated by alongshore dispersion. This thesis emphasizes the importance of explicitly recognizing - and ideally quantifying - these distinct phases during the design process. Coupled modelling tools like ShorelineS-Crocodile are well-suited to simulate both shoreline evolution and volumetric profile development, enabling a more comprehensive evaluation than shoreline position or a volumetric balance alone. This integrated approach also supports the assessment of alternative nourishment programs, including submerged designs as shown in section 6.3.
- **Design for flexibility**: allow to adjust timing, placement, and nourishment dimensions based on observed system response. Rigid nourishment schemes - e.g., predefined volumes or frequency - can result in suboptimal outcomes when sand dispersion is slower than anticipated (Chapter 4). Moreover, nourishment may have unforeseen consequences due to system complexity (Chapter 2). An adaptive design philosophy does not imply abandoning strategic planning, but instead acknowledges the limits of predictability. It emphasizes flexibility in spatial placement, timing, and scale, and requires ongoing monitoring and recalibration of used models.
- **Schedule eco-friendly**: Allow enough time between nourishment projects for beach organisms to recolonize and reproduce. High-frequency, low-volume strategies (e.g., hold-the-line approaches) offer flexibility but can lead to chronic ecological disturbance, particularly under accelerating sea level rise (Chapter 4 and Section 6.1). To reduce long-term biodiversity loss, strategies

should consider increasing individual nourishment volumes and preserving adjacent undisturbed areas as ecological refuges and sources for recolonization (Hanley et al., 2014; Ocaña et al., 2022). Modeling tools such as ShorelineS–Crocodile can help explore placement and scheduling options that create boundary conditions more favorable for ecological health.

7 Conclusions

7.1 Recap – Context and aim of thesis

Sandy shores are multifunctional zones, providing flood protection while supporting ecological habitats, human recreation and coastal economic activities (Manning et al., 2018). Yet, their capacity to sustain these roles is increasingly strained by accelerating sea level rise, sand deficits and coastal squeeze (Barbier et al., 2011; Bendixen et al., 2019; Lansu et al., 2024.; Luijendijk et al., 2018). As traditional hard-engineering solutions, such as seawalls, groynes, and dikes, are increasingly viewed as inflexible and unsustainable (Cooper and Pilkey, 2012; Nawarat et al., 2024), sand nourishment has emerged as a leading strategy for coastal protection while preserving or enhancing natural and recreational values (de Vriend et al., 2015; Hanson et al., 2002). This strategy not only prevents shoreline retreat, but also aims to deliver multifunctionality, supplying ecosystem services that meet multiple policy goals (Borsje et al., 2011; Manning et al., 2018). These include supporting coastal habitats, facilitating dune development, and maintaining recreational beach width.

However, despite a common optimistic framing of sand nourishment as a 'win-win' solution, the actual system-wide impacts of nourishment programmes are not yet fully understood, especially over decadal timeframes. Morphological responses to (recurrent) sand nourishment vary significantly by volume, placement depth, and placement frequency, thereby governing the evolution of the landscape (Beck et al., 2012; Ludka et al., 2016; Stive, 1991). These morphologic responses play a critical role in determining the overall success of the nourishment programme, as unintended trade-offs may occur. For example, certain designs may lead to undesirable outcomes such as steepening of the beach profile (Walstra et al., 2011), disruption of local ecosystems (Hanley et al., 2014; Ocaña et al., 2022), or reduced beach user satisfaction when artificially widened beaches exceed preferred dimensions for recreation (Cabezas-Rabadán et al., 2019).

At the same time, morphologic modelling tools that may be used to guide nourishment strategic planning have struggled to resolve these dynamics at the relevant temporal and spatial scales. Most existing tools either simulate short-term dynamics in high detail (e.g., XBeach, Delft-3D) but lack feasibility for decadal applications (Giardino et al., 2010; Montaño et al., 2020), or rely on long-term empirical formulations (e.g., Bruun Rule, ShoreTrans) that fail to capture depth- and time-dependent patterns in sand redistribution (McCarroll et al., 2021; Bruun, 1962).

This thesis addresses this gap by developing and applying new modelling tools to simulate decadal-scale sandy coastal morphology under varying nourishment strategies, focusing on outcomes that can inform long-term coastal protection

management. The approach supports the growing need for predictive, system-level understanding of how nourishments evolve morphologically, and by extension, how they shape the potential for multifunctionality over time. Summarized, the overall thesis aim was formulated: "to inform the sustainable and multifunctional design of coastal management strategies by developing, validating and applying a morphodynamic modelling framework that can simulate the multi-decadal evolution of nourished sandy coasts under varying design strategies and sea level rise rates." The research followed a cyclic structure, progressing from identifying relevant processes and indicators, to modelling these processes, to synthesizing the results in relation to coastal functions.

To identify and interpret the processes and indicators most relevant for sustainable and multifunctional designs, the thesis began with the development of a conceptual framework (Chapter 2), derived from a literature review spanning socio-economic, geomorphological, ecological, and ecosystem service dimensions. The morphologic indicators that linked these processes were subsequently simulated in the cross-shore direction (Chapter 3), whereby we developed and validated the numerical model Crocodile. This tool was applied to simulate different nourishment strategies comprising recurrent beach- or shoreface nourishment under present-day to high sea level rise scenarios, with the aim to contribute to a broader system-level understanding of long-term impacts (Chapter 4). Moreover, a combined alongshore-cross-shore modelling framework, ShorelineS-Crocodile. was developed and tested to capture the depth-dependent behaviour and design implications of mega-nourishment interventions with a feeding function (Chapter 5). We concluded by evaluating the potential of the simulated nourishment strategies to support coastal multifunctionality (Chapter 6). Detailed overview of these components and subsequent research contributions are given below.

7.2 Research contributions

7.2.1 From multifunctionality towards morphology

Designing an effective nourishment strategy to adapt to sea level rise involves making informed choices about the diverse, and sometimes conflicting, effects nourishments have on coastal functions, such as biodiversity and recreational quality, and overall multifunctionality (Cooke et al., 2012; De Schipper et al., 2021; Singhvi et al., 2022). To structure and interpret these effects, we developed a qualitative model illustrating the potential processes and interactions following sand nourishment design. This model is grounded in a literature review of four key dimensions of the coastal system: socioeconomics, geomorphology, ecology, and ecosystem services. It illustrates how nourishment-induced morphological change propagates through these domains to influence diverse coastal functions. Based on this framework and our empirical findings, we identify three key lessons for the design and evaluation of multifunctional nourishment strategies:

1. Conflicts between policy goals require informing political decision-making on prioritization between coastal functions. Multifunctional nourishments are not

always win–win solutions for nature, safety, and recreation. While synergies can occur, conflicts between policy goals are common and must be acknowledged. Planners benefit from assessing a broad range of strategic options, clarifying which goals each option serves, and engaging stakeholders to set priorities. In practice, this involves mapping how design choices (e.g. volume, location, return period) may enhance some ecosystem services (e.g. flood protection, recreation, habitat) while constraining others (e.g. beach access, sand supply).

2. Concreteness is needed on otherwise ambiguous functions. The outcomes of multifunctional sand nourishments may be ambiguous if the individual policy goals are not defined precisely. Broad aims like "enhance nature" or "improve recreation" must be translated into clear, measurable indicators, for example defining nature value by species richness or dune vegetation cover, and recreation by beach area or visitor counts. Literature reviews similarly highlight the need for transparent metrics. Distinctive aspects of recreation, safety and nature are affected differently by sand nourishment design. For instance, active recreationists (e.g., runners and hikers) may profit from a wider beach, while sunbathing and water-based recreation may be negatively affected by the increased distance to the waterline.
3. Ongoing, multidisciplinary system-wide monitoring is essential. In practice, this means measuring shoreline change, beach and dune volumes, habitat indices, and socioeconomic indicators (tourism, property impact) in tandem. Such system-wide datasets are needed to validate our modelled relationships and to adapt designs over time.

Throughout this thesis, the morphological research has been designed to couple nourishment strategies to expected evolution of morphologic indicators that can inform on the potential to deliver certain coastal functions, such as coastal volume, beach width and return periods. The development of these functions is complex, context-dependent, and in many cases influenced more by other boundary conditions than by morphology alone (Kindeberg et al., 2023; Stronkhorst et al., 2018; Temmerman et al., 2013). The relevance of particular functions varies by location, time, and stakeholder perspective. Nevertheless, our results show that nourishment design choices can, in some cases, lead to markedly different morphological outcomes, with implications for the delivery of coastal functions.

7.2.2 Cross-shore model development and validation

A cross-shore morphodynamic model Crocodile was developed to simulate decadal-scale sand redistribution resulting from beach and shoreface nourishment interventions (Chapter 3). The model is based on a diffusion-type equation (Stive et al., 1991) that allows sand to spread dynamically across the active cross-shore profile and includes components for sand exchange with the dune and alongshore losses. Using a long-term average profile and hydrodynamic climate, the model is specifically designed to approximate multi-year average profile behaviour on decadal timespans, rather than assessing year-to-year or event-driven nourishment evolution. It was tested

against multiple Dutch case studies at the Monster, Egmond, and Katwijk beaches, using over two decades of annual bathymetric data.

Quantitatively, model performance on morphologic indicators was within acceptable bounds for strategic planning purposes. The modelled coastal volume, shoreline position and beach width strongly resembled the observations with only a 12% overestimation in profile volume and 13% underestimation in beach width. Averaged over selected periods of nourishment, trends and trend reversals between different strategies were well replicated with slight overestimation for coastal volume trends by $1.5\ m^3/m/yr$ (10%), while beach width trends are underestimated by 0.2 m/yr (15%). Given that the added nourishment volumes are typically in the order of 100 m^3/m, these model errors are considered sufficiently low. It can therefore be concluded that Crocodile effectively simulates variations in coastal volume, coastline position and beach width over a decadal timeframe in response to different nourishment strategies within minutes - hours. Therefore, Crocodile can facilitate the evaluation of multi-decadal nourishment strategies with minimal computational power.

7.2.3 Evaluation of long-term nourishment strategies under sea level rise

Subsequently, Crocodile was applied to simulate present-day and sea level rise adapted nourishment strategies for several decades. The adapted strategies applied more sand, either through larger individual nourishment volumes or increased frequency of implementation. In such strategies, the nourished sand may lack time to effectively redistribute in the designated timeframe, leading to significant deformation of the profile over multiple nourishment cycles. The subsequent effects were analysed with a focus on profile steepening, nourishment lifetimes, and the feasibility of operational objectives. Two common nourishment policies were simulated at a Dutch case study location over a 50-year timespan under stationary sea level rise rates ranging from 2 to 32 mm/year. These were (1) a proactive sand balance policy, whereby nourishment volume and frequency were predetermined based on the conservation of sediment in the (regional) coastal system and (2) a reactive hold-the-line policy wherein the timing of placement is based on instantaneous shoreline position. These strategies reflect currently applied nourishment practices (Elko et al., 2021; Hamm et al., 2002).

The choice of strategy led to a variation of up to 75% in the total amount of sand used, with the proactive sand balance strategy requiring more sand. Our results show increasing profile deformation with nourishment volume applied and duration of the nourishment strategy, with sand accumulating in the nourished section and little dissipation to the upper shoreface. In our case study, the consequent profile steepening leads to reduced nourishment lifetimes by up to 30%. Such estimates should be interpreted as indicative rather than definitive, as nourishment dynamics are highly sensitive to site-specific coastal morphology and time-varying hydrodynamic conditions. Additionally, under high sea level rise rates, more erosive coasts experience a reduction in nourishment lifetimes to annual intervals, while less erosive areas require up to four times more sand than currently needed. These findings illustrate that nourishment volumes do not linearly translate from their

present-day effect to the future due to the slowness of the system response. Time-dependent morphological adaptation becomes increasingly important as the volume of applied sand increases.

7.2.4 Depth-dependent behaviour of mega-nourishments

In addition to regular-scale beach and shoreface nourishments, mega-nourishments are increasingly explored as adaptive responses to coastal erosion and sea level rise (e.g. Kroon et al., 2022; Lorenzoni et al., 2024; Stive et al., 2013). A method to evaluate depth-dependent spreading behaviour and design implications of mega nourishment strategies on a decadal timespan is developed and tested in Chapter 5 of this thesis. The ShorelineS coastline model is coupled with the Crocodile cross-shore diffusion model to simulate the 50-year evolution of gaussian-shaped mega nourishments with varying volume. The resulting modelling framework allows sand nourished in different parts of the profile to redistribute on different timescales, whereby the upper profile equilibrates relatively quickly (~O years) whereas sand deposited in lower-elevation, offshore parts of the profile disperses slowly (~O decades).

One of these Gaussian-shaped mega nourishments was designed as a simplified representation of the Dutch Sand Engine (Stive et al., 2013), allowing for model validation using available Sand Engine measurements. The model well reproduced sand volume, shoreline and decreasing rate of isobath retreat with depth. Simulation results revealed two morphodynamic phases. Specifically, our results show that explicitly including cross-shore deformation significantly improves model skill compared to an uncoupled, shoreline-only approach. The coupled model better reproduces observed changes in shoreline position, depth contour migration, and profile volume. Importantly, it captures a two-phase evolution: an initial decade dominated by cross-shore equilibration and alongshore dispersion, during which rapid shoreline retreat occurs. Immediately after implementation, about 73% of shoreline change is driven by cross-shore processes and 27% by alongshore processes. As equilibration progresses, the cross-shore contribution rapidly diminishes, and alongshore dispersion becomes the primary driver of shoreline change in the subsequent phase. These results highlight the added value of the coupled framework, offering detailed insight in both shoreline evolution and volumetric profile response, including the vertical distribution of nourished sand throughout the profile.

Alternative mega-nourishment scenarios with increased cross-shore extent and sand volume - representing future upscaled scenarios - led to slightly increased mobilization of sand in lower-elevation offshore parts of the profile and to marginally increased alongshore dispersion. Normalized per unit of nourished sand volume these dispersion rates were lower; leaving much of the additional sand immobile. These findings imply two design implications. The first is that mega-nourishments can leave a multi-decadal morphological footprint, particularly in lower-elevation, offshore parts of the profile. Sand deposited in these zones contributes little to protective or multifunctional outcomes due to its low mobility. Second, the feeding function does not scale linearly with nourishment volume or cross-shore extent.

7.2.5 Overarching morphologic findings

The research yielded several overarching findings:

- **Morphological response to nourishment is nonlinear, path-dependent, and controlled by cross-shore placement.** Increasing volume or frequency does not proportionally increase performance, due to physical limits in sand redistribution and profile adjustment times.
- **Nourishment effectiveness declines under accelerating sea level rise unless design adapts in frequency and volume.** Sand placed high in the profile may steepen the coast over time, reducing lifetime, whereas sand placed near the closure depth can remain immobile for decades.
- **Key indicators for nourishment effectiveness should reflect more than just volume, incorporating also frequency and spatial position.** Larger volumes or shorter return intervals alter profile shape in ways that change the behaviour of key indicators over time and space. Under sea level rise, maintaining present-day performance requires not just more sand, but flexible strategies that adapt to evolving morphological conditions. Mega-nourishments, while creating long-lasting footprints, often store large amounts of deep sand that remain immobile for decades—limiting short-term protective or multifunctional benefits despite their feeding potential.

7.2.6 From morphology towards multifunctionality

Our analysis (Chapter 2) exemplifies how specific morphodynamic indicators – shaped by sand nourishment programmes - translate to functional outcomes. These morphological outcomes are linked to ecosystem service proxies. Flood protection rises with increased dune and beach volume, recreation opportunities correlate with horizontal beach area, and ecological value increases with habitat area and with longer nourishment return periods. Hereby a method is demonstrated to evaluate how the volume, location, and frequency of nourishment affect these indicators, supporting informed and balanced sand nourishment strategy development.

Chapter 6 demonstrates this by applying this to nourishment strategies simulated in this thesis. For instance, in our simulations, high-frequency beach nourishments under accelerated sea level rise ($16\ mm/yr$) maintained optimal beach widths for recreation but required frequent intervention, lowering benthic ecosystem functioning due to insufficient recovery time. In contrast, large-scale interventions such as mega nourishments - either on the beach or shoreface - reduce disturbance frequency and thereby better support ecological functions. However, they may temporarily exceed optimal recreational conditions in the nourishment centre and show diminished efficiency in mobilizing deeply placed sand. A mega shoreface nourishment showed sustained recreationally suitable beach widths with potential for dune development, and minimized ecological disruption by avoiding repeated intervention.

These examples highlight that nourishment strategies can be designed to target specific functional outcomes, but synergies and trade-offs are inevitable. For instance, maximizing recreation and ecological value simultaneously may require spatial

differentiation - allowing some sections of the coast to remain undisturbed as ecological refuges, while others are optimized for human use.

Overall, the thesis shows that understanding the morphodynamic pathways from nourishment design to coastal function delivery is essential to support multifunctional and adaptive coastal strategies. By combining long-term morphological modelling with functional indicator frameworks, this research enables strategic evaluation of nourishment options, allowing coastal planners to tailor interventions to both current needs and future uncertainties.

7.3 Outlook

This thesis has demonstrated the utility of diffusion-type modelling tools such as Crocodile and ShorelineS for evaluating nourishment strategies on decadal timescales, with a focus on morphological outcomes and their links to multifunctional coastal use. Building on these findings, several pathways for further research and tool advancement can be outlined. These relate to the integration of available data, the refinement of existing models, and the increasing societal demand for multifunctional, adaptive coastal strategies.

7.3.1 Enhancing model accuracy through data integration and validation

Recently, an increasing number of nourished sites are systematically monitored (e.g. Brand et al., 2022; Elko et al., 2021; Stronkhorst et al., 2018). These datasets offer ground for model evaluation as well as insights into nourishment performance. Extended model calibration and evaluation in locations with varying hydrodynamic forcing, morphology and coastal maintenance schemes could help improving ShorelineS-Crocodile and help building a platform of knowledge for strategy design both in and outside of the Holland coast.

Additionally, recent decades have seen rapid growth in the availability and resolution of satellite-derived datasets, enabling more frequent and spatially extensive tracking of shoreline and nearshore dynamics. Advances in platforms such as the CoastSat toolkit (Vos et al., 2019) now allow for consistent extraction of shoreline positions from publicly available satellite imagery (e.g., Landsat, Sentinel-2), achieving temporal resolutions on the order of weeks for longer timespans. Such datasets, in combination with any available information on local hydrodynamic forcing and nourishment application, can allow models such as Crocodile-ShorelineS to perform analyses in much wider areas, and also in data-sparse or internationally less-monitored coastal regions.

Lastly, the integration with AI-based pattern recognition and data assimilation techniques may present opportunities. There are many recent examples where coastal engineering has included the automated detection of morphological features like shorelines or dune toes or in the forecasting of shoreline change (Bahrami and Siadatmousavi, 2025; Khan et al., 2025). Closer to the scope of this thesis, artificial neural networks have also been applied to predict cross-shore bathymetric profiles based on bathymetric datasets and wave forcing. (Hashemi et al., 2010; López et al.,

2018). However, much of this work remains focused on short to medium timescales—typically months to a few years (Khan et al., 2025). In combination with Crocodile and ShorelineS, machine learning could be used to enhance model performance and deepen system understanding in several ways. These include the automated calibration of parameters such as cross-shore diffusivity, dune exchange rates, or alongshore transport coefficients, particularly in data-rich environments. Moreover, machine learning techniques can support the analysis of increasingly complex datasets, including bathymetric surveys, LiDAR, UAV imagery, but also indicators of ecosystem services. Such data-driven insights could improve parameter estimation and model formulations, for example by refining how diffusion timescales vary with sediment grain size, profile shape and hydrodynamics or by empirically linking morphologic indicators to site-specific ecosystem service delivery. As monitoring networks and machine learning tools expand, coupling machine learning with behavioural models like Crocodile and ShorelineS offers a promising path for adaptive nourishment planning.

7.3.2 Advancing modelling tools presented in this thesis

The numerical models used in this thesis, Crocodile and ShorelineS, are most suitable for simulations spanning multiple decades, but their window of application can be widened by strategic coupling with other tools - an approach similar to the multi-timescale modelling by Montaño et al. (2021). For instance, combining the long-term cross-shore response modelled with Crocodile with a storm-scale event model (e.g., XBeach) can help assessing the influence of nourishment program design on flood safety under storm conditions.

Further development of Crocodile could focus on enhancing the parameterization of the diffusion coefficient, a key variable governing cross-shore sand redistribution. As discussed in Chapter 3, its current formulation involves several assumptions, including its maximum magnitude, its dependence on offshore water levels, and its profile across the shoreface which could be further tested and improved. Moreover, exploring how these relationships vary across different coastal morphologies and hydrodynamic regimes would enhance model reliability and transferability. In addition to validation against field observations, comparison to controlled experiments such as wave flume studies (e.g. Dean & Houston, 2016) and to analytical equilibrium profiles (Dean, 1991) may give additional insights in the model's ability to reproduce profile development.

For the coupled ShorelineS–Crocodile framework, future work could explore a tighter integration between the Crocodile model and other ShorelineS components that influence profile evolution, such as the module for beach-dune sand exchange, mud transport, and interactions with hard coastal structures. Synchronizing the calibration of both Crocodile and ShorelineS could enhance coherence in system representation. Finally, a significant advancement would be the extension of the coupled model, including one-line alongshore, to a multi-line configuration, enabling the simulation of lateral sand exchange at multiple depth levels. In its current form, alongshore transport is parameterized solely as a function of shoreline position. Incorporating

depth-specific transport would capture interactions between cross-shore profile shape and alongshore transport gradients, allowing the model to account for orientation-dependent processes and morphodynamic feedbacks.

7.3.3 Embedding developed models in real-world coastal management

The morphologic modelling tools presented in this thesis provide a foundation for scenario testing and functional evaluation, with potential to be embedded in broader decision-making frameworks that reflect local priorities. They are particularly valuable in the strategic phases of nourishment strategy design, where long-term performance must be assessed under uncertainty and broad design options are still open. At this stage, decision-makers must choose between nourishment types (e.g., beach vs. shoreface), determine placement location, volume and estimated return frequency - choices that significantly influence both costs and functional outcomes over time. These models can also help address more fundamental questions, such as whether nourishment is worthwhile and feasible under projected sea level rise. For example, they can support assessments of whether sufficient volumes can be placed effectively, or whether shifting towards larger, less frequent nourishments could improve efficiency. This can reduce the tendency toward conservative "over-nourishment" undertaken purely for safety margins, by quantifying how long nourishments persist and how quickly sediment is redistributed. The morphological models developed in this thesis enable rapid testing of nourishment strategies, quantifying trade-offs in shoreline evolution, beach width, profile volume, nourishment longevity, coastal steepening, and cross-/alongshore sediment redistribution.

A key advantage of these tools is their ability to simulate both cross-shore and alongshore sediment transport, making them applicable to a wide range of nourishment strategies. This includes interventions with primarily cross-shore dynamics (e.g., shoreface and beach nourishments) as well as large-scale, feeder-type nourishments with dominant alongshore dispersion (e.g., mega-nourishments). This wide applicability allows for side-by-side comparison of design options with relatively fast and simple setup, enabling efficient exploration of adaptive strategies. In addition, the models support visualization of morphodynamic trajectories over time, which can aid in stakeholder engagement and public communication by making the impacts of nourishment strategies more tangible. These visual outputs are also valuable for explaining choices to what is often referred to as "the environment" in practice—that is, municipalities, water boards, provinces, and coastal residents. For example, questions from stakeholders about when and where the next Sand Engine will be placed can be addressed more clearly, as the model outputs are accessible even to non-specialists and can transparently illustrate the reasoning behind strategic decisions.

In the Dutch context, Rijkswaterstaat (the Dutch national agency responsible for main roads, waterways, and water systems) monitors the coast annually using the JARKUS dataset (Wijnberg and Terwindt, 1995b) and updates the coastal nourishment plan (Suppletieprogramma) every four years, with execution spanning the subsequent five years (Rijkswaterstaat, 2024). These plans guide nourishment placement and sand

budgeting based on observed coastline trends, sediment deficit estimates derived from long-term coastal monitoring and policy goals (Lodder and Slinger, 2022). The models developed in this thesis can support this planning phase by explicitly modelling sand redistribution and thereby forecasting nourishment effectiveness, redistribution patterns, and functional impacts decades into the future. For example, sediment demand estimates generated with Crocodile or the coupled model could be compared to long-term projections in the coastal nourishment plan, helping to refine nourishment timing and placement and local sand demand. Moreover, during the implementation phase, Rijkswaterstaat's annual monitoring can inform whether observed morphodynamics align with predicted trajectories and allow recalibration of model parameters such as diffusion (scaling) coefficients, supporting adaptive coastal management.

It is important to recognize the current scope and limitations of these tools. In their present form, the models are best suited for open, sandy, wave-dominated coasts, where sediment transport processes are primarily governed by wave and tide-driven hydrodynamics, and where large-scale, long-term nourishment strategies are being considered. They are not intended for highly sheltered environments, mixed sand–gravel or muddy coasts, or settings dominated by complex nearshore structures where local hydrodynamics play a disproportionate role. Likewise, they are designed for strategic, long-term assessments rather than the detailed optimization of small, localized interventions. In such cases, more site-specific, process-rich modelling may be required. Within their intended domain, however, the tools can provide valuable, rapid insights into trade-offs, performance, and feasibility, thereby strengthening the evidence base for adaptive coastal management under changing boundary conditions.

7.3.4 Responding to evolving coastal management demands

Looking ahead, the value of coastal zones is increasingly being recognized not just for flood protection, but for ecosystem services, cultural value, recreational space, and blue economy opportunities (Barbier et al., 2008; De Schipper et al., 2021; Temmerman et al., 2013a). Consequently, future nourishment designs may be required to meet multifunctional objectives under increasing spatial constraints and environmental pressures. Sea level rise may demand larger, more frequent nourishment, while potential sand scarcity due to extraction limits or environmental regulation (Bendixen et al., 2019) may force a down-scale of sand use. In this context, tools that can quickly evaluate the efficiency and trade-offs of nourishment options across multiple functions and scales will become increasingly valuable (Biest et al., 2017; Kindeberg et al., 2023). A key opportunity lies in advancing the coupled modelling frameworks: for example, integrating ShorelineS–Crocodile with event-based storm models (e.g. XBeach) and ecosystem service models (e.g. Manning et al., 2018) to simulate compound effects and functional synergies.

However, in these 'functions' also lies a great challenge for future research. Nourishment also presents ecological trade-offs that are still insufficiently addressed, unknown or ignored. The construction process can cause widespread mortality

among intertidal fauna, alter sediment characteristics, and disrupt prey availability for shorebirds and other species (Gittman et al., 2016; Schipper et al., 2021; Schlacher et al., 2012). Recovery times vary; some species recolonize within a year, while long-lived or site-dependent species may take decades or never fully return (Hanley et al., 2014; Leewis et al., 2012). Additionally, eroding nourishments can degrade offshore water quality and may degrade adjacent habitats such as seagrass beds and reefs, while sand mining for nourishment supply can degrade source environments, raising sustainability concerns (Nunes da Silva and Barbosa Viana, 2024). Greater insight and consideration of these ecological consequences are essential if sand nourishment is to be regarded as a genuinely sustainable coastal adaptation strategy.

These consequences moreover underscore the importance of embedding functional and environmental considerations into early-stage design. Tools like ShorelineS–Crocodile can support this process by simulating scenarios with limited sand availability, varying sea level rise projections, and alternative nourishment strategies—assessing their performance not only in terms of shoreline stability but also in relation to ecological resilience and multifunctionality. It is evident that excessively short nourishment return periods lead to ecological and operational drawbacks; in this regard, mega-nourishments may offer advantages through reduced disturbance frequency (Herman et al., 2021), although more research is needed to better understand how these large-scale interventions affect coastal habitats, species recovery, and system dynamics over time.

In some high-risk or ecologically constrained settings, neither nourishment nor hard protection may be sustainable. Here, planned retreat may emerge as a legitimate alternative, enabling long-term resilience at reduced ecological cost (Haasnoot et al., 2013). Future strategies should therefore be adaptive, informed by integrated modelling, and designed to weigh functional benefits against environmental thresholds over decadal timescales.

In conclusion, adapting to evolving coastal management demands will require balancing functionality, sustainability, and system resilience. This calls for integrated modelling with expert judgement, cross-disciplinary collaboration, and flexible, adaptive design pathways that reflect not only physical drivers but also morphologic and socio-ecological responses.

Bibliography

Akerlof, G.A., Kranton, R.E., 2010. Identity Economics. https://doi.org/10.1515/9781400834181

Albada, E., Goshow, C., Beach, P.D.-F., 2007. Effect of beach nourishment on surfing–observations from the St. Johns county shore protection project, in: SBPA National Conference on Beach Preservation Technology.

Almar, R., Kestenare, E., Reyns, J., Jouanno, J., Anthony, E.J., Laibi, R., Hemer, M., Du Penhoat, Y., Ranasinghe, R., 2015. Response of the Bight of Benin (Gulf of Guinea, West Africa) coastline to anthropogenic and natural forcing, Part1: Wave climate variability and impacts on the longshore sediment transport. Cont Shelf Res 110, 48–59. https://doi.org/10.1016/J.CSR.2015.09.020

Alongi, D.M., 2020. Coastal Ecosystem Processes. Coastal Ecosystem Processes. https://doi.org/10.1201/9781003057864

Alves, B., Angnuureng, D.B., Morand, P., Almar, R., 2020. A review on coastal erosion and flooding risks and best management practices in West Africa: what has been done and should be done. J Coast Conserv 24, 1–22. https://doi.org/10.1007/S11852-020-00755-7/METRICS

Amrouni, O., Heggy, E., Hzami, A., 2024. Shoreline retreat and beach nourishment are projected to increase in Southern California. Commun Earth Environ 5, 1–17. https://doi.org/10.1038/S43247-024-01388-6;SUBJMETA=172,2737,4081,704,829;KWRD=ENVIRONMENTAL+IMPACT,PHYSICAL+OCEANOGRAPHY

Arriaga, J., Rutten, J., Ribas, F., Falqués, A., Ruessink, G., 2017. Modeling the long-term diffusion and feeding capability of a mega-nourishment. Coastal Engineering 121, 1–13. https://doi.org/10.1016/j.coastaleng.2016.11.011

Atkinson, A.L., Baldock, T.E., 2020. Laboratory investigation of nourishment options to mitigate sea level rise induced erosion. Coastal Engineering 161, 103769. https://doi.org/10.1016/j.coastaleng.2020.103769

Baeyens, G, Martínez, M., 2008. Animal Life on Coatal Dunes: From Exploitation and Prosecution to Protection and Monitoring. Coastal dunes: ecology and conservation 279–296. https://doi.org/10.1007/978-3-540-74002-5.PDF

Baeyens, G., Martínez, M.L., 2008. Animal Life on Coatal Dunes: From Exploitation and Prosecution to Protection and Monitoring 279–296. https://doi.org/10.1007/978-3-540-74002-5_17

Bahrami, N., Siadatmousavi, S.M., 2025. Prediction of coastline evolution using remote sensing and deep learning approach; Case study of the Northwest of the Persian Gulf. Mar Geol 480, 107472. https://doi.org/10.1016/J.MARGEO.2024.107472

Bakhshianlamouki, E., Augustijn, E.W., Brugnach, M., Voinov, A., Wijnberg, K., 2023. A participatory modelling approach to cognitive mapping of the socio-environmental system of sandy anthropogenic shores in the Netherlands. Ocean Coast Manag 243, 106739. https://doi.org/10.1016/J.OCECOAMAN.2023.106739

Baptist, M., Tamis, J., … B.B.-I.C., 2009, undefined, 2009. Review of the geomorphological, benthic ecological and biogeomorphological effects of nourishments on the shoreface and surf zone of the Dutch coast. core.ac.ukMJ Baptist, JE Tamis, BW Borsje, JJ Van der WerfIMARES C113/08, Deltares Z, 2009•core.ac.uk.

Baramiya, D., Gorbenko, N., Lavrentiev, M., Spigler, R., 2019. Diffusion model to predict coastal profile evolutions. OCEANS 2019 - Marseille, OCEANS Marseille 2019 2019-June. https://doi.org/10.1109/OCEANSE.2019.8867524

Barbier, E.B., Hacker, S.D., Kennedy, C., Koch, E.W., Stier, A.C., Silliman, B.R., 2011. The value of estuarine and coastal ecosystem services. Wiley Online Library 81, 169–193. https://doi.org/10.1890/10-1510.1

Barbier, E.B., Koch, E.W., Silliman, B.R., Hacker, S.D., Wolanski, E., Primavera, J., Granek, E.F., Polasky, S., Aswani, S., Cramer, L.A., Stoms, D.M., Kennedy, C.J., Bael, D., Kappel, C. V., Perillo, G.M.E., Reed, D.J., 2008. Coastal ecosystem-based management with nonlinear ecological functions and values. Science (1979) 319, 321–323. https://doi.org/10.1126/science.1150349

Bauer, B.O., Davidson-Arnottt, R.G., Nordstrome, K.F., Ollerhead, J., Jackson, N.L., 1996. Indeterminacy in Aeolian Sediment Transport Across Beaches. J Coast Res 12, 641–653.

Bauer, W., 2023. Reframing Urban Nature-Based Solutions Through Perspectives of Environmental Justice and Privilege. Urban Plan 8, 334–345. https://doi.org/10.17645/UP.V8I1.6018

Baykal, C., Tarakcıoğlu, G.Ö., Aydın, D., Çınar, G., 2017. Application of XBeach in a beach nourishment and restoration project a case study: Alanya-Turkler, Turkey, in: XBeach X (10th Year Anniversary) Conference. pp. 1–3.

Beck, T.M., Rosati, J.D., Rosati, J., 2012. An update on nearshore berms in the Corps of Engineers: Recent projects and future needs.

Bendixen, M., Best, J., Hackney, C., Iversen, L.L., 2019. Time is running out for sand. Nature 571, 29–31. https://doi.org/10.1038/d41586-019-02042-4

Blake, B.F., 1974. Topophilia: A Study of Environmental Perception, Attitudes and Values. By Yi-Fu Tuan. J Leis Res 6, 323–325. https://doi.org/10.1080/00222216.1974.11970208

Bonte, D., Batsleer, F., Provoost, S., Reijers, V., Vandegehuchte, M.L., Van De Walle, R., Dan, S., Matheve, H., Rauwoens, P., Strypsteen, G., Suzuki, T., Verwaest, T., Hillaert, J., 2021. Biomorphogenic Feedbacks and the Spatial Organization of a Dominant Grass Steer Dune Development. Front Ecol Evol 9, 761336. https://doi.org/10.3389/FEVO.2021.761336/BIBTEX

Booij, N., Holthuijsen, L.H., Ris, R.C., 1997. The" SWAN" wave model for shallow water. ascelibrary.org 1, 668–676. https://doi.org/10.1061/9780784402429.053

Borsje, B.W., van Wesenbeeck, B.K., Dekker, F., Paalvast, P., Bouma, T.J., van Katwijk, M.M., de Vries, M.B., 2011. How ecological engineering can serve in coastal protection. Ecol Eng 37, 113–122. https://doi.org/10.1016/J.ECOLENG.2010.11.027

Brambilla, M., Ronchi, S., 2020. Cool species in tedious landscapes: Ecosystem services and disservices affect nature-based recreation in cultural landscapes. Ecol Indic 116, 106485. https://doi.org/10.1016/J.ECOLIND.2020.106485

Brand, E., Ramaekers, G., Lodder, Q., 2022. Dutch experience with sand nourishments for dynamic coastline conservation – An operational overview. Ocean Coast Manag 217, 106008. https://doi.org/10.1016/j.ocecoaman.2021.106008

Brière, C., Janssen, S.K.H., Oost, A.P., Taal, M., Tonnon, P.K., 2018. Usability of the climate-resilient nature-based sand motor pilot, The Netherlands. J Coast Conserv 22, 491–502. https://doi.org/10.1007/S11852-017-0527-3/TABLES/2

Broer, J., De Pater, M., Blikman, D., 2011. Ruimte voor recreatie op het strand: Onderzoek naar een recreatiebasiskustlijn, vliz.be. Amsterdam.

Brown, J.M., Phelps, J.J.C., Barkwith, A., Hurst, M.D., Ellis, M.A., Plater, A.J., 2016. The effectiveness of beach mega-nourishment, assessed over three management epochs. J Environ Manage 184, 400–408. https://doi.org/10.1016/J.JENVMAN.2016.09.090

Bruun, P., 1962. Sea-level rise as a cause of shore erosion. Journal of the Waterways and Harbors division 88.1, 117–132.

Bruun, P., 1954. Coast erosion and the development of beach profiles, Beach Erosion Board Technical Memorandum. US Beach Erosion Board, US Army Engineer Waterways Experiment Station, Vicksburg.

Cabezas-Rabadán, C., Pardo-Pascual, J.E., Almonacid-Caballer, J., Rodilla, M., 2019a. Detecting problematic beach widths for the recreational function along the Gulf of Valencia (Spain) from Landsat 8 subpixel shorelines. Applied Geography 110, 102047. https://doi.org/10.1016/j.apgeog.2019.102047

Cabezas-Rabadán, C., Rodilla, M., Pardo-Pascual, J.E., Herrera-Racionero, P., 2019b. Assessing users' expectations and perceptions on different beach types and the need for diverse management frameworks along the Western Mediterranean. Land use policy 81, 219–231. https://doi.org/10.1016/j.landusepol.2018.10.027

Capobianco, M., De Vriend, H.J., Nicholls, R.J., Stive, M.J.F., 1994. Application of a parametric long term model concept to the Delray beach nourishment program, in: Coastal Dynamics - Proceedings of the International Conference. pp. 391–401.

Capobianco, M., Hanson, H., Larson, M., Steetzel, H., Stive, M.J.F., Chatelus, Y., Aarninkhof, S., Karambas, T., 2002. Nourishment design and evaluation: applicability of model concepts. Coastal Engineering 47, 113–135. https://doi.org/10.1016/S0378-3839(02)00123-0

Cardinale, B.J., Duffy, J.E., Gonzalez, A., Hooper, D.U., Perrings, C., Venail, P., Narwani, A., MacE, G.M., Tilman, D., Wardle, D.A., Kinzig, A.P., Daily, G.C., Loreau, M., Grace, J.B., Larigauderie, A., Srivastava, D.S., Naeem, S., 2012. Biodiversity loss and its impact on humanity. Nature 486, 59–67. https://doi.org/10.1038/NATURE11148;SUBJMETA=158,2458,670,704;KWRD=BIODIVERSITY,ECOSYSTEM+SERVICES

Cardoso, R.S., Mattos, G., Caetano, C.H.S., Cabrini, T.M.B., Galhardo, L.B., Meireis, F., 2012. Effects of environmental gradients on sandy beach macrofauna of a semi-enclosed bay. Marine Ecology 33, 106–116. https://doi.org/10.1111/J.1439-0485.2011.00457.X;PAGE:STRING:ARTICLE/CHAPTER

Carter, J., Dyer, P., Sharma, B., 2007. Dis-placed voices: sense of place and place-identity on the Sunshine Coast. Soc Cult Geogr 8, 755–773. https://doi.org/10.1080/14649360701633345

Chan, K.M., Gould, R.K., Pascual, U., 2018. Editorial overview: Relational values: what are they, and what's the fuss about? Curr Opin Environ Sustain 35, A1–A7. https://doi.org/10.1016/J.COSUST.2018.11.003

Chen, W.L., Dodd, N., 2021. A nonlinear perturbation study of a shoreface nourishment on a multiply barred beach. Cont Shelf Res 214, 104317. https://doi.org/10.1016/j.csr.2020.104317

Chen, W.L., Dodd, N., 2019. An idealised study for the evolution of a shoreface nourishment. Cont Shelf Res 178, 15–26. https://doi.org/10.1016/j.csr.2019.03.010

Chiva, L., Pagán, J.I., López, I., Tenza-Abril, A.J., Aragonés, L., Sánchez, I., 2018. The effects of sediment used in beach nourishment: Study case El Portet de Moraira beach. Science of The Total Environment 628–629, 64–73. https://doi.org/10.1016/J.SCITOTENV.2018.02.042

Coelho, C., Larson, M., Hanson, H., 2017. Simulating Cross-Shore Evolution Towards Equilibrium of Different Beach Nourishment Schemes, in: Coastal Dynamics. pp. 1732–1746.

Cooke, B.C., Jones, A.R., Goodwin, I.D., Bishop, M.J., 2012. Nourishment practices on Australian sandy beaches: A review. J Environ Manage 113, 319–327. https://doi.org/10.1016/j.jenvman.2012.09.025

Cooper, J., Pilkey, O., 2012. Pitfalls of Shoreline Stabilization: Selected Case Studies. Springer Science & Business Media.

Correljé, A., Broekhans, B., 2015. Flood risk management in the Netherlands after the 1953 flood: A competition between the public value(s) of water. J Flood Risk Manag 8, 99–115. https://doi.org/10.1111/JFR3.12087;JOURNAL:JOURNAL:1753318X;REQUESTEDJOURNAL:JOURNAL:1753318X;WGROUP:STRING:PUBLICATION

Costanza, R., D'Arge, R., De Groot, R., Farber, S., Grasso, M., Hannon, B., Limburg, K., Naeem, S., O'Neill, R. V., Paruelo, J., Raskin, R.G., Sutton, P., Van Den Belt, M., 1997. The value of the world's ecosystem services and natural capital. Nature 387, 253–260. https://doi.org/10.1038/387253A0;KWRD=SCIENCE

Curry, P., 2011. Ecological ethics: An introduction.

Dallimer, M., Irvine, K.N., Skinner, A.M.J., Davies, Z.G., Rouquette, J.R., Maltby, L.L., Warren, P.H., Armsworth, P.R., Gaston, K.J., 2012. Biodiversity and the Feel-Good Factor: Understanding Associations between Self-Reported Human Well-being and Species Richness. Bioscience 62, 47–55. https://doi.org/10.1525/BIO.2012.62.1.9

Dally, W.R., Osiecki, D.A., 2018. Evaluating the Impact of Beach Nourishment on Surfing: Surf City, Long Beach Island, New Jersey, U.S.A. J Coast Res 34, 793–805. https://doi.org/10.2112/JCOASTRES-D-17-00162.1

Davidson, M., 2021. Forecasting coastal evolution on time-scales of days to decades. Coastal Engineering 168, 103928. https://doi.org/10.1016/J.COASTALENG.2021.103928

Davidson-Arnott, R.G.D., 2005. Conceptual model of the effects of sea level rise on sandy coasts. J Coast Res 21, 1166–1172. https://doi.org/10.2112/03-0051.1

Davidson-Arnott, R.G.D., Law, M.N., 1996. Measurement and Prediction of Long-Term Sediment Supply to Coastal Foredunes. J Coast Res 12, 654–663.

de Schipper, M., de Vries, S., Mil-Homens, J., Reniers, A., Ranasinghe, R., Stive, M., 2015. Initial volume losses at nourished beaches and the effect of surfzone slope, in: The Proceedings of the Coastal Sediments 2015. WORLD SCIENTIFIC. https://doi.org/10.1142/9789814689977_0050

de Schipper, M.A., de Vries, S., Ruessink, G., de Zeeuw, R.C., Rutten, J., van Gelder-Maas, C., Stive, M.J.F., 2016. Initial spreading of a mega feeder nourishment: Observations of the Sand Engine pilot project. Coastal Engineering 111, 23–38. https://doi.org/10.1016/J.COASTALENG.2015.10.011

De Schipper, M.A., De Vries, S., Stive, M., De Zeeuw, R., Rutten, J., Ruessink, G., Aarninkhof, S., Van Gelder-Maas, C., 2014. Morphological development of a mega-nourishment; first observations at the Sand Engine. Coastal Engineering Proceedings 1, 73. https://doi.org/10.9753/icce.v34.sediment.73

De Vriend, H.J., Stive, M.J.F., Nicholls, R.J., Capobianco, M., 1993. Cross-shore spreading of shore nourishment, in: Bruun, P. (Ed.), Proc. Hilton Head Island Coastal Symposium. pp. 175–179.

de Vriend, H.J., van Koningsveld, M., Aarninkhof, S.G.J., de Vries, M.B., Baptist, M.J., 2015. Sustainable hydraulic engineering through building with nature. Journal of Hydro-environment Research 9, 159–171. https://doi.org/10.1016/J.JHER.2014.06.004

De Vries, S., Arens, B., Stive, M., Ranasinghe, R., 2011. Dune growth trends and the effect of beach width on annual timescales, in: The Proceedings of the Coastal Sediments 2011. World Scientific Publishing Company, pp. 712–724. https://doi.org/10.1142/9789814355537_0054

de Winter, R.C., Ruessink, B.G., 2017. Sensitivity analysis of climate change impacts on dune erosion: case study for the Dutch Holland coast. Clim Change. https://doi.org/10.1007/s10584-017-1922-3

De Zeeuw, R.C., De Schipper, M.A., Roelvink, D., De Vries, S., Stive, M.J.F., 2012. Impact of nourishments on nearshore currents and swimmer safety on the Dutch coast. Coastal Engineering.

Dean, R., 2003. Beach nourishment: theory and practice, 18th ed. World scientific publishing company.

Dean, R.G., 1991. Equilibrium beach profiles: characteristics and applications. J Coast Res 1, 53–84.

Dean, R.G., Houston, J.R., 2016. Determining shoreline response to sea level rise. Coastal Engineering 114, 1–8. https://doi.org/10.1016/j.coastaleng.2016.03.009

Defeo, O., McLachlan, A., Schoeman, D.S., Schlacher, T.A., Dugan, J., Jones, A., Lastra, M., Scapini, F., 2009. Threats to sandy beach ecosystems: A review. Estuar Coast Shelf Sci 81, 1–12. https://doi.org/10.1016/j.ecss.2008.09.022

Deltares, 2025. UNIBEST-CL+ [WWW Document]. URL https://www.deltares.nl/en/software-and-data/products/unibest-cl (accessed 8.9.25).

Dhakal, S., Brown, K., Burgess, J., 2016. Beach Erosion and Nourishment in Gold Coast : Perceptions, policies and prospects, in: State of Australian Cities Conference. State of Australian Cities Research Network.

Díaz, R., Cutter Jr, G., Hobbs III, C., 2004. Potential Impacts of Sand Mining Offshore of Maryland and Delaware: Part 2—Biological Considerations. J Coast Res. https://doi.org/10.2112/1551-5036(2004)20[61:PIOSMO]2.0.CO;2.SHORT

Díaz, S., Pascual, U., Stenseke, M., Martín-López, B., Watson, R.T., Molnár, Z., Hill, R., Chan, K.M.A., Baste, I.A., Brauman, K.A., Polasky, S., Church, A., Lonsdale, M., Larigauderie, A., Leadley, P.W., Van Oudenhoven, A.P.E., Van Der Plaat, F., Schröter, M., Lavorel, S., Aumeeruddy-Thomas, Y., Bukvareva, E., Davies, K., Demissew, S., Erpul, G., Failler, P., Guerra, C.A., Hewitt, C.L., Keune, H., Lindley, S., Shirayama, Y., 2018a. Assessing nature's contributions to people: Recognizing culture, and diverse sources of knowledge, can improve assessments. Science (1979) 359, 270–272. https://doi.org/10.1126/SCIENCE.AAP8826/SUPPL_FILE/AAP8826-DIAZ-SM.PDF

Díaz, S., Pascual, U., Stenseke, M., Martín-López, B., Watson, R.T., Molnár, Z., Hill, R., Chan, K.M.A., Baste, I.A., Brauman, K.A., Polasky, S., Church, A., Lonsdale, M., Larigauderie, A., Leadley, P.W., Van Oudenhoven, A.P.E., Van Der Plaat, F., Schröter, M., Lavorel, S., Aumeeruddy-Thomas, Y., Bukvareva, E., Davies, K., Demissew, S., Erpul, G., Failler, P., Guerra, C.A., Hewitt, C.L., Keune, H., Lindley, S., Shirayama, Y., 2018b. Assessing nature's contributions to people: Recognizing culture, and diverse sources of knowledge, can improve assessments. Science (1979) 359, 270–272. https://doi.org/10.1126/SCIENCE.AAP8826/SUPPL_FILE/AAP8826-DIAZ-SM.PDF

Dillingh, D., Stolk, A., 1989. A short review of the Dutch coast. GWIO-89-004.

Doody, J.P., 2013. Coastal squeeze and managed realignment in southeast England, does it tell us anything about the future? Ocean Coast Manag 79, 34–41. https://doi.org/10.1016/j.ocecoaman.2012.05.008

Doorn, N., 2019. Water ethics: an introduction. Rowman & Littlefield.

Drijfhout, S., Le Bars, D., 2021. KNMI Klimaatsignaal '21 - Hoe het klimaat in Nederland snel verandert.

Duan, Z., Chen, J., Jiang, C., Liu, X., Zhao, B., 2020. Experimental study on uniform and mixed bed-load sediment transport under unsteady flow. Applied Sciences (Switzerland) 10. https://doi.org/10.3390/app10062002

Dunlop, T., Khojasteh, D., Cohen-Shacham, E., Glamore, W., Haghani, M., van den Bosch, M., Rizzi, D., Greve, P., Felder, S., 2024. The evolution and future of research on Nature-based Solutions to address societal challenges. Commun Earth Environ 5. https://doi.org/10.1038/S43247-024-01308-8

Elko, N., Briggs, T.R., Benedet, L., Robertson, Q., Thomson, G., Webb, B.M., Garvey, K., 2021. A century of U.S. beach nourishment. Ocean Coast Manag 199, 105406. https://doi.org/10.1016/J.OCECOAMAN.2020.105406

Faraci, C., Scandura, P., Foti, E., 2013. Bottom Profile Evolution of a Perched Nourished Beach. J Waterw Port Coast Ocean Eng 140, 04014021. https://doi.org/10.1061/(ASCE)WW.1943-5460.0000253

Feagin, R.A., Figlus, J., Zinnert, J.C., Sigren, J., Martínez, M.L., Silva, R., Smith, W.K., Cox, D., Young, D.R., Carter, G., 2015. Going with the flow or against the grain? The promise of vegetation for protecting beaches, dunes, and barrier islands from erosion. Front Ecol Environ 13, 203–210. https://doi.org/10.1890/140218;JOURNAL:JOURNAL:15409309;PAGE:STRING:ARTICLE/CHAPTER

Fiorentino, S., Sielker, F., of, J.T.-C.J., 2024, undefined, 2024. Coastal towns as "left-behind places": economy, environment and planning. academic.oup.comS Fiorentino, F Sielker, J TomaneyCambridge Journal of Regions, Economy and Society, 2024•academic.oup.com 17, 103–116. https://doi.org/10.1093/cjres/rsad045

Fletemeyer, J., Hearin, J., Haus, B., Sullivan, A., 2018. The impact of sand nourishment on beach safety. J Coast Res 34, 1–5. https://doi.org/10.2112/JCOASTRES-D-17A-00006.1

Geelen, L., Salman, A., Kuipers, M., 2015. Dynamic Dunes 2015: Daring Solutions for Natura 2000 Challenges: Zandvoort-Rockanje, the Netherlands, October 7-9, 2015. Waternet.

Gesing, F., 2019. The politics of artificial dunes: Sustainable coastal protection measures and contested socio-natural objects. DIE ERDE – Journal of the Geographical Society of Berlin 150, 145–157. https://doi.org/10.12854/ERDE-2019-423

Geukes, H., Pesch, U., Correljé, A., Taebi, B., 2021a. A healthy metaphor? The north sea consultation and the power of words. Sustainability (Switzerland) 13. https://doi.org/10.3390/SU132212905

Geukes, H., Pesch, U., Correljé, A., Taebi, B., 2021b. A Healthy Metaphor? The North Sea Consultation and the Power of Words. Sustainability 2021, Vol. 13, Page 12905 13, 12905. https://doi.org/10.3390/SU132212905

Geukes, H.H., van Bodegom, P.M., van Oudenhoven, A.P.E., 2024a. Setting the stage for decision-making on nature-based solutions for coastal climate adaptation. Ocean Coast Manag 247. https://doi.org/10.1016/J.OCECOAMAN.2023.106916

Geukes, H.H., van Bodegom, P.M., van Oudenhoven, A.P.E., 2024b. Setting the stage for decision-making on nature-based solutions for coastal climate adaptation. Ocean Coast Manag 247, 106916. https://doi.org/10.1016/J.OCECOAMAN.2023.106916

Giardino, A., Werf, J. Van Der, Ormondt, M. Van, 2010. Simulating Coastal Morphodynamics with Delft3D: case study Egmond aan Zee. Deltares Delft Hydraulics 80.

Gijsman, R., Visscher, J., Schlurmann, T., 2018. A method to systematically classify design characteristics of sand nourishments. Coastal Engineering Proceedings 95. https://doi.org/10.9753/icce.v36.papers.95

Gittman, R.K., Peterson, C.H., Currin, C.A., Joel Fodrie, F., Piehler, M.F., Bruno, J.F., 2016. Living shorelines can enhance the nursery role of threatened estuarine habitats. Wiley Online Library 26, 249–263. https://doi.org/10.1890/14-0716

González, S.A., Holtmann-Ahumada, G., 2017. Quality of tourist beaches of northern Chile: A first approach for ecosystem-based management. Ocean Coast Manag 137, 154–164. https://doi.org/10.1016/J.OCECOAMAN.2016.12.022

Greenhalgh, T., Thorne, S., Malterud, K., 2018. Time to challenge the spurious hierarchy of systematic over narrative reviews? Eur J Clin Invest 48, e12931. https://doi.org/10.1111/ECI.12931;REQUESTEDJOURNAL:JOURNAL:13652362;PAGE:STRING:ARTICLE/CHAPTER

Haasnoot, M., Brown, S., Scussolini, P., Jimenez, J.A., Vafeidis, A.T., Nicholls, R.J., 2019. Generic adaptation pathways for coastal archetypes under uncertain sea-level rise. Environ Res Commun 1. https://doi.org/10.1088/2515-7620/ab1871

Haasnoot, M., Kwadijk, J., Van Alphen, J., Le Bars, D., Van Den Hurk, B., Diermanse, F., Van Der Spek, A., Oude Essink, G., Delsman, J., Mens, M., 2020. Adaptation to uncertain sea-level rise; how uncertainty in Antarctic mass-loss impacts the coastal adaptation strategy of the Netherlands. Environmental Research Letters 15, 034007. https://doi.org/10.1088/1748-9326/ab666c

Haasnoot, M., Kwakkel, J.H., Walker, W.E., ter Maat, J., 2013a. Dynamic adaptive policy pathways: A method for crafting robust decisions for a deeply uncertain world. Global Environmental Change 23, 485–498. https://doi.org/10.1016/j.gloenvcha.2012.12.006

Haasnoot, M., Kwakkel, J.H., Walker, W.E., ter Maat, J., 2013b. Dynamic adaptive policy pathways: A method for crafting robust decisions for a deeply uncertain world. Global Environmental Change 23, 485–498. https://doi.org/10.1016/j.gloenvcha.2012.12.006

Haasnoot, M., Lawrence, J., Magnan, A.K., 2021. Pathways to coastal retreat: The shrinking solution space for adaptation calls for long-term dynamic planning starting now. Science (1979) 372, 1287–1290. https://doi.org/10.1126/SCIENCE.ABI6594

Haila, Y., Levins, R., 1992. Humanity and nature: Ecology, science and society, cir.nii.ac.jp.

Hallermeijer, R., 1981. Terminal settling velocity of commonly occurring sand grains. Sedimentology 28, 859–865. https://doi.org/10.1111/J.1365-3091.1981.TB01948.X;PAGEGROUP:STRING:PUBLICATION

Hallin, C., 2019. Long-term beach and dune evolution Development and application of the CS-model.

Hamm, L., Capobianco, M., Dette, H.H., Lechuga, A., Spanhoff, R., Stive, M.J.F., 2002. A summary of European experience with shore nourishment. Coastal Engineering 47, 237–264. https://doi.org/10.1016/S0378-3839(02)00127-8

Hamza, W., Cherif, F., Choura, M., 2018. Exploration of the bearing capacity of Taparura Artificial Beach using the standard penetration test. J Coast Conserv 22, 315–324. https://doi.org/10.1007/S11852-017-0579-4/METRICS

Hands, E.B., Allison, M.C., 1991. Mound migration in deeper water and methods of categorizing active and stable berm depths, in: Proceedings of a Specialty Conference on Quantitative Approaches to Coastal Sediment Processes. Seattle, Washington.

Hanley, M.E., Hoggart, S.P.G., Simmonds, D.J., Bichot, A., Colangelo, M.A., Bozzeda, F., Heurtefeux, H., Ondiviela, B., Ostrowski, R., Recio, M., Trude, R., Zawadzka-Kahlau, E., Thompson, R.C., 2014. Shifting sands? Coastal protection by sand banks, beaches and dunes. Coastal Engineering 87, 136–146. https://doi.org/10.1016/J.COASTALENG.2013.10.020

Hanson, H., Beach, W.P., 2003. Modelling of Coastal Evolution on Yearly to Decadal Time Scales Modelling of Coastal Evolution on Yearly to Decadal.

Hanson, H., Brampton, A., Capobianco, M., Dette, H.H., Hamm, L., Laustrup, C., Lechuga, A., Spanhoff, R., 2002. Beach nourishment projects, practices, and objectives—a European

overview. Coastal Engineering 47, 81–111. https://doi.org/10.1016/S0378-3839(02)00122-9

Hanson, H., Kraus, N.C., 1989. GENESIS: Generalized Model for Simulating Shoreline Change. Report 1. Technical Reference.

Hanson, H.I., Wickenberg, B., Alkan Olsson, J., 2020. Working on the boundaries—How do science use and interpret the nature-based solution concept? Land use policy 90. https://doi.org/10.1016/J.LANDUSEPOL.2019.104302

Hashemi, M.R., Ghadampour, Z., Neill, S.P., 2010. Using an artificial neural network to model seasonal changes in beach profiles. Ocean Engineering 37, 1345–1356. https://doi.org/10.1016/J.OCEANENG.2010.07.004

Hattam, C., Atkins, J.P., Beaumont, N., Börger, T., Böhnke-Henrichs, A., Burdon, D., De Groot, R., Hoefnagel, E., Nunes, P.A.L.D., Piwowarczyk, J., Sastre, S., Austen, M.C., 2015a. Marine ecosystem services: Linking indicators to their classification. Ecol Indic 49, 61–75. https://doi.org/10.1016/j.ecolind.2014.09.026

Hattam, C., Atkins, J.P., Beaumont, N., Börger, T., Böhnke-Henrichs, A., Burdon, D., De Groot, R., Hoefnagel, E., Nunes, P.A.L.D., Piwowarczyk, J., Sastre, S., Austen, M.C., 2015b. Marine ecosystem services: Linking indicators to their classification. Ecol Indic 49, 61–75. https://doi.org/10.1016/J.ECOLIND.2014.09.026

Herman, P.M.J., Huisman, B.J.A., Prins, T.C., 2022. Natuurlijk Veilig Cumulatief effect van zandsuppleties op sediment en bodemdieren.

Herman, P.M.J., Moons, J.J.S., Wijsman, J.W.M., Luijendijk, A.P., Ysebaert, T., 2021. A Mega-Nourishment (Sand Motor) Affects Landscape Diversity of Subtidal Benthic Fauna. Front Mar Sci 8, 643674. https://doi.org/10.3389/FMARS.2021.643674/BIBTEX

Hesp, P., Martínez, M., 2007. Disturbance processes and dynamics in coastal dunes. Plant disturbance ecology: the process and the response 215–247.

Hesp, P., Martinez, M., Da Silva, G.M., Rodríguez-Revelo, N., Gutierrez, E., Humanes, A., Laínez, D., Montaño, I., Palacios, V., Quesada, A., Storero, L., Trilla, G.G., Trochine, C., 2011a. Transgressive dunefield landforms and vegetation associations, Doña Juana, Veracruz, Mexico. Earth Surf Process Landf 36, 285–295. https://doi.org/10.1002/ESP.2035

Hesp, P., Martinez, M., Da Silva, G.M., Rodríguez-Revelo, N., Gutierrez, E., Humanes, A., Laínez, D., Montaño, I., Palacios, V., Quesada, A., Storero, L., Trilla, G.G., Trochine, C., 2011b. Transgressive dunefield landforms and vegetation associations, Doña Juana, Veracruz, Mexico. Earth Surf Process Landf 36, 285–295. https://doi.org/10.1002/ESP.2035

Hinkel, J., 2011. " Indicators of vulnerability and adaptive capacity": Towards a clarification of the science-policy interface. Global Environmental Change 21, 198–208. https://doi.org/10.1016/j.gloenvcha.2010.08.002

Hinkel, J., Lincke, D., Vafeidis, A.T., Perrette, M., Nicholls, R.J., Tol, R.S.J., Marzeion, B., Fettweis, X., Ionescu, C., Levermann, A., 2014. Coastal flood damage and adaptation costs under 21st century sea-level rise. Proc Natl Acad Sci U S A 111, 3292–3297. https://doi.org/10.1073/pnas.1222469111

Hinton, C., Nicholls, R.J., 1998. Spatial and temporal behaviour of depth of closure along the Holland coast. Proceedings of the Coastal Engineering Conference 3, 2913–2925. https://doi.org/10.1061/9780784404119.221

Hoonhout, B., de Vries, S., 2017. Aeolian sediment supply at a mega nourishment. Coastal Engineering 123, 11–20. https://doi.org/10.1016/J.COASTALENG.2017.03.001

Houston, J., 2021. The economic value of beach nourishment in South Carolina. Shore & Beach 89, 3–12. https://doi.org/10.34237/1008931

Huisman, B., Roelvink, D., De Bakker, A., De Beer Vassia, A., Review, D., Reyns, J., 2024. ShorelineS : Technical manual.
Huisman, B.J.A., Walstra, D.J.R., Radermacher, M., de Schipper, M.A., Ruessink, B.G., 2019. Observations and modelling of shoreface nourishment behaviour. J Mar Sci Eng 7. https://doi.org/10.3390/jmse7030059
Huisman, B.J.A., Wang, Z.B., De Ronde, J.G., Stronkhorst, J., Sprengers, C.J., 2013. Coastline modelling for nourishment strategy evaluation, in: 6th SCACR – International Short Course/Conference on Applied Coastal Research .
Huizer, S., Luijendijk, A.P., Bierkens, M.F.P., Oude Essink, G.H.P., 2019. Global potential for the growth of fresh groundwater resources with large beach nourishments. Sci Rep 9, 1–14. https://doi.org/10.1038/s41598-019-48382-z
Huizer, S., Oude Essink, G.H.P., Bierkens, M.F.P., 2016. Fresh groundwater resources in a large sand replenishment. Hydrol Earth Syst Sci 20, 3149–3166. https://doi.org/10.5194/hess-20-3149-2016
Hulskamp, R.L., Pregnolato, M., de Vries, S., 2025. Dynamics of engineered coastal dune landscapes at the Zandmotor. Discover Geoscience 3, 244. https://doi.org/10.1007/S44288-025-00360-X
Hynes, S., Ghermandi, A., Norton, D., Williams, H., 2018. Marine recreational ecosystem service value estimation: A meta-analysis with cultural considerations. Ecosyst Serv 31, 410–419. https://doi.org/10.1016/J.ECOSER.2018.02.001
IPCC, 2023. Oceans and Coastal Ecosystems and Their Services. Climate Change 2022 – Impacts, Adaptation and Vulnerability 379–550. https://doi.org/10.1017/9781009325844.005
IPCC AR6 Working Group I, 2021. IPCC, 2021: Climate change 2021-the physical science basis, Interaction. https://doi.org/10.3316/informit.315096509383738
IPCC AR6 Working Group II, 2022. IPCC, 2022: Climate change 2022-impacts, adaptation and vulnerability.
Jackson, N.L., Nordstrom, K.F., 2011. Aeolian sediment transport and landforms in managed coastal systems: A review. Aeolian Res 3, 181–196. https://doi.org/10.1016/J.AEOLIA.2011.03.011
Jacobs, S., Zafra-Calvo, N., Gonzalez-Jimenez, D., Guibrunet, L., Benessaiah, K., Berghöfer, A., Chaves-Chaparro, J., Díaz, S., Gomez-Baggethun, E., Lele, S., Martín-López, B., Masterson, V.A., Merçon, J., Moersberger, H., Muraca, B., Norström, A., O'Farrell, P., Ordonez, J.C., Prieur-Richard, A.H., Rincón-Ruiz, A., Sitas, N., Subramanian, S.M., Tadesse, W., van Noordwijk, M., Pascual, U., Balvanera, P., 2020a. Use your power for good: Plural valuation of nature – the Oaxaca statement. Global Sustainability 3. https://doi.org/10.1017/SUS.2020.2
Jacobs, S., Zafra-Calvo, N., Gonzalez-Jimenez, D., Guibrunet, L., Benessaiah, K., Berghöfer, A., Chaves-Chaparro, J., Díaz, S., Gomez-Baggethun, E., Lele, S., Martín-López, B., Masterson, V.A., Merçon, J., Moersberger, H., Muraca, B., Norström, A., O'Farrell, P., Ordonez, J.C., Prieur-Richard, A.H., Rincón-Ruiz, A., Sitas, N., Subramanian, S.M., Tadesse, W., van Noordwijk, M., Pascual, U., Balvanera, P., 2020b. Use your power for good: plural valuation of nature – the Oaxaca statement. Global Sustainability 3, e8. https://doi.org/10.1017/SUS.2020.2
Janssen, G., Mulder, S., 2005. Zonation of macrofauna across sandy beaches and surf zones along the Dutch coast. Oceanologia 47.
Kalligeris, N., Smit, P.B., Ludka, B.C., Guza, R.T., Gallien, T.W., 2020. Calibration and assessment of process-based numerical models for beach profile evolution in southern

California. Coastal Engineering 158, 103650. https://doi.org/10.1016/j.coastaleng.2020.103650

Karalinas, V., Jarmalavičius, D., Pupienis, D., Janušait, R., Zilinskas, G., Karlonien, D., 2020. Shore Nourishment Impact on Coastal Landscape Transformation: An Example of the Lithuanian Baltic Sea Coast. J Coast Res 95, 840–844. https://doi.org/10.2112/SI95-163.1

Kaufmann, M., Priest, S., Hudson, P., Löschner, L., Raška, P., Schindelegger, A., Slavíková, L., Stričević, R., Vleesenbeek, T., 2022. Win–Win for Everyone? Reflecting on Nature-Based Solutions for Flood Risk Management from an Environmental Justice Perspective. Handbook of Environmental Chemistry 107, 399–423. https://doi.org/10.1007/698_2021_759

Keijsers, J.G.S., Poortinga, A., Riksen, M.J.P.M., Maroulis, J., 2014. Spatio-temporal variability in accretion and erosion of coastal foredunes in the Netherlands: regional climate and local topography. journals.plos.orgJGS Keijsers, A Poortinga, MJPM Riksen, J MaroulisPloS one, 2014•journals.plos.org 9, 91115. https://doi.org/10.1371/JOURNAL.PONE.0091115

Kettler, T., de Schipper, M., Luijendijk, A., 2024. Simulating decadal cross-shore dynamics at nourished coasts with Crocodile. Coastal Engineering 190, 104491. https://doi.org/10.1016/J.COASTALENG.2024.104491

Key, I.B., Smith, A.C., Turner, B., Chausson, A., Girardin, C.A.J., Macgillivray, M., Seddon, N., 2022. Biodiversity outcomes of nature-based solutions for climate change adaptation: Characterising the evidence base. Front Environ Sci 10, 905767. https://doi.org/10.3389/FENVS.2022.905767/XML/NLM

Khan, A.R., Ab Razak, M.S. Bin, Yusuf, B.B., Mohd Shafri, H.Z. Bin, Mohamad, N.B., 2025. Harnessing artificial neural networks for coastal erosion prediction: A systematic review. Mar Policy 178, 106704. https://doi.org/10.1016/J.MARPOL.2025.106704

Kindeberg, T., Almström, B., Skoog, M., Olsson, P.A., Hollander, J., 2023a. Toward a multifunctional nature-based coastal defense: a review of the interaction between beach nourishment and ecological restoration. Nord J Bot 2023, e03751. https://doi.org/10.1111/NJB.03751;CSUBTYPE:STRING:SPECIAL;PAGE:STRING:ARTICLE/CHAPTER

Kindeberg, T., Almström, B., Skoog, M., Olsson, P.A., Hollander, J., 2023b. Toward a multifunctional nature-based coastal defense: a review of the interaction between beach nourishment and ecological restoration. Nord J Bot 2023, e03751. https://doi.org/10.1111/NJB.03751;CSUBTYPE:STRING:SPECIAL;PAGE:STRING:ARTICLE/CHAPTER

Klein, Y.L., Osleeb, J., 2010. Determinants of Coastal Tourism: A Case Study of Florida Beach Counties. J Coast Res 26, 1149–1156. https://doi.org/10.2112/JCOASTRES-D-09-00152.1

KNMI, 2023. KNMI'23-klimaatscenario's voor Nederland. De Bilt.

Kristensen, S.E., Drønen, N., Deigaard, R., Fredsoe, J., 2016. Impact of groyne fields on the littoral drift: A hybrid morphological modelling study. Coastal Engineering 111, 13–22. https://doi.org/10.1016/J.COASTALENG.2016.01.009

Kroon, A., de Schipper, M., de Vries, S., Aarninkhof, S., 2022a. Subaqueous and Subaerial Beach Changes after Implementation of a Mega Nourishment in Front of a Sea Dike. J Mar Sci Eng 10, 1152. https://doi.org/10.3390/jmse10081152

Kroon, A., De Schipper, M.A., De Vries, S., Aarninkhof, S., Coelho, B., De Schipper, M., 2022b. Subaqueous and Subaerial Beach Changes after Implementation of a Mega Nourishment in Front of a Sea Dike. researchgate.net. https://doi.org/10.3390/jmse10081152

Lamb, J., True, J., Piromvaragorn, S., Conservation, B.W.-B., 2014, undefined, 2014. Scuba diving damage and intensity of tourist activities increases coral disease prevalence. ElsevierJB Lamb, JD True, S Piromvaragorn, BL WillisBiological Conservation, 2014•Elsevier 178, 88–96. https://doi.org/10.1016/j.biocon.2014.06.027

Lamb, R.J., Purcell, A.T., 1990. Perception of naturalness in landscape and its relationship to vegetation structure. Landsc Urban Plan 19, 333–352. https://doi.org/10.1016/0169-2046(90)90041-Y

Lansu, E.M., Reijers, V.C., Höfer, S., Luijendijk, A., Rietkerk, M., Wassen, M.J., Lammerts, E.J., van der Heide, T., 2024. A global analysis of how human infrastructure squeezes sandy coasts. Nat Commun 15, 432. https://doi.org/10.1038/s41467-023-44659-0

Larson, M., 1998. SBEACH: Numerical Model for Simulating Storm-Induced Beach Change.

Lavrentiev, M.M., 2015. Diffusion model identification for long-term coastal profile evolution, in: The Twenty-Fifth International Ocean and Polar Engineering Conference. pp. 1271–1278.

Leewis, L., Bodegom, P., Rozema, J., Janssen, G., 2012. Does beach nourishment have long-term effects on intertidal macroinvertebrate species abundance? https://doi.org/10.5555/20123384145

Leewis, L., Bodegom, P. van, Estuarine, J.R.-, and, C., 2012, undefined, n.d. Does beach nourishment have long-term effects on intertidal macroinvertebrate species abundance? ElsevierL Leewis, PM van Bodegom, J Rozema, GM JanssenEstuarine, Coastal and Shelf Science, 2012•Elsevier.

Lesser, G.R., Roelvink, J.A., van Kester, J.A.T.M., Stelling, G.S., 2004. Development and validation of a three-dimensional morphological model. Coastal Engineering 51, 883–915. https://doi.org/10.1016/j.coastaleng.2004.07.014

Lippmann, T.C., Holman, R.A., 1989. Quantification of sand bar morphology: A video technique based on wave dissipation. J Geophys Res Oceans 94, 995–1011. https://doi.org/10.1029/JC094iC01p00995

Liquete, C., Zulian, G., Delgado, I., Stips, A., Maes, J., 2013a. Assessment of coastal protection as an ecosystem service in Europe. Ecol Indic 30, 205–217. https://doi.org/10.1016/j.ecolind.2013.02.013

Liquete, C., Zulian, G., Delgado, I., Stips, A., Maes, J., 2013b. Assessment of coastal protection as an ecosystem service in Europe. Ecol Indic 30, 205–217. https://doi.org/10.1016/J.ECOLIND.2013.02.013

Liu, X., Luo, X., Lu, C., Zhang, G., Ding, W., 2024. The Impact of Foreshore Slope on Cross-Shore Sediment Transport and Sandbar Formation in Beach Berm Nourishment. Water (Basel) 16, 2212. https://doi.org/10.3390/w16152212

Lodder, Q., Slinger, J., 2022. The 'Research for Policy' cycle in Dutch coastal flood risk management: The Coastal Genesis 2 research programme. Ocean Coast Manag 219, 106066. https://doi.org/10.1016/j.ocecoaman.2022.106066

Lodder, Q.J., Slinger, J.H., Wang, Z.B., van Gelder, C., 2020. Decision making in Dutch coastal research based on coastal management policy assumptions, in: Coastal Management 2019. ICE Publishing, pp. 291–300. https://doi.org/10.1680/cm.65147.291

López, I., Aragonés, L., Villacampa, Y., Satorre, R., 2018. Modelling the cross-shore beach profiles of sandy beaches with Posidonia oceanica using artificial neural networks: Murcia (Spain) as study case. Applied Ocean Research 74, 205–216. https://doi.org/10.1016/j.apor.2018.03.004

Lorenzoni, I., Day, S.A., Mahony, M., Tolhurst, T.J., Bark, R.H., 2024. Innovation in coastal governance: management and expectations of the UK's first sandscaping scheme. Reg Environ Change 24, 1–15. https://doi.org/10.1007/S10113-024-02248-X/TABLES/1

Ludka, B.C., Gallien, T.W., Crosby, S.C., Guza, R.T., 2016. Mid-El Niño erosion at nourished and unnourished Southern California beaches. Geophys Res Lett 43, 4510–4516. https://doi.org/10.1002/2016GL068612

Luijendijk, A., Hagenaars, G., Ranasinghe, R., Baart, F., Donchyts, G., Aarninkhof, S., 2018. The State of the World's Beaches. Sci Rep 8, 1–11. https://doi.org/10.1038/s41598-018-24630-6

Luijendijk, A.P., de Schipper, M.A., Ranasinghe, R., 2019. Morphodynamic acceleration techniques for multi-timescale predictions of complex sandy interventions. J Mar Sci Eng 7. https://doi.org/10.3390/jmse7030078

Luijendijk, A.P., Ranasinghe, R., de Schipper, M.A., Huisman, B.A., Swinkels, C.M., Walstra, D.J.R., Stive, M.J.F., 2017. The initial morphological response of the Sand Engine: A process-based modelling study. Coastal Engineering 119, 1–14. https://doi.org/10.1016/j.coastaleng.2016.09.005

Luo, S., Liu, Y., Jin, R., Zhang, J., Wei, W., 2016. A guide to coastal management: Benefits and lessons learned of beach nourishment practices in China over the past two decades. Ocean Coast Manag 134, 207–215. https://doi.org/10.1016/j.ocecoaman.2016.10.011

Manero, A., Mach, L., 2023. Valuing surfing ecosystems: an environmental economics and natural resources management perspective. Tourism Geographies 25, 1602–1629. https://doi.org/10.1080/14616688.2023.2261909

Manning, P., Van Der Plas, F., Soliveres, S., Allan, E., Maestre, F.T., Mace, G., Whittingham, M.J., Fischer, M., 2018. Redefining ecosystem multifunctionality. Nat Ecol Evol 2, 427–436. https://doi.org/10.1038/S41559-017-0461-7;SUBJMETA=158,2445,2458,670,704;KWRD=BIODIVERSITY,ECOLOGY,ECOSYSTEM+ECOLOGY,ECOSYSTEM+SERVICES

Marchesiello, P., Chauchat, J., Shafiei, H., Almar, R., Benshila, R., Dumas, F., Debreu, L., 2022. 3D wave-resolving simulation of sandbar migration. Ocean Model (Oxf) 180, 102127. https://doi.org/10.1016/J.OCEMOD.2022.102127

Marean, C.W., 2010. Pinnacle Point Cave 13B (Western Cape Province, South Africa) in context: The Cape Floral kingdom, shellfish, and modern human origins. J Hum Evol 59, 425–443. https://doi.org/10.1016/J.JHEVOL.2010.07.011

Marinho, B., Coelho, C., Larson, M., Hanson, H., 2017. Simulating Cross-Shore Evolution Towards Equilibrium of Different Beach Nourishment Schemes, in: Coastal Dynamics. pp. 1732–1746.

Martínez, M.L., Psuty, N.P., Lubke, R.A., 2008. A Perspective on Coastal Dunes 3–10. https://doi.org/10.1007/978-3-540-74002-5_1

Martino, S., Amos, C.L., 2015. Valuation of the ecosystem services of beach nourishment in decision-making: The case study of Tarquinia Lido, Italy. Ocean Coast Manag 111, 82–91. https://doi.org/10.1016/j.ocecoaman.2015.03.012

McCarroll, R.J., Masselink, G., Valiente, N.G., Scott, T., Wiggins, M., Kirby, J.-A., Davidson, M., 2021a. A rules-based shoreface translation and sediment budgeting tool for estimating coastal change: ShoreTrans. Mar Geol 435, 106466. https://doi.org/10.1016/j.margeo.2021.106466

McCarroll, R.J., Masselink, G., Valiente, N.G., Scott, T., Wiggins, M., Kirby, J.A., Davidson, M., 2021b. A rules-based shoreface translation and sediment budgeting tool for estimating coastal change: ShoreTrans. Mar Geol 435. https://doi.org/10.1016/J.MARGEO.2021.106466

McLachlan, A., Defeo, O., Jaramillo, E., Short, A.D., 2013. Sandy beach conservation and recreation: Guidelines for optimising management strategies for multi-purpose use. Ocean Coast Manag 71, 256–268. https://doi.org/10.1016/j.ocecoaman.2012.10.005

Mclachlan, A., Dorvlo, A., 2007. Species - area relationships for sandy beach macrobenthos in the context of intertidal width. Oceanologia 49.
McLachlan, A., Dorvlo, A., 2005. Global Patterns in Sandy Beach Macrobenthic Communities. J Coast Res 21, 674–687. https://doi.org/10.2112/03-0114.1
McLachlan, A., Jaramillo, E., Donn, T., Wessels, F., 1993. Sandy beach macrofauna communities and their control by the physical environment: a geographical comparison. J Coast Res 27–38.
McNamara, D.E., Gopalakrishnan, S., Smith, M.D., Murray, A.B., 2015. Climate Adaptation and Policy-Induced Inflation of Coastal Property Value. PLoS One 10, e0121278. https://doi.org/10.1371/JOURNAL.PONE.0121278
Melanidis, M.S., Hagerman, S., 2022. Competing narratives of nature-based solutions: Leveraging the power of nature or dangerous distraction? Environ Sci Policy 132, 273–281. https://doi.org/10.1016/j.envsci.2022.02.028
Montaño, J., Coco, G., Antolínez, J.A.A., Beuzen, T., Bryan, K.R., Cagigal, L., Castelle, B., Davidson, M.A., Goldstein, E.B., Ibaceta, R., Idier, D., Ludka, B.C., Masoud-Ansari, S., Méndez, F.J., Murray, A.B., Plant, N.G., Ratliff, K.M., Robinet, A., Rueda, A., Sénéchal, N., Simmons, J.A., Splinter, K.D., Stephens, S., Townend, I., Vitousek, S., Vos, K., 2020. Blind testing of shoreline evolution models. Sci Rep 10, 1–10. https://doi.org/10.1038/s41598-020-59018-y
Montaño, J., Coco, G., Chataigner, T., Yates, M., Le Dantec, N., Suanez, S., Cagigal, L., Floc'h, F., Townend, I., 2021. Time-Scales of a Dune-Beach System and Implications for Shoreline Modeling. J Geophys Res Earth Surf 126, e2021JF006169. https://doi.org/10.1029/2021JF006169;WEBSITE:WEBSITE:AGUPUBS;WGROUP:STRING:PUBLICATION
Mulder, J.P.M., 2000. Zandverliezen in het Nederlandse kustsysteem.
Muller, M.W., 2018. Beach replenishment and surf-zone injuries along the coast of Delmarva, USA. Ocean Coast Manag 151, 127–133. https://doi.org/10.1016/J.OCECOAMAN.2017.10.013
Mullin, M., Smith, M.D., McNamara, D.E., 2019. Paying to save the beach: effects of local finance decisions on coastal management. Clim Change 152, 275–289. https://doi.org/10.1007/S10584-018-2191-5/METRICS
Nawarat, K., Reyns, J., Vousdoukas, M.I., Duong, T.M., Kras, E., Ranasinghe, R., 2024. Coastal hardening and what it means for the world's sandy beaches. Nature Communications 2024 15:1 15, 1–8. https://doi.org/10.1038/s41467-024-54952-1
Nederbragt, G.J., 2006. Zandvoorraden van het kustsysteem: onderbouwing van een conceptueel model met behulp van trends van de winst- en verliesposten over de periode 1973-1997.
Nesshöver, C., Assmuth, T., Irvine, K.N., Rusch, G.M., Waylen, K.A., Delbaere, B., Haase, D., Jones-Walters, L., Keune, H., Kovacs, E., Krauze, K., Külvik, M., Rey, F., van Dijk, J., Vistad, O.I., Wilkinson, M.E., Wittmer, H., 2017. The science, policy and practice of nature-based solutions: An interdisciplinary perspective. Science of The Total Environment 579, 1215–1227. https://doi.org/10.1016/J.SCITOTENV.2016.11.106
Norgaard, R.B., 2010. Ecosystem services: From eye-opening metaphor to complexity blinder. Ecological Economics 69, 1219–1227. https://doi.org/10.1016/j.ecolecon.2009.11.009
Nunes da Silva, L.C., Barbosa Viana, M., 2024. Effects of artificial beach nourishment on water quality and marine biota: a critical review. Arquivos de Ciências do Mar 57. https://doi.org/10.32360/ACMAR.V57I2.93127

Ocaña, F.A., Cuevas, E., Sauma-Castillo, L., López-Castro, M., Guerra-Castro, E., 2022. A quantitative three-step approach for guiding sandy beach management. Ocean Coast Manag 229, 106337. https://doi.org/10.1016/J.OCECOAMAN.2022.106337

Ojeda, M C, Ojeda, Mariana Cecilia, 2008. Rasgos de la identidad del profesor de enseñanza media en su trayectoria de formación y desempeño profesionales: ¿Cómo, cuándo y con quiénes adquiere su condición de profesor? Revista electrónica de investigación educativa 10, 1–14.

Palinkas, C.M., Orton, P., Hummel, M.A., Nardin, W., Sutton-Grier, A.E., Harris, L., Gray, M., Li, M., Ball, D., Burks-Copes, K., Davlasheridze, M., De Schipper, M., George, D.A., Halsing, D., Maglio, C., Marrone, J., McKay, S.K., Nutters, H., Orff, K., Taal, M., Van Oudenhoven, A.P.E., Veatch, W., Williams, T., 2022. Innovations in Coastline Management With Natural and Nature-Based Features (NNBF): Lessons Learned From Three Case Studies. Front Built Environ 8. https://doi.org/10.3389/FBUIL.2022.814180

Pang, W., Dai, Z., Ma, B., Wang, J., Huang, H., Li, S., 2020. Linkage between turbulent kinetic energy, waves and suspended sediment concentrations in the nearshore zone. Mar Geol 425, 106190. https://doi.org/10.1016/j.margeo.2020.106190

Pang, W., Ge, Z., Dai, Z., Li, S., Huang, H., 2021. The behaviour of beach elevation contours in response to different wave energy environments. Earth Surf Process Landf 46, 443–454. https://doi.org/10.1002/esp.5036

Paprotny, D., Vousdoukas, M.I., Athanasiou, P., Mentaschi, L., Śledziowski, J., Terefenko, P., Feyen, L., 2025. Sandy coast erosion threatens vital ecosystem services. https://doi.org/10.21203/RS.3.RS-6716780/V1

Pearson, S.G., van Prooijen, B.C., Elias, E.P.L., Vitousek, S., Wang, Z.B., 2020. Sediment Connectivity: A Framework for Analyzing Coastal Sediment Transport Pathways. J Geophys Res Earth Surf 125, e2020JF005595. https://doi.org/10.1029/2020JF005595

Pelnard-Considère, R., 1957. Essai de théorie de l'évolution des formes de rivage en plages de sable et de galets. Journées de l'hydraulique 4, 289–298.

Pinto, C.A., Silveira, T.M., Teixeira, S.B., 2020. Beach nourishment practice in mainland Portugal (1950–2017): Overview and retrospective. Ocean Coast Manag 192. https://doi.org/10.1016/J.OCECOAMAN.2020.105211

Puijenbroek, L., Limpens, M.E.B.;, Groot, J.;, Riksen, A.;, Gleichman, M.J.P.M.;, Et Al, J.M., Van Puijenbroek, M.E.B., Limpens, J., De Groot, A. V, Riksen, M.J.P.M., Gleichman, M., Slim, P.A., Van Dobben, H.F., Berendse, F., 2017. Embryo dune development drivers: beach morphology, growing season precipitation, and storms. Wiley Online LibraryMEB van Puijenbroek, J Limpens, AV de Groot, MJPM Riksen, M Gleichman, PA SlimEarth Surface Processes and Landforms, 2017•Wiley Online Library 42, 1733–1744. https://doi.org/10.1002/ESP.4144

Ranasinghe, R., 2020. On the need for a new generation of coastal change models for the 21st century. Sci Rep 10, 1–6. https://doi.org/10.1038/s41598-020-58376-x

Ranasinghe, R., 2016a. Assessing climate change impacts on open sandy coasts: A review. Earth Sci Rev. https://doi.org/10.1016/j.earscirev.2016.07.011

Ranasinghe, R., 2016b. Assessing climate change impacts on open sandy coasts: A review. Earth Sci Rev 160, 320–332. https://doi.org/10.1016/j.earscirev.2016.07.011

Ranasinghe, R., Turner, I.L., 2006. Shoreline response to submerged structures: A review. Coastal Engineering 53, 65–79. https://doi.org/10.1016/J.COASTALENG.2005.08.003

Rawls, J., 1971. A theory of justice, in: Applied Ethics. https://doi.org/10.4324/9781315097176-4/THEORY-JUSTICE-JOHN-RAWLS

Refulio-Coronado, S., Lacasse, K., Dalton, T., Humphries, A., Basu, S., Uchida, H., Uchida, E., 2021. Coastal and Marine Socio-Ecological Systems: A Systematic Review of the Literature. Front Mar Sci 8. https://doi.org/10.3389/FMARS.2021.648006

Richards, M.P., Schulting, R.J., 2006. Touch not the fish: the Mesolithic-Neolithic change of diet and its significance. Antiquity 80, 444–456. https://doi.org/10.1017/S0003598X00093765

Rijkswaterstaat, 2024. Kustonderhoud [WWW Document]. URL https://www.rijkswaterstaat.nl/water/waterbeheer/bescherming-tegen-het-water/maatregelen-om-overstromingen-te-voorkomen/kustonderhoud?utm_source=chatgpt.com (accessed 7.21.25).

Rijkswaterstaat, 2020. Kustgenese 2.0: kennis voor een veilige kust.

Rodil, I.F., Lastra, M., 2022. Beyond physical control: Macrofauna community diversity across sandy beaches and its relationship with secondary production. Estuar Coast Shelf Sci 277, 108083. https://doi.org/10.1016/J.ECSS.2022.108083

Rodrigues Garcia, J., Conides, A.J., Rodriguez Rivero, S., Raicevich, S., Pita, P., Kleisner, K.M., Pita, C., Lopes, P.F.M., Roldán Alonso, V., Ramos, S.S., Klaoudatos, D., Outeiro, L., Armstrong, C., Teneva, L., Stefanski, S., Böhnke-Henrichs, A., Kruse, M., Lillebø, A.I., Bennett, E.M., Belgrano, A., Murillas, A., Pinto Sousa, I., Burkhard, B., Villasante, S., 2017. Marine and coastal cultural ecosystem services: Knowledge gaps and research priorities. One Ecosystem 2. https://doi.org/10.3897/ONEECO.2.E12290

Roelvink, D., Huisman, B., Elghandour, A., Ghonim, M., Reyns, J., 2020. Efficient Modeling of Complex Sandy Coastal Evolution at Monthly to Century Time Scales. Front Mar Sci 7, 535. https://doi.org/10.3389/fmars.2020.00535

Roelvink, D., Reniers, A., Van Dongeren, A., 2010. XBeach model description and manual, ccee.ncsu.edu.

Rosati, J.D., Dean, R.G., Walton, T.L., 2013. The modified Bruun Rule extended for landward transport. Mar Geol 340, 71–81. https://doi.org/10.1016/j.margeo.2013.04.018

Ruggiero, P., Komar, P.D., McDougal, W.G., Beach, R.A., 1997. Extreme Water Levels, Wave Runup and Coastal Erosion, in: Coastal Engineering 1996. American Society of Civil Engineers, New York, NY, pp. 2793–2805. https://doi.org/10.1061/9780784402429.216

Scheffer, M., 2010. Complex systems: Foreseeing tipping points. Nature 467, 411–412. https://doi.org/10.1038/467411A

Schipper, M.A. De, Ludka, B.C., Raubenheimer, B., Luijendijk, A.P., Schlacher, T.A., 2021. Beach nourishment has complex implications for the future of sandy shores. Nat Rev Earth Environ 1–15. https://doi.org/10.1038/s43017-020-00109-9

Schlacher, T.A., Noriega, R., Jones, A., Dye, T., 2012. The effects of beach nourishment on benthic invertebrates in eastern Australia: Impacts and variable recovery. Science of The Total Environment 435–436, 411–417. https://doi.org/10.1016/J.SCITOTENV.2012.06.071

Schooler, N.K., Dugan, J.E., Hubbard, D.M., 2019. No lines in the sand: Impacts of intense mechanized maintenance regimes on sandy beach ecosystems span the intertidal zone on urban coasts. Ecol Indic 106, 105457. https://doi.org/10.1016/j.ecolind.2019.105457

Schröter, M., Başak, E., Christie, M., Church, A., Keune, H., Osipova, E., Oteros-Rozas, E., Sievers-Glotzbach, S., van Oudenhoven, A.P.E., Balvanera, P., González, D., Jacobs, S., Molnár, Z., Pascual, U., Martín-López, B., 2020. Indicators for relational values of nature's contributions to good quality of life: the IPBES approach for Europe and Central Asia. Ecosystems and People 16, 50–69.

https://doi.org/10.1080/26395916.2019.1703039;WEBSITE:WEBSITE:TFOPB;PAGEGROUP:STRING:PUBLICATION

Seddon, N., Chausson, A., Berry, P., Girardin, C.A.J., Smith, A., Turner, B., 2020. Understanding the value and limits of nature-based solutions to climate change and other global challenges. Philosophical Transactions of the Royal Society B 375. https://doi.org/10.1098/RSTB.2019.0120

Seekamp, E., Jurjonas, M., Bitsura-Meszaros, K., 2019. Influences on coastal tourism demand and substitution behaviors from climate change impacts and hazard recovery responses. Taylor & FrancisE Seekamp, M Jurjonas, K Bitsura-MeszarosJournal of Sustainable Tourism, 2019•Taylor & Francis 27, 629–648. https://doi.org/10.1080/09669582.2019.1599005

Seymour, R., Guza, R.T., O'Reilly, W., Elgar, S., 2005. Rapid erosion of a small southern California beach fill. Coastal Engineering 52, 151–158. https://doi.org/10.1016/J.COASTALENG.2004.10.003

Shivlani, M.P., Letson, D., Theis, M., 2003. Visitor preferences for public beach amenities and beach restoration in South Florida. Coastal Management 31, 367–385. https://doi.org/10.1080/08920750390232974;PAGE:STRING:ARTICLE/CHAPTER

Silva, F., Wijnberg, K., Groot, A. de, Geomorphology, S.H.-, 2019, undefined, 2019. The effects of beach width variability on coastal dune development at decadal scales. ElsevierFG Silva, KM Wijnberg, AV de Groot, SJMH HulscherGeomorphology, 2019•Elsevier 329, 58–69. https://doi.org/10.1016/j.geomorph.2018.12.012

Small, C., Nicholls, R., 2003. A global analysis of human settlement in coastal zones. J Coast Res.

Speybroeck, J., Bonte, D., Courtens, W., Gheskiere, T., Grootaert, P., Maelfait, J.P., Mathys, M., Provoost, S., Sabbe, K., Stienen, E.W.M., Van Lancker, V., Vincx, M., Degraer, S., 2006a. Beach nourishment: An ecologically sound coastal defence alternative? A review. Aquat Conserv 16, 419–435. https://doi.org/10.1002/AQC.733;REQUESTEDJOURNAL:JOURNAL:10990755

Speybroeck, J., Bonte, D., Courtens, W., Gheskiere, T., Grootaert, P., Maelfait, J.P., Mathys, M., Provoost, S., Sabbe, K., Stienen, E.W.M., Van Lancker, V., Vincx, M., Degraer, S., 2006b. Beach nourishment: An ecologically sound coastal defence alternative? A review. Aquat Conserv 16, 419–435. https://doi.org/10.1002/AQC.733;REQUESTEDJOURNAL:JOURNAL:10990755

Splinter, K.D., Coco, G., 2021. Challenges and Opportunities in Coastal Shoreline Prediction. Front Mar Sci 8, 788657. https://doi.org/10.3389/FMARS.2021.788657/BIBTEX

Staudt, F., Gijsman, R., Ganal, C., Mielck, F., Wolbring, J., Hass, H.C., Goseberg, N., Schüttrumpf, H., Schlurmann, T., Schimmels, S., 2021. The sustainability of beach nourishments: a review of nourishment and environmental monitoring practice. J Coast Conserv 25, 1–24. https://doi.org/10.1007/S11852-021-00801-Y/TABLES/1

Stedman, R.C., 2002. Toward a social psychology of place: Predicting behavior from place-based cognitions, attitude, and identity. Environ Behav 34, 561–581. https://doi.org/10.1177/0013916502034005001;PAGEGROUP:STRING:PUBLICATION

Stirling, A., 2008. "Opening up" and "closing down": Power, participation, and pluralism in the social appraisal of technology. Sci Technol Human Values 33, 262–294. https://doi.org/10.1177/0162243907311265

Stive, M., de Schipper, M.A., Luijendijk, A.P., Aarninkhof, S.G.J., van Gelder-Maas, C., van Thiel de Vries, J.S.M., de Vries, S., Henriquez, M., Marx, S., Ranasinghe, R., 2013. A New Alternative to Saving Our Beaches from Sea-Level Rise: The Sand Engine. J Coast Res 290, 1001–1008. https://doi.org/10.2112/JCOASTRES-D-13-00070.1

Stive, M., Roelvink, D., 1990, H. de V.-C.E., 1991, undefined, n.d. Large-scale coastal evolution concept: the Dutch coast: paper no. 9. ascelibrary.orgMJF Stive, DJA Roelvink, HJ de VriendCoastal Engineering 1990, 1991•ascelibrary.org.

Stive, M.J.F., 1991. Shore nourishment and the active zone: a time scale dependent view 2464–2473.

Stive, M.J.F., de Vriend, H.J., 1995. Modelling shoreface profile evolution. Mar Geol 126, 235–248. https://doi.org/10.1016/0025-3227(95)00080-I

Stive, M.J.F., Nicholls, R.J., de Vriend, H.J., 1991. Sea-level rise and shore nourishment: a discussion. Coastal Engineering 16, 147–163. https://doi.org/10.1016/0378-3839(91)90057-N

Stronkhorst, J., Huisman, B., Giardino, A., Santinelli, G., Santos, F.D., 2018. Sand nourishment strategies to mitigate coastal erosion and sea level rise at the coasts of Holland (The Netherlands) and Aveiro (Portugal) in the 21st century. Ocean Coast Manag 156, 266–276. https://doi.org/10.1016/j.ocecoaman.2017.11.017

Taal, M., Quataert, E., van der Spek, A., Huisman, B., Elias, E., Wang, Z., Vermeer, N., 2023. Sedimentbehoefte Nederlands kustsysteem bij toegenomen zeespiegelstijging. Delft.

Taebi, B., 2017. Bridging the Gap between Social Acceptance and Ethical Acceptability. Risk Analysis 37, 1817–1827. https://doi.org/10.1111/RISA.12734

Taebi, B., Kwakkel, J.H., Kermisch, C., 2020. Governing climate risks in the face of normative uncertainties. Wiley Interdiscip Rev Clim Change 11. https://doi.org/10.1002/WCC.666

Temmerman, S., Meire, P., Bouma, T.J., Herman, P.M.J., Ysebaert, T., De Vriend, H.J., 2013a. Ecosystem-based coastal defence in the face of global change. Nature 504, 79–83. https://doi.org/10.1038/NATURE12859;SUBJMETA=106,158,172,2151,631,704;KWRD=CLIMATE+SCIENCES,ECOLOGY,ENVIRONMENTAL+SCIENCES,SOLID+EARTH+SCIENCES

Temmerman, S., Meire, P., Bouma, T.J., Herman, P.M.J., Ysebaert, T., De Vriend, H.J., 2013b. Ecosystem-based coastal defence in the face of global change. Nature 504, 79–83. https://doi.org/10.1038/NATURE12859;SUBJMETA=106,158,172,2151,631,704;KWRD=CLIMATE+SCIENCES,ECOLOGY,ENVIRONMENTAL+SCIENCES,SOLID+EARTH+SCIENCES

Thaler, T., Fuchs, S., Priest, S., Doorn, N., 2018. Social justice in the context of adaptation to climate change—reflecting on different policy approaches to distribute and allocate flood risk management. Reg Environ Change 18, 305–309. https://doi.org/10.1007/S10113-017-1272-8

Tonnon, P K, Huisman, B.J.A., Stam, G.N., Rijn, L.C. Van, 2018. Numerical modelling of erosion rates , life span and maintenance volumes of mega nourishments. Coastal Engineering 131, 51–69. https://doi.org/10.1016/j.coastaleng.2017.10.001

Tonnon, P.K., Huisman, B.J.A., Stam, G.N., van Rijn, L.C., 2018. Numerical modelling of erosion rates, life span and maintenance volumes of mega nourishments. Coastal Engineering 131, 51–69. https://doi.org/10.1016/j.coastaleng.2017.10.001

Torres, A., Brandt, J., Lear, K., Liu, J., 2017. A looming tragedy of the sand commons. Science (1979) 357, 970–971. https://doi.org/10.1126/SCIENCE.AAO0503

Usher, L.E., 2021. Virginia and North Carolina surfers' perceptions of beach nourishment. Ocean Coast Manag 203, 105471. https://doi.org/10.1016/J.OCECOAMAN.2020.105471

Valdemoro, H.I., Jiménez, J.A., 2006. The Influence of Shoreline Dynamics on the Use and Exploitation of Mediterranean Tourist Beaches. Coastal Management 34, 405–423. https://doi.org/10.1080/08920750600860324

Valloni, R., Médit, M.B., 2007. Artificial beach nourishment projects in Italy, in: Intervento Presentato al Convegno 38th CONGRÉS CIESM Tenutosi a ISTANBUL Nel 9-13 Mars 2007. pp. 706–706.

Valverde, H.R., Trembanis, A.C., Pilkey, O.H., 1999. Summary of Beach Nourishment Episodes on the U.S. East Coast Barrier Islands. J Coast Res 15, 1100–1118.

Van Den Berg, A.E., Vlek, C.A.J., Coeterier, J.F., 1998. GROUP DIFFERENCES IN THE AESTHETIC EVALUATION OF NATURE DEVELOPMENT PLANS: A MULTILEVEL APPROACH. J Environ Psychol 18, 141–157. https://doi.org/10.1006/JEVP.1998.0080

Van der Biest, K., De Nocker, L., Provoost, S., Boerema, A., Staes, J., Meire, P., 2017a. Dune dynamics safeguard ecosystem services. Ocean Coast Manag 149, 148–158. https://doi.org/10.1016/j.ocecoaman.2017.10.005

Van der Biest, K., De Nocker, L., Provoost, S., Boerema, A., Staes, J., Meire, P., 2017b. Dune dynamics safeguard ecosystem services. Ocean Coast Manag 149, 148–158. https://doi.org/10.1016/j.ocecoaman.2017.10.005

van der Meulen, F., IJff, S., van Zetten, R., 2023. Nature-based solutions for coastal adaptation management, concepts and scope, an overview. Nord J Bot 2023. https://doi.org/10.1111/NJB.03290

Van Der Spek, A., Elias, E., 2013. The effects of nourishments on autonomous coastal behaviour. - Google Scholar, in: Proceedings of the 7th International Conference on Coastal Dynamics. Arcachon, France, pp. 24–28.

van der Spek, A., Lodder, Q.J., 2015. A new sediment budget for The Netherlands; the effects of 15 years of nourishing (1991-2005), in: The Proceedings of the Coastal Sediments 2015. WORLD SCIENTIFIC. https://doi.org/10.1142/9789814689977_0074

van der Spek, A.J.F., de Kruif, A.C., Spanhoff, R., 2007. Richtlijnen onderwatersuppleties.

van Duin, M.J.P., Wiersma, N.R., Walstra, D.J.R., van Rijn, L.C., Stive, M.J.F., 2004. Nourishing the shoreface: observations and hindcasting of the Egmond case, The Netherlands. Coastal Engineering 51, 813–837. https://doi.org/10.1016/j.coastaleng.2004.07.011

van Duin, M. J.P., Wiersma, N.R., Walstra, D.J.R., van Rijn, L.C., Stive, M.J.F., 2004. Nourishing the shoreface: Observations and hindcasting of the Egmond case, The Netherlands. Coastal Engineering 51, 813–837. https://doi.org/10.1016/j.coastaleng.2004.07.011

van Egmond, E.M., van Bodegom, P.M., Berg, M.P., Wijsman, J.W.M., Leewis, L., Janssen, G.M., Aerts, R., 2018. A mega-nourishment creates novel habitat for intertidal macroinvertebrates by enhancing habitat relief of the sandy beach. Estuar Coast Shelf Sci 207, 232–241. https://doi.org/10.1016/j.ecss.2018.03.003

Van Koningsveld, M., Mulder, J.P.M., 2004. Sustainable coastal policy developments in the Netherlands. A systematic approach revealed. J Coast Res 20, 375–385. https://doi.org/10.2112/1551-5036(2004)020[0375:SCPDIT]2.0.CO;2

van Oudenhoven, A.P.E., Aukes, E., Bontje, L.E., Vikolainen, V., van Bodegom, P.M., Slinger, J.H., 2018a. 'Mind the Gap' between ecosystem services classification and strategic decision making. Ecosyst Serv 33, 77–88. https://doi.org/10.1016/j.ecoser.2018.09.003

van Oudenhoven, A.P.E., Schröter, M., Drakou, E.G., Geijzendorffer, I.R., Jacobs, S., van Bodegom, P.M., Chazee, L., Czúcz, B., Grunewald, K., Lillebø, A.I., Mononen, L., Nogueira, A.J.A., Pacheco-Romero, M., Perennou, C., Remme, R.P., Rova, S., Syrbe, R.U., Tratalos, J.A., Vallejos, M., Albert, C., 2018b. Key criteria for developing ecosystem service indicators to inform decision making. Ecol Indic 95, 417–426. https://doi.org/10.1016/j.ecolind.2018.06.020

van Puijenbroek, M.E.B., Teichmann, C., Meijdam, N., Oliveras, I., Berendse, F., Limpens, J., 2017. Does salt stress constrain spatial distribution of dune building grasses Ammophila arenaria and Elytrichia juncea on the beach? Ecol Evol 7, 7290–7303. https://doi.org/10.1002/ECE3.3244

van Rijn, L.C., Huisman, B.J.A., 2025. Long term modelling of longshore sand transport and coastline changes along central COAST of Holland. Coastal Engineering 202, 104841. https://doi.org/10.1016/J.COASTALENG.2025.104841

Van Well, L., Isayeva, A., Axel Olsson, P., Hollander, J., 2023. Public perceptions of cultural ecosystem services provided by beach nourishment and eelgrass restoration in southern Sweden. Nord J Bot 2023, e03654. https://doi.org/10.1111/NJB.03654;JOURNAL:JOURNAL:17561051;CTYPE:STRING:JOURNAL

van Westen, B., Luijendijk, A.P., de Vries, S., Cohn, N., Leijnse, T.W.B., de Schipper, M.A., 2024. Predicting marine and aeolian contributions to the Sand Engine's evolution using coupled modelling. Coastal Engineering 188, 104444. https://doi.org/10.1016/J.COASTALENG.2023.104444

Velpen, A. Vander, Smeets, A., Torres, A., Matheson, A., 2022. Sand and sustainability: 10 strategic recommendations to avert a crisis.

Verhagen, H.J., 1996. Analysis of beach nourishment schemes. J Coast Res 12, 179–185.

Verhagen, H.J., 1993. Method for Artificial Beach Nourishment, in: Coastal Engineering 1992. American Society of Civil Engineers, New York, NY, pp. 2474–2485. https://doi.org/10.1061/9780872629332.189

Vidal, R., Van Oord, G., 2010. Environmental Impacts in Beach Nourishment: A Comparision of Options.

Vos, K., Splinter, K.D., Harley, M.D., Simmons, J.A., Turner, I.L., 2019. CoastSat: A Google Earth Engine-enabled Python toolkit to extract shorelines from publicly available satellite imagery. Environmental Modelling & Software 122, 104528. https://doi.org/10.1016/J.ENVSOFT.2019.104528

Vousdoukas, M.I., Ranasinghe, R., Mentaschi, L., Plomaritis, T.A., Athanasiou, P., Luijendijk, A., Feyen, L., 2020a. Sandy coastlines under threat of erosion. Nat Clim Chang. https://doi.org/10.1038/s41558-020-0697-0

Vousdoukas, M.I., Ranasinghe, R., Mentaschi, L., Plomaritis, T.A., Athanasiou, P., Luijendijk, A., Feyen, L., 2020b. Sandy coastlines under threat of erosion. Nat Clim Chang 10, 260–263. https://doi.org/10.1038/S41558-020-0697-0;SUBJMETA=106,215,2151,2739,2786,694,704;KWRD=CLIMATE-CHANGE+IMPACTS,GEOMORPHOLOGY,PROJECTION+AND+PREDICTION

Vries, S. De, Southgate, H.N., Kanning, W., Ranasinghe, R., 2012. Dune behavior and aeolian transport on decadal timescales. Coastal Engineering 67, 41–53. https://doi.org/10.1016/j.coastaleng.2012.04.002

Walstra, D.-J., Hoyng, C.W., Tonnon, P.K., Van Rijn, L.C., 2011. EXPERIMENTAL STUDY INVESTIGATING VARIOUS SHOREFACE NOURISHMENT DESIGNS. Coastal Engineering Proceedings 1, 30. https://doi.org/10.9753/icce.v32.management.30

Walstra, D.J.R., 2000. Unibest-TC userguide, repository.tudelft.nl. Delft, The Netherlands.

Wijnberg, K.M., Kroon, A., 2002. Barred beaches. Geomorphology 48, 103–120. https://doi.org/10.1016/S0169-555X(02)00177-0

Wijnberg, K.M., Terwindt, J.H.J., 1995a. Extracting decadal morphological behaviour from high-resolution, long-term bathymetric surveys along the Holland coast using eigenfunction analysis. Mar Geol 126, 301–330. https://doi.org/10.1016/0025-3227(95)00084-C

Wijnberg, K.M., Terwindt, J.H.J., 1995b. Extracting decadal morphological behaviour from high-resolution, long-term bathymetric surveys along the Holland coast using eigenfunction analysis. Mar Geol 126, 301–330. https://doi.org/10.1016/0025-3227(95)00084-C

Wijsman, K., Berbés-Blázquez, M., 2022. What do we mean by justice in sustainability pathways? Commitments, dilemmas, and translations from theory to practice in nature-based solutions. Environ Sci Policy 136, 377–386. https://doi.org/10.1016/j.envsci.2022.06.018

Willson, K., Thomson, G., Briggs, T., … N.E.-S.&, 2017, undefined, n.d. Beach nourishment profile equilibration: What to expect after sand is placed on a beach. files.municipalone.comK Willson, G Thomson, TR Briggs, N Elko, J MillerShore & Beach, 2017•files.municipalone.com.

Wilsoncroft, C., 2017. Effective Contract-Type Selection in the Dredging Industry.

Witteveen&Bos, 2006. Evaluatie onderwatersuppleties Noord- en Zuid-Holland. Eindrapport. Witteveen&Bos rapport Rw1472-2.

Wong, T.E., Ledna, C., Rennels, L., Sheets, H., Errickson, F.C., Diaz, D., Anthoff, D., 2022. Sea level and socioeconomic uncertainty drives high-end coastal adaptation costs. Wiley Online Library 10. https://doi.org/10.1029/2022EF003061

Woodroffe, C.D., 2002. Coasts: form, process and evolution. Cambridge University Press.

Wooldridge, T., Henter, H.J., Kohn, J.R., 2016. Effects of beach replenishment on intertidal invertebrates: A 15-month, eight beach study. Estuar Coast Shelf Sci 175, 24–33. https://doi.org/10.1016/J.ECSS.2016.03.018

Yao, Z., Chen, J., Jiang, C., Liang, H., Wu, Z., Deng, B., Long, Y., Bian, C., 2024. Experimental Analysis of the Changes in Coral Sand Beach Profiles under Regular Wave Conditions. J Mar Sci Eng 12. https://doi.org/10.3390/jmse12020287

Yates, M., Seymour, R., Guza, R., O'Reilly, W., 2009. Overview of seasonal sand level changes on southern California beaches. Shore & beach.

Propositions

Accompanying the dissertation

Simulating Sand Nourishment Strategies

from morphology towards multifunctionality

by

Tosca Kettler

1. *Sand nourishment simulations should expose how coasts behave, rather than forecast where the shoreline will be.*
2. *The path from coastal morphology to multifunctionality is unmapped, marked only by signs pointing toward resilience.*
3. *More sand does not necessary result in proportionally more benefits (this thesis).*
4. *The more detailed the model is, the more it hides its uncertainty.*
5. *Coastal change is not the problem; any perception of a static coastline is.*
6. *A nature-based solution is not necessarily a nature-friendly solution.*
7. *If underwater destruction were as visible as deforestation, coastal defence would face more societal threats.*
8. *Sitting is toxic - each hour seated demands an hour in motion.*
9. *Computers are masters of work, but thieves of play.*

These propositions are regarded as opposable and defendable, and have been approved as such by the promotor: Dr. ir. M.A. de Schipper, and the copromotor: Dr. ir. A.P. Luijendijk.

Acknowledgments

Model run: *PhD_Thesis_TTK*
Simulation period: 2020–2025

Main function

$$\frac{d(PhD)}{dt} = \frac{d}{dx}\left\{D(z') \frac{d(PhD)}{dx}\right\} + M(PhD) + A(PhD) + S\,\delta(t\text{-}t_0) + W(t)$$

With

$$z' = C + O + A + S + T$$

Wherein

- **PhD** = the evolving state variable
- **t** = time
- **x** = distance along the PhD trajectory
- **D** = Diffusion coefficient, shaped by **z'**
- **z'** = **C + O + A + S + T** = local conditions of the phD run, composed of:
    - **C = Coffee** (high-frequency external forcing function)
    - **O = Orbits** (repeated cycles/iterations around the same problems until convergence)
    - **A = Antecedents** (those who worked on this topic before me)
    - **S = Sleep** (equilibrium restoration)
    - **T = Training** (hydrodynamic forcing - rowing)
- **M(PhD) = Matthieu** (promotor, supervisor): the most reliable calibration constant in this model run. Always supportive and patient in guiding the work, providing sharp insights, and encouraging improvements with enthusiasm. A strong drive to set up new research and bring it to completion proved invaluable. Even under an overfull agenda, availability for "recomputations" was nearly constant: with only a few words the dynamics were understood, and just as quickly a practical solution emerged.
- **A(PhD) = Arjen** (co-promotor): a constructive gradient, consistently sharpening iterations and adding clarity. Also a source of new ideas already during the planning phase, keeping the trajectory innovative and well-structured. Always enthusiastic, supportive, and generous with feedback, ensuring the model state stayed on track.
- **S δ(t−t0) = Stefan** (initial promotor, main C-SCAPE applicant): the crucial initial impulse, providing the project's starting momentum and boundary conditions.

Constructive and enthusiastic throughout, and instrumental in bringing fresh ideas that helped set the long-term course of this run.

- **W(t) = wider system support**. The composite forcing that kept the model adaptive, stable, and fun, composed of:
    - **Consortium and institutions**
        - C-SCAPE consortium (with special thanks to junior colleagues Eva, Haye, Vincent)
        - Department of Hydraulic Engineering, TU Delft
        - Funding agencies: NWO (grant 17595), Rijkswaterstaat, Province of Noord-Holland, Municipality of Veere/Region Fund Zeeuwse Kust, Van Oord, Witteveen+Bos, HHNK Water Board, Staatsbosbeheer, Dutch Coastline Challenge, OBN, Natuurmonumenten, WWF
    - **Initial conditions (home base)**
        - Agnes & Rob (parents)
        - Celeste & Myrthe (sisters)
        - Jasper (favourite human)
        - Joan (housemate & friend)
    - **Essential support variables**
        - Collaborations with Deltares (among others, Bas, Renske), Rijkswaterstaat (among others, Laura), Svasek Hydraulics (Anna)
        - Thesis students: Aaron, Ka-Way, Luke
        - Fellow PhD travellers and colleagues: Anna, Anne, Bart, Bas, Christa, Inge, Marlies
        - Friends and fam: Agnes, Bas, Bertine, Carlos, Celeste, Eline, Ger, Gerco, Jasper, Jiska, Joan, Jonna, Jolanda, Jessica, Lisanne, Manon, Marieke, Maurits, Myrthe, Myrza, Pauline, Reinette, Rob, Romy, Rowan, Sander, Sieb, Tessa
        - Rowing coaches: Edwin, Elout, Gerco, Iza, Jethri, Jonna, Olof, Pim, Sophie, Steffen

Model performance
Without the above parameters, this run would have quickly diverged.
With them, the system remained stable and fun!

Output
One completed PhD thesis and immense gratitude.

Curriculum Vitae

Tosca Thalia Kettler

21-06-1996, Eindhoven, the Netherlands

Pre-university education

2008 – 2014	*Christelijk Gymnasium Utrecht, Utrecht, the Netherlands – Gymnasium Diploma*

Higher education

2014 – 2017	*Bachelor of Science in Geological and Earth Sciences/Geosciences, Utrecht University, Utrecht, the Netherlands*
2017 – 2020	*Master of Science in Climate Physics, Utrecht University, Utrecht, the Netherlands*

Professional practice after Master's degree

2020 – Present	*PhD Candidate in Hydraulic Engineering at Delft University of Technology, Delft, the Netherlands*

Institution where the research was conducted

Delft University of Technology (TU Delft), Faculty of Civil Engineering and Geosciences, Delft, the Netherlands

List of publications

***Kettler**, T., de Schipper, M., Luijendijk, A., 2024. Simulating decadal cross-shore dynamics at nourished coasts with Crocodile. Coastal Engineering 190, 104491. https://doi.org/10.1016/J.COASTALENG.2024.104491*

*Geukes, H. H., **Kettler**, T. T., Lansu, E. M., Bax, V., Höfer, S., de Schipper, M. A., de Winter, R., Luijendijk, A. P., Reijers, V. C., van Bodegom, P. M., van de Lageweg, W. I., van der Heide, T., & van Oudenhoven, A. P. E., 2024. Sand nourishment for multifunctional coastal climate adaptation: three key implications for researchers. Nature-Based Solutions, 6, 100191. https://doi.org/10.1016/J.NBSJ.2024.100191*

*Gleeson, E., Kurzeneva, E., de Rooy, W., Rontu, L., Martín Pérez, D., Clancy, C., Ivarsson, K.-I., Engdahl, B.J., Tijm, S., Nielsen, K.P., Shapkalijevski, M., Maalampi, P., Ukkonen, P., Batrak, Y., Kähnert, M., **Kettler**, T., van den Brekel, S.M.E., Adriaens, M.R., Theeuwes, N., Pálmason, B., Rieutord, T., Fannon, J., Whelan, E., Viana, S., Homleid, M., Bessardon, G., Onvlee, J., Samuelsson, P., Santos-Muñoz, D., Vignes, O.N., Stappers, R., 2024. The Cycle 46 Configuration of the HARMONIE-AROME Forecast Model. Meteorology 3(4), 354–390. https://doi.org/10.3390/meteorology3040021*

***Kettler**, T., de Schipper, M., Luijendijk, A., 2025. Exploring decadal beach profile dynamics in response to nourishment strategies under accelerated sea level rise." Ocean & Coastal Management 260., (2025), 107477. https://doi.org/10.1016/j.ocecoaman.2024.107477*

*Geukes, H.H., **Kettler**, T.T., De Schipper, M.A., Van Bodegom, P.M., Van Oudenhoven, A. P.E., 2025. Evaluating coastal multifunctionality: sand nourishment strategies at decadal timescales. Ecol. Indic. 181. https://doi.org/10.1016/j.ecolind.2025.114487.*

***Kettler**, T., de Schipper, M., Huisman, B., Luijendijk, A. " Numerical assessment of decadal redistribution and profile equilibration at mega nourishments." Coastal Engineering, submitted.*